

Charakterisierung der Expression von Humanen Endogenen Retroviren und ihre mögliche Bedeutung für die Pathogenese von Tumorerkrankungen und der Multiplen Sklerose

Kumulative Dissertation

zur Erlangung des

Doktorgrades der Naturwissenschaften (Dr. rer. nat.)

an der Naturwissenschaftlichen Fakultät I

– Biowissenschaften –

der Martin-Luther-Universität Halle-Wittenberg

vorgelegt von

Frau Lisa Marie Wieland



Gutachter:

1. Prof. Gary Sawers
2. apl. Prof. Martin Sebastian Staeger
3. Prof. Steffen Roßner

Tag der öffentlichen Verteidigung: 05.11.2024

In Liebe meiner Familie und Freunden.

Ihr habt mich auf dieser Reise zugleich geerdet, wie beflügelt.

Hypocritical, egotistical

Don't wanna be the parenthetical, hypothetical

Working onto something that I'm proud of, out of the box

An epoxy to the world and the vision we've lost

I'm an apostrophe

I'm just a symbol to remind you that there's more to see

I'm just a product of the system, a catastrophe

And yet a masterpiece, and yet I'm half-diseased

And when I am deceased

At least I go down to the grave and die happily

Leave the body and my soul to be a part of thee

I do what it takes

- Imagine Dragons

Inhaltsverzeichnis

Abbildungs- und Tabellenverzeichnis	6
Abkürzungsverzeichnis	7
1. Einleitung	11
1.1. Ursprung, Aufbau und Nomenklatur humaner endogener Retroviren (HERVs)	11
1.2. Mechanismen zur Stilllegung von HERVs	15
1.3. Physiologische Bedeutung	17
1.4. HERVs und ihre mögliche Bedeutung für die Pathogenese von Tumor- und Autoimmunerkrankungen	18
1.5. Zielstellung	22
2. Kumulativer Teil	25
2.1. <i>Formation of HERV-K and HERV-Fc1 Envelope Family Members is Suppressed on Transcriptional and Translational Level</i>	26
2.1.1. Zusammenfassung	26
2.1.2. Darlegung des Eigenanteils, Manuskript und Zitierung	27
2.1.3. Bestätigung des Betreuers der vorliegenden Dissertation	28
2.2. <i>Overexpression of Endogenous Retroviruses and Malignancy Markers in Neuroblastoma Cell Lines by Medium-Induced Microenvironmental Changes</i>	69
2.2.1. Zusammenfassung	69
2.2.2. Darlegung des Eigenanteils, Manuskript und Zitierung	70
2.2.3. Bestätigung des Betreuers der vorliegenden Dissertation	71
2.3. <i>Epstein-Barr Virus-Induced Genes and Endogenous Retroviruses in Immortalized B Cells from Patients with Multiple Sclerosis</i>	90
2.3.1. Zusammenfassung	90
2.3.2. Darlegung des Eigenanteils, Manuskript und Zitierung	91
2.3.3. Bestätigung des Betreuers der vorliegenden Dissertation	92
3. Diskussion	133
3.1. Kodon-Optimierung überwindet die limitierte Proteinsynthese nativer ENV <i>in vitro</i> und führt zur Akkumulation überexprimierter ENV im ER	133
3.2. Seltene Nukleotidtriplets haben einen negativen Effekt auf die Expression des ENV von HERV-K113 in Säugerzellen und im zellfreien System	134
3.3. Mögliche Bedeutung der mRNA-Sekundärstruktur für die Synthese nativer HERV-Proteine	135

3.4.	Induktion eines HERV-K/CD133-positiven Phänotyps in SiMa-Zellen und weiterer, bekannter Malignitätsmarker in NB-Zelllinien durch Kultivierung in Serum-depletiertem Stammzell-Medium	136
3.5.	Aktivierung des Immuncheckpunkt-Moleküls CD200 und Identifizierung ko-exprimierter HERV-Loci mittels Virus-Metagenomanalysen unter Stammzell-fördernden Bedingungen	138
3.6.	Virus-Metagenomanalysen führen zur Identifizierung aktivierter HERV-Loci über den B-Zell-Rezeptor/CD40-Signalweg in EBV-immortalisierten B-Zelllinien	140
3.7.	Immortalisierung mittels EBV führt ausschließlich in MS-assoziierten LCL zur Induktion distinkter HERV-Loci	141
3.8.	Darstellung potentiell prädiktiver Gen- <i>Panel</i> für die MS und deren krankheitsrelevante Faktoren mittels differenzieller Genexpressionsmuster in EBV-immortalisierten B-Zelllinien	144
3.9.	Mögliche Bedeutung <i>in vitro</i> exprimierter EBV-Genprodukte im Zusammenhang mit Umwelt-bedingten und klinischen Parametern in der MS	145
4.	Zusammenfassung und Ausblick	150
5.	Literaturverzeichnis	155
6.	Anhang	197
6.1.	Eidesstattliche Erklärung / Declaration of Oath	197
6.2.	Lebenslauf	198
6.3.	Publikationen	199
6.4.	Konferenzbeiträge (<i>Abstracts</i>) und Publikationen ohne <i>Peer-Review</i> -Verfahren	200
6.5.	Danksagung	202

Abbildungs- und Tabellenverzeichnis

Abbildung 1. Transponierbare Elemente (TE) des menschlichen Genoms.	12
Abbildung 2. Der Ursprung humaner endogener Retroviren (HERV), sowie deren physiologische und pathophysiologische Bedeutung.	13
Tabelle 1. Übersicht zu den allgemeinen Daten der Fachzeitschriften.	25
Tabelle 2. Übersicht zu den Beiträgen aller Autoren der Publikation I.	27
Tabelle 3. Übersicht zu den Beiträgen aller Autoren der Publikation II.	70
Tabelle 4. Übersicht zu den Beiträgen aller Autoren der Publikation III.	91

Abkürzungsverzeichnis

-1PRF	<i>Programmed -1 Ribosomal Frameshifting</i>
AK	Antikörper
ALS	Amyotrophe Lateralsklerose
APC	Antigen-präsentierende Zelle
APOBEC3	<i>Apolipoprotein B mRNA-editing Enzyme Catalytic Polypeptide-like 3</i>
BCR	B-Zell-Rezeptor
bzw.	Beziehungsweise
CA	Kapsid
CAR-T	Chimäre Antigenrezeptor T-Zellen
CD200R	CD200 Rezeptor
cDNA	Komplementäre DNA
CDR	<i>Complementarity Determining Region</i>
CIS	Klinisch isoliertes Syndrom
coLCL	Lymphoblastoide B-Zelllinie aus PBMC eines gesunden Kontrollspenders
CpG	Cytosin-Guanin-Dinukleotid
CSC	<i>Cancer-like Stem Cells</i>
CSF	<i>Cerebrospinal Fluid</i> , engl. für Rückenmarksflüssigkeit
Da	Dalton
DNA	Desoxyribonukleinsäure
DMT	<i>Disease Modifying Therapy</i>
ds	Doppelsträngig
e. g.	<i>Exempli Gratia</i> , lat. für zum Beispiel
EBNA	<i>EBV Nuclear Antigen</i>
EBV	Epstein-Barr-Virus
EDSS	<i>Expanded Disability Status Scale</i>
EMT	Epithelial-Mesenchymale Transition
ENV	<i>Envelope</i> , engl. für Hüllprotein
ER	Endoplasmatisches Retikulum
ERV	Endogenes Retrovirus
FBS	Fetales Kälberserum
FDR	<i>False Discovery Rate</i>
FGFR1	Fibroblasten-Wachstumsfaktor-Rezeptor 1
FP	Fusionspeptid
FPKM	<i>Fragments per Kilobase per Million Mapped Fragments</i>

GAG	Gruppen-spezifische Antigene
GBM	Glioblastom
GCT	Keimzelltumor
H3K9me3	Tri-Methylierungen von Histon H3 an Lysin 9
HCC	Hepatozelluläres Karzinom
HERV	Humanes Endogenes Retrovirus
HHV-6	Humanes Herpesvirus 6
HIV-1	Humanes Immundefizienz Virus Typ 1
HML	<i>Human MMTV-like</i>
HRP	Meerrettich-Peroxidase
ID	<i>Inhibitor of Differentiation/DNA binding</i>
IFN	Interferon
IM	Infektiöse Mononukleose
INT	Integrase
ISD	Immunsuppressive Domäne
KRAB-ZFP	K rüppel-assoziertes B ox-Domänen- Z inkfingerprotein
LCL	Lymphoblastoide B-Zelllinie
LINE	<i>Long Interspersed Nuclear Elements</i>
lncRNA	<i>Long Non-Coding RNA</i>
LTR	<i>Long Terminal Repeat</i>
MA	Matrix
mESC	Embryonale Stammzellen von Mäusen
MHC	<i>Major Histocompatibility Complex</i>
miRNA	Mikro-RNA
MMTV	Murines Mammatumovirus
MOG	Myelin-Oligodendrozytenprotein
MOV10	<i>Moloney Leukemia Virus Homolog 10</i>
mRNA	<i>Messenger RNA</i>
MRT	Magnetresonanztomografie
MS	Multiple Sklerose
MSLCL	Lymphoblastoide B-Zelllinie aus PBMC eines Patienten mit Multipler Sklerose
MSRV	Multiple Sklerose-assoziiertes Retrovirus
NB	Neuroblastom
NC	Nukleokapsid
NCBI	<i>National Center of Biotechnology Information</i>
ORF	<i>Open Reading Frame</i> , engl. für Offener Leserahmen
PA	<i>Pituitary Adenoma</i> , engl. für Hypophysenadenom

PAGE	Polyacrylamid-Gelelektrophorese
PBL	Lymphozyten des peripheren Blutes
PBMC	Mononukleäre Zellen des peripheren Blutes
PBS	Primerbindungsstelle
PGC	Primordiale Keimzellen
piRNA	Piwi-interagierende RNA
PMA	Phorbolmyristat-Acetat
POL	Polymerase
PPMS	Primär Progrediente MS
PPT	Polypurintrakt
PRF	<i>Programmed Ribosomal Frameshifting</i>
PRO	Protease
qRT-PCR	Quantitative <i>Real Time</i> Polymerase-Kettenreaktion
R	<i>Redundant</i>
RA	Rheumatoide Arthritis
Rb	Retinoblastom
RNA	Ribonukleinsäure
RNAseq	Transkriptomsequenzierung
RRMS	Schubförmig Remittierende MS
RT	Reverse Transkriptase
RTE	<i>Retrotransposable Element</i>
SAg	Superantigen
SAMHD1	<i>SAM Domain and HD Domain-containing Protein 1</i>
SDS	Natrium-Dodecylsulfat
shRNA	<i>Small Hairpin RNA</i>
SINE	<i>Short Interspersed Nuclear Element</i>
siRNA	<i>Small Interfering RNA</i>
SLE	Systemischer Lupus Erythematoses
SP	Signalpeptid
SPMS	Sekundär Progrediente MS
SRA	<i>Sequence Read Archive</i>
SU	<i>Surface Unit</i> , engl. für Oberflächeneinheit
SVA	<i>SINE-R, Variable-Number-of-Tandem-Repeats and Alu-like elements</i>
TCR	T-Zellrezeptor
TCRBV13	V β 13+ T-Zellen
TE	Transponierbares Element

TIR	<i>Terminal Inverted Repeat</i>
TLR	<i>Toll-like Receptor</i>
TM	Transmembraneinheit
TPase	Transposase
TRIM5	<i>Tripartite Motif-containing 5</i>
tRNA	Transfer-RNA
U3	<i>Unique 3'</i>
U5	<i>Unique 5'</i>
UPR	<i>Unfolded Protein Response</i>
V β	Variable Region der β -Kette
WT	Wildtyp
z. B.	Zum Beispiel
z. T.	Zum Teil
ZFP	Zinkfingerprotein

1. Einleitung

Die Veröffentlichung der ersten nahezu vollständigen menschlichen Genomsequenz im Jahr 2001 war der geschichtsträchtige Meilenstein einer internationalen Wissenschaftskooperation und setzte zugleich den Grundstein für neue Forschungsbereiche der Humangenetik (1, 2). Die Auffassung des menschlichen Erbguts als Aneinanderreihung Protein-kodierender Genabschnitte und sogenannter „*junk DNA*“ (engl. für Schrott) (3-5) wich einem Verständnis für das Ausmaß an zwischenmenschlicher Nukleotidvielfalt und der Erkenntnis, dass sich fast die Hälfte unseres Genoms von transponierbaren Elementen (TEs) ableitet und der Anteil an Protein-kodierenden Regionen nur 1,5 % beträgt (6). TEs sind mobile DNA-Stücke, die sich von einer Stelle im Genom zu einer anderen Stelle bewegen können und deshalb umgangssprachlich auch als „springende Gene“ bezeichnet werden (7). Hierbei unterscheidet man eukaryotische TEs grundlegend in Retrotransposons und DNA-Transposons (8). Die Replikation der Retrotransposons erfolgt über ein RNA-Intermediat, welches mittels reverser Transkription in DNA wieder umgeschrieben und andernorts ins Genom integriert wird. Neben der neuen DNA-Kopie bleibt das ursprüngliche Element intakt, weshalb man diese Akkumulation von Elementen auch als „*copy and paste*“ (engl. für Kopieren und Einfügen)-Mechanismus bezeichnen kann. Im Gegensatz dazu werden die meisten DNA-Transposons über einen „*cut and paste*“ (engl. für Ausschneiden und Einfügen)-Mechanismus von einem Ort im Genom zu einem anderen Ort mobilisiert (9). Bei DNA-Transposons wird dieser Prozess durch die Transposase (TPase) vermittelt. Bei der „*cut and paste*“-Mobilisation stellt die TPase das zentrale und zumeist einzig kodierte Gen dar, welches im 5'- und 3'-Bereich von sogenannten *terminal inverted repeats* (TIRs) flankiert wird. Anhand der TPase werden diese TIR-tragenden Elemente verschiedenen Superfamilien zugeordnet: Tc1/Mariner, hAT, Mutator, Merlin, Transib, P, PiggyBac, PIF/Harbinger und CACTA, wobei sich die beiden Letzten durch einen weiteren offenen Leserahmen (ORF) auszeichnen (10, 11). Helitrons und Polinton/Maverick gehören zu einer zweiten Subklasse innerhalb der DNA-Transposons, welche andere Mobilisationsmechanismen verwenden (s. Abb. 1). Nachfolgend soll auf die Subklassen innerhalb der Retrotransposons und deren Bedeutung weiter eingegangen werden.

1.1. Ursprung, Aufbau und Nomenklatur humaner endogener Retroviren (HERVs)

Innerhalb der Retrotransposons gibt es Sequenzen, die von langen repetitiven Elementen am 5'- und 3'-Ende, sogenannten *long terminal repeats* (LTRs), begrenzt sind. Die allermeisten Retrotransposons zählen jedoch zur non-LTR Klasse und beanspruchen in etwa ein Drittel des Genoms (12). Zu den wichtigsten Vertretern der non-LTR Klasse zählen *long interspersed nuclear elements* (LINEs), *short interspersed nuclear elements* (SINEs), *Alu*-Elemente, SVAs

(SINE-R, *Variable-Number-of-Tandem-Repeats* und *Alu*-ähnliche Elemente), sowie die Gruppe der *retrotransposable elements* (RTEs) (13). LTR-tragende Elemente machen in etwa 8 % des Genoms aus und werden auch als endogene Retroviren (ERV) bezeichnet. In Abbildung 1 ist die Gruppe der ERV innerhalb der TE, sowie deren Unterteilung in Klassen unter Angabe wichtiger ERV-Familien dargestellt.

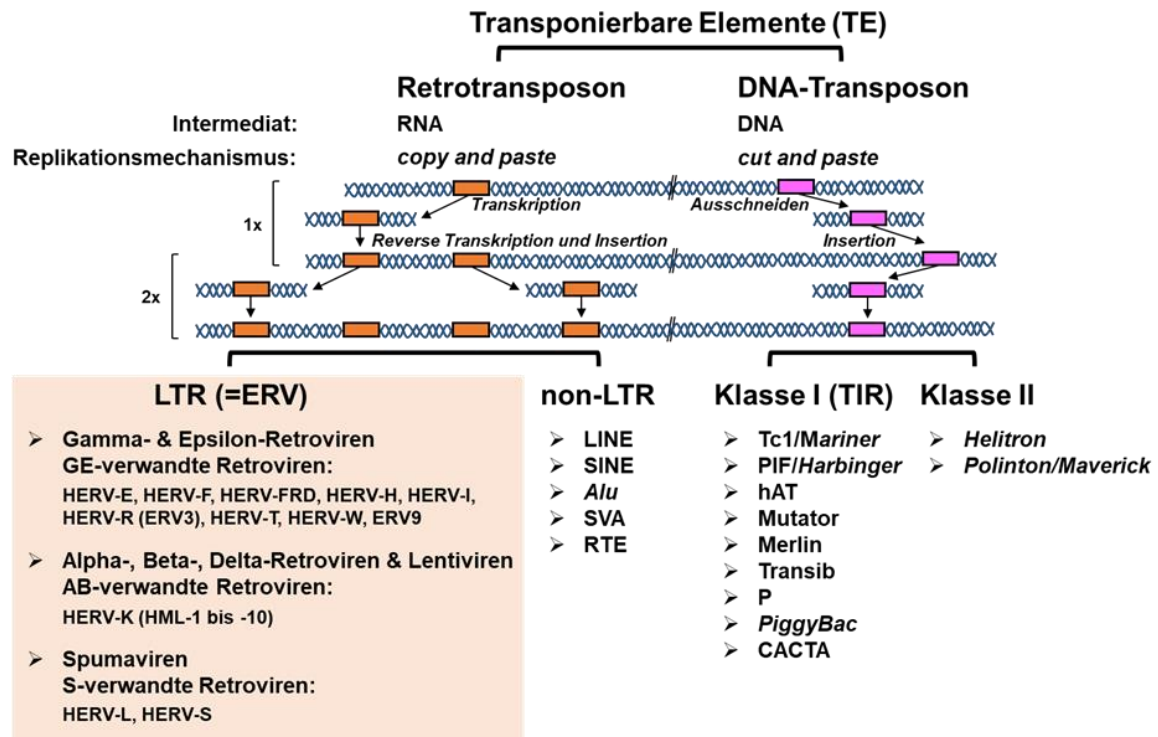


Abbildung 1. Transponierbare Elemente (TE) des menschlichen Genoms. Die Unterschiede in der Replikation und Mobilisierung von DNA- und Retrotransposons ist schematisch dargestellt. Die wichtigsten Subfamilien der DNA- und Retrotransposons sind hier aufgeführt und im Text ausführlicher beschrieben. Endogene Retroviren (ERV) sind Retrotransposons, die Bereiche sogenannter *long terminal repeats* (LTRs) enthalten. Anhand ihrer Abstammung von exogenen Retroviren können humane ERV (HERV) aufgeteilt werden. Wichtige HERV-Familien sind den jeweiligen Gruppen zugeordnet. TIR: terminal inverted region.

Der Ursprung dieser großen Anzahl retroviraler Elemente im Genom geht auf einstige Infektionsereignisse der Keimbahn mit exogenen Retroviren und der Integration der daraus resultierenden Proviren zurück, die seither vertikal als Wirtsallel an die nächste Generation weitergegeben werden (14). Phylogenetisch gehören ERV daher zur Familie der *Retroviridae* und lassen sich grundlegend in die sieben Genera α -, β -, γ -, δ - und ε -Retroviren, sowie Lenti- und Spumaviren einteilen. Bei humanen ERV (HERV) gruppiert man diese Genera in drei Klassen, wobei diese Unterteilung auf Sequenzhomologien ihrer Protein-kodierenden Regionen beruht. Die provirale Sequenz der HERV entspricht dem Aufbau ihrer exogenen Verwandten. Die Integration und der Aufbau sind in Abbildung 2 schematisch dargestellt.

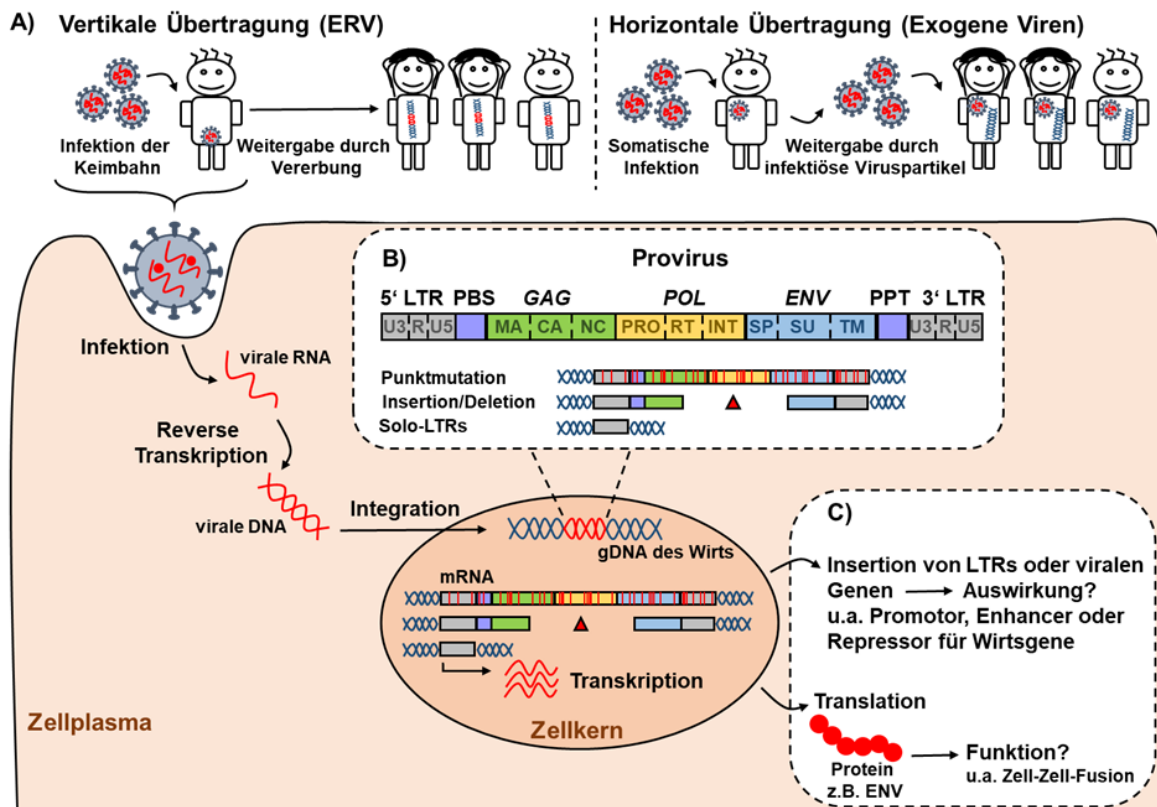


Abbildung 2. Der Ursprung humaner endogener Retroviren (HERV), sowie deren physiologische und pathophysiologische Bedeutung. Die Integration von HERVs in das Genom, die damit einhergegangenen Veränderungen in der proviralen Sequenz, sowie mögliche Auswirkungen der HERV-Expression sind schematisch zusammengefasst. **A)** Im Unterschied zur rein horizontalen Virusübertragung in somatische Zellen waren diejenigen exogenen Retroviren, aus denen die HERVs entstanden sind, in der Lage, Keimbahnzellen zu infizieren. Bei der Replikation wird retrovirale RNA in ein doppelsträngiges DNA (dsDNA)-Intermediat umgeschrieben und in das zelluläre Genom integriert. Als integraler Bestandteil des Genoms werden HERV nach den Mendelschen Gesetzen an die nächste Generation weitergegeben (vertikale Übertragung). **B)** Die Endogenisierung und Fixierung hatte zur Folge, dass im Lauf der Evolution Mutationen, Insertionen und Deletionen in der viralen Sequenz stattgefunden haben, welche die Vollständigkeit ihrer kodierenden Regionen der Gruppen-spezifischen Antigene (*GAG*), der Polymerase (*POL*) und des Hüllproteins (*ENV*) beeinträchtigen. Die Homologie der flankierenden LTR-Sequenzen führte auch oftmals zu LTR-LTR-Rekombinationsereignissen in dessen Folge der gesamte interne provirale Teil eliminiert wurde und sich sogenannte solo-LTRs im Genom akkumulierten. **C)** Die Transkription proviraler mRNA unterliegt vielschichtigen, epigenetischen Kontrollmechanismen, weshalb HERVs unter physiologischen Bedingungen kaum exprimiert werden. Ausgenommen davon ist die Expression von HERV-ENVs in der Plazenta und während der Embryonalentwicklung, wo insbesondere deren Eigenschaft zur Zell-Zell-Fusion eine wichtige Rolle zu spielen scheint. Im Kontext verschiedener Tumor- und Autoimmunerkrankungen wird eine gesteigerte transkriptionelle Aktivität von HERVs beobachtet. Eine De-Regulierung der Transkription durch die Insertion von LTRs und anderen proviralen Sequenzen innerhalb bzw. in unmittelbarer Nähe von Wirtsgenen mit proto-onkogenen oder immunmodulierenden Eigenschaften könnte die Entstehung pathogener Signalwege begünstigen, sowie die

genomische Instabilität im Allgemeinen fördern. Zudem könnten virale Proteine, wie ENVs, selbst einen schadhafte Einfluss auf umliegende Zellen und Gewebe haben. *U3: unique 3', R: redundant, U5: unique 5', PBS: primer binding site, MA: matrix, CA: capsid, NC: nucleocapsid, PRO: protease, RT: reverse transcriptase, INT: integrase, SP: signal peptide, SU: surface unit, TM: transmembrane uni, PPT: polypurine tract.*

Nach dem LTR am 5'-Ende befindet sich die Region der Gruppen-spezifischen Antigene (GAG), welche die Strukturproteine des viralen Nukleus, wie Matrix- (MA), Kapsid- (CA) und Nukleokapsid (NC)-Protein, enthält. In 3'-Richtung weitergehend folgt der Bereich des Polymerase-Komplexes (POL) innerhalb dessen die zur Replikation und Integration wichtigen Enzyme Protease (PRO), Reverse Transkriptase (RT) und Integrase (INT) enthalten sind. Die dritte Region kodiert für das virale Hüllprotein (ENV), das sich aus dem Signalpeptid (SP), der Oberflächen- (SU), sowie der Transmembraneinheit (TM) zusammensetzt. Zudem gibt es HERVs, die akzessorische Gene besitzen, wie *REC* oder *NP9* bei β -Retrovirus-verwandten HERVs (z. B. HERV-K) oder *TAS/BEL1* oder *BET* bei Spumavirus-verwandten HERVs (z. B. HERV-L) (15). Neben den kodierenden Regionen enthält die provirale Sequenz die Primerbindungsstelle (PBS) und den Polypurintrakt (PPT). Der PPT dient als Primer für die Plus-Strang-Synthese der viralen DNA. Die PBS dient als Bindestelle für die zelluläre tRNA des Wirts, die die DNA-Synthese vom Minus-Strang initiiert (16).

Auf die getragene Aminosäure der ersten tRNA, unter Verwendung des Einbuchstabencodes, bezieht sich auch die Nomenklatur der allermeisten ERV, sowie die damit einhergehende Einteilung in Unterfamilien. Wird die Transkription eines ERV mit einer Lysin (K)-gekoppelten tRNA initiiert, so wird die Bezeichnung ERV-K verwendet. Diese Nomenklatur wird häufig kritisiert. Die Hauptgründe dafür sind, dass sie entfernt verwandte Proviren nur aufgrund derselben tRNA-Nutzung innerhalb einer Unterfamilie vereint und sie die Klassifizierung für Proviren mit unvollständigen Informationen über diese Region unmöglich macht bzw. sie mit einer erhöhten Fehlerrate einhergeht (17). Für zusätzliche Verwirrung sorgen willkürlich vergebene Labornamen oder Erweiterungen vieler ERV-Proviren (18). Zur eindeutigen Identifizierung innerhalb der Unterfamilie wird eine Nummer vergeben, z. B. ERV-K5, wobei diese fortlaufend ist, um das Nomenklatur-System möglichst einfach erweitern zu können (19). Die Nummerierung enthält hierbei keine Information über die Position des ERVs im Genom, noch folgt sie einer chronologischen Ordnung ihrer zeitlichen Erst-Veröffentlichung und dient lediglich der eindeutigen Benennung des ERVs, die so kurz wie möglich gehalten sein soll. Trotz der genannten Kritikpunkte, wird diese Nomenklatur von der Forschungsgemeinschaft derzeit weitestgehend akzeptiert. Aufgrund dessen wurde dieses System in der vorliegenden Arbeit, sowie den inbegriffenen Veröffentlichungen verwendet. Es gibt Bestrebungen ein einheitlicheres Nomenklatur-System zu etablieren, welches auch Spezies-übergreifende Verwandtschaftsverhältnisse der ERV eindeutiger erkennbar machen soll (20), so dass die hier

verwendete Bezeichnung der HERVs von denen in zukünftigen Arbeiten abweichen könnte. Zur Minimierung potentieller Unklarheiten und Missverständnisse wurde bei der erstmaligen Nennung eines HERV die Position im Genom, sowie (wenn vorhanden) die Annotation in der Datenbank des *National Center for Biotechnology Information* (NCBI) angegeben.

1.2. Mechanismen zur Stilllegung von HERVs

Wie in Abbildung 2B schematisch dargestellt ist, sind die allermeisten HERV-Proviren durch Punktmutationen, Insertionen und Deletionen beeinträchtigt. Diese Unterbrechungen der ORFs sind auf Inaktivierungs- und *Silencing*-Mechanismen (engl. für Stilllegen) des Wirts, sowie auf Rekombinationsereignisse während der langen Persistenz im Primaten-Genom von bis zu 55 Millionen Jahren, zurückzuführen (21). Im menschlichen Genom sind alle bislang bekannten HERVs von Mutationen in den Bereichen der *RT* und des *ENV* betroffen, welche zum Verlust der Replikationsfähigkeit geführt haben und somit keine Viruspartikel gebildet werden können (22-24). In der Konsequenz gelten HERVs als nicht infektiös, obgleich deren „*copy-and-paste*“-Anreicherung durch Transposition und Amplifikation, sowie die Weitergabe durch Vererbung zu zahlreichen proviralen Kopien in der DNA aller Zellen führte (25).

Die Kontrolle der Chromatinstruktur durch DNA- und Histonmodifizierungen stellt hierbei den epigenetisch wichtigsten Mechanismus dar, welcher die Transkription der HERV bereits während der Embryonalentwicklung streng reguliert und in adulten Geweben in der Regel gänzlich inaktiviert (26, 27). DNA-Methylierungen unterdrücken die Transkription entweder durch direkte Interferenz mit Sequenz-spezifischen Transkriptionsfaktoren oder indirekt über die Rekrutierung von Proteinen mit Methyl-CpG-Bindedomänen, die zur Histon-Deacetylierung führen (28). In embryonalen Stammzellen von Mäusen (mESC) wurde gezeigt, dass in ERVs Tri-Methylierungen von Histon H3 an Lysin 9 (H3K9me3) angereichert sind, welche durch die Methyltransferase SETDB1 gesetzt werden (29). Die Rekrutierung von SETDB1 erfolgt durch Krüppel-assoziierte Box-Domänen-Zinkfingerproteine (KRAB-ZFPs), deren Sequenz-spezifische Bindung über ihre C-terminalen Domänen unter anderem an die PBS-Region der ERV führt (30-33). Als Konsequenz wurde beobachtet, dass ERVs in mESCs und primordialen Keimzellen (PGCs) stärker transkribiert werden, in denen SETDB1 oder KRAB-assoziiertes Protein 1 (KAP1) depletiert waren (34-36). Darüber hinaus ist denkbar, dass die ERV-Transkription über kleine regulatorische RNAs, z. B. *microRNAs* (miRNAs) oder *Piwi-interacting RNAs* (piRNAs), unterdrückt wird. Bisher gibt es nur wenige Hinweise, wie ausreichend hohe Sequenzhomologien, die eine Koinzidenz von miRNAs und HERVs vermuten lassen (37, 38). Das Zusammenspiel von piRNAs und HERV ist weitestgehend ungeklärt. Funktionell könnten die piRNAs bei der gezielten Markierung der HERV eine Rolle spielen, da sie in der Lage sind „körpereigene“ und „fremde“ Gene, wie Transposons, zu unterscheiden. Dies

würde zum direkten Abbau oder zur Stilllegung der HERV über DNA-Methylierungen führen (39, 40). Zusammenfassend sind regulatorische RNAs nach heutigem Verständnis ein eher zweitrangiger bzw. adaptiver Mechanismus zur Stilllegung von HERVs.

Neben epigenetischem *Silencing* stellen antivirale Verteidigungsmechanismen eine zentrale Barriere für die Replikation von Viren, sowie deren Gene dar. Die allermeisten Erkenntnisse über die zelluläre Abwehr von Retroviren sind den Forschungsanstrengungen zur Aufklärung der Replikation des Humanen Immundefizienz Virus Typ 1 (HIV-1) zu verdanken. Zu den wichtigsten Restriktionsfaktoren zählen Tetherin, *Tripartite motif containing 5* (TRIM5), *SAM domain and HD domain-containing protein 1* (SAMHD1), das *Moloney leukemia virus homolog 10* (MOV10)-Protein, sowie die *Apolipoprotein B mRNA-editing enzyme catalytic polypeptide-like 3* (APOBEC3)-Proteine. Für eine ausführliche Beschreibung aller genannten Restriktionsfaktoren sei auf eine Veröffentlichung von Zheng und Kollegen verwiesen (41). Nachfolgend soll lediglich auf die beiden Letzteren näher eingegangen werden. APOBEC3-Proteine sind evolutionär konservierte Cytidin-Desaminasen, die retrovirale einzelsträngige cDNA erkennen, an sie binden und die enthaltenen Cytosine zu Uracilen deaminieren können. In Folge dessen kommt es zu Hypermutationen von G zu A der genomischen DNA oder zum Abbau der viralen DNA (42). Hierbei ist von den sieben APOBEC3-Proteinen, das APOBEC3G am besten charakterisiert. Studien weisen darauf hin, dass APOBEC3G über einen weiteren Deaminase-unabhängigen Mechanismus zur Hemmung der Aktivität des HIV-1 verfügt, wobei APOBEC3G durch Bindung an die virale RNA die Funktion der reversen Transkriptase sterisch behindert (43, 44). Im Hinblick auf HERV sind zwei Mitglieder der Familie HERV-K beschrieben, HERV-K23 (21q21.1, chr21: 19933916-19941962, Alias: HERV-K60) und HERV-K4 (3q21.2, chr3: 125609302-125618416, Alias: HERV-KI), deren Hypermutationen auf die Deaminierungs-Ereignisse durch APOBEC3G zurückgeführt werden (45, 46). Des Weiteren konnte dieselbe Studie zeigen, dass das Einbringen von artifiziellen HERV-K-Proviren, die mittels eines rekonstruierten replikationskompetenten HERV-K-Vektors generiert wurden, durch die Expression verschiedener APOBEC-Proteine (-3A, -3B, -3C, -3F und -3G) *in vitro* unterbunden werden konnte.

MOV10 ist wie APOBEC3 ein Bestandteil zytoplasmatischer Proteinkomplexe zur RNA-Prozessierung, den sogenannten *P-bodies*, welche den Transport viraler Proteine ermöglichen können. Hierbei kann es dazu kommen, dass zelluläre Proteine mit in die Virionen verpackt werden, wie es u.a. für MOV10 in HIV-1-Virionen nachgewiesen werden konnte (47). In MOV10-überexprimierenden Zellen konnte eine Hemmung der Virusproduktion und der Infektiosität von HIV-1 (48, 49), sowie dem Maus-Mammatumovirus (MMTV) beobachtet werden (50). Interessanterweise ist das β -Retrovirus MMTV eng mit proviralen Sequenzen innerhalb der HERV-K-Familie, den humanen MMTV-ähnlichen Elementen (HML), verwandt.

Inwiefern die Expression von MOV10 einen Einfluss auf HERV-rekonstruierte Sequenzen oder *vice versa* hat, ist bislang nicht untersucht.

1.3. Physiologische Bedeutung

Bemerkenswerterweise werden ERV nicht ausschließlich bekämpft, sondern können auch Teil der antiviralen Antwort sein. Für virale ENV-Proteine von Mäusen und Schafen konnte gezeigt werden, dass die endogen exprimierten Genprodukte vor der Infektion mit ihren verwandten exogenen Retroviren schützen (51, 52). Zwar wurde ein derartiger Mechanismus für HERV oder den Menschen im Allgemeinen noch nicht beschrieben, jedoch können HERV durch ihre virale RNA, als auch ihre ENV-Proteine von *Toll-like* Rezeptoren (TLRs) erkannt werden und so die Produktion pro-inflammatorischer Zytokine auslösen (53-55), was einen essentiellen Bestandteil der antiviralen Signalkaskade des angeborenen Immunsystems darstellt (56, 57). Zudem gibt es Hinweise darauf, dass eine ausgelöste Immunantwort gegen HERV-K-Proteine in HIV-infizierten Patient:innen die HIV-1-Replikation und -Expansion beeinträchtigen kann (58-62). Als mögliche Erklärung für die Aktivierung von insbesondere Mitgliedern der HERV-K-Familie (63, 64) wird auf die strukturelle Homologie zwischen den akzessorischen Proteinen des HIV-1 (Rev) und HERV-K (Rec) verwiesen (65, 66). In Summe lassen die vielschichtigen Kontrollmechanismen in Kombination mit der hohen Anzahl an retroviralen Elementen im Genom die Vermutung zu, dass diese regelhafte Domestizierung der HERV sehr wahrscheinlich einen evolutionären Vorteil mit sich gebracht hat. Es ist denkbar, dass insbesondere LTR als Expression-verstärkende oder -unterdrückende Regionen innerhalb oder der Nähe von Genen eine erleichterte bzw. schnellere Regulierung von Signalwegen ermöglichen (67). Als retrovirale Kontrollelemente können LTRs über Entfernungen von mehreren 100 bis 1000 Basenpaaren Einfluss auf benachbarte Gene nehmen (68). Für das Interferon (IFN)-Transkriptionsnetzwerk konnte beispielsweise gezeigt werden, dass HERV-Insertionen in hohem Maße zur Verstärkung IFN-induzierter Gene beitragen und sie damit aktiv an der Regulierung und Entwicklung unseres Immunsystems beteiligt sind (69).

Zudem sind ERV-Proteine, die funktionell bei der Ausbildung der Plazenta und im Verlauf der Schwangerschaft eine bedeutende Rolle spielen, in nahezu allen höheren Säugetieren beschrieben (70). Im Menschen werden diese sogenannten Synzytine von den ENV-Proteinen von HERV-W1 (Synzytin-1, NCBI-Genbank-Nr.: NM_001130925.2) und HERV-FRD1 (Synzytin-2, NCBI-Genbank-Nr.: NM_207582.3) kodiert und fördern die Zell-Zell-Fusion von Zytotrophoblasten zur Bildung des Synzytiotrophoblasten, welcher die maternal-fetale Schnittstelle der Plazenta darstellt (71). Aktuelle Studien gehen davon aus, dass neben den zwei Haupt-Fusogenen HERV-W1 und HERV-FRD1 mindestens sechs weitere ENV-kodierende HERVs (HERV-V1, HERV-V2, HERV-H48-1, HERV-MER34-1, HERV3-1, HERV-K13-1) im Trophoblasten während der

gesamten Schwangerschaftsdauer exprimiert werden (zusammengefasst in (72)). Interessanterweise verfügen viele dieser ERV über eine immunsuppressive Domäne (ISD), die beim Aufbau der mütterlichen Immuntoleranz gegenüber dem Fötus eine Rolle spielen könnte. Die ISD beschreibt einen 17 Aminosäuren-langen Bereich innerhalb der TM-Untereinheit des ENV, welcher innerhalb der HERV-Klassen, sowie deren Verwandten in anderen Säugetieren, hoch konserviert zu sein scheint (73, 74). Für verschiedene ISDs konnte *in vitro* und *in vivo* eine Hemmung der zellulären Immunantwort beobachtet werden (75-80). Hierbei wurde u.a. festgestellt, dass in Gegenwart eines synthetisch hergestellten ISD-Peptids injizierte Tumorzellen zur Ausbildung größerer, solider Tumore in immunkompetenten Mäusen führte, wohingegen sich ohne ISD-Peptid keine oder nur rasch abgestoßene Tumore bildeten (79). Anhand dieser Beispiele wird deutlich, dass HERVs und deren Proteinprodukte starke immunmodulatorische Eigenschaften besitzen, die einer strengen epigenetischen Regulierung bedürfen. Unter unvorteilhaften Bedingungen könnte die unkontrollierte Expression von HERVs zur Entstehung pathologischer Prozesse beitragen, auf die nachfolgend weiter eingegangen werden soll.

1.4. HERVs und ihre mögliche Bedeutung für die Pathogenese von Tumor- und Autoimmunerkrankungen

HERVs werden insbesondere im Zusammenhang mit der Entstehung von Autoimmunität, inflammatorischen Erkrankungen und verschiedenen Tumorentitäten genannt (16, 81-84). Hauptursächlich dafür ist das verstärkte Auftreten von HERV-mRNA z. B. in mononukleären Zellen des peripheren Bluts (PBMCs) oder der Nachweis von anti-HERV-Antikörpern im Serum (85-88), in Rückenmarksflüssigkeit (CSF) (89, 90), sowie pathologisch veränderten Geweben (91-93), in denen HERVs im Normalfall nicht oder nur schwach exprimiert sind. Ob HERVs ursächlich oder nur in Folge des Verlaufs der jeweiligen Erkrankung auftreten, wird bis heute kontrovers diskutiert (23, 94-97). Viele Erkrankungen die im Zusammenhang mit einer möglichen HERV-Beteiligung diskutiert werden, sind in ihrer Pathogenese unvollständig oder nur teilweise aufgeklärt, was eine eindeutige Beantwortung der Frage zusätzlich erschwert. Eine kurze Zusammenfassung der wichtigsten, derzeit bekannten Aspekte zur HERV-Reaktivierung und deren Auswirkung in pathogenen Prozessen soll im Rahmen der vorliegenden Arbeit zur besseren Einordnung und Beurteilung dieser Frage dienen.

Wie in Abschnitt 1.2 näher erläutert, unterliegt die HERV-Expression einer strengen epigenetischen Regulation, wozu Histon-Modifikationen und DNA-Methylierungen gehören. Mittels verschiedener *in vitro*- und *in vivo*-Modelle wurde eine Re-Aktivierung in Folge der Aufhebung dieser Stilllegungsmechanismen beobachtet (32, 34, 35, 98-100). Eine unerwünschte bzw. unkontrollierte Aufhebung der transkriptionellen Repression von HERV-Loci könnte im

Zuge der altersbedingt zunehmenden De-Methylierung des Genoms auftreten (101, 102). Interessanterweise korreliert die Hypo-Methylierung von HERV-Loci mit einer geringeren Überlebenswahrscheinlichkeit, sowie einer im Allgemeinen eher ungünstigen Prognose bei Patient:innen mit Tumorerkrankungen (103, 104), weshalb sie für das erhöhte Krebsrisiko im Alter, sowie als Kennzeichen der zellulären Seneszenz relevant sein könnten (105, 106). Neben der epigenetisch-vermittelten Regulierung können HERVs auch durch äußere Faktoren und Umwelteinflüsse, wie UV- oder ionisierende Strahlung (107, 108), verschiedene chemische Substanzen und Medikamente (109-113), Hormone (114-116), Vitamine (117, 118), Zytokine (119), sowie exogene Viren (120-127) transaktiviert werden.

Die Re-Aktivierung von HERV durch exogene Viren, die zumeist zur Familie der Herpesviren zählen, wird am häufigsten mit der Entstehung von Autoimmunerkrankungen, wie rheumatoider Arthritis (RA) (128-131), systemischem Lupus Erythematoses (SLE) (132-134), amyotropher Lateralsklerose (ALS) (135, 136) und multipler Sklerose (MS) (126, 137, 138) diskutiert. Hierbei konzentrieren sich die Theorien über mögliche Konsequenzen der HERV-Expression auf die starken immunmodulatorischen Eigenschaften von HERV-Proteinen, insbesondere den ENVs. HERV-ENVs könnten über (I) den Mechanismus der molekularen Mimikry (139) oder (II) als Superantigen (120) zur Über-Stimulierung des Immunsystems beitragen. In beiden Fällen ist das Ergebnis die Auslösung einer Entzündungskaskade, die zur Schädigung umliegender Zellen und Gewebe führt (140, 141). Bei der molekularen Mimikry kommt es zur Kreuz-Reaktivität von viralen Proteinen mit wirtseigenen Proteinen, da diese ähnliche Sequenz- oder Struktur motive aufweisen (142). Das bedeutet, dass gegen ein virales Peptid generierte Antikörper und T-Zellen fälschlicherweise durch ein homologes, körpereigenes Protein aktiviert werden und es zum Verlust der Immuntoleranz gegenüber den exprimierenden Zellen kommt (143, 144). Zudem könnten Auto-Antikörper (Auto-AK) gegen HERV-Antigene, die einen Sonderfall des körpereigenen Protein-Pools darstellen, an der resultierenden Immunantwort beteiligt sein (139, 145, 146). Durch unvorteilhafte Polymorphismen an Regionen des Haupt-Histokompatibilitätskomplexes (MHC), welche die Antigenerkennung beeinträchtigen, könnten nicht-optimal bzw. fehlgefaltete HERV-Proteine als „körperfremd“ identifiziert werden, was zur Induktion von Auto-AKs führen und im Allgemeinen die Entstehung von Autoimmunität begünstigen würde (147). Virale oder bakterielle Superantigene können B- und T-Zellen unabhängig von der Spezifität ihrer Antigenrezeptoren aktivieren. Im Normalfall werden aufgenommene Antigene als mindestens 13-17 AS-lange Fragmente in einer Peptidantigen-Furche von MHC-Klasse II-Molekülen präsentiert (148). Anschließend kommt es über die hochvariable Komplementarität-bestimmende Region (CDR, engl. für *complementarity determining region*) am T-Zellrezeptor (TCR) per Schlüssel-Schloss-Prinzip zur Erkennung des Antigens und spezifischen Aktivierung von T-Zellen (149). Superantigene (SAg) binden außerhalb der klassischen Furche an Peptidbereiche von MHC-Klasse II-Molekülen der Antigen-

präsentierenden Zelle (APC) und verbinden diese direkt mit Elementen der variablen Region der β -Kette (V β) des TCR (82, 150, 151). Im Vergleich zur CDR des TCR sind V β -Elemente weniger vielfältig, weshalb SAg mit 5-20 %, anstelle von 0,01-1 %, aller T-Zellen interagieren und zur oligoklonalen Expansion aktivierter T-Zellen führen können (140, 152-154). Für zwei Allel-Varianten von HERV-K18 (NCBI GenBank-Nr.: 100775105), K18.1 (NCBI GenBank-Nr.: AF012336.2) und K18.2 (NCBI GenBank-Nr.: AF333069.1), wobei K18.2 für ein vollständiges ENV kodiert, konnte eine SAg-Aktivität für V β 13+ T-Zellen (TCRBV13) beobachtet werden (120, 155). Diese und weiterführende Arbeiten von Sutkowski *et al.* zeigten eine Transaktivierung des SAg von HERV-K18 durch verschiedene Genprodukte des Epstein-Barr-Virus (EBV) (120, 121) und begründeten sie durch die Lokalisation des HERV-K18 im ersten Intron des EBV-induzierbaren CD48-Gens (156). Das EBV ist der Erreger der infektiösen Mononukleose (IM), auch besser bekannt als Pfeiffersches Drüsenfieber. Nach der Infektion bleibt das Herpesvirus latent im Gedächtnispool der B-Zellen vorhanden und persistiert ein Leben lang im menschlichen Körper ohne Symptome auszulösen (157, 158). Im Falle einer Immunschwäche kann es jedoch zur unkontrollierten Vermehrung von Virus-infizierten B-Zellen kommen und EBV zum Auslöser für lymphoproliferative Störungen werden (159, 160). Zudem wird insbesondere eine altersmäßig verzögerte EBV-Serokonversion als möglicher Risikofaktor bei der Entstehung der MS diskutiert (161-164). Interessanterweise führten stabil mit EBV-immortalisierte B-Lymphozyten (LCL) *in vitro* zur polyklonalen Aktivierung von T-Zellen mit einer ähnlichen Spezifität für die TCRBV13-Elemente (165). Eine einzige Meta-Studie, die Daten von über 5000 Patient:innen mit Typ 1 Diabetes, RA und MS und über 4000 ethnisch-passenden Kontroll-Proband:innen zusammenfasst, konnte ein höheres MS-Risiko für homozygote Träger:innen des HERV-K18.3 Allels, nicht aber für K18.1 oder K18.2, feststellen (166, 167). In Ermangelung weiterer Studien kann über die Relevanz von HERV-K18 in MS lediglich spekuliert werden. Für ENV der HERV-K (HML-2)-Familie, wozu auch das HERV-K18 zählt, wird eine Beteiligung an der Pathogenese der ALS diskutiert, da es im CSF von ALS-Patient:innen beobachtet wurde und die ENV-Expression *in vivo* einen toxischen Effekt auf neuronale Zellen von Mäusen hatte (90). In Bezug auf die Pathogenese der MS ist nach der aktuellen Studienlage ein Mitglied der HERV-W-Familie, das MS-assoziierte Retrovirus (MSRV) von höherer Relevanz (98, 168, 169). Ähnlich zu HERV-K18 ist für das MSRV ENV (NCBI GenBank-Nr.: AF331500.1) der HERV-W-Familie ein pro-inflammatorischer Stimulus mittels einer polyklonalen Aktivierung von T-Zellen im Sinne eines SAg beschrieben worden (170). Nachfolgend ist das Krankheitsbild der MS kurz zusammengefasst, um die Beobachtungen einer möglichen Beteiligung von EBV und HERVs besser einordnen und diskutieren zu können. Die MS ist eine chronisch entzündliche Erkrankung des zentralen Nervensystems (ZNS), die zu fortschreitender Neurodegeneration und neurologischen Behinderungen führt. Aus Daten des *Atlas of MS* der *Multiple Sclerosis International Federation* geht hervor, dass im Jahr 2020 weltweit 2,8 Millionen Menschen von

MS betroffen waren, womit die Prävalenz bei schätzungsweise 36 Fällen pro 100.000 Einwohner lag. Hierbei sind Frauen durchschnittlich doppelt so häufig von MS betroffen, wie Männer (171). Eine erste Episode von neurologischen Symptomen beginnt zumeist zwischen dem 20. und 40. Lebensjahr. Dabei ist die Art der Symptomatik vielfältig und hängt von den betroffenen ZNS-Regionen ab. Frühe Anzeichen können Müdigkeits- und Schwächegefühle, sowie Seh- und Gleichgewichtsstörungen sein, welche durch eine Entzündung oder Demyelinisierung ausgelöst werden. Durch Magnetresonanztomografie (MRT) können Läsionen der weißen Substanz bereits sichtbar sein, bevor die ersten klinischen Symptome auftreten, was auf neurodegenerative Veränderungen in Frühphasen der MS hinweist (172, 173). Weitere pathologische Merkmale der MS sind Demyelinisierung und Schädigung der Oligodendrozyten durch aktivierte selbstreaktive T-Zellen, die über die sich auflösende Blut-Hirn-Schranke aus der Peripherie ins ZNS infiltrieren können (174, 175). Typischerweise lässt sich die MS in drei klinische Subtypen unterteilen: die schubförmig remittierende MS (RRMS), die sekundär progrediente MS (SPMS) und die primär progrediente MS (PPMS), wobei sich die Kennzeichen für entzündliche Prozesse und Neurodegeneration unterschiedlich stark ausprägen. Die akute axonale Schädigung mit aktiven Hirnläsionen der grauen und weißen Materie ist in den frühen Stadien von RRMS und SPMS am stärksten ausgeprägt, während der Abbau von Axonen bei PPMS konstanter über den Krankheitsverlauf (176) und der zunehmende Grad der Behinderung unabhängig von distinkten Schüben ist (177). Als wichtigste Beobachtungen im Zusammenhang mit MS soll der Nachweis von HERV-W/MSRV ENV in aktiven Hirnläsionen von Patient:innen (91, 178, 179) und der negative Einfluss der Expression von HERV-W/MSRV ENV *in vitro* auf die Differenzierung von Oligodendrozyten-Vorläuferzellen (55, 180), sowie die Aktivierung eines pro-inflammatorischen Mikroglia-Phänotyps (181) genannt werden. Zum aktuellen Zeitpunkt konnte eine randomisierte, klinische Studie mit dem monoklonalen Antikörper Temelimab gegen besagtes HERV-W/MSRV ENV nach Abschluss der Phase 2b keine signifikante Verringerung der MS-Läsionsherde oder der Schubrate erzielen (182).

Wie im Abschnitt 1.3 erwähnt, können HERV neben einer immunstimulierenden, auch eine immunsupprimierende Wirkung haben (78, 183). Die Umgehung der Überwachung durch das Immunsystem von Zellen mit einem entarteten Selbsterneuerungs-, Proliferation- und (De-) Differenzierungspotential ist ein wichtiger Mechanismus bei der Entstehung von Tumoren und Metastasen (184, 185). Diese Krebszellen mit Stammzell-ähnlichen Eigenschaften (CSCs, engl. *cancer-like stem cells*) weisen durch die Aufrechterhaltung eines undifferenzierten Zellstadiums eine hohe Plastizität aus, was bedeutet, dass sie sehr anpassungsfähig gegenüber äußeren Einflüssen und Stressbedingungen, wie z. B. Radio-, Immun- oder Chemotherapie sind (186-191). Interessanterweise könnte eine gesteigerte HERV-Expression die Bildung dieser CSC-Subpopulationen durch die Regulierung der Zell-Differenzierung begünstigen, wie sie in Melanom-Zelllinien bereits beobachtet wurde (192). Ob die Bildung einer Stammzell-ähnlichen

HERV-K/CD133-positiven Population in Folge Medium-induzierter Veränderungen der Mikroumgebung auch bei anderen Tumoren aus der Neuralleiste auftritt, wie beispielsweise dem Neuroblastom (NB), ist jedoch bislang ungeklärt. Das NB ist der häufigste solide Tumor außerhalb des ZNS bei Säuglingen und Kindern, welcher sich durch seine Heterogenität auszeichnet (193). NB-Tumore der Hochrisiko-Stadien 3 und 4 (*International Neuroblastoma Staging System*, INSS) sind häufig durch Chemotherapieversagen und Nichtansprechen auf Immuntherapie mit Checkpunkt-Inhibitoren gekennzeichnet, weshalb die Patient:innen eine schlechte Prognose mit einer niedrigen Überlebensrate haben (194-196). Ein Zusammenhang von HERV-Expressionsaktivität, Pluripotenz und einer gesteigerten Immuntoleranz kann auch im Kontext der Embryonalentwicklung (35, 99) und Plazentagenese (74) beobachtet werden. Untersuchungen mit Keimzelltumor-Zelllinien (GCTs, engl. *germ cell tumors*) konnten zeigen, dass die Expression von HERV-K (HML-2)-Transkripten invers mit dem Differenzierungsstadium und der Expression von Pluripotenzmarkern, wie *OCT4* und *NANOG*, korreliert (100). Mit z. T. relativ kurzen Integrationszeiten von 100.000-500.000 Jahren, zählen einige Mitglieder der HERV-K (HML-2)-Familie zu den 1,5 % der HERVs mit vollständigen ORFs für alle viralen Gene (197). In der Konsequenz könnten in undifferenzierten Zellstadien exprimierte HERV-K-Antigene, wie z. B. HERV-K ENV und dessen Splicevarianten *REC* und *NP9*, die Bildung eines tumorfördernden Mikromilieus begünstigen (198, 199). Erste Studien mit HERV-K ENV-spezifischen chimären Antigenrezeptor (CAR)-T-Zellen konnten bereits eine Reduzierung des Tumorwachstums und der Metastasierung in andere Organe in Xenograft-Maus-Modellen von Brustkrebs- (200) und Melanomzellen (201) beobachten und damit einen potentiellen therapeutischen Einsatz von HERV-Antikörpern bzw. HERV-CAR-Ts demonstrieren.

1.5. Zielstellung

Im Verlauf der Pathogenese von Tumor- oder Autoimmunerkrankungen exprimierte HERV-Transkripte und -Proteine weisen auf ihre mögliche Relevanz als diagnostische oder therapeutische Zielstrukturen hin. Durch zahlreiche homologe HERV-Kopien derselben Familie und z. T. unspezifische Angaben in der Literatur (202, 203), ist die Auswahl geeigneter HERVs erschwert. Ein Ziel dieser Arbeit soll daher die Identifizierung distinkter HERV-Loci sein, die potentiell als Biomarker oder im Falle vollständiger ORFs, als Antigene geeignet wären.

Für das EBV wird seit Langem eine bedeutsame Rolle in der Pathogenese der MS vermutet. Kürzlich konnten weitere, überzeugende Hinweise für einen kausalen Zusammenhang zwischen MS und EBV dargelegt werden (164). Für einige HERV-Loci wurde eine Transaktivierung durch EBV bereits impliziert. Im Rahmen dieser Arbeit soll die Transkription von HERVs in EBV-infizierten Zellen im Kontext der MS untersucht werden. Zu diesem Zweck soll die EBV-

spezifische Eigenschaft der latenten Infektion und Immortalisierung von B-Zellen *in vitro* genutzt werden, um stabile Zelllinien aus PBMC-Isolaten von MS-Patient:innen (MSLCL) und gesunden Kontrollen (coLCL) zu erzeugen. Die benötigten PBMCs sollen aus einem Teil des Vollbluts isoliert werden, welches im Rahmen der routinemäßigen Diagnostik seitens der neurologischen Ambulanzen des Universitätsklinikums Halle (Saale) und des Martha-Maria Klinikums in Halle-Dörlau abgenommen wird. Diese MSLCL und coLCL sollen zur Identifizierung differenziell exprimierter Gene und HERVs mittels Transkriptomsequenzierung (RNAseq) und quantitativer *real-time* Polymerasekettenreaktion (qRT-PCR) verwendet werden. Aufgrund der geringen Anzahl annotierter HERV-Loci in der menschlichen Transkriptomversion hg38/GRCh38 sollen zusätzlich Sequenzanalysen mit einem in der Arbeitsgruppe entwickelten Virus-Transkriptom durchgeführt werden. Neben nicht menschlichen ERVs und exogenen Virussequenzen enthält dieses Virus-Transkriptom eine Sammlung von über 100 HERV-Sequenzen aus 14 HERV-Familien, wobei die Auswahl vor allem HERVs mit vollständigen ORFs für einen oder ggf. mehrere kodierende Bereiche von *GAG*, *POL*, *ENV* umfasst (204). Zudem sollen mögliche Korrelationen ausgewählter EBV- und HERV-Transkripte und klinisch-pathologischen Merkmalen der Patient:innen untersucht werden. Deshalb werden u. a. Alter und Geschlecht, sowie klinische Parameter, wie die Anzahl der Schübe in den letzten 2 Jahren und der *Expanded Disability Status Scale* (EDSS), als auch die aktuelle Medikation der Proband:innen in pseudonymisierten Fragebögen erfasst und ausgewertet.

Solide Tumore mit einer hohen Heterogenität sind oftmals durch eine erhöhte Therapieresistenz und Rückfallrate gekennzeichnet (205, 206). Eine mögliche Strategie zur Steigerung der Chancen einer langfristigen Heilung ist die gezielte Zerstörung der CSCs (207). Studien legen nahe, dass HERVs an der Aufrechterhaltung eines undifferenzierten Zellstadiums und damit der Entstehung der CSC-Nische beteiligt sein könnten (100). Insbesondere bei Melanom-Zelllinien konnte eine Aktivierung von HERV-K108 *ENV* in Folge einer Medium-induzierten Veränderungen in Verbindung mit der Ausbildung einer CD133-positiven Stammzellpopulation beobachtet werden (192). Unklar ist, ob eine derartige HERV-Aktivierung auch in anderen Entitäten von entarteten Zellen der Neuralleiste auftritt und ggf. weitere HERV-Loci verstärkt transkribiert werden. Hierzu sollen differenzielle Expressionsanalysen unter Verwendung unseres Virus-Transkriptoms von NB-Zelllinien vor und nach Inkubation in Stammzell-Medium durchgeführt werden. Zudem soll die Analyse bekannter NB-Malignitätsmarker zur Charakterisierung des Phänotyps der NB-Zellen beitragen.

Um die biologische Rolle und das pathogenetische Risiko von insbesondere HERV-ENVs zu verstehen, ist eine funktionelle Charakterisierung erforderlich. Im Rahmen dieser Arbeit soll die Expression von drei ENVs, sowie deren Reifung und Lokalisierung in verschiedenen Säugerzelllinien analysiert werden. Zudem sollen mögliche Gründe für die beobachtete, limitierte

Expression von nativen HERV ENVs untersucht werden. Als biologische aktivste HERV-Familie mit z. T. vollständig erhaltenen ORFs für alle viralen Gene stellen die HERV-K (HML-2)-Mitglieder geeignete Kandidaten für eine funktionelle Charakterisierung dar. HERV-K18 (1q23.3; NCBI GenBank-Nr.: AF333069.1) und dessen ENV werden mutmaßlich superantigene Eigenschaften, sowie eine putative Beteiligung in der Entstehung von Autoimmunerkrankungen zugeschrieben, weshalb es ein interessantes Zielprotein für weitere Untersuchungen darstellt. Das HERV-K113 (19p13.11; NCBI-Genbank-Nr.: NC_022518.1) ist durch seine kurze Integrationszeit ein geeigneter Kandidat. Als eines der best-erhaltenen HERV im menschlichen Genom und einer noch unvollständigen, weltweiten „Durchseuchung“, sollte dessen native Expression und Sequenzintegrität durch den evolutionären Selektionsdruck noch am wenigsten beeinträchtigt sein. Mit Hilfe artifizierlicher Varianten des HERV-K113 ENV soll eine suboptimale Kodon-Verwendung als möglicher Faktor der limitierten Expression nativer ENV untersucht werden. Zuletzt wurde das ENV von HERV-Fc1 (Xq21.33; NCBI-Genbank-Nr.: XM_011531085.2) ausgewählt, welches in jüngerer Zeit mit Autoimmunkrankheiten in Verbindung gebracht wurde. Mit sechs bekannten Proviren hat die HERV-Fc-Familie zudem eine begrenzte Verbreitung im menschlichen Genom (208), was sie als potentielle Zielstruktur für einen therapeutischen Antikörper interessant macht.

2. Kumulativer Teil

Im Folgenden sind drei Publikationen aufgeführt, welche als *Research Articles* dem anerkannten *Peer Review* Verfahren unterzogen und bei den nachfolgend aufgeführten Fachzeitschriften veröffentlicht wurden. Die Publikationen bilden den Schwerpunkt der im Rahmen der Promotion ausgeführten Experimente und fassen die erzielten Ergebnisse zusammen.

Tabelle 1: Übersicht zu den allgemeinen Daten der Fachzeitschriften.

Titel	<i>Impact Factor</i> (Jahr der Veröffentlichung)	<i>5-year Impact Factor</i> (2022)	Herausgeber
<i>International Journal of Molecular Sciences (IJMS)</i>	5,924 (2020)	6,2	MDPI, St Alban-Anlage 66, CH-4052 Basel, Switzerland
<i>Frontiers in Oncology (Front Oncol)</i>	5,738 (2021)	5,2	FRONTIERS MEDIA SA, Avenue du tribunal federal 34, CH-1015 Lausanne, Switzerland
<i>Cells</i>	6,0 (2022)	6,7	MDPI, St Alban-Anlage 66, CH-4052 Basel, Switzerland

Die Publikationen stellen verschiedene Aspekte der untersuchten Aktivierung endogener Retroviren in der Pathogenese von Tumor- und Autoimmunerkrankungen vor.

2.1. Formation of HERV-K and HERV-Fc1 Envelope Family Members is Suppressed on Transcriptional and Translational Level

2.1.1. Zusammenfassung

Im Lauf der Evolution wurden ins Genom integrierte Sequenzen retroviralen Ursprungs, die so genannten HERVs, weitestgehend mittels Mutation oder Rekombination inaktiviert. Es sind einige HERVs bekannt, die offene Leserahmen in Protein-kodierenden Regionen besitzen. Da die Folgen aktivierter proviraler Sequenzen im menschlichen Körper weitgehend unerforscht sind, wurden in der vorliegenden Studie ausgewählte HERV-ENV, die mit entzündlichen Erkrankungen des Immunsystems in Verbindung gebracht werden, nämlich HERV-K18, HERV-K113 und HERV-Fc1, untersucht. Die Bildung von glykosylierten Hüllproteinen wurde in verschiedenen Säugerzelllinien nachgewiesen. Allerdings schien die Proteinreifung unvollständig zu sein, da kein Transport zur Plasmamembran beobachtet wurde. Stattdessen verblieben die Proteine im endoplasmatischen Retikulum (ER), wo sie die Expression von Genen induzierten, die an der Signalkaskade fehlgefalteter Proteine (*unfolded protein response*, UPR) beteiligt sind, wie *HSPA5* und *sXBP1*. Darüber hinaus wurde die niedrige Expression der nativen Hüllproteine durch den Einsatz Kodon-optimierter ENV-Varianten erhöht. Zellfreie Expressionssysteme zeigten, dass die Kodon-Optimierung sowohl die Transkriptions-, als auch die Translationsebene beeinflusste. Mittels verschiedener artifizieller Kodon-optimierter Varianten des HERV-K113 ENV konnte der Einfluss seltener tRNA-Pools in bestimmten Zelllinien untersucht werden. Die mRNA-Sekundärstruktur könnte hierbei auch eine wichtige Rolle bei der Translation der getesteten viralen ENV spielen. Zusammenfassend lässt sich sagen, dass die Bildung bestimmter HERV-Proteine anhand ihrer im Genom vorliegenden Sequenz grundsätzlich möglich ist. Ihre vollständige Reifung und damit ihre volle biologische Aktivität scheint jedoch von zusätzlichen Faktoren abzuhängen, die möglicherweise krankheitsspezifisch sind und in weiterführenden Studien aufgeklärt werden müssen.

2.1.2. Darlegung des Eigenanteils, Manuskript und Zitierung

Im Folgenden ist der experimentelle und schriftliche Eigenanteil aller Autoren prozentual angegeben und die Beteiligung mehrerer Personen an der Veröffentlichung durch einen Betreuer bestätigt.

Publikation I:

Gröger, V., **Wieland, L.**, Naumann, M., Meinecke, A. C., Meinhardt, B., Rossner, S., Ihling, C., Emmer, A., Staeger, M. S., & Cynis, H. (2020). Formation of HERV-K and HERV-Fc1 Envelope Family Members is Suppressed on Transcriptional and Translational Level. *International journal of molecular sciences*, 21(21), 7855. <https://doi.org/10.3390/ijms21217855>

Tabelle 2: Übersicht zu den Beiträgen aller Autoren der Publikation I.

	Entwurf (Design)	Umsetzung (Implementation)	Auswertung (Analysis)	Schreiben (Writing)
Gröger, V.	5 %	30 %	30 %	30 %
Wieland, L.		30 %	35 %	30 %
Naumann, M.		10 %		
Meinecke, A.		10 %		
Meinhardt, B.		5 %		
Rossner, S.	15 %			
Ihling, C.		10 %		
Emmer, A.	20 %			
Staeger, M. S.	25 %	5 %	15 %	20 %
Cynis, H.	35 %		20 %	20 %

Datum: 15.03.2024



Lisa Wieland

Dr. med. Alexander Emmer

2.1.3. Bestätigung des Betreuers der Dissertation von Frau Lisa Wieland

Hiermit bestätige ich als Betreuer der o. g. Dissertation, dass die gemeinsame Arbeit mehrerer Personen an der Arbeit durch den Forschungsgegenstand gerechtfertigt ist.

Mit freundlichen Grüßen,



Dr. med. Alexander Emmer

Datum: 15.03.2024

Nachfolgend sind die Publikation und die supplementären Daten aufgeführt.



Article

Formation of HERV-K and HERV-Fc1 Envelope Family Members is Suppressed on Transcriptional and Translational Level

Victoria Gröger ^{1,†}, Lisa Wieland ^{2,3,†} , Marcel Naumann ¹, Ann-Christin Meinecke ¹, Beate Meinhardt ^{2,3}, Steffen Rossner ⁴, Christian Ihling ⁵, Alexander Emmer ², Martin S. Staeger ^{3,*} and Holger Cynis ^{1,*}

¹ Department of Drug Design and Target Validation, Fraunhofer Institute for Cell Therapy and Immunology, Weinbergweg 22, 06120 Halle, Germany; victoria.groeger@izi.fraunhofer.de (V.G.); marcel.naumann@izi.fraunhofer.de (M.N.); ann-christin.meinecke@web.de (A.-C.M.)

² Department of Neurology, Medical Faculty, Martin Luther University Halle-Wittenberg, Ernst-Grube-Str. 40, 06097 Halle, Germany; lisa.wieland@uk-halle.de (L.W.); beate.meinhardt@uk-halle.de (B.M.); alexander.emmer@uk-halle.de (A.E.)

³ Department of Surgical and Conservative Pediatrics and Adolescent Medicine, Medical Faculty, Martin Luther University Halle-Wittenberg, Ernst-Grube-Str. 40, 06097 Halle, Germany

⁴ Paul Flechsig Institute for Brain Research, Leipzig University, Liebigstraße 19, 04103 Leipzig, Germany; Steffen.Rossner@medizin.uni-leipzig.de

⁵ Department of Pharmaceutical Chemistry & Bioanalytics, Institute of Pharmacy, Martin Luther University Halle-Wittenberg, Charles Tanford Protein Center, Kurt-Mothes-Str. 3a, 06120 Halle, Germany; christian.ihling@pharmazie.uni-halle.de

* Correspondence: martin.staeger@uk-halle.de (M.S.S.); holger.cynis@izi.fraunhofer.de (H.C.); Tel.: +49-345-5577280 (M.S.S.); +49-345-13142835 (H.C.); Fax: +49-345-5577275 (M.S.S.); +49-345-13142801 (H.C.)

† These authors contributed equally to this study.

Received: 4 September 2020; Accepted: 21 October 2020; Published: 23 October 2020



Abstract: The human genome comprises 8% sequences of retroviral origin, so-called human endogenous retroviruses (HERVs). Most of these proviral sequences are defective, but some possess open reading frames. They can lead to the formation of viral transcripts, when activated by intrinsic and extrinsic factors. HERVs are thought to play a pathological role in inflammatory diseases and cancer. Since the consequences of activated proviral sequences in the human body are largely unexplored, selected envelope proteins of human endogenous retroviruses associated with inflammatory diseases, namely HERV-K18, HERV-K113, and HERV-Fc1, were investigated in the present study. A formation of glycosylated envelope proteins was demonstrated in different mammalian cell lines. Nevertheless, protein maturation seemed to be incomplete as no transport to the plasma membrane was observed. Instead, the proteins remained in the ER where they induced the expression of genes involved in unfolded protein response, such as *HSPA5* and *sXBP1*. Furthermore, low expression levels of native envelope proteins were increased by codon optimization. Cell-free expression systems showed that both the transcriptional and translational level is affected. By generating different codon-optimized variants of HERV-K113 envelope, the influence of single rare t-RNA pools in certain cell lines was demonstrated. The mRNA secondary structure also appears to play an important role in the translation of the tested viral envelope proteins. In summary, the formation of certain HERV proteins is basically possible. However, their complete maturation and thus full biologic activity seems to depend on additional factors that might be disease-specific and await elucidation in the future.

Keywords: human endogenous retroviruses; expression; codon usage; transcription; translation

1. Introduction

In the course of evolution, a large number of retroviral elements were incorporated into the genomes of vertebrates. At present, the human genome consists of up to 8% of such transposable elements (TE) resulting from infections with ancient retroviruses, which circulated millions of years ago [1]. Since the integration occurred by infection of the germ line, the resulting provirus of the so-called endogenous retroviruses (ERV) can be transmitted vertically as a host allele [2,3]. The retroviral provirus typically possesses three coding regions: the group-specific antigen (*GAG*) gene, which provides the capsid- and matrix proteins of the nucleus, the polymerase (*POL*) gene encoding the viral enzymes for reverse transcription and integration into the host genome, and the envelope (*ENV*) gene, encoding the viral glycoproteins on the virus surface important for fusion with the host cell membrane during infection. Additionally, these regions are flanked on either side by long terminal repeats (LTR) that regulate transcription of enclosed viral genes [4].

Due to their long persistence in the genome, the proviruses were subject to selective pressure, which resulted in inactivation of most viral sequences by (I) disruption of open reading frames (ORFs) by mutations or (II) complete loss of all viral genes by recombination between flanking LTR sequences. As a consequence, nearly all human ERV (HERV) show defective protein products [5]. Nevertheless, there are few HERV with almost complete ORFs, which are able to form functional proteins. Under normal conditions proviral sequences are epigenetically silenced, but disease or developmental stages can activate transcription. As popular examples, the envelope proteins (*ENV*) of the HERV-W family, e.g., syncytin-1 and the HERV-FRD family, e.g., syncytin-2, are important during pregnancy and embryogenesis [6,7].

Besides a beneficial effect, some HERV *ENV* are thought to contribute to diseases including cancer and autoimmune disorders [8–12]. Transcriptional activation of retroviral elements in pathologic tissues of soft tissue sarcoma patients or elevated antibody titers against viral proteins in the sera of patients with autoimmune rheumatic diseases were observed [13–15]. Little is known about the protein expression of *ENV* in mammals. For understanding the biological role and the pathogenetic risk of *ENV*, a functional characterization including analysis of maturation, localization and limitations of native *ENV* expression is necessary. For this purpose, we investigated in this study the expression of three selected *ENV* possessing intact ORFs in the human genome and a known correlation to diseases, such as Multiple Sclerosis [16–19].

We focused on two members of *ENV* from the HERV-K family: HERV-K18 *ENV* and HERV-K113 *ENV*. Additionally, one member from the HERV-H/F family, HERV-Fc1 *ENV*, was investigated. HERV-K *ENV* belong to the human endogenous mouse mammary tumor virus-like (HML2)-subset of the HERV-K family, which comprises the most complete and biological active members among all HERVs [20–22]. The studied HERV-K18 on chromosome 1 is a locus of 9235 bp with three allelic variants. The variants K18.1 and K18.2 are most common in the Caucasian population ($\approx 90\%$), but only K18.2 encodes a full-length *ENV* of 553 amino acids [23–25]. Interestingly, the K18.2 allele (NCBI accession no.: AF333069.1) is located in the first intron of the *CD48* gene, which can be transactivated by Epstein–Barr virus (EBV) and might promote the expression of *ENV* with putative super-antigenic properties [18,25–27]. The third allelic variant, K18.3, has been identified as risk factor for Multiple Sclerosis [28].

HERV-K113 is located on chromosome 19p12 (NCBI accession no.: NC_022518.1). Despite its short integration time, it possesses mutations in the reverse transcriptase gene, which leads to the loss of replication competency of the provirus [29]. Interestingly, the fixation of HERV-K113 in the human population is still ongoing. Today the provirus is present in about 30% of humans and it is one of few retroviruses with known ORFs for all viral proteins [30]. In addition, we studied HERV-Fc1 *ENV*, which is located on the X chromosome (NCBI accession no.: XM_011531085.2). HERV-Fc1 contains a full-length *ENV* open reading frame. In addition to small in-frame deletions and insertions, the *GAG* and *POL* regions contain stop codons. The stop codon in *GAG* is located near the 3' end [31]. *POL* contains two stop codons and frame shifts. Compared with HERV-H consensus sequences [32] translation of

this sequence would result in a protein with a large C terminal truncation. The HERV-Fc1 locus seems to be genetically associated with Multiple Sclerosis (MS) [19,33,34]. Unlike the HERV-K members, the HERV-Fc family has a very limited expansion with only a few proviruses in the human genome [35].

In the present study, we analyzed the expression of all three *ENV* in several mammalian cell lines with a closer view on protein localization and protein maturation. Our second aim was to examine reasons for the observed limited protein synthesis efficacy of native *ENV*. Therefore, we investigated rare codon bias as a factor for the limited protein biosynthesis of the native proteins of HERV-K113 in mammalian cell lines and in a cell-free system.

2. Results

2.1. ORFs of HERV-K18, HERV-K113, and HERV-Fc1 form Envelope Proteins

The expression of three different HERV *ENV* (Fc1, K18, K113, Figure 1a) was analyzed in transfected HEK293 cells. The expression of wild type (WT) *ENV* sequences as found in the human reference genome led to barely detectable amounts of protein for HERV-Fc1 (Figure 1b,c) and HERV-K113 (Figure 1b,d) despite application of equal protein amounts, exemplarily shown for HERV-K113 (Supplementary Figure S1). In addition, no protein could be detected for WT HERV-K18. However, when codon-optimized variants were expressed under the same conditions, all envelope proteins were readily detected (Figure 1b).

This result was corroborated by LC-MS/MS analysis of HERV-K113 and HERV-Fc1 expressing HEK293 cells. The sequence coverage, which is to a limited extent indicative for the protein concentration, coincided well with the Western blot detection of HERV proteins (Table 1, Supplementary Figure S2). The highest sequence coverage was observed for HERV proteins identified in cells with a codon-optimized protein sequence (coFc1 and coK113, Supplementary Figure S2). In cells that expressed the WT sequences, either the identified HERV protein showed only a reduced sequence coverage (K113, Supplementary Figure S2) or no HERV protein was detected at all (Fc1) by this method. In this regard, the low intracellular abundance was not due to secretion of the proteins from cells. An antibody specifically binding to the surface unit (SU) of HERV-K did not detect K18 and K113 in cell culture supernatants up to 48 h post-transfection but corroborated the intracellular accumulation of the tested proteins (Supplementary Figure S3).

Table 1. Sequence coverage and proteolytic peptides identified by LC-MS/MS for expressed HERV proteins and the ER chaperone BiP.

Sample	Protein	Sequence Coverage (%)	Proteolytic Peptides #
Control	K113, Fc1 envelope proteins	n.d.	n.d.
	ER chaperone BiP	20	7
K113	K113 envelope protein	4	3
	ER chaperone BiP	47	31
coK113	K113 envelope protein	20	10
	ER chaperone BiP	48	27
Fc1	Fc1 envelope protein	n.d.	n.d.
	ER chaperone BiP	53	36
coFc1	Fc1 envelope protein	39	25
	ER chaperone BiP	54	38

BiP: binding immunoglobulin protein, n.d.: not detected.

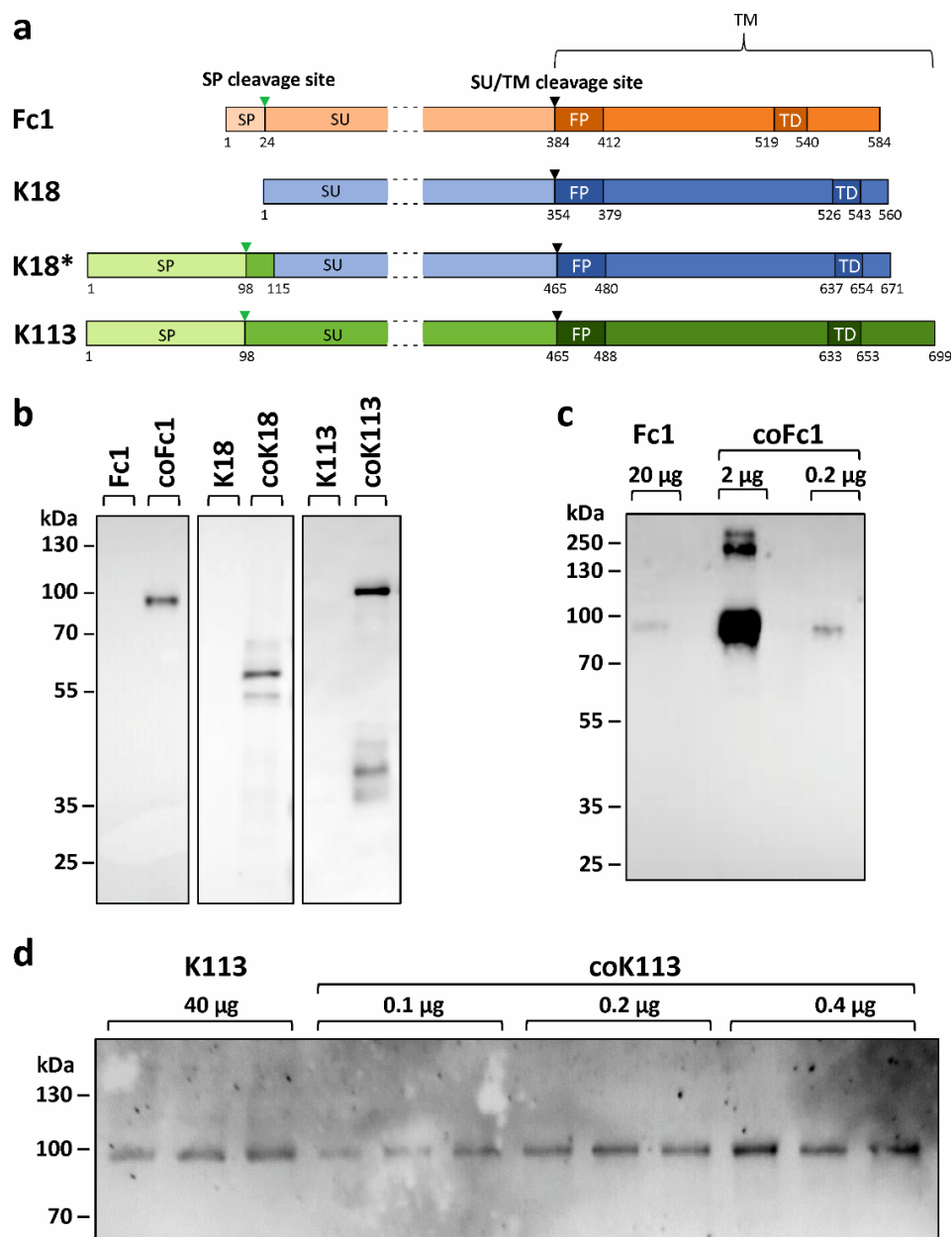


Figure 1. Expression and quantification of HERV envelope proteins in HEK293 cells. (a) Schematic representation of expressed HERV ENV. The pro-peptides are processed co- and post-translationally: The signal peptide (SP) is cleaved by signal peptidases (green triangle). The surface unit (SU) is separated from the transmembrane unit (TM) by furin-like proteases at a highly conserved consensus sequence (black triangle). The fusion peptide (FP) and the transmembrane domain (TD) are particularly hydrophobic regions within the TM. The chimeric K18* is composed of the signal peptide and another 17 amino acids of K113 plus amino acids 5–560 from K18. The numbers correspond to the amino acid positions. The SU is not shown to scale, but shortened. (b) Influence of codon optimization on protein biosynthesis of HERV ENV. Cell lysates were analyzed by Western blot 24 h after transient transfection of HEK293 cells with expression plasmids containing either the WT sequence or codon-optimized (co) sequences of the envelope proteins of HERV-Fc1, -K18, and -K113. Each lane was loaded with 20 μ g total protein. (c,d) Representative Western blots used for densitometric quantification of expression increase caused by codon-optimization. The amount of total protein load is indicated for each lane. Representative loading controls are presented as Supplementary Figure S1. The following antibodies were used: Primary antibodies: anti-FLAG 1:1000 (Fc1), anti-HERV-K TM 1:1000 (K18, K113). Secondary antibodies: anti-rabbit IgG-HRP 1:2000, anti-mouse IgG-HRP 1:2000.

For quantification of the increase in protein synthesis resulting from codon-optimization, different total protein amounts were applied to SDS-PAGE. This was necessary to enable visualization of both variants (WT vs. codon-optimized) on the same blot. Densitometric analysis of resulting proteins revealed a 150-fold (K113) or 290-fold (Fc1) increase in ENV levels caused by codon-optimization (Figure 1c,d and Supplementary Figure S4). A fold-change for K18 could not be determined, since the WT variant could not be identified by Western blot.

2.2. Analysis of Post-Translational Processing of HERV ENV

Protein maturation of HERV ENV was studied in terms of N-glycosylation, cleavage of precursor proteins, and oligomerization (Figure 2). The precursors for all HERV ENV investigated in this study were detected by Western blot analysis (Figures 1b and 2a).

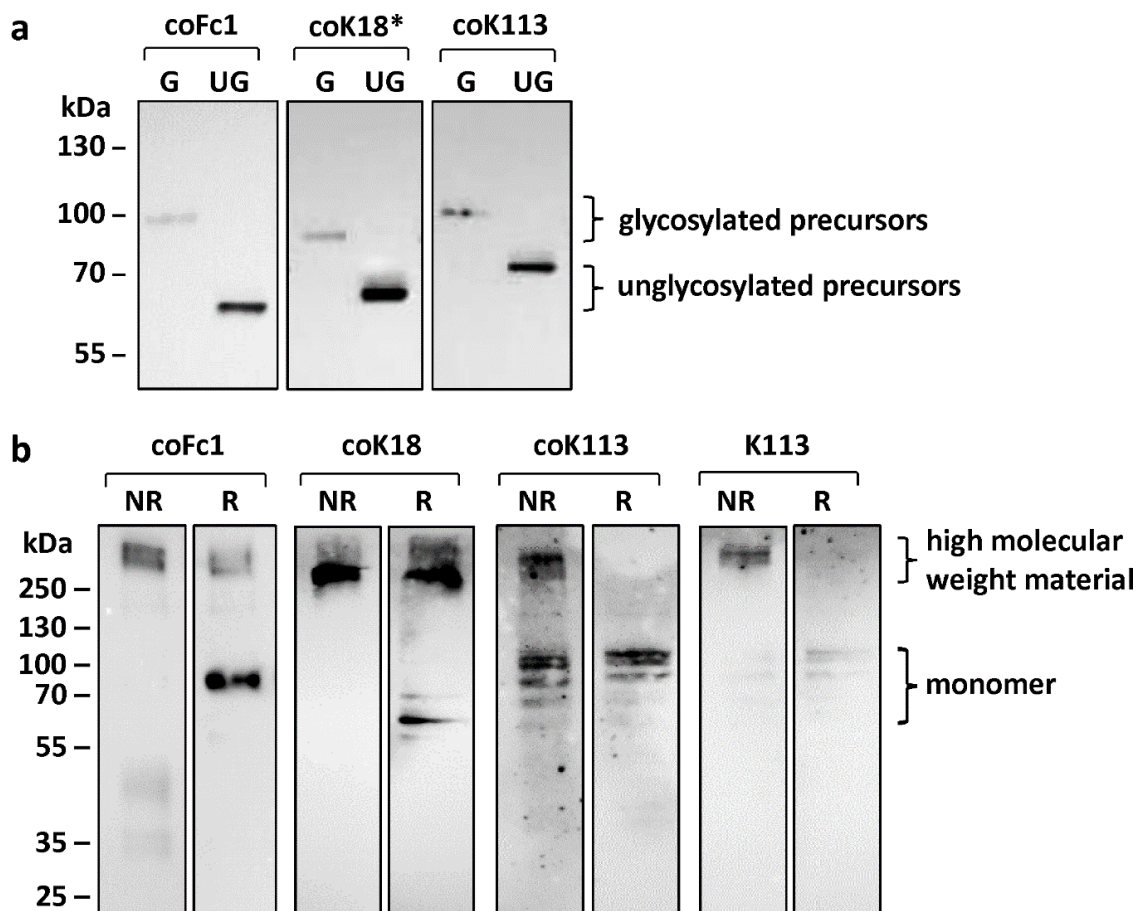


Figure 2. Western blot analysis for characterization of post-translational modifications of HERV ENV. (a) Detection of glycosylated (G) or unglycosylated (UG) envelope proteins in cell lysates of transiently transfected HEK293 cells. Notice the shift in protein size after deglycosylation by PNGase F. (b) Higher molecular weight material resulting from expression of HERV ENV precursors via intramolecular disulfide bridges analyzed by comparison of non-reducing (NR) and reducing (R) sample buffer conditions. The monomers are only visible when reducing (R) sample buffer was used. Either anti-FLAG antibody (coFc1) or anti-HERV-K SU HERM1821-5 antibody (coK18*, coK113) was used for detection of ENV.

The envelope precursors of HERV-Fc1, HERV-K18*, and HERV-K113 are glycosylated as shown by treatment of cell lysates from transfected HEK293 cells with the peptide N-glycosidase (PNGase F) (Figure 2a). The protein size after de-glycosylation corresponded to the theoretical molecular mass of

ENV precursors (Fc1: 64 kDa, K113: 80 kDa, K18*: 66 kDa,). Hence, it can be concluded that these ENV are post-translationally glycosylated in the ER.

For HERV-K18, the size of the detected ENV in HEK293 cell lysates corresponded to the theoretical molecular mass of 63 kDa. In addition, treatment with PNGase F did not lead to a change in the molecular mass of the protein (Supplementary Figure S5). In contrast, HERV-K18*, which has a reconstructed signal peptide, was glycosylated. Thus, a defective signal peptide in HERV-K18 ENV prevents glycosylation due to an altered subcellular localization.

Furthermore, retroviral envelope proteins are synthesized as precursors, which are cleaved by proprotein convertases such as furin into two functional subunits (SU and TM). For all HERV ENV investigated in this study, the precursor was detected by Western blot analysis (Figures 1b and 2a). For coFc1 and coK18 no cleavage of the precursor protein into SU and TM was detected. However, for coK113 we were able to visualize the appearance of the TM as detected by the TM-specific HERV-K antibody (Figure 1b, Supplementary Figure S5b). Here, additional proteins with a molecular mass of 35–40 kDa were observed. These correspond to the glycosylated TM, since after de-glycosylation proteins with the theoretical molecular mass of TM were detectable (Supplementary Figure S5b). Furthermore, protein detected by a corresponding SU-specific HERV-K antibody in lysates of HERV-K113 expressing HEK293 cells corroborated the at least partial processing of the HERV-K113 precursor into the SU and TM subunit (Supplementary Figure S5b,c). Therefore, it can be assumed that the precursor of HERV-K113 ENV is processed into TM and SU to some extent. However, the most abundant form of the envelope proteins appears to be the unprocessed precursor.

In addition, functional retroviral envelope proteins form oligomers at the plasma membrane. For all tested HERV ENV it could be shown that the expressed envelope proteins are present as an oligomer within the cell after analyzing cell lysates of transfected HEK293 cells under non-reducing (NR) conditions (Figure 2b). By omitting the reducing agent, possible disulfide bridges remain intact. Furthermore, in the non-reduced sample, the monomer did not appear, which suggests that it forms disulfide bonds with other monomers. The high-molecular double band found in these samples may therefore likely be trimers or tetramers. In contrast, under reducing conditions mainly the monomers are visible (Figure 2b), except for coFc1 and coK18. For coFc1 the oligomer band is weaker under reducing conditions but did not disappear. In addition, the oligomer band for coK18 was stable and only minor amounts of monomer were formed suggesting aggregation of the protein in the cytosol.

2.3. Analyzed HERV Envelope Proteins are not Transported to the Plasma Membrane but Reside within the Endoplasmic Reticulum

The subcellular localization of envelope proteins from HERV-K113, HERV-K18, and HERV-Fc1 was studied using flow cytometry and immunocytochemistry. First, transfected and non-permeabilized HEK293 cells, COS-7 cells, and LN-405 cells were incubated with anti-HERV-K TM specific antibody HERM1811-5 in order to detect envelope proteins at the cellular surface. Exemplarily, transfected and non-permeabilized HEK293 cells and COS-7 cells are depicted in Figure 3a and do not reveal the presence of envelope proteins on the cellular surface (Figure 3a). Only when using permeabilized cells, a robust percentage of cells showed increased fluorescence intensities as can exemplarily be seen in the dot plot of coK113-FLAG-transfected HEK293 cells (Figure 3b). Empty vector controls stained with primary and secondary antibodies served as controls (Figure 3b). Interestingly, the percentage of ENV-producing cells depends both on the cell line (39.0% coK113-positive HEK293 cells vs. 21.8% coK113-positive COS-7 cells) and the transfected expression plasmid (13.9% coK18-positive HEK293 cells vs. 39.0% coK113-positive HEK293 cells). In this regard, shedding of the SU did not account for the low abundance on the cellular surface, since we were not able to detect K18 or K113 ENV in the cell culture supernatant using a SU-specific antibody (Supplementary Figure S3).

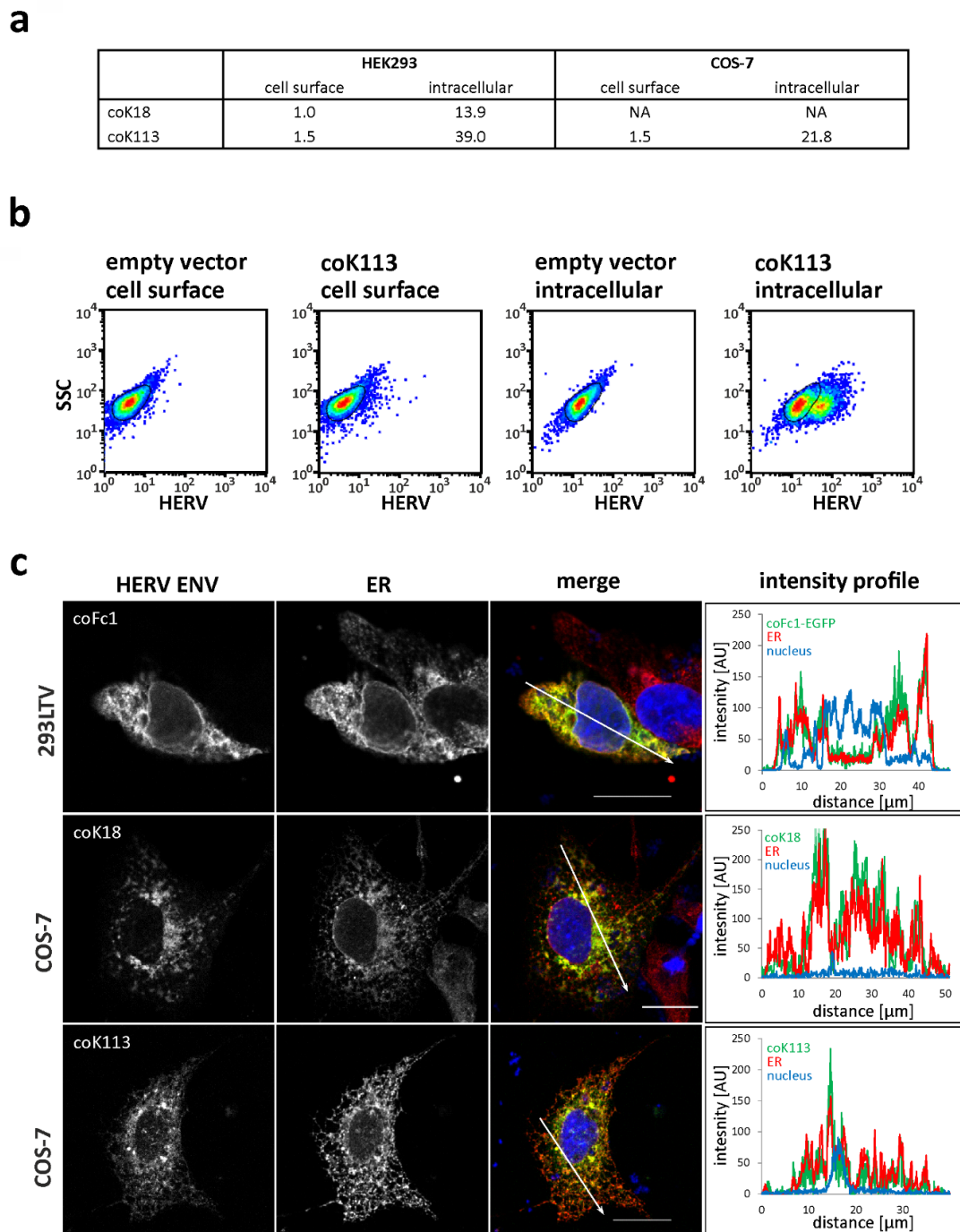


Figure 3. Localization of HERV ENV in transfected HEK293 cells, 293LTV cells, and COS-7 cells. (a,b) Flow cytometry of transiently transfected, non-permeabilized or permeabilized HEK293 cells and COS-7 cells stained for HERV-K ENV. The table in (a) shows the percentage of fluorescent cells. NA, not analyzed. In (b) the dot plots of HEK293 cells transiently transfected with coK113-FLAG and empty vector are shown. No staining without primary antibody was observed (Supplementary Figure S6). (c) Fluorescence microscopic images showing the subcellular localization of specified HERV ENV and the endoplasmic reticulum (ER) in transiently transfected COS-7 cells and 293LTV cells. The merge image is a z-projection (maximum intensity) of the three recorded channels (green: HERV ENV, red: ER, blue (DAPI): cell nucleus). Pixels with red and green fluorescence appear yellow. The graphs show a fluorescence intensity profile along the arrows drawn in the merge image. The detection of envelope proteins was performed using anti-HERV-K-TM antibody HERM1811-5 (coK18, coK113) or EGFP tag (coFc1). The ER was visualized by an anti-calnexin antibody. Scale: 20 μm .

To further study the localization of envelope proteins, double immunofluorescence staining of transfected and permeabilized 293LTV cells, COS-7 cells, and LN-405 cells was performed using anti-FLAG tag or anti-HERV-K TM-specific antibodies and cell organelle specific antibodies. For the envelope proteins of HERV-K18, HERV-K113, and HERV-Fc1 a similar localization in the form of branched net-like, partially vesicle- or cistern-like structures within the entire cell, excluding the cell nucleus, was observed (Figure 3c). The signal intensity was higher in areas close to the nucleus than in areas far away from the nucleus. For HERV-K18*, an unusually large number of cells with sharply defined regions of very high fluorescence intensity was observed (Figure 4 and Supplementary Figure S7). These are probably aggregated ENV within the ER lumen. The double immunofluorescence staining with the ER marker protein calnexin showed a partial overlay with the envelope protein signals, which appear yellow in the pseudo-colored Z-projection (Figure 3c). In addition to the concurrence of the signals presented in this way, intensity profiles provided evidence that the fluorescence signals of HERV ENV and ER were even colocalized, since pixels with high green (HERV ENV) fluorescence also showed high red (ER) fluorescence along a drawn distance (Figure 3c).

Furthermore, we used Golgi-specific markers GP73 for analysis of HERV-Fc1 and golgin-97 for analysis of HERV-K in order to determine the appearance of the ENV proteins in the Golgi complex. We observed only a partial overlap with Golgi markers especially for HERV-K113 (Figure 4). However, since we observed incomplete cleavage of the full-length precursor of coK113 into SU and TM (Supplementary Figure S5b,c), at least coK113 is not fully retained in the ER. Furthermore, staining using anti-tubulin corroborated the cytosolic localization of coK18 possessing a defective signal sequence (Supplementary Figure S7). In conclusion, HERV-K ENV could not be detected on the cellular surface, whereas all studied HERV ENV seem to be trapped inside the ER of transfected mammalian cells. The partial processing of the HERV-K113 precursor, however suggested only inefficient transport to the Golgi complex.

2.4. HERV Envelope Proteins Increase Gene Expression of Markers for Unfolded Protein Response but Trigger no Antiviral Response

As HERV ENV were shown to accumulate inside the ER, it was further studied whether this induces an unfolded protein response (UPR) in transfected HEK293 cells. The UPR is part of the cellular protein quality control that facilitates correct protein folding and prevents the accumulation of misfolded proteins in the ER lumen. Using qRT-PCR analyses of transiently HERV ENV transfected HEK293 cells, the transcript levels of different genes involved in the UPR (*HSPA5*, *ATF4*, *sXBP1*, *DDIT3*) were determined (Figure 5a). The *HSPA5* transcript levels of coK113 were nonsignificantly elevated when compared to control vector transfected cells.

Furthermore, *sXBP1* levels were significantly increased for coK113 as well as *DDIT3* mRNA levels for K18 and coK18 compared to control vector expression (one-way ANOVA, Dunnett's post-test, $p < 0.05$). In addition, we analyzed *HSPA5* (BiP) in WT and codon-optimized K113 and Fc1-expressing HEK cells using LC-MS/MS. As done for HERV-expression, we used sequence coverage as an indicator of protein abundance in these cells (Supplementary Figure S8). We could show that the sequence coverage and the number of proteolytic peptides increases in HERV-expressing cells compared to a vector-transfected control (Table 1). Therefore, we suggest that overexpression of HERV ENV activates UPR to some extent but focused studies for this topic are required in the future.

In addition, if a retrovirus infects a host cell, a number of cellular defense reactions occur. Among others, the group of apolipoprotein B mRNA editing enzyme, catalytic polypeptide-like 3 (APOBEC3) proteins plays an important role. These evolutionarily conserved cytidine deaminases recognize and bind retroviral single-stranded DNA to deaminate cytosine to uracil. As a result, hypermutations or degradation of viral DNA occurs. In the present study we were not able to see significant changes in *APOBEC3G* and *MOV10* expression in HEK293 cells (Figure 5b). Expression of *APOBEC3G* was always very low in HEK293 cells (Supplementary Figure S9a).

Additionally, no changes in *APOBEC3B* could be detected in HERV ENV-expressing cells in comparison to empty vector-transfected cells (Supplementary Figure S9b).

Another gene activated in response to retroviral infection is *BST2*. It encodes the protein tetherin, which prevents the budding of viral particles by binding viral envelope proteins. The restriction factor *TRIM22* is also an important component of innate antiviral immunity as it recognizes viral proteins and LTRs. The transcript levels of both genes were quantified in the present study after transfection of HERV ENV expressing plasmids in HEK293 cells. No differences in comparison to the control were found (Supplementary Figure S9b).

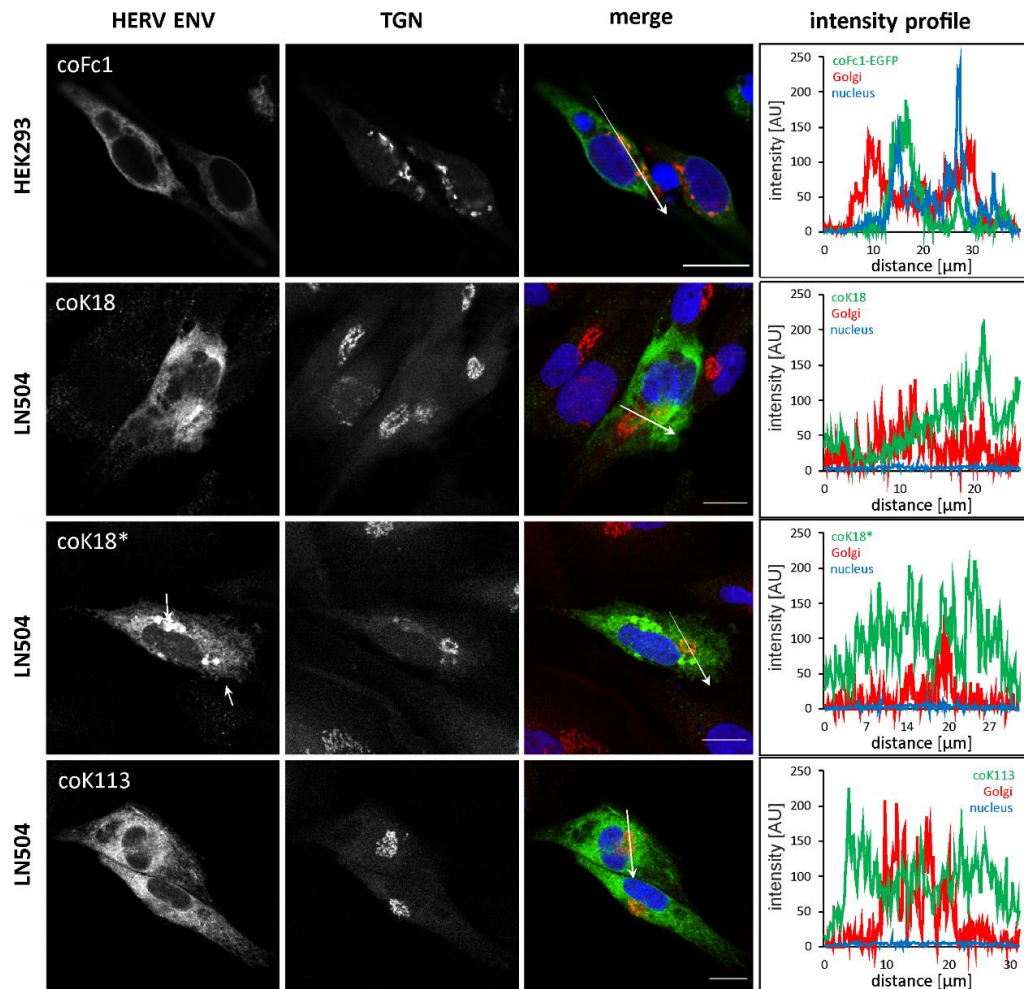


Figure 4. Localization of HERV ENV with trans Golgi network in transfected HEK293 and LN405 cells. Fluorescence microscopic images showing the subcellular localization of specified HERV ENV and the trans Golgi network (TGN) in transiently transfected HEK293 and LN405 cells. The merge image is a z-projection (maximum intensity) of the three recorded channels (green: HERV ENV, red: TGN, blue (DAPI): cell nucleus). Pixels with red and green fluorescence appear yellow. The graphs show a fluorescence intensity profile along the arrows drawn in the merge image. The detection of the envelope proteins was performed using anti-HERV-K-TM antibody HERM1811-5 for HERV-K and anti-FLAG for HERV-Fc1. The TGN was visualized by an anti-golgin-97 antibody for HERV-K and anti-GP73 antibody for HERV-Fc1. Scale bar: 20 μm .

2.5. Rare Leucine and Valine Codons Result in Decreased ENV Protein Synthesis in Human Cell Lines

The limited expression of native ENV raised the question of a possible mechanism that might be involved in increased protein synthesis after codon-optimization. Interestingly, the wild-type envelopes of HERV-K family members contained a high number of rare leucine (CUA and UUA)

or valine (GUA) coding triplets. Those codons can be seen as rare, because they are less served through the human tRNA pool. In the sequence of codon-optimized K113 ENV 43 of these codons were changed to the more common CUG or GUG triplets, respectively. The generation of different codon-optimized variants of K113 ENV with partial back-mutation to respective native codons for leucine or valine (mutcoK113) should lead to a decrease in protein synthesis through the limited availability of tRNAs. The expression of the complete codon-optimized K113 ENV (coK113) and five mutants including different rare codons (7× CUA; 23× UUA; 30× CUA and UUA; 13× GUA; 43× CUA and UUA and GUA) was analyzed in four mammalian cell lines, three from human origin, HEK293, 293LTV and A549, and one originating from African green monkey, COS-7. The results of Western blots of three independent transfection experiments of each vector normalized to expression of β -actin by densitometric analysis are shown (Figure 6).

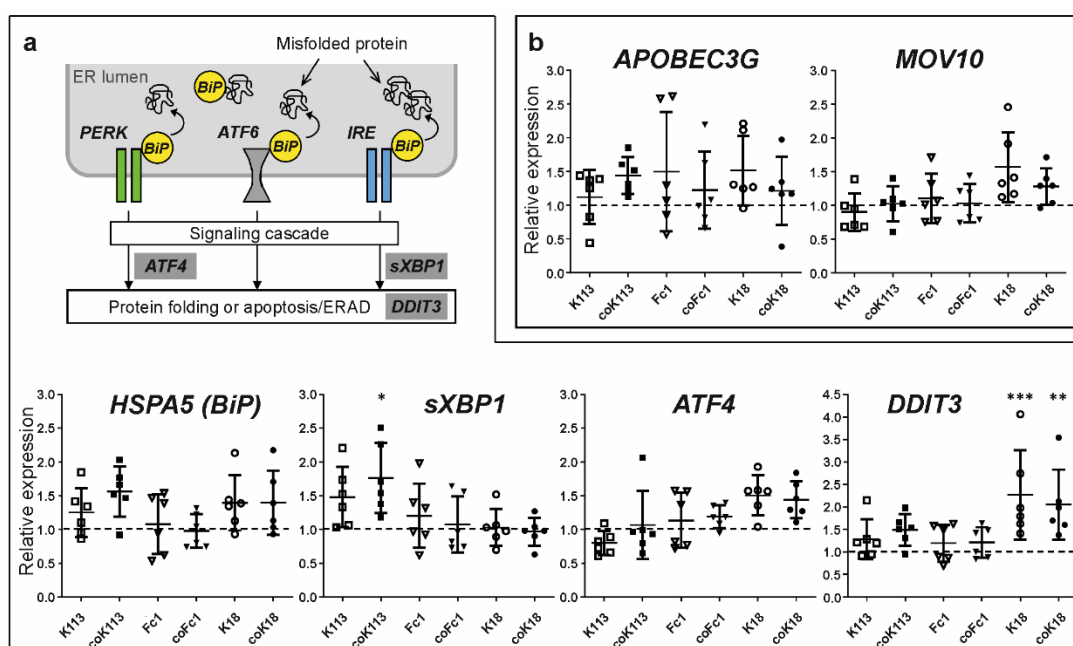


Figure 5. Influence of HERV ENV expression on antiviral response and unfolded protein response in transfected HEK293 cells. **(a)** The simplified scheme shows key players of the unfolded protein response (UPR). The ER chaperone immunoglobulin binding protein (BiP), which is encoded by the gene *HSPA5*, is transiently bound to three protein sensors anchored in the ER membrane: PKR-like ER kinase (PERK), activating transcription factor 6 (ATF6), and inositol-requiring enzyme (IRE). If misfolded proteins accumulate in the ER lumen, BiP selectively binds to hydrophobic regions of these proteins and detaches from the membrane sensors at the same time. Hence, they become activated via oligomerization, autophosphorylation, or glycosylation. As a result, a signaling cascade is triggered, which leads to enhanced protein folding or ER-associated degradation (ERAD). The expression normalized to *GAPDH* and relative to empty vector-transfected cells (dashed grey line) was determined. The graphs show single data points and mean values \pm standard deviation. Statistics: one-way ANOVA with Dunnett's multiple comparison test; *** $p < 0.001$; ** $p < 0.01$; * $p < 0.05$, $n = 6$. **(b)** Relative expression of genes involved in viral defense mechanisms after transfection of WT and codon-optimized HERV envelope protein sequences in HEK293 cells. Expression was normalized to *GAPDH* and empty vector-transfected cells were set as one (dashed grey line).

Assuming coK113 ENV levels as 100%, alterations for leucine and valine codon mutants were calculated. In all human cell lines, we observed decreasing K113 ENV level with increasing number of rare leucine (in total 30) codons with strongest drop in A549 cells (1/500th for mutcoK113*CUA*UUA). Interestingly, the usage of rare leucine codons alone showed no influence on expression of ENV in COS-7 cells. Here, we first observed decreasing protein level after introduction of rare valine codons

(mutcoK113*GUA: 3-fold; mutcoK113*GUA*CUA*UUA: 5.6-fold). The vector with back mutations of rare valine codon GUA led to decrease of protein synthesis in A549 cells (1/200th), whereas in contrast no effect was measured in HEK293 cells or 293LTV cells. The vector containing all 43 rare codons (mutcoK113*GTA*CTA*TTA) showed lower expression of K113 ENV in all three human cell lines (HEK293: 13.5-fold; 293LTV: 1/6th), with no detectable protein in A549 cells.

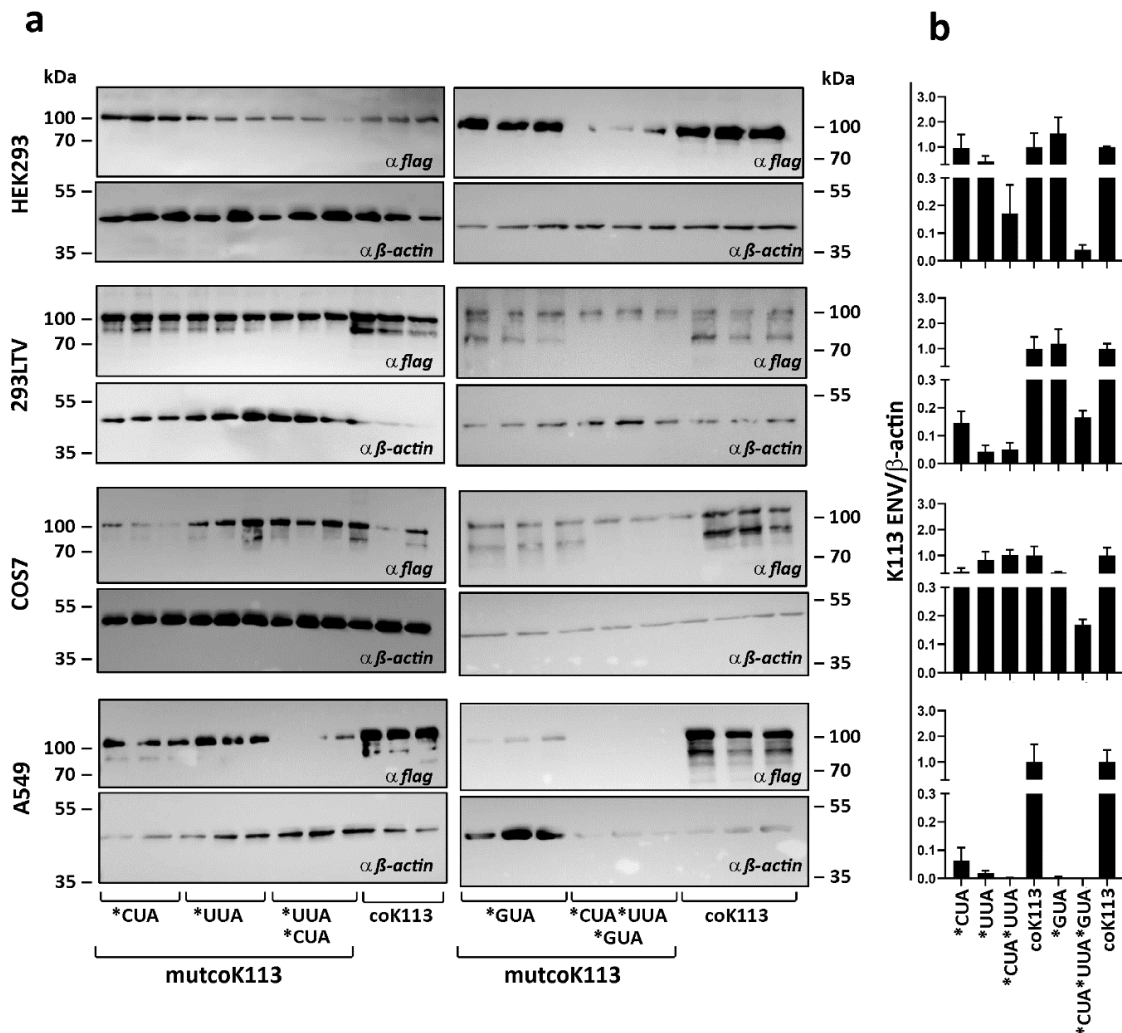


Figure 6. Expression of coK113 ENV mutants in mammalian cells. (a) Three human cell lines (HEK293, 293LTV, and A549) and monkey COS7 cells were transfected with expression vectors containing codon-optimized (coK113) or rare codon mutants of this sequence (mutcoK113). After 24 h the cells were harvested. Total amount of 20 μ g protein from three independent experiments was analyzed by Western blotting. For detection of ENV, staining against their C-terminal FLAG tag was performed. As reference the expression of β -actin was observed. (b) Densitometric analysis of normalized expression level is shown. The expression of ENV precursors was measured and normalized to expression of β -actin by densitometric analysis using ImageJ software. The complete codon-optimized ENV was set as 1. Mean and standard errors were calculated and visualized by GraphPad Prism5.

2.6. Rare Codons have a Negative Effect on Expression of HERV-K113 Envelope Protein in a Cell-Free Expression System

In addition to expression in mammalian cells, cell-free synthesis of K113 ENV sequences was performed to minimize the influence of environmental factors on efficiency and reproducibility, such as e.g., cell stress or days in culture. The quantification of absolute mRNA levels using standard curves of WT or codon-optimized DNA vectors in qRT-PCR resulted in lower amounts of transcripts for

the WT ENV, with 5.8×10^{-14} mol, compared to all codon-optimized variants, on average approx. 8×10^{-14} mol (Figure 7a).

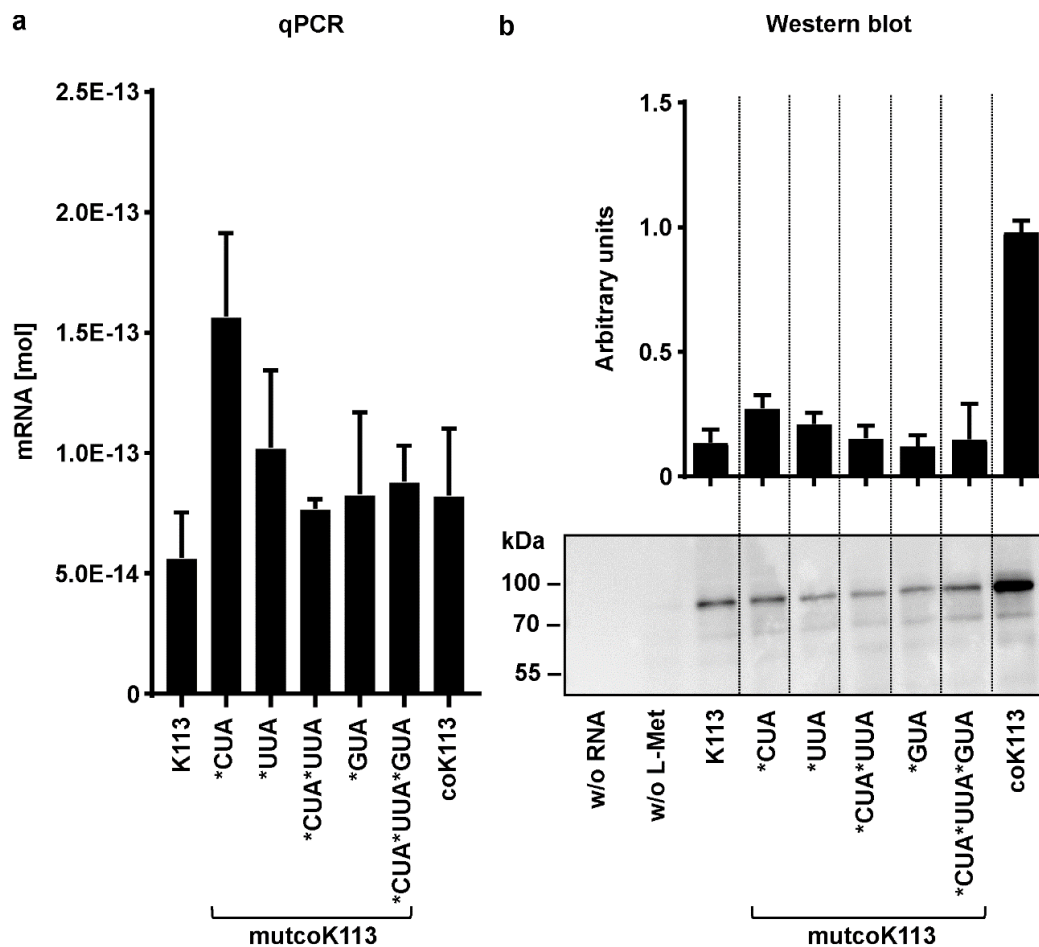


Figure 7. Cell-free expression of HERV-K113 envelope variants in qRT-PCR and Western blotting analysis. K113 envelope sequences of native (K113), codon-optimized (coK113), or its mutants with rare codons (mutcoK113) were in-vitro transcribed into mRNA and then translated into protein in a cell-free expression system. Mean and standard errors were calculated from at least two (four of native and codon-optimized K113 envelope) individual experiments with GraphPad Prism5. (a) In total, 1 μ g of linearized expression vector DNA was used for generation of mRNA by transcription starting at T7 promoter site upstream of ENV by RNA polymerase. A total of, 1 μ g of mRNA was reverse transcribed into cDNA and used as template in qRT-PCR. The calculation of absolute mRNA levels was performed using standard curves with native or codon-optimized vector DNA, respectively. (b) In total, 4 μ g of transcribed mRNA of ENV in (a) were translated into protein using reticulocyte lysate from New Zealand white rabbits including a mixture of all components necessary for translation. A translation reaction without RNA and a sample of codon-optimized RNA without amino acid methionine (L-Met) served as negative controls. An equal aliquot of all reactions was loaded for Western blotting. Densitometric analysis was performed by using ImageJ software, n=4. The de-glycosylated precursor of K113 ENV was observed at 80 kDa using anti-HERV-K-TM (HERM1811-5) antibody.

The transcript levels of mutcoK113 variant with back-mutated leucine codons CUA were increased (1.5×10^{-13} mol). In cell-free protein synthesis with rabbit reticulocyte lysate, the full-length and de-glycosylated ENV precursor could be detected for all K113 ENV variants at 80 kDa using an equal aliquot of all reactions in Western blotting. The expression of coK113 was increased by six times compared to the native ENV shown by densitometric analysis of four individual experiments.

Mutants of coK113 ENV expressed protein levels comparable to those of native ENV in two individual experiments (Figure 7b and Supplementary Figure S10).

Although the transcript levels of the variants are almost equal to or higher than those of coK113, protein biosynthesis seems to be impaired in all of these variants.

2.7. Inefficient Synthesis of Native HERV ENV—A Problem of Secondary RNA Structure?

The weak synthesis of native HERV ENV prompted us to investigate the folding of mRNA secondary structures as a possible reason.

The secondary structures of WT and codon-optimized HERV ENV mRNAs of Fc1, K18 and K113 were predicted using *The mfold Web Server* (<http://unafold.rna.albany.edu/?q=mfold>; last accessed data 14.02.2020). The in-silico models of envelope RNAs revealed differences in the secondary structure of native mRNAs compared to their codon-optimized counterparts (Figure 8). Interestingly, the calculated minimum free energy (ΔG) of all codon-optimized sequences was lower than that of WT sequences. The difference of ΔG of WT and codon-optimized versions was 218.95 for K113, 203.31 for K18, and 147.93 for Fc1, respectively.

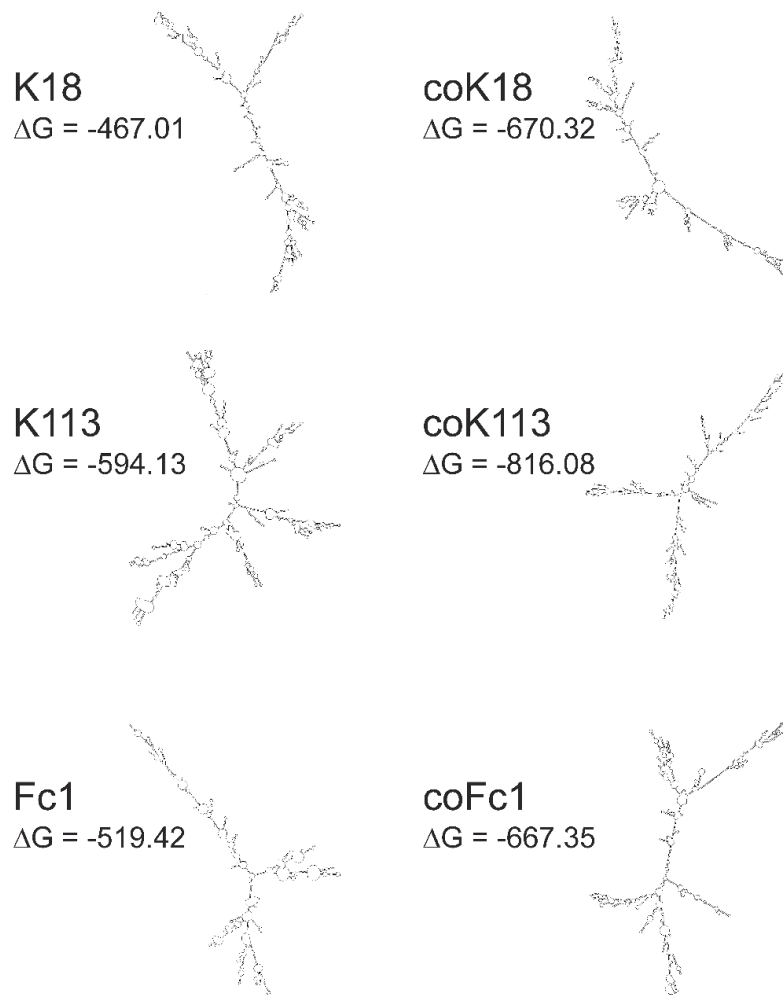


Figure 8. In-silico models of mRNA secondary structure of cloned native and codon-optimized HERV envelope RNAs. For all RNAs the sequence between the predicted transcription start site and the poly(A) site from the vector pcDNA3.1(+) was used for modeling. Models were calculated using *The mfold Web Server* (<http://unafold.rna.albany.edu/?q=mfold>, last accessed data 14.02.2020). For all RNAs the calculated structure with the lowest ΔG is shown.

3. Discussion

In the present study, we investigated the expression of three selected ENV, which are frequently associated with inflammatory diseases and cancer.

First, we observed limited expression of native ENV by transient transfection in mammalian cells (see Figure 1b–d). Codon optimization of sequences increasing ENV expression up to 150-fold (K113) and 290-fold (Fc1) was essential for further analysis of maturation, glycosylation and localization. In 2009, Hanke and colleagues also observed a 50-fold increase by codon optimization for K113 ENV [36]. This deviation is probably a result of different optimization algorithms and due to use of an artificial envelope sequence, which according to the authors corresponds to the suggested K113 ENV at the time of integration [36]. Interestingly, the reconstructed ENV showed increased proteolytic cleavage in SU and TM and additional glycosylation sites at the TM compared to the K113 ENV in our study [36]. We found that the majority of detected K113, Fc1, K18 and K18* ENV in all cell lysates is composed of the unprocessed ENV precursor (Figure 2a and Supplementary Figure S1). With exception of K18 all studied ENV were glycosylated and the protein sizes after de-glycosylation corresponded to the theoretical molecular mass of ENV precursors (K113: 80 kDa, K18*: 66 kDa, Fc1: 64 kDa). Of particular interest is that glycosylation of K18 ENV precursor could be rescued by reconstruction of a signal peptide sequence in K18* ENV (Figure 2a). Therefore, it can be suggested that in type 1 proviruses of the HERV-K (HML-2) family, e.g., K18, the loss of the signal peptide sequence by the characteristically 292 bp deletion in the *POL-ENV* region, prevents glycosylation by an altered subcellular localization.

In double immunostaining experiments by antibody labelling of organelle marker proteins, we demonstrated localization of HERV-K18, -Fc1, and -K113 ENV inside the ER (Figure 3c). The appearance especially of HERV-K113 ENV in the compartment of the Golgi can also be suggested due to (I) a partial overlap of fluorescence signals of the applied trans-Golgi network marker and ENV (Figure 4) and (II) the cleavage of precursor proteins into subunits SU and TM as shown for HERV-K113 (Figure 1b, Supplementary Figure S5b,c). The cleavage by furin proteases, which are active in the Golgi apparatus, is essential in protein maturation of retroviruses promoting membrane fusion and infectivity [37,38]. Our results for K113 ENV are in line with previous reports, detecting a reduced surface expression in comparison to K108 ENV [39]. Our study suggests the absence of K113 ENV at the plasma membrane as detected by immunohistochemistry and flow cytometry (Figure 3) and could explain absence of K113 ENV in pseudotyping experiments using simian immunodeficiency virus [39]. In this regard, an inaccessibility of the utilized antibody to its epitope is unlikely, since prior reports using the same antibody showed HERV-K ENV on the cellular surface of transfected HeLa cells and human PBMCs [39,40]. The accumulation of HERV ENV inside the ER was further supported by investigating the induction of genes involved in the unfolded protein response (UPR). Overexpression of proteins after codon-optimization lead to a strong enrichment of protein in the ER promoting misfolding [41]. As a result, coK113 ENV and K18/coK18 ENV showed elevation of e.g., *sXBP1* and *DDIT3* (Figure 5). In addition, LC-MS/MS experiments suggested a higher abundance of *HSPA5* (BiP) after expression of K113/coK113 and Fc1/coFc1 (Table 1). The physiological relevance of the observations remains elusive, since it is poorly understood to what extent the expression of dormant proviral sequences can be reactivated in the human genome. The applied codon-optimization would mimic a stronger activation according to the low level of protein synthesis from native sequences. Therefore, we suggest that the lack of efficient intracellular trafficking is (I) due to the defective signal sequence in K18 or (II) inefficient cleavage of the precursor as shown for coK113. In this regard, it has been shown previously, that inefficient cleavage of the ENV precursor interferes with intracellular trafficking, e.g., as shown for bovine HERV-K [42]

In accordance to that, we also investigated the altered nucleotide sequence during codon-optimization of ENV. The majority of optimized nucleotides in the ENV of K113 belonged to triplets coding for leucine (CUA and UUA) or valine (GUA) indicating that the low protein amounts of native ENV might be due to a limited availability of appropriate cognate t-RNAs. Interestingly, we observed that gradually elevation of rare leucine codons in the codon-optimized

ENV led to a decreased ENV expression in human cell lines (Figure 6). With the exception of A549 cells, the re-introduction of rare valine codons only caused a reduced protein expression in the monkey cell line, COS7. Thus, a different tRNA pool in the applied human and monkey cells might be part of an explanation. Furthermore, we decided to investigate expression of all K113-ENV variants in a cell-free system, which offers the advantage of a controlled transcription and translation process. As a result, we detected the expression of all K113 ENVs as de-glycosylated precursor with a molecular mass of 80 kDa (Figure 7b and Supplementary Figure S10). Interestingly, the native ENV could be detected next to the codon-optimized ENV by loading equal amounts of protein lysate, which implicates that the protein yield of native ENV was much higher in the cell-free system than in the mammalian cells. In this regard it is of interest that we observed a discrepancy in transcript amounts between the native and all codon optimized ENV sequences by using equal RNA amounts for synthesis of cDNA and equal amounts of cDNA performing qRT-PCR, respectively (Figure 7a). In-silico prediction of mRNA secondary structures using the *mfold Web Server* algorithm revealed (I) an apparently different modelling of native and codon-optimized ENV and (II) a lower minimum free energy of all codon-optimized sequences indicating a higher thermodynamic stability of these structures (Figure 8). These increased thermodynamic stabilities might influence translation efficiency. In addition, Zhang and colleagues observed that stable RNA secondary structures, e.g., stem loops, could be skipped by the reverse transcriptase, resulting in shortened transcripts and early termination of cDNA synthesis [43]. The algorithm used for codon optimization (see Section 4) considers not only the codon usage bias but also multiple parameters influencing transcriptional and translational efficiency, e.g., the GC content or the presence of RNA destabilizing elements. Interestingly, codon composition has been shown to directly influence mRNA stability. The impact of codon usage on stability varies between species or cell types [44] and cannot be predicted certainly today. Moreover, the tRNA pool seems to be dynamic [45] and not all cells of a given species must behave identically. Codon usage has also been shown to influence transcription independent of RNA stability [46,47]. Finally, mRNAs are subjected to epitranscriptomic modifications that influence RNA stability and gene expression, which has been studied especially in viruses [48,49]. All these factors might be responsible for the different impact of codon composition on HERV ENV expression in different cell lines. The complexity of secondary structures of native ENV should be investigated in future analysis.

4. Materials and Methods

4.1. Generation of Expression Plasmids

The cDNA for HERV-Fc1 ENV was isolated from the human embryonic testicular carcinoma cell line H12.5 [50]. The obtained sequence contained a silent mutation C705T compared to the sequence of the reference sequence (NCBI accession no.: 105373297), which was mutated back via site-directed mutagenesis. For subsequent cloning in expression vectors, a restriction site for *NcoI* was mutated so that the silent mutation A438T was inserted (used primers are specified in Supplementary Table S1). The sequences of the envelope proteins of HERV-K18.2 (NCBI accession no.: 100775105) and HERV-K113 (NCBI accession no.: 17099689) were synthesized de novo (Eurofins Genomics, Ebersberg, Germany; GenScript, Piscataway, NJ, USA). Codon-optimized gene sequences for all three envelope genes were generated using the OptimumGene algorithm (GenScript, Piscataway, NJ, USA). Additionally, K18* comprising a functional signal peptide was generated by combining the codon-optimized signal sequence of HERV-K113 with codon-optimized HERV-K18. All sequences contained a 3'-FLAG tag sequence. In addition, for HERV-Fc1, also an EGFP was fused C-terminally. Amplification of the target sequences was accomplished by conventional PCR using Phusion High Fidelity Polymerase (New England Biolabs, Ipswich, MA, USA) according to the manufacturer's protocol. All used primer sequences are listed in Supplementary Table S1. The PCR product was purified using the Wizard® SV Gel and PCR Clean-Up System (Promega GmbH, Mannheim, Germany). After restriction digestion of the purified PCR product and the expression vector

pcDNA3.1(+) (Thermo Fisher Scientific, Waltham, MA, USA) using appropriate restriction enzymes (New England Biolabs, Ipswich, MA, USA) as specified in Supplementary Table S1, ligation was performed using T4 DNA Ligase (Thermo Fisher Scientific) according to the manufacturer's protocol and transformed into *E. coli* DH5alpha. Thereafter, the DNA of one overnight colony grown in 1 mL LB medium supplemented with selection antibiotics was isolated using GeneJET Plasmid Miniprep Kit (Thermo Fisher Scientific) according to the manufacturer's protocol. The corresponding expression vectors are designated as follows: Fc1-FLAG; Fc1-EGFP; coFc1-FLAG; K18-FLAG; coK18-FLAG, coK18*-FLAG, K113-FLAG; coK113-FLAG, where "co" stands for codon-optimized.

4.2. Cell Lines

The human embryonic kidney cell line HEK293 [51] and the African green monkey cell line COS-7 [52] was obtained from the *Deutsche Sammlung für Mikroorganismen und Zellkulturen* (DSMZ), Braunschweig, Germany). 293LTV cells were obtained from Cell Biolabs, San Diego, CA, USA. The human glioblastoma cell line LN-405 [53] was a kind gift from I. Schulz, Probiobdrug AG, Halle, Germany. The human lung adenocarcinoma cell line A549 [54] was obtained from CLS, Eppelheim, Germany. HEK293 cells, LN-405 cells, and COS-7 cells were grown in DMEM (Life Technologies, Carlsbad, CA, USA), supplemented with 10% FBS (Life Technologies, Carlsbad, CA, USA). 293LTV cells were grown in DMEM, supplemented with 10% FBS, 1x GlutaMAX (Life Technologies, Carlsbad, CA, USA) and 1x non-essential amino acids (Life Technologies, Carlsbad, CA, USA). A549 cells were cultivated in RPMI1640 medium supplemented with 10% FBS. All cell lines were cultivated at 37 °C with 5% CO₂ (HEK293, 293LTV, COS-7) or 10% CO₂ (LN-405).

4.3. Transfection

Unless otherwise stated, cells were seeded at 1.4×10^6 cells/well (HEK293 cells), 1.2×10^6 cells/well (293LTV cells), 0.4×10^6 cells/well (COS-7 cells), or 1.3×10^6 cells/well (A549 cells) in 6-well plates. After 24 h, transfection with the appropriate vectors using Opti-MEM reduced-serum medium (Life Technologies, Carlsbad, CA, USA) and Lipofectamine 2000 (Life Technologies, Carlsbad, CA, USA) was carried out according to the manufacturer's protocol. In total, 4 µg vector and 7.5 µL Lipofectamine 2000 were used for each well. Empty vector-transfected cells served as controls. The transfected cells were incubated for 24 h before further use.

4.4. Protein Extraction

Cells were detached from the culture flask by incubation with trypsin (Life Technologies, Carlsbad, CA, USA) and separated from the cell culture medium by centrifugation (300× *g*, 5 min). The cell pellet was washed twice with 0.5 mL cold PBS (300× *g*, 5 min). The cells were then resuspended in 200 µL cell extraction buffer (CEB, Life Technologies, Carlsbad, CA, USA) supplemented with 10 mM AEBSF Protease Inhibitor (Sigma Aldrich, St. Louis, MO, USA) and 1x Complete Mini EDTA-free Protease Inhibitor Cocktail (Roche Diagnostics GmbH, Basel, Switzerland) and incubated on ice for 30 min with regular mixing. After centrifugation at 13,000× *g* for 30 min at 4 °C, the cell lysates were transferred to new reaction tubes. The concentration was determined by UV/VIS spectrophotometry using Bradford reagent. For LC-MS/MS analysis, pellets of HERV-expressing HEK293 cells were dissolved in 75 µL of 0.1% (*w/v*) SDS (in 50 mM NH₄HCO₃, pH 8.0), incubated for 10 min at 95 °C, and chilled on ice for 5 min. Then, 75 µL of cell extraction buffer (Invitrogen, FNN0011) were added and samples were again incubated on ice for 30 min and subsequently treated with ultrasound for 2 min. Cell debris were removed by centrifugation (10 min with 16,000× *g* at 4 °C) and 100 µL of the supernatant were mixed with 25 µL of 5 × SDS sample buffer.

4.5. Deglycosylation

Deglycosylation was carried out using the PNGase F Deglycosylation Kit (New England Biolabs, Ipswich, MA, USA) on 20 µg total protein lysates under denaturing reaction conditions according to the manufacturer's protocol. A reaction mixture without PNGase F served as control.

4.6. SDS-PAGE

SDS polyacrylamide gel electrophoresis (PAGE) was performed according to Laemmli [55]. The polyacrylamide gels used contained a stacking gel fraction (5% acrylamide) and a separating gel fraction (10% or 12% acrylamide). The samples were mixed with reducing sample buffer and boiled at 95 °C for 10 min before application. Electrophoretic separation was performed at 90 V (20 min), followed by 140 V.

For LC-MS/MS analysis, samples were incubated for 5 min at 95 °C and subsequently allowed to cool down at room temperature. Then, 50 µL of each sample were applied on a 6% stacking gel and run with 60 V for 25 min. Proteins were stained with Coomassie Brilliant Blue for 30 min at room temperature and de-stained with MeOH/H₂O/acetic acid (500/400/100; *v/v/v*) for 2 h (Supplementary Figure S11).

4.7. Western Blot Analysis

SDS gels, the nitrocellulose membrane (GE Life Sciences, Freiburg, Germany), and four filter papers were soaked in Towbin Buffer (0.025 mol/L TRIS pH 8.3; 0.192 mol/L glycine; 20% (*v/v*) methanol) for at least 20 min. Protein transfer to the nitrocellulose membrane was performed with a semidry blot system under a constant electrical voltage of 15 V for 45 min. The membrane was then incubated for 1 h in blocking buffer (5% (*w/v*) milk powder in TBS-T), followed by incubation with the appropriate primary antibody in blocking buffer at 4 °C for 12–16 h. For detection of the FLAG tag, anti-DYKDDDDK antibody (Cell signaling, Cambridge, Great Britain) diluted 1:1000 was used. For detection of the HERV-K, TM subunit anti-HERV-K TM HERM1811-5 and anti-HERV-K SU HERM1821-5 (Austral Biologicals, San Ramon, CA, USA) diluted 1:1000 were used. Please refer to Supplementary Table S2 for a complete list of applied antibodies. Thereafter, the membrane was washed three times in TBS-T for 10 min each before incubation with secondary antibodies anti-rabbit IgG-HRP (Cell signaling, Cambridge, Great Britain) or anti-mouse IgG-HRP (Cell signaling, Cambridge, Great Britain) diluted 1:2000 for 1 h at room temperature. After two washes in TBS-T and one wash in TBS, immunodetection by chemiluminescence was performed using the SuperSignal West Pico/Femto Chemiluminescent Substrate Kit (Thermo Fisher Scientific) according to the manufacturer's instructions. The signal strength of the chemiluminescent signals was recorded using the Fusion FX-7 imager (Vilber Lourmat Deutschland GmbH, Eberhardzell, Germany).

4.8. Sample Preparation for Mass Spectrometry

Proteins from SDS gels were excised and Coomassie Brilliant Blue was removed by repeated incubation (five cycles at 30 min) in 100 mM NH₄HCO₃ (in H₂O, pH 8.0) and 100 mM NH₄HCO₃ (in ACN/H₂O (500/500; *v/v*), pH 8.0) at 37 °C. Gel bands were dehydrated by incubation in neat ACN for 10 min and finally dried by rotational vacuum concentration (10 min at ≈30 °C). Disulfide bonds were reduced by incubation in DTT solution for 45 min at 50 °C. Samples were allowed to cool down and DTT was exchange for iodoacetamide solution. Alkylation of cysteine residues was carried out for 1 h at room temperature in the dark. The iodoacetamide solution was discarded and gel bands were washed 2x with 100 mM NH₄HCO₃ followed by dehydration in neat ACN for 10 min and drying by rotational vacuum concentration (10 min at ≈30 °C).

Trypsin (Promega, V5280) stock solution (*c* = 1 µg/µL) was thawed on ice and diluted 1:50 with 40 mM NH₄HCO₃ (in H₂O/ACN (900/100; *v/v*), pH 8.0). Gel bands were incubated for 1 h at room temperature with 75 µL of digestion solution. The latter was removed and 150 µL of 40 mM NH₄HCO₃ (in H₂O/ACN (900/100; *v/v*), pH 8.0) were added. Gel bands were incubated for 8 h at

37 °C. Afterwards, proteolytic peptides were extracted by incubation of the gel bands in H₂O with frequent vortexing and treatment with ultrasound for 1 min. This extraction step was repeated with ACN/H₂O/TFA (500/450/50; *v/v/v*) and neat ACN. Digestion buffer and extraction solutions of each sample were combined in one tube and subsequently concentrated by rotational vacuum concentration (1 h at ≈30 °C). Concentrated gel extracts were purified with C₁₈ stage-tips (10 layers). Elution was carried out with 10 μL of ACN/H₂O/FA (600/390/10; *v/v/v*).

4.9. LC-MS/MS Data Acquisition and Analysis

Samples were analyzed on an Ultimate 3000 RSLC nano-HPLC system coupled with an Orbitrap Fusion mass spectrometer (Thermo Fisher Scientific). Chromatography was performed by applying 240-min gradients with reversed phase C18 columns (μPAC 900 nL C18 trapping column and μPAC™ 50 cm C18 chip-based separation column, Pharmafluidics). For MS data acquisition, a data-dependent top 5s method was used. FTMS survey scans were acquired in the *m/z* range 300–1700 (*R* = 120,000 at *m/z* 200). MS/MS scans of the most abundant signals of the survey scan were acquired in parallel by FTMS and ITMS. For FTMS higher energy collision-induced dissociation (HCD) was used with 27% normalized collision energy (NCE), an isolation window of 1.5 Th and an intensity threshold of 30,000. For ITMS collision induced dissociation (CID) was used with a NCE of 35%, an isolation window of 2.2 Th, and an intensity threshold of 5000). Dynamic exclusion was enabled and exclusion time was set to 60 s.

Data analysis was carried out with PEAKS Studio (version 7.5) using the human sequences of the UniProt/SwissProt database (release 2019_11). Refinement of raw mass spectrometry data included merging of MS/MS scans (0.1 min retention time window, 5.0 ppm precursor *m/z* error tolerance, merging of CID and HCD scans was enabled) and precursor mass correction. The database search was performed using the following mass tolerances: 5.0 ppm for MS and 20 mDa for MS/MS. The maximum number of both, post-translational modifications per peptide and missed cleavage sites, was 3. Non-specific proteolytic cleavage was allowed for both termini. The FDR value was set to 0.01%.

4.10. Flow Cytometry

A total of 24 h after transfection the cells were washed with PBS and incubated with Accutase (PAA Laboratories, Pasching, Germany) for 5 min at room temperature to remove them from the cell culture vessel. Flow cytometry was performed essentially using standard methods. In short, cells were incubated with anti-HERV-K TM HERM1811-5 (diluted 1:500 in staining buffer) for 45 min on ice. Goat anti-mouse Cy2 (Supplementary Table S3), diluted 1:200 in staining buffer, was used as secondary antibody for 45 min on ice in the dark. After two washes with staining buffer the cell pellet was finally resuspended in 100 μL PBS. For intracellular staining, the protocol was essentially the same except for fixation (4% PFA) and permeabilization (0.1% saponin in PBS) steps before application of the primary antibody. The samples were analyzed using a FACSCalibur (Becton Dickinson, Franklin Lakes, NJ, USA). For each sample 10,000 cells were counted. Data analysis was performed with the FlowJo v10.3 software (Becton Dickinson, Franklin Lakes, NJ, USA).

4.11. Immunocytochemistry

Cells were seeded at 7×10^4 cells/well (293LTV cells) or 4×10^4 cells/well (LN-405 cells, COS-7 cells) in chamber slides and 24 h later cells were transfected with appropriate vectors as described before using 0.7 μg vector and 2 μL Lipofectamine 2000 per well. The following day the cells were washed with PBS (Life Technologies, Carlsbad, CA, USA) and fixed in 4% PFA in PBS for 15 min at room temperature. This was followed by a PBS washing step and a 5-min incubation with 50 mM ammonium chloride in PBS to quench aldehyde autofluorescence. The cells were then permeabilized for 10 min with 0.1% saponin in PBS (PBS-S), incubated for 30 min in blocking buffer (0.1% saponin, 3% goat serum (Life Technologies, Carlsbad, CA, USA) in PBS), and incubated overnight at 4 °C with the appropriate primary antibody diluted in blocking buffer. The cells were then washed twice with PBS-S

and incubated for 1 h with the appropriate secondary antibody in blocking buffer. After two washes with PBS-S and PBS each, the cells were incubated for 2 min in the dark with DAPI staining solution (5 ng/mL, Molecular Probes, Eugene, OR, USA) and then washed twice with PBS. Finally, the cells were embedded in Citifluor AF1 mounting medium (Citifluor, Hatfield, PA, USA) and sealed with cover glasses. Unless otherwise indicated, all incubation steps were performed at room temperature. If the localization of HERV ENV on the cell surface was to be checked, the permeabilization step and the use of saponin were omitted in all subsequent steps. If a HERV ENV coupled to EGFP was transfected, the cells were only fixed as described above, incubated with ammonium chloride, and DAPI stained before they were cover slipped. All used antibodies with corresponding dilutions are listed in Supplementary Table S3. The fluorescence images were taken with a 40× or 63× water immersion objective using a laser scanning microscope LSM 780 (Carl Zeiss AG, Oberkochen, Germany).

4.12. RNA Extraction and cDNA Generation

Total RNA was isolated using the NucleoSpin XS kit (Macherey-Nagel, Düren, Germany) as specified by the manufacturer. Transcription into complementary DNA (cDNA) was accomplished by mixing 200 ng total RNA with 1 µL of 100 µM random hexanucleotide primers (Roche Diagnostics GmbH, Basel, Switzerland), 1 µL of 10 mM dNTPs (Thermo Fisher Scientific), filled to 14 µL with nuclease-free water and incubated for 5 min at 65 °C. Then, 4 µL first-strand 5 × buffer (Thermo Fisher Scientific), 2 µL of 100 mM DTT solution (Thermo Fisher Scientific), 0.5 µL SuperScript II reverse transcriptase (Life Technologies, Carlsbad, CA, USA), and 1.5 µL nuclease-free water were added. The preparation was incubated for 10 min at 25 °C, followed by 50 min at 42 °C and finally 15 min at 70 °C. For quantification of in vitro transcribed HERV ENV, 1 µg RNA was diluted in 16 µL nuclease-free water and 4 µL of cDNA mix (qScript cDNA Synthesis Kit, QuantaBio), containing reverse transcriptase, enzymes, and buffer, was added. Synthesis was done in three steps: 5 min at 22 °C, 30 min at 42 °C, and 5 min at 85 °C. The transcribed cDNA was stored at −20 °C.

4.13. Quantitative Real Time PCR (qRT-PCR)

Quantification of gene expression by qRT-PCR was performed using PowerUP SYBR Green Mastermix (ThermoFisher, Germany). Each reaction contained 12.5 ng of cDNA, 500 nM of forward and reverse primer, 5 µL 2 × PowerUP SYBR Green Mastermix and 4 µL of water. Used primer sequences are listed in Supplementary Table S4. For amplification a QuantStudio3 cyclor (ThermoFisher) with QuantStudio Design and Analysis Software v.1.4.3 was used. After an initial denaturation step at 95 °C for 10 min, amplification was performed by 40 cycles with denaturation at 95 °C for 15 s and primer annealing and extension at 60 °C for 60 s. Two to three technical replicates were measured for each sample in six independent experiments (biological replicates). GAPDH was used as reference gene for normalization and quantification was performed according to the $2^{-\Delta(\Delta)Ct}$ method [56]. To quantify in vitro transcribed RNA qRT-PCR, GoTaq qPCR Master Mix (Promega, Walldorf, Germany) was used. In this case, a 20 µL-reaction with 10 µL (2×) SybrGreen mix, 1250 nM forward and reverse primer, nuclease-free water, and 1 µL cDNA was mixed. Standard curves with serial dilutions of plasmid DNA containing WT or codon-optimized K113 ENV sequences were used for calculation of absolute amounts. As reference, the amplification of a vector specific target (neomycinR) was analyzed.

4.14. Cell-Free In Vitro Transcription and Translation

All expression vectors containing K113 ENV sequences were digested after the poly(A) site using restriction enzyme *Sma*I (10 U/µL, ThermoScientific) at 30 °C for 4 h. After inactivation at 65 °C for 20 min, the reaction was loaded with 6× DNA loading dye on a 1% agarose gel and the linearized vector was eluted with GeneJet Gel Extraction Kit (ThermoScientific) according to manufacturer's protocol. In vitro transcription starting at the T7 promotor was performed with 1 µg linearized vector according to the manufacturer's protocol (MEGAscript T7 Kit, ThermoScientific) at 37 °C for 4 h. For DNA digest, 1 µL of TURBO DNase Kit was applied to the mixture and incubated for 15 min. The transcribed mRNA

was precipitated with lithium chloride suspension and finally resuspended with 60 µL nuclease-free water. The concentration was measured using spectrophotometer NanoDrop2000 and aliquots of mRNA were stored at -80°C .

Cell-free protein synthesis was performed using the Rabbit Reticulocyte Lysate System (Promega). In total, 4 µg in vitro transcribed mRNA of all K113 ENV was used per reaction. A total of 1 µL of RiboLock RNase inhibitor (ThermoScientific) was used. One reaction without RNA and one reaction without the amino acid L-methionine were used as negative controls. The reactions were set up according to manufacturer's protocol and incubated in a water bath at 30°C for 90 min. Subsequently, the digestion of RNA was done using RNaseA (ThermoScientific) at final concentration of 0.2 mg/mL for 5 min. The tubes were set on ice for 10 min to stop the reaction. The translation reaction was stored in SDS sample buffer at -20°C . For further analysis of protein by SDS-PAGE, an aliquot of 12 µL was mixed with SDS sample buffer and nuclease-free water to 60 µL and boiled for 5 min at 95°C .

4.15. In-Silico Determination of mRNA Secondary Structure

The in-silico prediction of mRNA secondary structure was performed using *The mfold Web Server* (<http://unafold.rna.albany.edu/?q=mfold>; last accessed data 14.02.2020) [57]. The nucleotide sequences starting at the putative transcription start site and ending at the poly(A) site of the vectors with cloned wildtype or codon optimized HERV ENV of K18, K113, and Fc1 were analyzed.

4.16. Statistics

For comparison of relative mRNA levels measured with qRT PCR one-way ANOVA followed by Dunnett's multiple comparison test was performed. Statistical significance was indicated by asterisks (*, $p < 0.05$; ***, $p < 0.001$).

Supplementary Materials: Supplementary Materials can be found at <http://www.mdpi.com/1422-0067/21/21/7855/s1>.

Author Contributions: Conceptualization, V.G., A.E., M.S.S. and H.C.; methodology, V.G., L.W., M.N., B.M., A.-C.M. and C.I.; validation, M.S.S. and H.C.; formal analysis, V.G., L.W., M.S.S. and H.C.; investigation, V.G., L.W., M.N., C.I., B.M., and A.-C.M.; resources, S.R.; data curation, V.G., L.W., A.E., M.S.S. and H.C.; writing—original draft preparation, V.G., L.W.; writing—review and editing, M.S.S. and H.C.; visualization, V.G., L.W. and M.S.S.; supervision, S.R., A.E., M.S.S. and H.C.; project administration, A.E., M.S.S. and H.C.; funding acquisition, A.E., M.S.S. and H.C. All authors have read and agreed to the published version of the manuscript.

Funding: The work was supported by grants ZS/2018/12/96228 (to University of Halle) and ZS/2018/12/96169 (to Fraunhofer Society) from European Regional Development Fund within the local program "Sachsen-Anhalt WISSENSCHAFT Schwerpunkte".

Acknowledgments: The authors are grateful to B. Hause for generous support and helpful discussions.

Conflicts of Interest: The authors declare no conflict of interest.

References

1. Griffiths, D.J. Endogenous retroviruses in the human genome sequence. *Genome Biol.* **2001**, *2*, 1017. [[CrossRef](#)] [[PubMed](#)]
2. Belshaw, R.; Pereira, V.; Katzourakis, A.; Talbot, G.; Paces, J.; Burt, A.; Tristem, M. Long-term reinfection of the human genome by endogenous retroviruses. *Proc. Natl. Acad. Sci. USA* **2004**, *101*, 4894–4899. [[CrossRef](#)] [[PubMed](#)]
3. Christensen, T. HERVs in neuropathogenesis. *J. Neuroimmune Pharmacol.* **2010**, *5*, 326–335. [[CrossRef](#)] [[PubMed](#)]
4. Gifford, R.J.; Blomberg, J.; Coffin, J.M.; Fan, H.; Heidmann, T.; Mayer, J.; Stoye, J.; Tristem, M.; Johnson, W.E. Nomenclature for endogenous retrovirus (ERV) loci. *Retrovirology* **2018**, *15*, 59. [[CrossRef](#)]
5. de Parseval, N.; Heidmann, T. Human endogenous retroviruses: From infectious elements to human genes. *Cytogenet. Genome Res.* **2005**, *110*, 318–332. [[CrossRef](#)]

6. Blond, J.L.; Lavillette, D.; Cheynet, V.; Bouton, O.; Oriol, G.; Chapel-Fernandes, S.; Mandrand, B.; Mallet, F.; Cosset, F.L. An envelope glycoprotein of the human endogenous retrovirus HERV-W is expressed in the human placenta and fuses cells expressing the type D mammalian retrovirus receptor. *J. Virol.* **2000**, *74*, 3321–3329. [[CrossRef](#)]
7. Grandi, N.; Tramontano, E. HERV envelope proteins: Physiological role and pathogenic potential in cancer and autoimmunity. *Front. Microbiol.* **2018**, *9*, 462. [[CrossRef](#)]
8. Balada, E.; Vilardell-Tarrés, M.; Ordi-Ros, J. Implication of human endogenous retroviruses in the development of autoimmune diseases. *Int. Rev. Immunol.* **2010**, *29*, 351–370. [[CrossRef](#)]
9. Lemaître, C.; Tsang, J.; Bireau, C.; Heidmann, T.; Dewannieux, M. A human endogenous retrovirus-derived gene that can contribute to oncogenesis by activating the ERK pathway and inducing migration and invasion. *PLoS Pathog.* **2017**, *13*, e1006451. [[CrossRef](#)] [[PubMed](#)]
10. Gröger, V.; Cynis, H. Human endogenous retroviruses and their putative role in the development of autoimmune disorders Such as multiple sclerosis. *Front. Microbiol.* **2018**, *9*, 265. [[CrossRef](#)] [[PubMed](#)]
11. Staeger, M.S.; Emmer, A. Editorial: Endogenous viral elements—links between autoimmunity and cancer? *Front. Microbiol.* **2018**, *9*, 3171. [[CrossRef](#)] [[PubMed](#)]
12. Grabski, D.F.; Hu, Y.; Sharma, M.; Rasmussen, S.K. Close to the bedside: A systematic review of endogenous retroviruses and their impact in oncology. *J. Surg. Res.* **2019**, *240*, 145–155. [[CrossRef](#)] [[PubMed](#)]
13. Herve, C.A.; Lugli, E.B.; Brand, A.; Griffiths, D.J.; Venables, P.J.W. Autoantibodies to human endogenous retrovirus-K are frequently detected in health and disease and react with multiple epitopes. *Clin. Exp. Immunol.* **2002**, *128*, 75–82. [[CrossRef](#)] [[PubMed](#)]
14. Marni, G.; Erre, G.L.; Caggiu, E.; Mura, S.; Cossu, D.; Bo, M.; Cadoni, M.L.; Piras, A.; Mundula, N.; Colombo, E.; et al. Identification of a HERV-K env surface peptide highly recognized in rheumatoid arthritis (RA) patients: A cross-sectional case-control study. *Clin. Exp. Immunol.* **2017**, *189*, 127–131. [[CrossRef](#)]
15. Giebler, M.; Staeger, M.S.; Blauschmidt, S.; Ohm, L.I.; Kraus, M.; Würfl, P.; Taubert, H.; Greither, T. Elevated HERV-K expression in soft tissue sarcoma is associated with worsened relapse-free survival. *Front. Microbiol.* **2018**, *9*, 211. [[CrossRef](#)]
16. Johnston, J.B.; Silva, C.; Holden, J.; Warren, K.G.; Clark, A.W.; Power, C. Monocyte activation and differentiation augment human endogenous retrovirus expression: Implications for inflammatory brain diseases. *Ann. Neurol.* **2001**, *50*, 434–442. [[CrossRef](#)]
17. Moyes, D.L.; Martin, A.; Sawcer, S.; Temperton, N.; Worthington, J.; Griffiths, D.J.; Venables, P.J. The distribution of the endogenous retroviruses HERVK113 and HERV-K115 in health and disease. *Genomics* **2005**, *86*, 337–341. [[CrossRef](#)]
18. de la Hera, B.; Varadé, J.; García-Montojo, M.; Lamas, J.R.; de la Encarnación, A.; Arroyo, R.; Fernández-Gutiérrez, B.; Alvarez-Lafuente, R.; Urcelay, E. Role of the human endogenous retrovirus HERV-K18 in autoimmune disease susceptibility: Study in the Spanish population and meta-analysis. *PLoS ONE* **2013**, *8*, e62090. [[CrossRef](#)]
19. Nexø, B.A.; Villesen, P.; Nissen, K.K.; Lindegaard, H.M.; Rossing, P.; Petersen, T.; Tarnow, L.; Hansen, B.; Lorenzen, T.; Hørslev-Petersen, K.; et al. Are human endogenous retroviruses triggers of autoimmune diseases? Unveiling associations of three diseases and viral loci. *Immunol. Res.* **2016**, *64*, 55–63. [[CrossRef](#)]
20. Garcia-Montojo, M.; Doucet-O’Hare, T.; Henderson, L.; Nath, A. Human endogenous retrovirus-K (HML-2): A comprehensive review. *Crit. Rev. Microbiol.* **2018**, *44*, 715–738. [[CrossRef](#)]
21. Buzdin, A.; Ustyugova, S.; Khodosevich, K.; Mamedov, I.; Lebedev, Y.; Hunsmann, G.; Sverdlöv, E. Human-specific subfamilies of HERV-K (HML-2) long terminal repeats: Three master genes were active simultaneously during branching of hominoid lineages. *Genomics* **2003**, *81*, 149–156. [[CrossRef](#)]
22. Wildschutte, J.H.; Williams, Z.H.; Montesion, M.; Subramanian, R.P.; Kidd, J.M.; Coffin, J.M. Discovery of unfixed endogenous retrovirus insertions in diverse human populations. *Proc. Natl. Acad. Sci. USA* **2016**, *113*, E2326–E2334. [[CrossRef](#)] [[PubMed](#)]
23. Tönjes, R.R.; Czauderna, F.; Kurth, R. Genome-wide screening, cloning, chromosomal assignment, and expression of full-length human endogenous retrovirus type K. *J. Virol.* **1999**, *73*, 9187–9195. [[CrossRef](#)] [[PubMed](#)]
24. Stauffer, Y.; Marguerat, S.; Meylan, F.; Ucla, C.; Sutkowski, N.; Huber, B.; Pelet, T.; Conrad, B. Interferon-alpha-induced endogenous superantigen. a model linking environment and autoimmunity. *Immunity* **2001**, *15*, 591–601. [[CrossRef](#)]

25. Sutkowski, N.; Conrad, B.; Thorley-Lawson, D.A.; Huber, B.T. Epstein-Barr virus transactivates the human endogenous retrovirus HERV-K18 that encodes a superantigen. *Immunity* **2001**, *15*, 579–589. [[CrossRef](#)]
26. Thorley-Lawson, D.A.; Schooley, R.T.; Bhan, A.K.; Nadler, L.M. Epstein-Barr virus superinduces a new human B cell differentiation antigen (B-LAST 1) expressed on transformed lymphoblasts. *Cell* **1982**, *30*, 415–425. [[CrossRef](#)]
27. Barth, M.; Gröger, V.; Cynis, H.; Staeger, M.S. Identification of human endogenous retrovirus transcripts in Hodgekin Lymphoma cells. *Mol. Biol. Rep.* **2019**, *46*, 1885. [[CrossRef](#)]
28. Tai, A.K.; O'Reilly, E.J.; Alroy, K.A.; Munger, K.L.; Huber, B.T.; Ascherio, A. Human endogenous retrovirus-K18 Env as a risk factor in multiple sclerosis. *Mult. Scler.* **2008**, *14*, 1175–1180. [[CrossRef](#)] [[PubMed](#)]
29. Beimforde, N.; Hanke, K.; Ammar, I.; Kurth, R.; Bannert, N. Molecular cloning and functional characterization of the human endogenous retrovirus K113. *Virology* **2008**, *371*, 216–225. [[CrossRef](#)]
30. Turner, G.; Barbulescu, M.; Su, M.; Jensen-Seaman, M.I.; Kidd, K.K.; Lenz, J. Insertional polymorphisms of full-length endogenous retroviruses in humans. *Curr. Biol.* **2001**, *11*, 1531–1535. [[CrossRef](#)]
31. Jern, P.; Sperber, G.O.; Blomberg, J. Definition and variation of human endogenous retrovirus H. *Virology* **2004**, *327*, 93–110. [[CrossRef](#)]
32. Jern, P.; Sperber, G.O.; Blomberg, J. Use of endogenous retroviral sequences (ERVs) and structural markers for retroviral phylogenetic interference and taxonomy. *Retrovirology* **2005**, *2*, 50. [[CrossRef](#)] [[PubMed](#)]
33. Hansen, D.T.; Petersen, T.; Christensen, T. Retroviral envelope proteins: Involvement in neuropathogenesis. *J. Neurol. Sci.* **2017**, *380*, 151–163. [[CrossRef](#)]
34. Laska, M.J.; Brudek, T.; Nissen, K.K.; Christensen, T.; Møller-Larsen, A.; Petersen, T.; Nexø, B.A. Expression of HERV-Fc1, a human endogenous retrovirus, is increased in patients with active multiple sclerosis. *J. Virol.* **2012**, *86*, 3713–3722. [[CrossRef](#)] [[PubMed](#)]
35. Benit, L.; Calteau, A.; Heidmann, T. Characterization of the low-copy HERV-Fc family: Evidence for recent integrations in primates of elements with coding envelope genes. *Virology* **2003**, *312*, 159–168. [[CrossRef](#)]
36. Hanke, K.; Kramer, P.; Seeher, S.; Beimforde, N.; Kurth, R.; Bannert, N. Reconstitution of the ancestral glycoprotein of human endogenous retrovirus k and modulation of its functional activity by truncation of the cytoplasmic domain. *J. Virol.* **2009**, *83*, 12790–12800. [[CrossRef](#)]
37. Heinrich, S.; Cameron, A.; Bourenkov, G.P.; Kiefersauer, R.; Huber, R.; Lindberg, I.; Bode, W.; Than, M.E. The crystal structure of the proprotein processing proteinase furin explains its stringent specificity. *Nat. Struct. Mol. Biol.* **2003**, *10*, 520–526. [[CrossRef](#)] [[PubMed](#)]
38. Apte, S.; Sanders, D.A. Effects of retroviral envelope-protein cleavage upon trafficking, incorporation, and membrane fusion. *Virology* **2010**, *405*, 214–224. [[CrossRef](#)] [[PubMed](#)]
39. Dewannieux, M.; Blaise, S.; Heidmann, T. Identification of a functional envelope protein from the HERV-K family of human endogenous retroviruses. *J. Virol.* **2005**, *79*, 15573–15577. [[CrossRef](#)] [[PubMed](#)]
40. Michaud, H.-A.; de Mulder, M.; SenGupta, D.; Deeks, S.G.; Martin, J.N.; Pilcher, C.D.; Hecht, F.M.; Sacha, J.B.; Nixon, D.F. Trans-activation, post-transcriptional maturation, and induction of antibodies to HERV-K (HML-2) envelope transmembrane protein in HIV-1 infection. *Retrovirology* **2014**, *11*, 10. [[CrossRef](#)] [[PubMed](#)]
41. Hanson, G.; Collier, J. Codon optimality, bias and usage in translation and mRNA decay. *Nat. Rev. Mol. Cell. Biol.* **2018**, *19*, 20–30. [[CrossRef](#)]
42. Nakaya, Y.; Takayuki, M. Dysfunction of bovine endogenous retrovirus K2 envelope glycoprotein is related to unsuccessful intracellular trafficking. *J. Virol.* **2014**, *88*, 6869–6905. [[CrossRef](#)] [[PubMed](#)]
43. Zhang, Y.J.; Pan, H.Y.; Gao, S.J. Reverse transcription slippage over the mRNA secondary structure of the LIP1 gene. *Biotechniques* **2001**, *31*, 1286–1294. [[CrossRef](#)]
44. Forrest, M.E.; Pinkard, O.; Martin, S.; Sweet, T.J.; Hanson, G.; Collier, J. Codon and amino acid content are associated with mRNA stability in mammalian cells. *PLoS ONE* **2020**, *15*, e0228730. [[CrossRef](#)]
45. Torrent, M.; Chalancon, G.; de Groot, N.S.; Wuster, A.; Babu, M.M. Cells alter their tRNA abundance to selectively regulate protein synthesis during stress conditions. *Sci. Signal.* **2018**, *11*, eaat6409. [[CrossRef](#)] [[PubMed](#)]
46. Zhou, Z.; Dang, Y.; Zhou, M.; Li, L.; Yu, C.H.; Fu, J.; Chen, S.; Liu, Y. Codon usage is an important determinant of gene expression levels largely through its effect on transcription. *Proc. Natl. Acad. Sci. USA* **2016**, *113*, E6117–E6125. [[CrossRef](#)] [[PubMed](#)]
47. Fu, J.; Dang, Y.; Counter, C.; Liu, Y. Codon usage regulates human KRAS expression at both transcriptional and translational levels. *J. Biol. Chem.* **2018**, *293*, 17929–17940. [[CrossRef](#)] [[PubMed](#)]

48. Tsai, K.; Jaguva Vasudevan, A.A.; Martinez Campos, C.; Emery, A.; Swanstrom, R.; Cullen, B.R. Acetylation of cytidine residues boosts HIV-1 gene expression by increasing viral RNA stability. *Cell Host Microbe*. **2020**, *28*, 306–312. [[CrossRef](#)]
49. Tsai, K.; Cullen, B.R. Epigenetic and epitranscriptomic regulation of viral replication. *Nat. Rev. Microbiol.* **2020**, *18*, 559–570. [[CrossRef](#)]
50. Caspar, J.; Schmoll, H.J.; Schnaidt, U.; Fonatsch, C. Cell lines of human germinal cancer. *Int. J. Androl.* **1987**, *10*, 105–113. [[CrossRef](#)]
51. Graham, F.L.; Smiley, J.; Russell, W.C.; Nairn, R.J. Characteristics of a human cell line transformed by DNA from human adenovirus type 5. *Gen. Virol.* **1977**, *36*, 59–74. [[CrossRef](#)] [[PubMed](#)]
52. Gluzman, Y. SV40-transformed simian cells support the replication of early SV40 mutants. *Cell* **1981**, *23*, 175–182. [[CrossRef](#)]
53. Bodmer, S.; Strommer, K.; Frei, K.; Siepl, C.; de Tribolet, N.; Heid, I.; Fontana, A. Immunosuppression and transforming growth factor-beta in glioblastoma. Preferential production of transforming growth factor-beta 2. *J. Immunol.* **1989**, *143*, 3222–3229. [[PubMed](#)]
54. Giard, D.J.; Aaronson, S.A.; Todaro, G.J.; Arnstein, P.; Kersey, J.H.; Dosik, H.; Parks, W.P. In vitro cultivation of human tumors: Establishment of cell lines derived from a series of solid tumors. *J. Natl. Cancer. Inst.* **1973**, *51*, 1417–1423. [[CrossRef](#)] [[PubMed](#)]
55. Laemmli, U.K. Cleavage of structural proteins during the assembly of the head of bacteriophage T4. *Nature* **1970**, *227*, 680–685. [[CrossRef](#)]
56. Livak, K.J.; Schmittgen, T.D. Analysis of relative gene expression data using real-time quantitative PCR and the 2⁻(Delta Delta C(T)) Method. *Methods* **2001**, *25*, 402–408. [[CrossRef](#)]
57. Zuker, M. Mfold web server for nucleic acid folding and hybridization prediction. *Nucleic Acids Res.* **2003**, *31*, 3406–3415. [[CrossRef](#)]

Publisher's Note: MDPI stays neutral with regard to jurisdictional claims in published maps and institutional affiliations.



© 2020 by the authors. Licensee MDPI, Basel, Switzerland. This article is an open access article distributed under the terms and conditions of the Creative Commons Attribution (CC BY) license (<http://creativecommons.org/licenses/by/4.0/>).

Supplementary Data for

Formation of HERV-K and HERV-Fc1 envelope family members is suppressed on transcriptional and translational level

Victoria Gröger, Lisa Wieland, Marcel Naumann, Ann-Christin Meinecke, Beate Meinhardt, Steffen Rossner, Christian Ihling, Alexander Emmer, Martin S. Staege and Holger Cynis

This file contains:

- Supplementary Table S1-S4
- Supplementary Fig. S1-S11

Supplementary Table S1. List of Primers for cloning HERV sequences. The primer sequences show restriction sites in bold and the respective tag underlined.

Primer name	Sequence 5'-3'	Restriction site
<i>Fc1_mut_C705T_for</i> <i>Fc1_mut_C705T_rev</i>	CCTAGTCCGCCACGGGGCTCGCCTTG CAAGGCGAGCCCCGTGGCGGACTAGG	
<i>Fc1_mut_A438T_for</i> <i>Fc1_mut_A438T_rev</i>	CCTAGTCCGCCACGGGGCTCGCCTTG CAAGGCGAGCCCCGTGGCGGACTAGG	
<i>pcDNA_Fc1-Flag_for</i> ; <i>pcDNA_Fc1-EGFP_for</i>	TATAGGATCCATGGGCAGACCTTCCCCAC	<i>Bam</i> HI
<i>pcDNA_Fc1-Flag_rev</i> ; <i>pcDNA_coFc1-Flag_rev</i>	TATAGCGGCCGCTCACTTGTTCGTCATCGTCTT <u>TGTAGTCTCTGGCTGCTTCCTGCTG</u>	<i>Not</i> I
<i>pcDNA_Fc1-EGFP_rev</i>	TATAGCGGCCGCTTTTCTGGCTGCTTCCTGCTG	<i>Not</i> I
<i>pcDNA_coFc1-Flag_for</i>	TATAGGATCCATGGCCCCGCCCTTAC	<i>Bam</i> HI
<i>pcDNA_K18-Flag_for</i>	TATAAAGCTTATGGTAACACCAGTCACATG	<i>Hind</i> III
<i>pcDNA_K18-Flag_rev</i>	TATAGCGGCCGCTCACTTGTTCGTCATCGTCTT <u>TGTAGTCTGGCCCGTTCTCGATGTC</u>	<i>Not</i> I
<i>pcDNA_coK18-Flag_for</i>	ATATAAAGCTTGCCGCCACCATGGTGACACCT GTGACTTG	<i>Hind</i> III
<i>pcDNA_coK113-Flag_for</i> ; <i>pcDNA_coK18*-Flag_for</i>	ATGCATCTAGATAAAGCTTGCCGCCACCATG	<i>Hind</i> III
<i>pcDNA_coK113-Flag_rev</i>	CGATGCGGCCGCTTACTTATCGTCATC	<i>Not</i> I
<i>pcDNA_coK18*-Flag_rev</i> ; <i>pcDNA_coK18-Flag_rev</i>	CGATGCGGCCGCTTATTTATCGTCATC	<i>Not</i> I

Supplementary Table S2. Antibodies used for Western Blot analysis

Name	Type	Organism	Dilution	Manufacturer
anti-DYKDDDDK (FLAG) tag	primary	rabbit	1:1000	Cell signaling, Cambridge, Great Britain
anti-HERV-K TM HERM1811-5	primary	mouse	1:1000	Austral Biologicals, San Ramon, CA, USA
Anti-HERV-K SU HERM1821-5	primary	mouse	1:1000	Austral Biologicals, San Ramon, CA, USA
anti- β -Aktin	primary	rabbit	1:1000	Cell signaling, Cambridge, Great Britain
anti-mouse IgG-HRP	secondary	horse	1:2000	Cell signaling, Cambridge, Great Britain
anti-rabbit IgG-HRP	secondary	goat	1:2000	Cell signaling, Cambridge, Great Britain

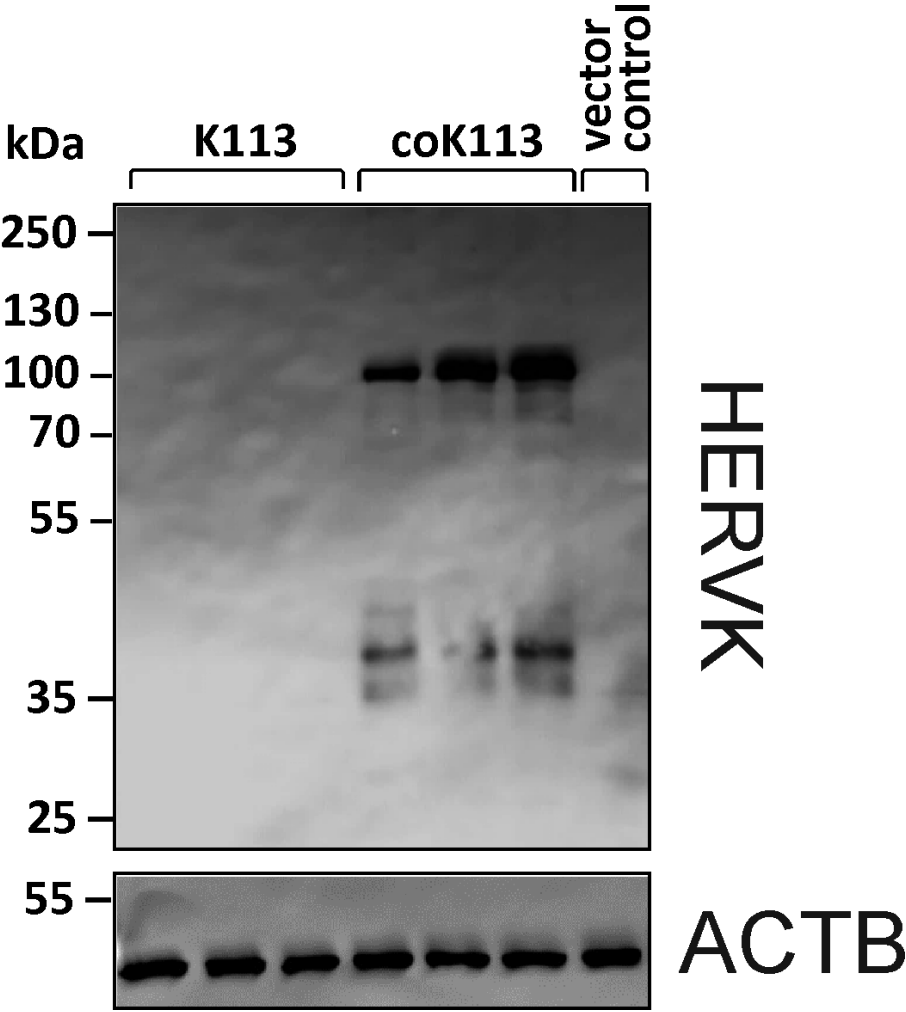
Supplementary Table S3. Antibodies used for immunofluorescence and FACS analysis

Antibody	Dilution	Manufacturer
anti-DYKDDDDK (FLAG) tag	1:800	Cell signaling, Cambridge, Great Britain
anti-HERV-K TM HERM1811-5	1:500	Austral Biologicals, San Ramon, CA, USA
anti-calnexin	1:50	Cell signaling, Cambridge, Great Britain
anti-golgin-97	1:100	Cell signaling, Cambridge, Great Britain
anti-GP73	1:50	Santa Cruz, Heidelberg, Germany
anti-tubulin- α	1:250	BioLegend, San Diego, USA
Cy TM 2 anti-rabbit IgG	1:200	Dianova, Hamburg, Germany
Cy TM 2 anti-mouse IgG	1:200	Dianova, Hamburg, Germany
Cy TM 3 anti-rabbit IgG	1:400	Dianova, Hamburg, Germany
Cy TM 3 anti-mouse IgG	1:200	Dianova, Hamburg, Germany

Supplementary Table S4. Primer sequences for qRT PCR

Target gene	Sequence of forward primer 5'-3'	Sequence of reverse primer 5'-3'
<i>DDIT3</i>	TTGCCTTTCTCCTTCGGGAC	TGATTCTTCCTCTTCATTTCC
<i>APOBEC3B</i>	CCATCCTCTATGGTCGGAGC	GAGGCTTCAAATACACCTGGC
<i>APOBEC3G</i>	GCATCGTGACCAGGAGTATGA	GTCAGGGTAACCTTCGGGT
<i>MOV10</i>	GGGCCAGTGTTTCGAGAGTTT	TCTTGGTGACGTAGGCCAGA
<i>HSPA5</i>	GAACGTCTGATTGGCGATGC	TCAACCACCTTGAACGGCAA
<i>sXBP1</i>	CTGAGTCCGCAGCAGGTG	ATGACTGGGTCCAAGTTGTCC
<i>ATF4</i>	TCCAACAACAGCAAGGAGGAT	TCCAACGTGGTCAGAAGGTC
<i>GAPDH</i>	ACCCAGAAGACTGTGGATGG	TTCTAGACGGCAGGTCAGGT
<i>K113 ENV</i>	CCTTGTGTGCCTGTTTTGTC	ATCTCTCTTGCTTTTCCCACA
<i>coK113 ENV</i>	TGTCTGCTGCTGGTGTATAGG	ATCTGGTCCCTTTTGCTTTTGC
<i>Neo^R</i>	AGACAATCGGCTGCTCTGAT	AGTGACAACGTGAGCACAG
<i>HPRT1</i>	ACCAGTCAACAGGGGACATAA	CTTCGTGGGGTCCTTTTCACC

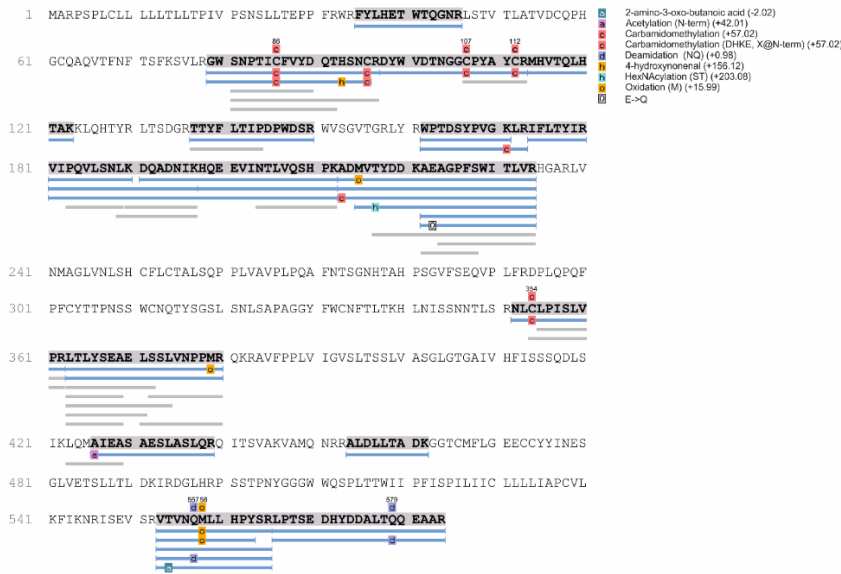
Supplementary Figure S1



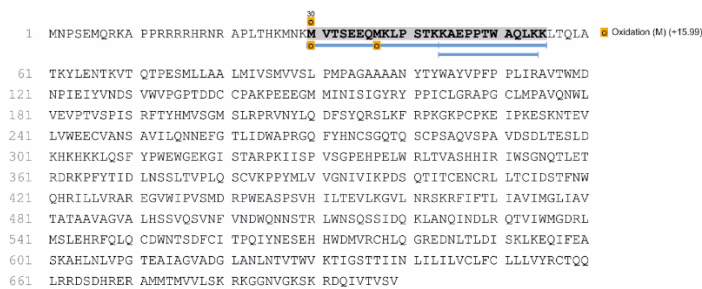
Supplementary Figure S1. Representative Western Blot Image showing the expression of K113 and codon-optimized coK113 in HEK 293 cells in relation to the loading control ACTB (beta-Actin).

Supplementary Figure S2

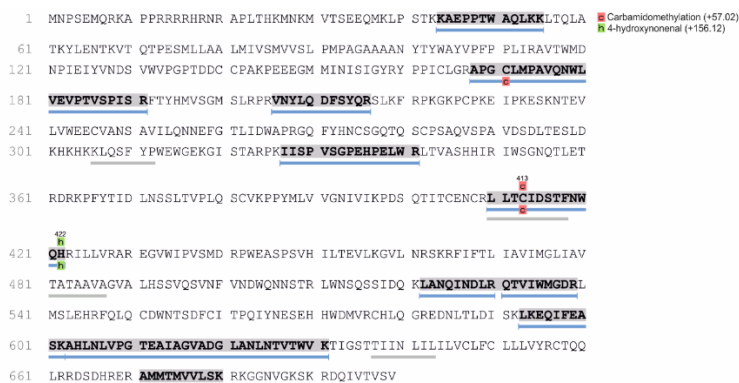
a



b

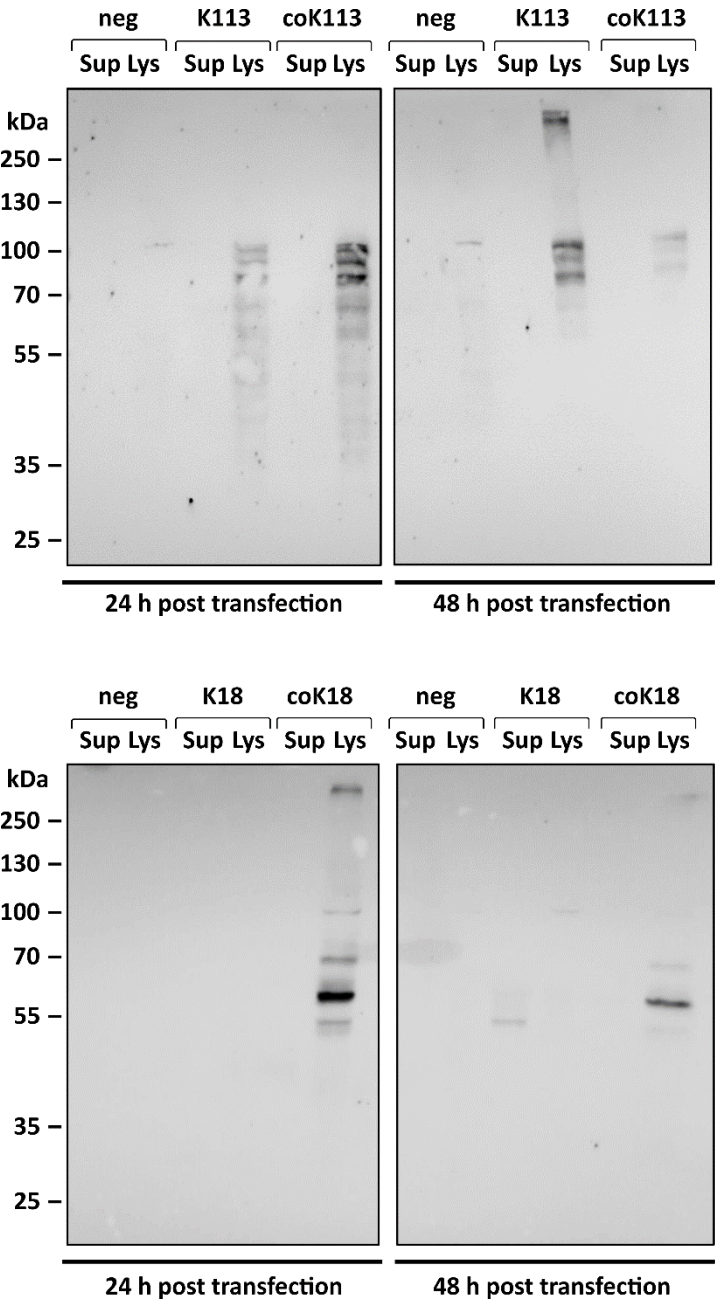


c



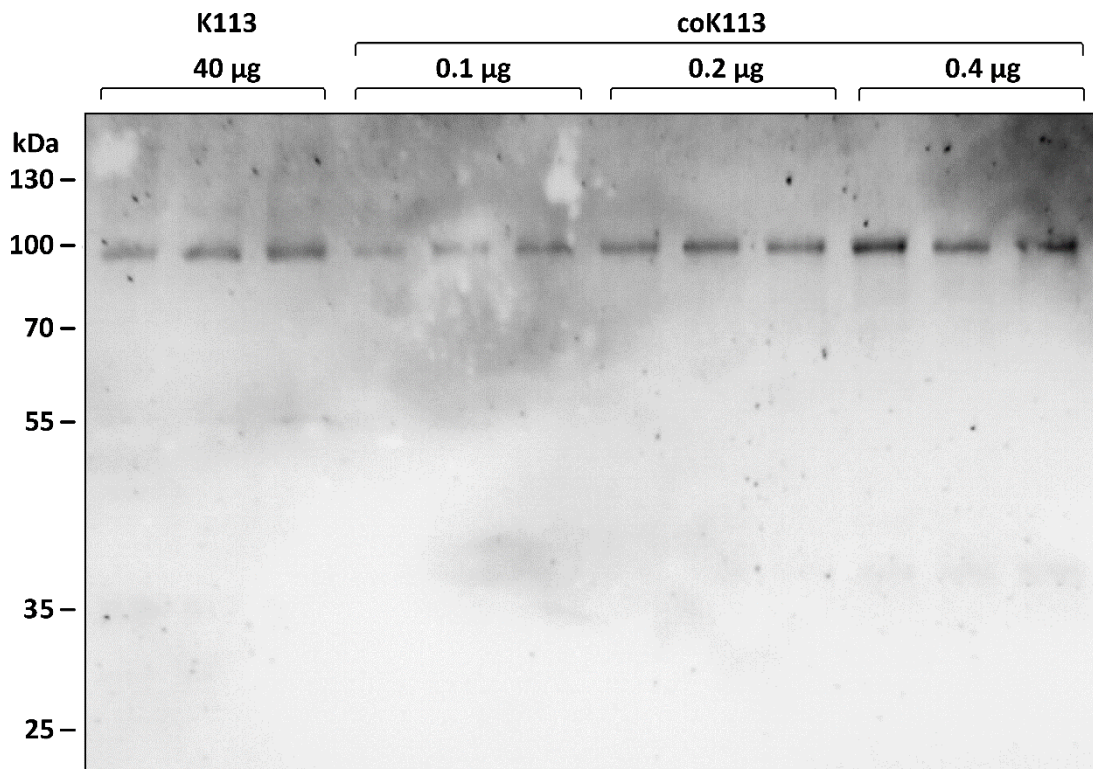
Supplementary Figure S2. Sequence coverage for the envelope proteins of the (a) endogenous retrovirus group Fc1 (UniProt: P60507) identified in HEK293 cells expressing coFc1, (b) endogenous retrovirus group K member 113 (UniProt: Q902F9) identified in HEK293 cells expressing K113 and (c) endogenous retrovirus group K member 113 (UniProt: Q902F9) identified in HEK293 cells expressing coK113.

Supplementary Figure S3



Supplementary Figure S3. Time-dependent expression of WT and codon-optimized variants of K113 and K18. Cell harvest was 24h and 48h post-transfection. For each time-point, 40 µg of cell lysate (Lys) and 20 µl of cell culture supernatant (Sup) were analyzed using a HERV-K antibody specific for the surface unit. HERV expression was compared to empty vector control (neg).

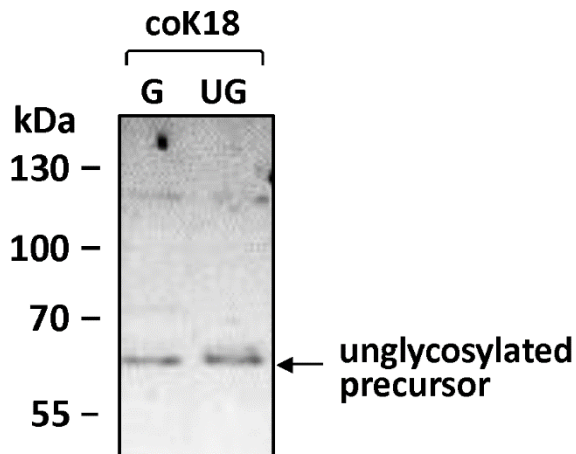
Supplementary Figure S4



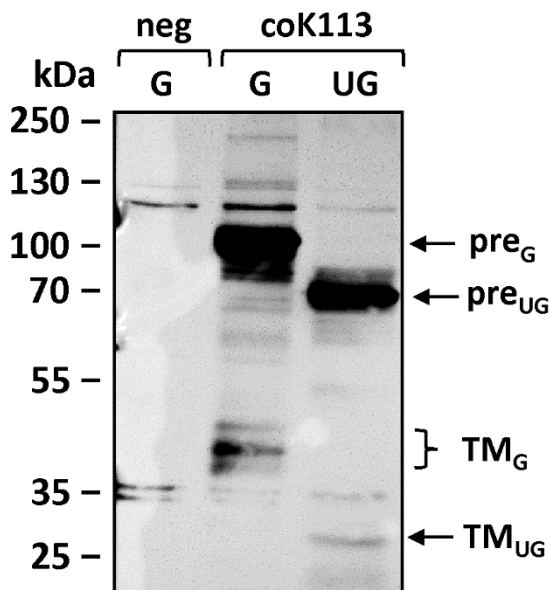
Supplementary Figure S4. Entire image of the blot used for densitometric quantification of expression increase caused by codon-optimization and depicted as Fig. 1d in the main body of the manuscript.

Supplementary Figure S5

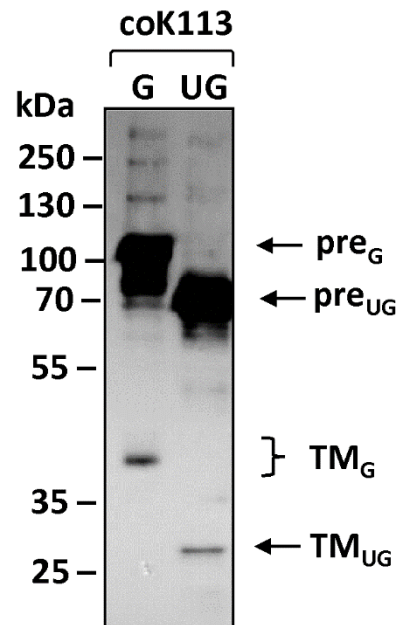
a



b

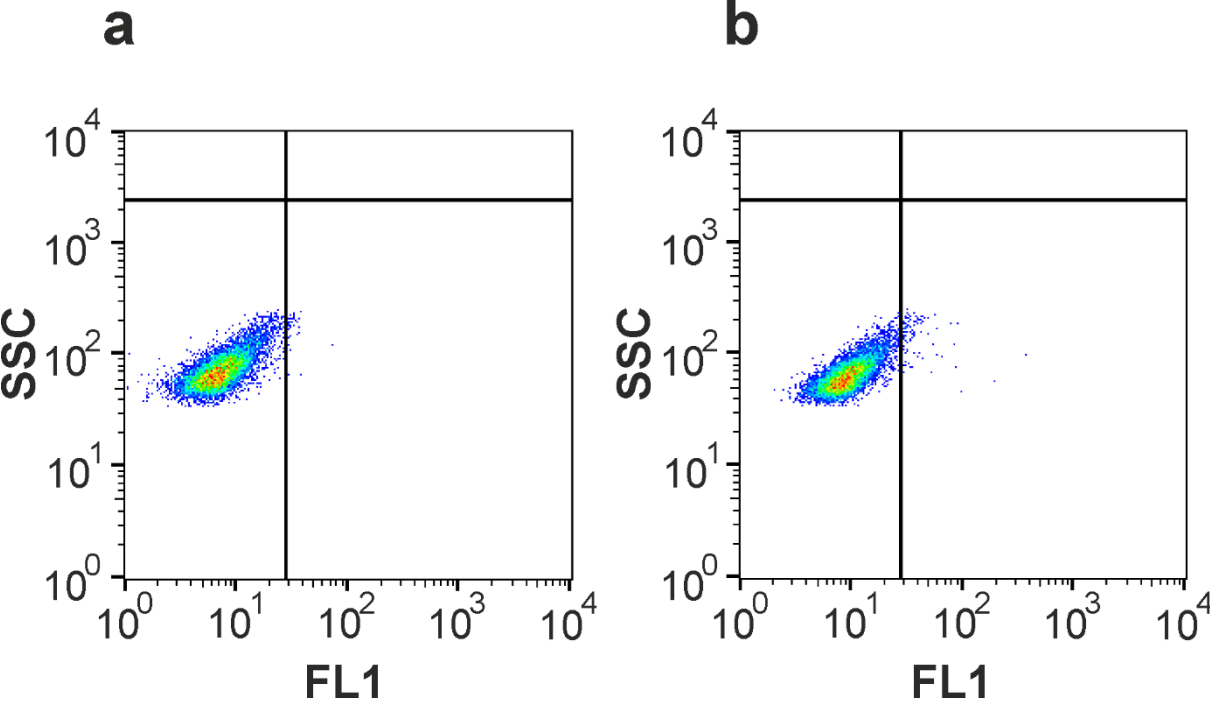


c



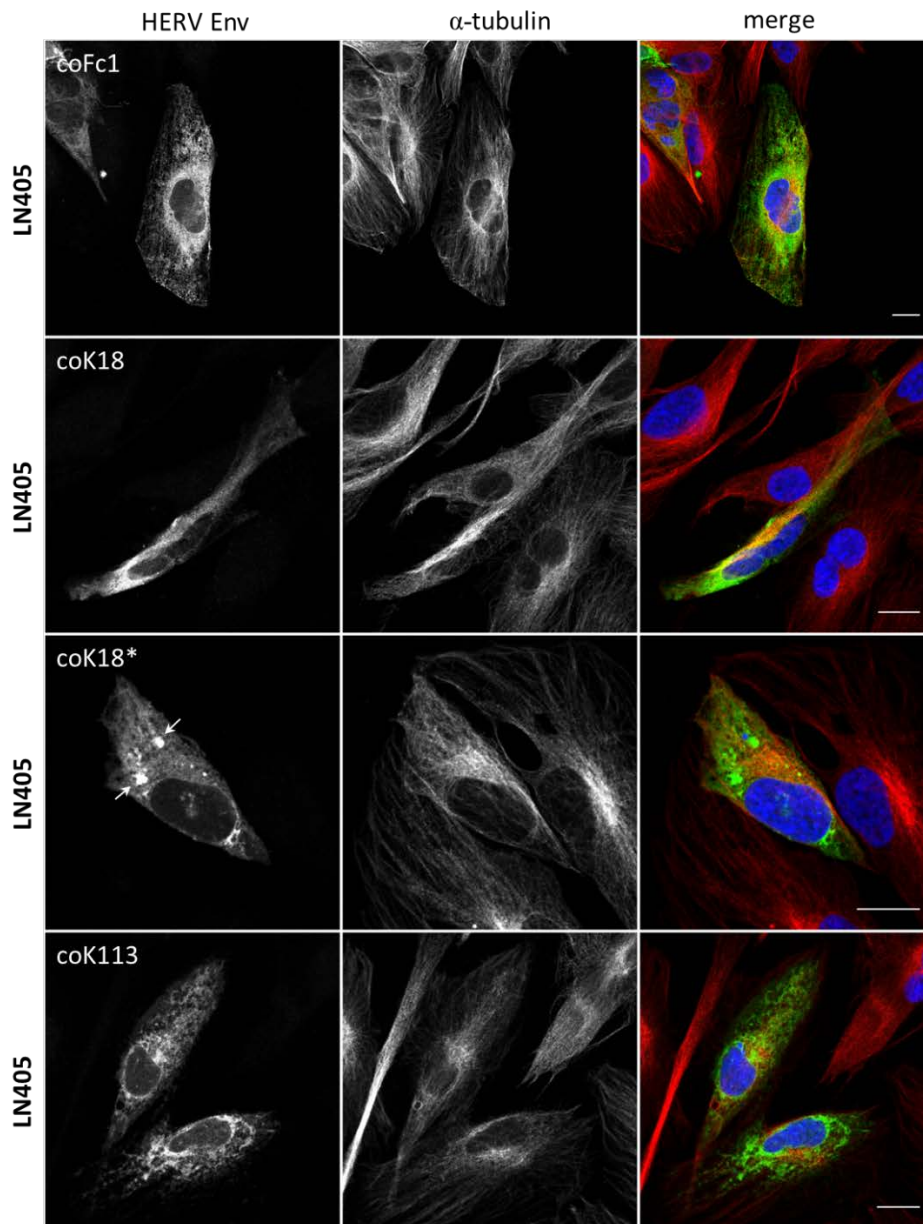
Supplementary Figure S5. (a) No glycosylation of HERV-K18 ENV without signal peptide in transfected HEK293 cells. Cell lysates were analyzed via Western blot 24 h after transient transfection of HEK293 cells with expression plasmids containing codon-optimized (co) sequence of the envelope proteins of HERV-K18 and subsequent treatment with (UG) or without (G) de-glycosylating agent PNGase F. Each lane was loaded with 20 μ g total protein. (b) and (c) The cleavage of the precursor (pre) of coK113 into SU and TM is visible, whereby only the precursor and TM were detected by the anti-HERV-K TM HERM1811-5 antibody (two independent experiments). In (b) empty vector-transfected cells served as negative control (neg).

Supplementary Figure S6



Supplementary Figure S6. Dot plots of HEK293 as determined by FACS analysis. (a) Native HEK293 cells were compared to (b) HEK293 cells incubated with Cy2-labeled secondary antibody goat anti-mouse IgG. No unspecific adhesion to HEK293 cells was observed.

Supplementary Figure S7



Supplementary Figure S7. Localization of HERV ENV with α -tubulin in transfected LN405 cells. Fluorescence microscopic images showing the subcellular localization of specified HERV ENV and α -tubulin in transiently transfected LN405 cells. The merge image is a z-projection (maximum intensity) of the 3 recorded channels (green: HERV ENV, red: α -tubulin, blue (DAPI): cell nucleus). Pixels with red and green fluorescence appear yellow. The detection of the envelope proteins was performed using anti-HERV-K-TM antibody HERM1811-5 (coK18, coK18*, coK113) or EGFP tag (Fc1). The α -tubulin was visualized by an anti-tubulin- α antibody. Scale bar: 20 μ m.

Supplementary Figure S8

a

```

1  MKLSLVAAML LLLSAARAE EKKKEDVGTV VGIDLGTYS CVGVFKNGR V EIIANDQGNR
61  ITPSYVAFTP EGERLIGDAA KNQLTSNPN TVFDKRLIG R TWNDPSVQQ DIKFLPFKVV
121  EKKTKPYIQV DIGGGQKTF APEEISAMVL TKMKETAEAY LGRKVTHAVV TVPAYFNDAQ
181  RQATK DAGTI AGLNVMRIIN EPTAAAIAYG LDKRREGKNI LVFDLGGGTF DVSLITDNG
241  VFEVATNGD THLGGEDFDQ RVMEHFIRLY KKRKTKDVRK DNRAVQKLRR EVEKAKRALS
301  SOHQARIEIE SFYEGEDFSE TLTRAKFPEL NMDLFRSTMK PVQRVLESDS LKKSIDIEIV
361  LVGGSTRIPK IQQLVKEFFN GKEPSRGINP DEAVAYGAAV QAGVLSGDQD TGDVLVLDVC
421  PLTLGIEITVG GVMTKLIPRN TVVPTKRSQI FSTASDNQPT VTIKRYEGER PLTKDNHLLG
481  TFDLTGIPPA PRGVVPIEVT FEIDVNGILR VTAEDKGTGN KNKITITNDQ NRLTPEEIER
541  MVNDAERFAE EDKRLKERID TRNELESYAY SLKNQIGDKE PLGGKLSSED KETMEKAVEE
601  KIEWLESHQD ADIEDFKAKK KELEEIVQPI ISKLYGSAGP PPTGEEDTAE KDEE
    
```

b

```

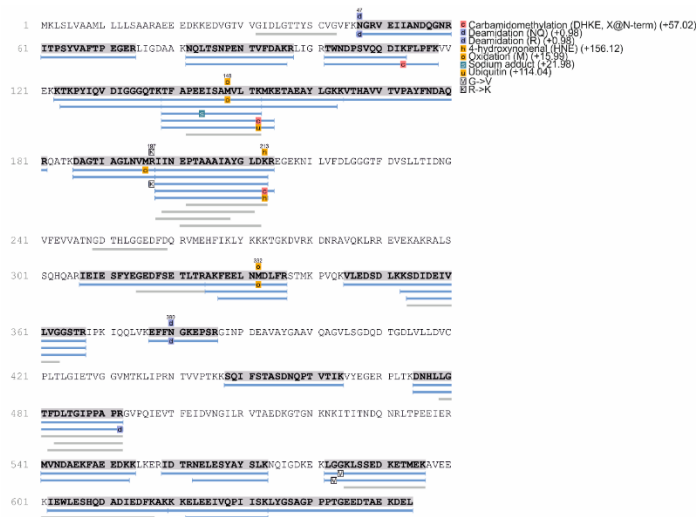
1  MKLSLVAAML LLLSAARAE EKKKEDVGTV VGIDLGTYS CVGVFKNGR V EIIANDQGNR
61  ITPSYVAFTP EGERLIGDAA KNQLTSNPN TVFDKRLIG R TWNDPSVQQ DIKFLPFKVV
121  EKKTKPYIQV DIGGGQKTF APEEISAMVL TKMKETAEAY LGRKVTHAVV TVPAYFNDAQ
181  RQATK DAGTI AGLNVMRIIN EPTAAAIAYG LDKRREGKNI LVFDLGGGTF DVSLITDNG
241  VFEVATNGD THLGGEDFDQ RVMEHFIRLY KKRKTKDVRK DNRAVQKLRR EVEKAKRALS
301  SOHQARIEIE SFYEGEDFSE TLTRAKFPEL NMDLFRSTMK PVQRVLESDS LKKSIDIEIV
361  LVGGSTRIPK IQQLVKEFFN GKEPSRGINP DEAVAYGAAV QAGVLSGDQD TGDVLVLDVC
421  PLTLGIEITVG GVMTKLIPRN TVVPTKRSQI FSTASDNQPT VTIKRYEGER PLTKDNHLLG
481  TFDLTGIPPA PRGVVPIEVT FEIDVNGILR VTAEDKGTGN KNKITITNDQ NRLTPEEIER
541  MVNDAERFAE EDKRLKERID TRNELESYAY SLKNQIGDKE PLGGKLSSED KETMEKAVEE
601  KIEWLESHQD ADIEDFKAKK KELEEIVQPI ISKLYGSAGP PPTGEEDTAE KDEE
    
```

c

```

1  MKLSLVAAML LLLSAARAE EKKKEDVGTV VGIDLGTYS CVGVFKNGR V EIIANDQGNR
61  ITPSYVAFTP EGERLIGDAA KNQLTSNPN TVFDKRLIG R TWNDPSVQQ DIKFLPFKVV
121  EKKTKPYIQV DIGGGQKTF APEEISAMVL TKMKETAEAY LGRKVTHAVV TVPAYFNDAQ
181  RQATK DAGTI AGLNVMRIIN EPTAAAIAYG LDKRREGKNI LVFDLGGGTF DVSLITDNG
241  VFEVATNGD THLGGEDFDQ RVMEHFIRLY KKRKTKDVRK DNRAVQKLRR EVEKAKRALS
301  SOHQARIEIE SFYEGEDFSE TLTRAKFPEL NMDLFRSTMK PVQRVLESDS LKKSIDIEIV
361  LVGGSTRIPK IQQLVKEFFN GKEPSRGINP DEAVAYGAAV QAGVLSGDQD TGDVLVLDVC
421  PLTLGIEITVG GVMTKLIPRN TVVPTKRSQI FSTASDNQPT VTIKRYEGER PLTKDNHLLG
481  TFDLTGIPPA PRGVVPIEVT FEIDVNGILR VTAEDKGTGN KNKITITNDQ NRLTPEEIER
541  MVNDAERFAE EDKRLKERID TRNELESYAY SLKNQIGDKE PLGGKLSSED KETMEKAVEE
601  KIEWLESHQD ADIEDFKAKK KELEEIVQPI ISKLYGSAGP PPTGEEDTAE KDEE
    
```

d



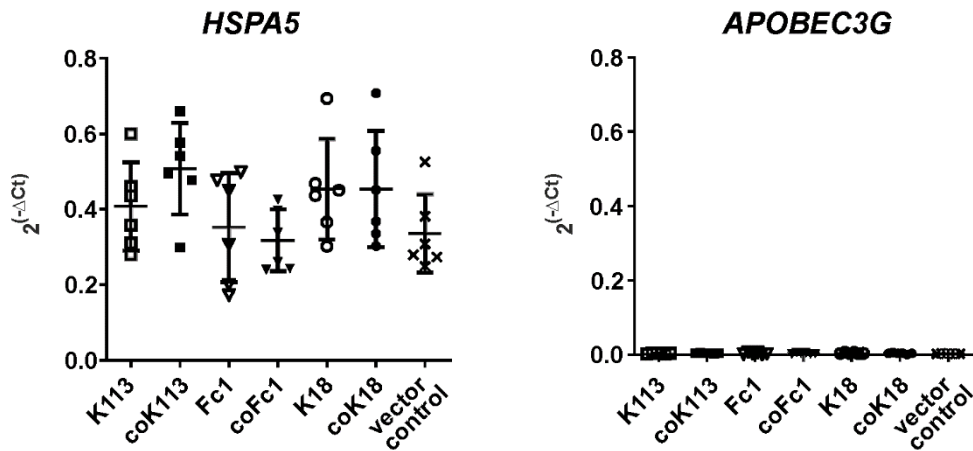
e



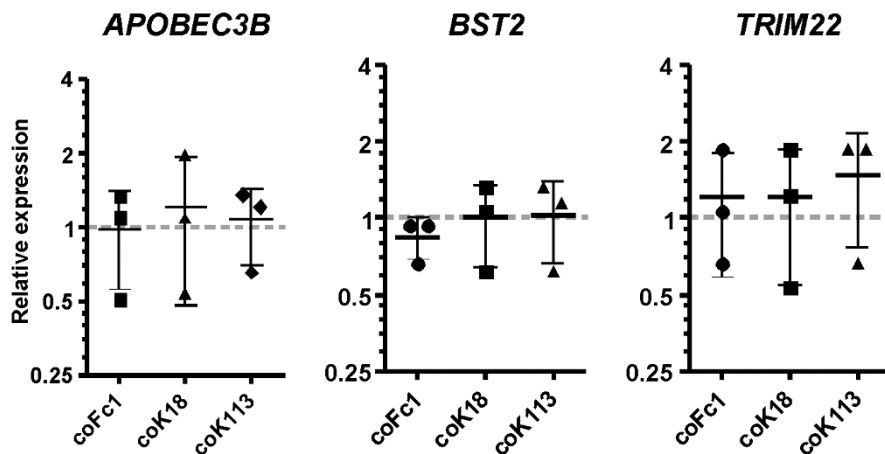
Supplementary Figure S8. Sequence coverage for the endoplasmic reticulum chaperone BiP (UniProt: P11021) identified in (a) the empty vector (pcDNA3.1)-expressing HEK293 cells, (b) K113-expressing HEK293 cells, (c) coK113-expressing HEK293 cells, (d) Fc1-expressing HEK293 cells and (e) coFc1-expressing HEK293 cells.

Supplementary Figure S9

a

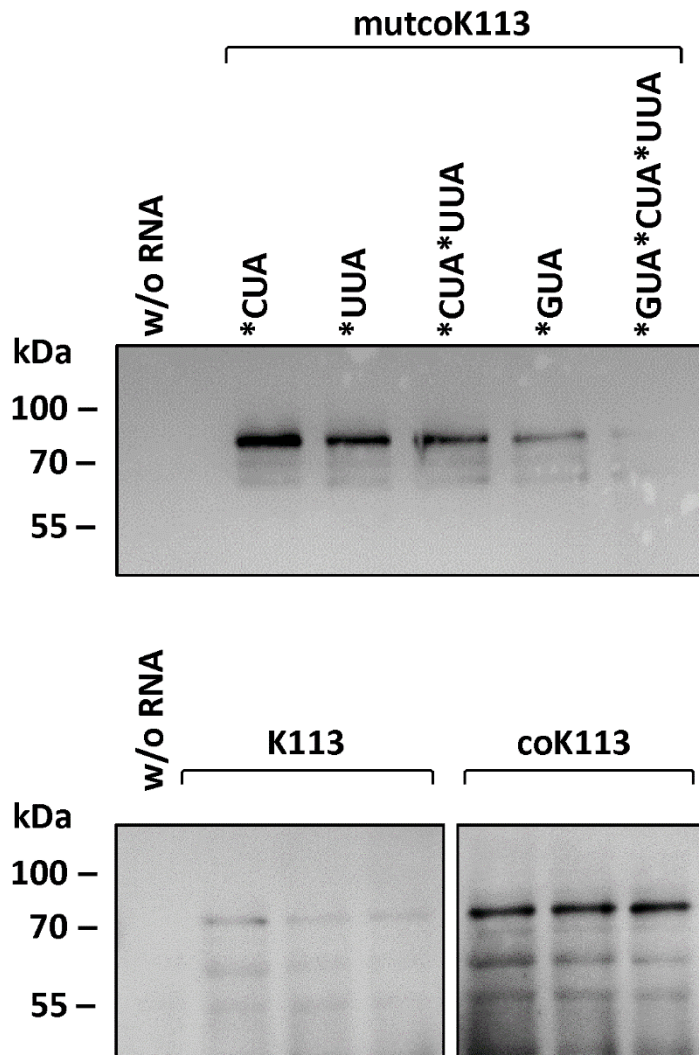


b



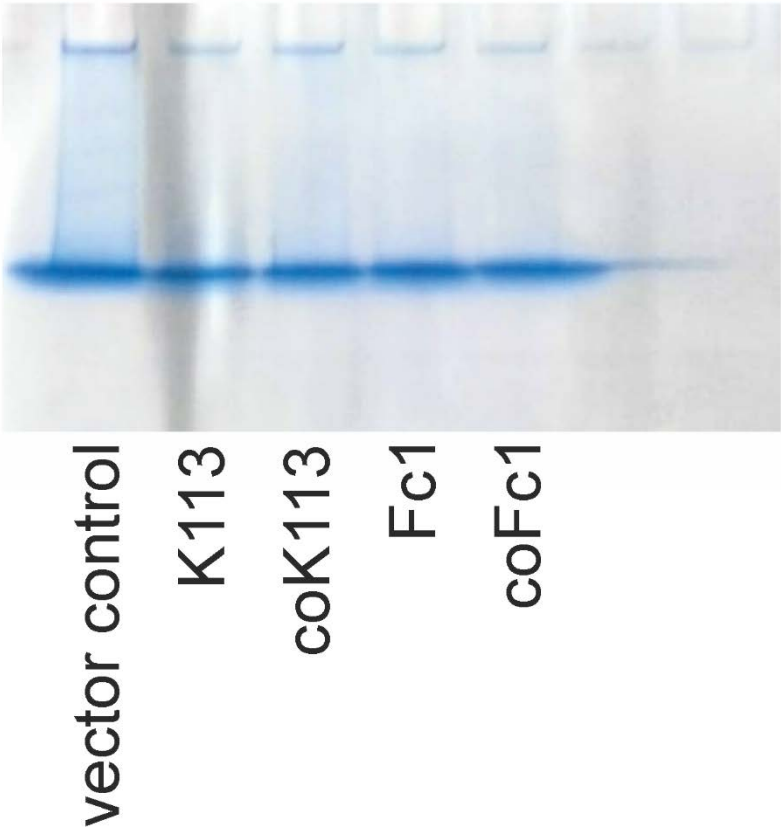
Supplementary Figure S9. (a) Comparison of $2^{-\Delta Ct}$ values for *HSPA5* and *APOBEC3G* in HEK293 cells. Expression of *HSPA5* and *APOBEC3G* was analyzed in transfected HEK293 cells by quantitative PCR. The expression was normalized to *GAPDH*. (b) Relative gene expression of additional genes involved in viral defense mechanisms after transfection of codon-optimized HERV envelope protein sequences studied in COS-7 cells (*APOBEC3B*) or HEK293 cells (*BST2*, *TRIM22*). The expression was normalized to *GAPDH* and relative to empty vector-transfected cells (dashed grey line)

Supplementary Figure S10



Supplementary Figure S10. Cell-free expression of HERV-K113 envelope variants. 4 μ g of transcribed mRNA of K113 envelope sequences were translated into protein using reticulocyte lysate from New Zealand white rabbits including mixture of all components necessary for translation. Three independent experiments of wildtype and codon-optimized and one experiment of mutant variants of codon-optimized K113 envelope protein are shown. A translation reaction without RNA served as negative control. An equal aliquot of all reactions was loaded for Western blotting. The non-glycosylated precursor of K113 ENV was observed at 80 kDa using anti-HERV-K-TM (HERM1811-5) antibody. Densitometric analysis of expression level is shown in Figure 7 of the manuscript.

Supplementary Figure S11



Supplementary Figure S11. 6 % PAA stacking gel used to focus cellular lysates that were subsequently applied to tryptic digestion and LC-MS/MS analysis.

2.2. Overexpression of Endogenous Retroviruses and Malignancy Markers in Neuroblastoma Cell Lines by Medium-Induced Microenvironmental Changes

2.2.1. Zusammenfassung

Im Säuglings- und Kindesalter ist das Neuroblastom (NB) der am häufigsten auftretende solide Tumor außerhalb des Zentralnervensystems. NB sind biologisch sehr heterogen. Bei Patient:innen mit fortgeschrittenen, metastasierenden Tumoren sind Therapieversagen und eine schlechte Prognose oft durch Resistenzen gegen Chemo- oder Immuntherapie gekennzeichnet. Daher scheint die Identifizierung robuster Biomarker für das Verständnis der Tumorphysion und die Entwicklung wirksamer Therapien unerlässlich. In dieser Studie haben wir die Expression von HERVs als potenzielle Zielstrukturen in NB-Zelllinien während der Inkubation in Standard-, sowie Stammzell-Medium mit und ohne FBS-Serum untersucht. Mittels quantitativer PCR wurde beobachtet, dass die relative Expression der HERV-K (HML-2)-Familie und von HERV-W1 *ENV* in allen drei untersuchten NB-Zelllinien durch Inkubation in Serum-depletiertem Stammzell-Medium erhöht war. Mittels eines Mapping-Verfahrens mit einem in unserem Labor designten Virus-Transkriptom stellten wir die Aktivierung von drei endogenen Retrovirus-Elementen: HERV-R *ENV* (ERV3-1), HERV-E1 und HERV-Fc2 *ENV* (ERVFC1-1) in NB-Linien in Serum-freiem Stammzell-Medium fest. Bekannte Malignitätsmarker in NB, z. B. onkogenes *MYC* oder *MYCN*, wurden in den drei untersuchten NB-Zelllinien sehr heterogen exprimiert, wobei sie durch das Serum-freie Stammzell-Medium in den jeweiligen Zelllinien ebenfalls hochreguliert wurden. Darüber hinaus veränderten SiMa-Zellen in Stammzell-Medium ihren Phänotyp von locker adhären Monolayern zu schwach proliferierenden traubenartigen Zellaggregaten in Suspension, was mit einer verstärkten CD133-Expression einherging. Interessanterweise war die Überexpression von HERVs sowohl in der quantitativen PCR-, als auch in der Analyse mittels RNAseq mit einem signifikanten Anstieg des Immun-Checkpoint-Moleküls CD200 verbunden, was auf einen Tumor-Escape-Mechanismus in NB-Zelllinien hindeuten könnte.

2.2.2. Darlegung des Eigenanteils und Zitierung

Im Folgenden ist der experimentelle und schriftliche Eigenanteil aller Autoren prozentual angegeben und die Beteiligung mehrerer Personen an der Veröffentlichung durch einen Betreuer bestätigt.

Publikation II:

Wieland, L., Engel, K., Volkmer, I., Krüger, A., Posern, G., Kornhuber, M. E., Staege, M. S., & Emmer, A. (2021). Overexpression of Endogenous Retroviruses and Malignancy Markers in Neuroblastoma Cell Lines by Medium-Induced Microenvironmental Changes. *Frontiers in oncology, 11*, 637522. <https://doi.org/10.3389/fonc.2021.637522>

Tabelle 3: Übersicht zu den Beiträgen aller Autoren der Publikation II.

	Entwurf (Design)	Umsetzung (Implementation)	Auswertung (Analysis)	Schreiben (Writing)
Wieland, L.	40 %	80 %	80 %	65 %
Engel, K.		10 %	10 %	
Volkmer, I.	5 %	5 %		
Krüger, A.		5 %		5 %
Posern, G.				10 %
Kornhuber, M. E.	5 %			5 %
Staege, M. S.	40 %		10 %	10 %
Emmer, A.	10 %			5 %

Datum: 15.03.2024



Lisa Wieland

Dr. med. Alexander Emmer

2.2.3. Bestätigung des Betreuers der Dissertation von Frau Lisa Wieland

Hiermit bestätige ich als Betreuer der o. g. Dissertation, dass die gemeinsame Arbeit mehrerer Personen an der Arbeit durch den Forschungsgegenstand gerechtfertigt ist.

Mit freundlichen Grüßen,



Dr. med. Alexander Emmer

Datum: 15.03.2024

Nachfolgend sind die Publikation und die supplementären Daten aufgeführt.



Overexpression of Endogenous Retroviruses and Malignancy Markers in Neuroblastoma Cell Lines by Medium-Induced Microenvironmental Changes

Lisa Wieland^{1,2}, Kristina Engel², Ines Volkmer², Anna Krüger², Guido Posern³, Malte E. Kornhuber¹, Martin S. Staeger^{2*} and Alexander Emmer¹

OPEN ACCESS

Edited by:

Tara Patricia Hurst,
Birmingham City University,
United Kingdom

Reviewed by:

Alessandro Giovino,
National Research Council (CNR), Italy
Hervé Perron,
Geneuro Innovation, France

*Correspondence:

Martin S. Staeger
martin.staeger@uk-halle.de

Specialty section:

This article was submitted to
Cancer Molecular Targets
and Therapeutics,
a section of the journal
Frontiers in Oncology

Received: 03 December 2020

Accepted: 09 April 2021

Published: 07 May 2021

Citation:

Wieland L, Engel K, Volkmer I,
Krüger A, Posern G, Kornhuber ME,
Staeger MS and Emmer A (2021)
Overexpression of Endogenous
Retroviruses and Malignancy
Markers in Neuroblastoma Cell
Lines by Medium-Induced
Microenvironmental Changes.
Front. Oncol. 11:637522.
doi: 10.3389/fonc.2021.637522

¹ Department of Neurology, Medical Faculty, Martin Luther University Halle-Wittenberg, Halle, Germany, ² Department of Surgical and Conservative Pediatrics and Adolescent Medicine, Medical Faculty, Martin Luther University Halle-Wittenberg, Halle, Germany, ³ Institute for Physiological Chemistry, Medical Faculty, Martin Luther University Halle-Wittenberg, Halle, Germany

Neuroblastoma (NB) is the commonest solid tumor outside the central nervous system in infancy and childhood with a unique biological heterogeneity. In patients with advanced, metastasizing neuroblastoma, treatment failure and poor prognosis is often marked by resistance to chemo- or immunotherapy. Thus, identification of robust biomarkers seems essential for understanding tumor progression and developing effective therapy. Here, we have studied the expression of human endogenous retroviruses (HERV) as potential targets in NB cell lines during stem-cell medium-induced microenvironmental change. Quantitative PCR revealed that relative expression of the HERV-K family and HERV-W1 ENV were increased in all three NB cell lines after incubation in stem-cell medium. Virus transcriptome analyses revealed the transcriptional activation of three endogenous retrovirus elements: HERV-R ENV (ERV3-1), HERV-E1 and HERV-Fc2 ENV (ERVFC1-1). Known malignancy markers in NB, e.g. proto-oncogenic MYC or MYCN were expressed highly heterogeneously in the three investigated NB cell lines with up-regulation of MYC and MYCN upon medium-induced microenvironmental change. In addition, SiMa cells exclusively showed a phenotype switching from loosely-adherent monolayers to low proliferating grape-like cellular aggregates, which was accompanied by an enhanced CD133 expression. Interestingly, the overexpression of HERV was associated with a significant elevation of immune checkpoint molecule CD200 in both quantitative PCR and RNA-seq analysis suggesting tumor escape mechanism in NB cell lines after incubation in serum-free stem cell medium.

Keywords: endogenous retrovirus, human endogenous retrovirus, neuroblastoma, CD133, CD200, biomarker

INTRODUCTION

In the course of evolution, a large number of retroviral elements have entered the genome of vertebrates. Since integration occurred by infection of the germ line with their exogenous relatives, the resulting proviruses of the so-called endogenous retroviruses (ERV) can be transmitted vertically as a host allele (1, 2). The human genome is comprised of approximately 8% of such elements (3, 4). During their long persistence in the genome, the proviruses suffered from multiple inactivation or silencing mechanisms that lead to disruption of open reading frames (ORF) by mutations and to defective protein products in nearly all human HERV (5). Nevertheless, there are few HERV with almost complete ORF, which are able to form functional proteins even if their intracellular trafficking seems to be inefficient (6).

As most controversially discussed HERV, the envelope (*ENV*) of the HERV-W locus on chromosome 7 (NCBI accession no.: NP_001124397.1; also known as ERVWE-1) can be mentioned. The encoded protein called syncytin-1 is expressed in the placenta, where it mediates cytotrophoblast fusion to the syncytiotrophoblast layer based on its fusogenic properties (7, 8). On the other hand, activation of HERV-W *ENV* has been associated with neurological disorders like multiple sclerosis (MS) due to its localization in brain lesions and detection of anti-HERV-W antibodies *in sera* of MS patients (9–11). In addition to the usual increase in autoreactive antibodies in the course of activation of the immune system (12), abnormally expressed HERV-W *ENV* has been shown to trigger inflammatory cascades including polyclonal activation of T lymphocytes [reviewed in (13)]. Another HERV that was associated more recently with autoimmune disorders is the *ENV* of HERV-Fc1 (NCBI accession no.: XM_011531085.2) (14, 15). Interestingly, the HERV-Fc family has an only limited expansion with six known proviruses in the human genome (16). Among the HERV families, HERV-K (HML-2) is the most active family, which comprises several complete members due to still ongoing fixation in the human population (17–19). Stronger expression of HERV-K family members including their group-specific antigens (GAG) has been mainly identified in tissues and cell lines established from different types of tumors including germ cell tumors, lymphoma, sarcoma and melanoma (20–25). Like melanoma, neuroblastoma (NB) is a tumor originating from cells of the neural crest and unique for its heterogeneity. NB is the most frequent solid tumor outside the central nervous system in infants and children with an incidence of approximately 10 cases per million children under 15 years of age (26). An important prognostic marker is *MYCN* amplification, which is associated with deregulated growth and proliferation and can be found in 30–40% of high risk NB (27). *MYCN* is a member of the *MYC* family of transcription factors. Another family member, *c-myc* (*MYC*), shares oncogenic ability to sustain multiple pathways leading to malignancy, but is reported to be expressed only in a small group of advanced NB showing poor clinical outcome identical to that of patients with amplification of the *MYCN* gene (28, 29). Although overall outcome of patients have been improved in the last decades, survival for patients with

high risk NB (stages 3 and 4 by the International Neuroblastoma Staging System INSS) remains poor due to chemotherapy failure or unresponsiveness to checkpoint blockade immunotherapy (30–32). In the course of focusing on individualized targeted therapy for more effective treatment, modulation of tumor microenvironment seems to be crucial (33, 34). In this context, lack of immunotherapeutic targets, like programmed cell death ligand-1 (PD-L1), in CD24 overexpressing NB, as well as amplification of multidrug resistance-associated genes and overexpression of immune checkpoint molecule CD200 in NB is of particular interest (35–38).

Studies from an Italian group strongly suggest that the stem cell-like CD133 positive subtype of melanoma cells is promoted by HERV-K activation in response to microenvironmental change (39). It remains unknown, whether such effects also occur in other neural crest-derived tumor cells. Therefore, we investigated the expression of above mentioned NB malignancy markers and selected HERV in three NB cell lines in standard and stem cell-promoting media with or without serum by quantitative real time PCR (RT-qPCR). For the RT-qPCR analysis, we focused on the *ENV* of human HERV-W1 and HERV-Fc1 due to their strong association with neurological disorders. In addition, the *GAG* region (HERV-K *GAG*) of the HERV-K (HML-2) family was investigated, because of its putative role in the progression of several tumor malignancies (19). In accordance, we previously reported a robust HERV-K *GAG* expression in soft tissue sarcoma patients, which was significantly correlated with clinicopathological features, such as shortened relapse-free survival, and hypoxia-related gene expression (24). In addition, the targeting of HERV-K *GAG* is beneficial as it allows the detection of numerous members of the most biologically active HERV-K (HML-2) family, which might be hampered by the presence of intact (type 1) and non-intact ORF (type 2) in the *ENV* region (18). Considering the broadest distribution across HERV families and the overall high sequence similarity, the detection of additional HERV-K families (e.g. HML-6) is not excluded by our study. In addition, we analyzed activation of retroviral sequences by mapping RNA-seq reads against a synthetic virus metagenome.

MATERIALS AND METHODS

Cell Lines

In this study the human NB cell lines SH-SY5Y (40), IMR-32 (41) and SiMa (42) were used (all from the German Collection of Microorganisms and Cell Cultures GmbH, Braunschweig, Germany). All cell lines were cultured as adherent or loosely-adherent (SiMa) cells in DMEM medium supplemented with 10% (v/v) heat-inactivated fetal bovine serum (FBS) and penicillin-streptomycin at 37°C in a humidified 5% CO₂ atmosphere (all reagents by Life Technologies, Carlsbad, CA, USA). Twice weekly the cells were passaged after detachment with 0.05% trypsin/EDTA solution (Life Technologies, Carlsbad, CA, USA) for 30–60 s at room temperature and were seed out at 3x10⁶ cells per 75 cm² flask (SH-SY5Y cells and IMR-32 cells) or at 5 × 10⁶ cells per 75 cm² flask (SiMa cells), respectively.

To investigate the medium-induced microenvironmental changes, the three NB cell lines were seed out at 1×10^6 cells (SH-SY5Y cells and IMR-32 cells) or at 3×10^6 cells (SiMa cells) per 25 cm² flask and cultured either in DMEM complete medium, stem-cell medium Panserin 401 (PAN-Biotech GmbH, Aidenbach, Germany) supplemented with 10% FBS and penicillin–streptomycin or Panserin 401 medium with penicillin–streptomycin for 72 h at 37 °C in a humidified 5% CO₂ atmosphere. Morphological analyses were performed by phase contrast microscopy using Keyence microscope BZ-X810 and BZ-X800 Analyzer software version 1.1.1.8 (Keyence, Itasca, IL, USA).

RNA Extraction, cDNA Generation and Quantitative Real-Time PCR

Cells were harvested after 72 h and total cellular RNA was isolated using NucleoSpin RNA kit (Machery-Nagel GmbH & Co. KG, Düren, Germany) following the manufacturer's instructions. Transcription into cDNA was performed using 1 µg total RNA in 16 µl nuclease-free water and 4 µl qScript cDNA 5× SuperMix (QuantaBio, Beverly MA, USA). The mix was incubated for 5 min at 25°C, followed by 30 min at 42°C and finally for 5 min at 82°C.

For quantitative real-time PCR (RT-qPCR) each reaction contained 0.5 µl of cDNA, 500 nM of forward and reverse primer, 5 µl PowerUP SYBR Green 2× Master Mix (Applied Biosystems by Thermo Fisher Scientific, Waltham MA, USA) and 4 µl of nuclease-free water. All used primers were purchased from Invitrogen Thermo Fisher Scientific (Waltham, MA, USA) and were listed in **Table 1**. The amplification protocol included an initial denaturation step at 95°C for 10 min, followed by 40 cycles with denaturation at 95°C for 15 s and primer annealing, amplification and extension at 60°C for 60 s. Two technical

replicates were measured for each sample in three independent experiments (biological replicates). The analysis was performed using QuantStudio3 and QuantStudio Design and Analysis Software v.1.4.3 (Thermo Fisher Scientific). The quantification of relative mRNA levels was performed using the $2^{-\Delta\Delta C_t}$ method (44). Hypoxanthine phosphoribosyltransferase 1 (HPRT1) was used as reference gene for normalization and the median of all samples was set as 1.

Statistics

For comparison of relative mRNA levels measured with RT-qPCR, two-way ANOVA followed by Tukey test was performed using GraphPad Prism (version 8.0.0 for Windows, GraphPad Software, San Diego, California USA). Statistical significance was indicated by asterisks (**, $p < 0.01$; ***, $p < 0.001$; ****, $p < 0.0001$).

RNA-seq

Generation of RNA-seq data was performed by Novogene UK Co., Ltd. (Cambridge, United Kingdom) using Illumina Novaseq6000 system. The quantification of human transcripts mapping to genome version GRCh38/hg38 was calculated as Fragments Per Kilobase per Million reads (FPKM) by Novogene. RNA-seq data can be downloaded from the NCBI Short Read Archive (SRA) under BioProject PRJNA684790. For quantification of ERV expression, reads were mapped against a synthetic virus metagenome, which consists of 119 individual human endogenous viral sequences including three endogenous bornavirus-like elements with almost complete ORF for their *GAG*, *POL* and *ENV* genes, four sequences of housekeeping genes and 124 sequences from unrelated exogenous viruses or non-human endogenous viruses used as spacers. The HERV-K (HML-2) family has more than 100 integrated copies in the human genome, of which we added the 92 full-length sequences to our virus metagenome. All sequences were collected from the nucleotide database from the National Center for Biotechnology Information (NCBI). For detailed information, refer to Engel et al. (45). The Galaxy server at usegalaxy.org (46) was used for mapping of the paired-end reads by Bowtie2 analysis and quantification of all uniquely mapped reads using FeatureCounts (47). To obtain the HERV family specific FPKM, the fragment read counts and the gene length of a family was calculated by summarization of individual family members.

Flow Cytometry

Cells were harvested after 72 h under medium-induced microenvironmental changes. Therefore, loosely-adherent or suspensory cells were loosened by gentle pipetting. Adherent cells were harvested by detachment with 0.05% trypsin/EDTA solution. For antibody staining, cells were resuspended in ice-cold PBS with 2 mM EDTA and 5 µl of the antibody solution was added. Cells were stained using CD200-APC (Miltenyi Biotech, Bergisch Gladbach, Germany) or IgG1-APC control (BD Biosciences, Franklin Lakes, NJ, USA) for 30 min at 4°C in the dark. Unbound antibody was removed with 1 ml PBS/EDTA solution and centrifugation for 10 min at 300 ×g. Finally, cells were suspended in 0.5 ml PBS/EDTA solution and analyzed on a LSRII cytometer using the FACSDiva software version 8.0.1 (BD Biosciences, Franklin Lakes, NJ, USA).

TABLE 1 | Primers used for quantitative real time PCR.

Target	Exemplary accession number (reference)	Sequence of forward (f) and reverse (r) primer (5'-3')
ABCC5	NM_001023587	f: CGAAGGGTTGTGTGGATCTT r: TCTCCCCTCCCTCAGATTTTT
CD24	NM_013230	f: ACCACGCAGATTTATTCCA r: ACCACGAAGAGACTGGCTGT
CD133	NM_006017	f: GCCACCGCTCTAGATACTGC r: TGTTGTGATGGGCTTGTGCAT
CD200	NM_005944	f: AAGTGGTGACCCAGGATGAAA r: AGGTGATGGTTGAGTTTTGGAG
HERV-Fc1 ENV	XM_011531085	f: CTCCCCATCTCTGGTGC r: TGAGGAGGCTGGTTTCTACTAAG
HERV-K GAG	JN675025 (23)	f: GGCCATCAGAGTCTAAACCACG r: CTGACTTTCTGGGGGTGGCCG
HERV-W1 ENV	NM_014590 (43)	f: TGCTAACCGCTGAAAGAGGG r: CGAAGCTCCTCTGCTCTACG
HPRT1	NM_000194	f: ACCAGTCAACAGGGGACATAA r: CTTCTGGGGTCTTTTACC
MYC	NM_002467	f: GGCTCCTGGCAAAGGTCA r: CTGCGTAGTTGTGCTGATGT
MYCN	NM_001293228	f: TGATCCTCAAACGATGCCTTC r: GGACGCCTCGCTCTTATCT

RESULTS

Transcriptional Activation of Tumor Progression Markers and HERV by Medium-Induced Microenvironmental Changes in Neuroblastoma Cell Lines

In order to investigate the expression of selected HERV and cellular markers involved in NB tumor progression or invasiveness under microenvironmental modifications, the three NB cell lines SH-SY5Y, IMR-32 and SiMa were cultured in serum-supplemented DMEM standard medium or serum-supplemented stem cell medium (Panserin 401), or Panserin without serum. Using RT-qPCR analyses, the transcript levels of all investigated HERV were shown to be up-regulated upon exposure to serum-free stem cell medium (**Figure 1**). Both, elevation of HERV-K GAG in SH-SY5Y cells ($p < 0.0001$) and IMR-32 cells ($p < 0.01$), as well as activation of HERV-W1 *ENV* in SH-SY5Y cells ($p < 0.001$) were statistically significant. In SiMa cells, a tendency for increase of the relative HERV expression was observed (black bars). No significant regulation was observed for HERV-Fc1 *ENV*, while the expression was comparatively low with CT values around 30. Concordantly, enhanced expressions of CD24 and CD200 were observed in all three NB lines following cultivation in stem cell media, which was highly significant ($p < 0.0001$) for CD200 compared to both serum-supplemented incubations. An increased CD200 expression at protein level was confirmed in all three NB cell lines by flow cytometry analyses (**Supplementary Figure 1**). Furthermore, relative expression of ABCC5, also known as multidrug resistance-associated protein 5, was increased in SiMa cells and significantly increased in SH-SY5Y cells, whereas no effect was observed in IMR-32 cells. The members of the proto-oncogene MYC family, MYCN and MYC, were expressed heterogeneously in the three studied NB lines. High expression of MYCN was seen in SiMa cells and IMR-32 cells, but not in SH-SY5Y cells. Upon medium-induced microenvironmental changes, MYCN levels were increased by factor 1.6 in IMR-32 cells only. In contrast, MYC expression was exclusive for SH-SY5Y cells and increased by at least factor 4 ($p < 0.0001$) in serum-free stem cell medium. Interestingly, SiMa was the only NB cell line that underwent morphological changes from loosely-adherent monolayers to low proliferating grape-like cellular aggregates upon exposure to serum-free stem cell medium (**Supplementary Figure 2**), accompanied by highly significant ($p < 0.0001$) enrichment of CD133 expression. The NB cell lines SH-SY5Y and IMR-32 did show neither phenotype switching nor transcriptional activation of CD133 during medium-induced microenvironmental changes.

Differential Gene Expression Pattern in HERV-Expressing Neuroblastoma Cell Lines

Secondly, we investigated the overall gene expression in medium-induced HERV-transcriptional active NB cell lines. Therefore, RNA-seq data were collected in duplicates from all three NB cell lines in serum-supplemented standard and stem cell media or stem cell medium without serum. After mapping

against the human genome GRCh38/hg38, the $2^{-\Delta\Delta CT}$ -values were used to filter for transcripts that showed either a high positive ($r \geq 0.7$) or negative ($r \leq -0.7$) correlation to expression of HERV-K GAG. The strongest up- and downregulated genes are presented in **Figure 2**. The list of all 198 up- and downregulated genes can be found in the supplement of this manuscript (**Supplementary Tables 1, 2**). **Figure 2A** shows that stem cell medium led to a shift in gene expression of all three NB cell lines, accompanied by the formation of individual expression signatures. No differences in the overall expression pattern were observed between the serum-supplemented standard and stem cell media incubated cells, indicating serum deprivation as the major factor affecting transcription. This, together with increasing levels of CD200 and ABCC5 in serum-free medium, shows that the RNA-seq analysis is in line with our previously observed RT-qPCR results (**Figure 2B**). Furthermore, TAR (HIV-1) RNA Binding Protein 1 (TARBP1) was increased by 1.46 times in NB incubated in serum-free stem cell medium, which might be of interest regarding potential host interaction partners of the activated HERV. As two of the 78 strongest up-regulated genes, the long non-coding RNA (lncRNA) Myocardial Infarction Associated Transcript (MIAT) by fold change of 2.11 and the transcription factor Myeloid Zinc Finger 1 (MZF1) by fold change of 1.87 were observed (**Figure 2B** and **Supplementary Table 2**). In addition, enhanced expression of the P21 Activated Kinase (PAK) 3 (fold change: 1.51) and PAK5 (fold change: 1.79) were observed. In contrast, 120 genes were found to be down-regulated by serum-free medium and correlated negatively with HERV expression (**Figure 2A** and **Supplementary Table 2**). Hereby, Inhibitor of DNA Binding Protein (ID) 1 and ID2 that are typically expressed by cells of the neural crest were both among the strongest decreased genes. Furthermore, vimentin (VIM), a known regulator of tumor suppressor p21, was reduced in all three NB cell lines after exposure to serum-free media.

Identification of Additional Stem Cell Medium-Induced HERV Members by Using a Virus Metagenome

To study viral transcription and their potential activation in a pathogenic context using RNA-seq, we designed a combined virus metagenome including a collection of exogenous viruses, endogenous retrovirus elements and other endogenous viral elements (EVE), e.g. endogenous bornavirus sequences. Using this virus metagenome, we were able to investigate the differential expression pattern of 115 HERV elements representing 14 HERV families and three EVE of the bornavirus family (EBLN-1, EBLN-2 and EBLN-3P) in the three NB cell lines under medium-induced microenvironmental change. We found that overall expression of EVE was low. But half of studied endogenous virus families were up-regulated upon removal of serum supplementation in stem cell medium (**Figure 3A**). Interestingly, three HERV elements showed strongest differential expression across all three NB cell lines: the *ENV* of HERV-R (ERV3-1; NCBI accession no.: NC_000007.14:6499 0356-65006687), the full-length HERV-E1 (NCBI accession no.: AB062274.1) and the *ENV* of HERV-Fc2 (NCBI accession no.: AC073236.8:162447-165176). As shown in **Figure 3B**, HERV-E1

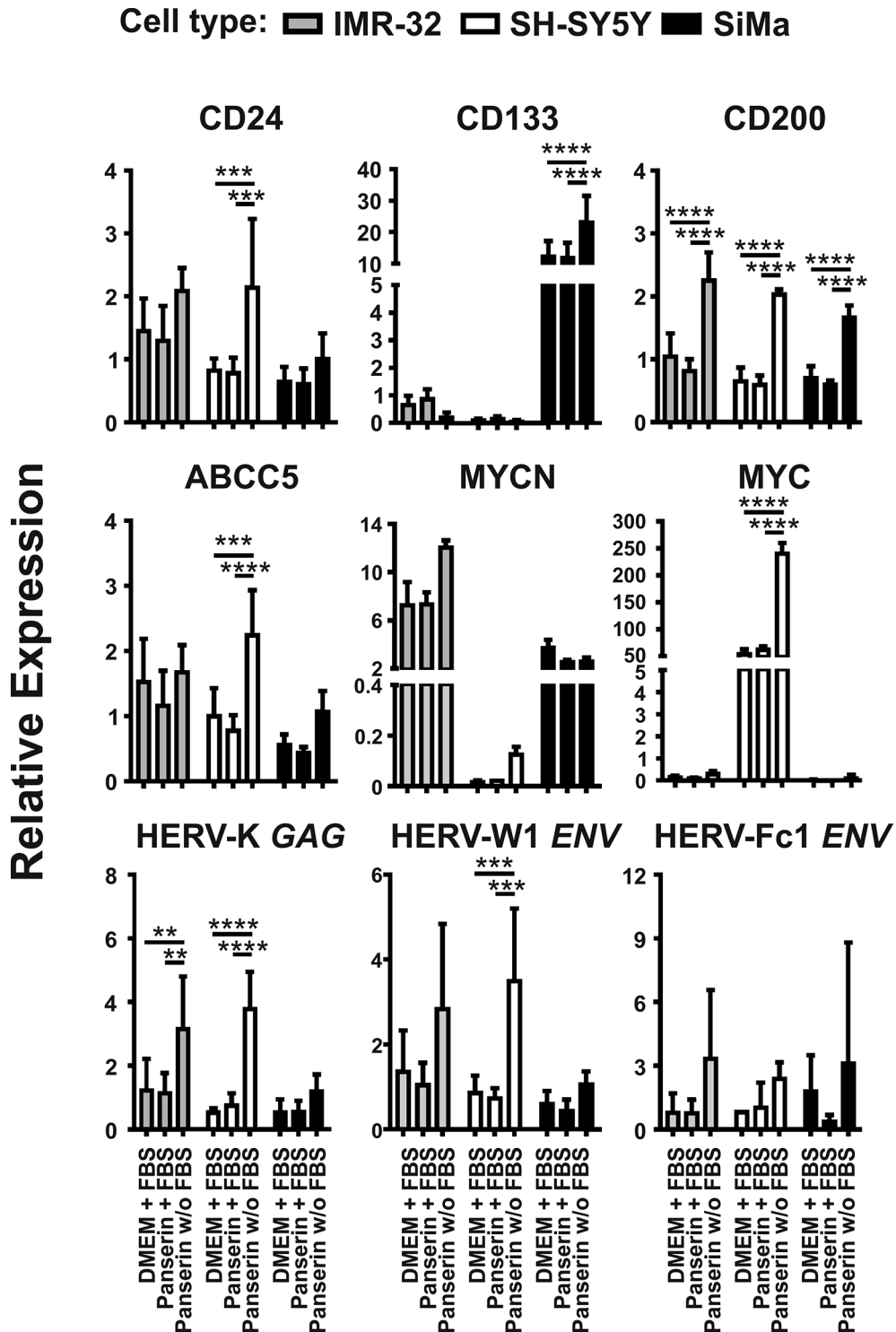
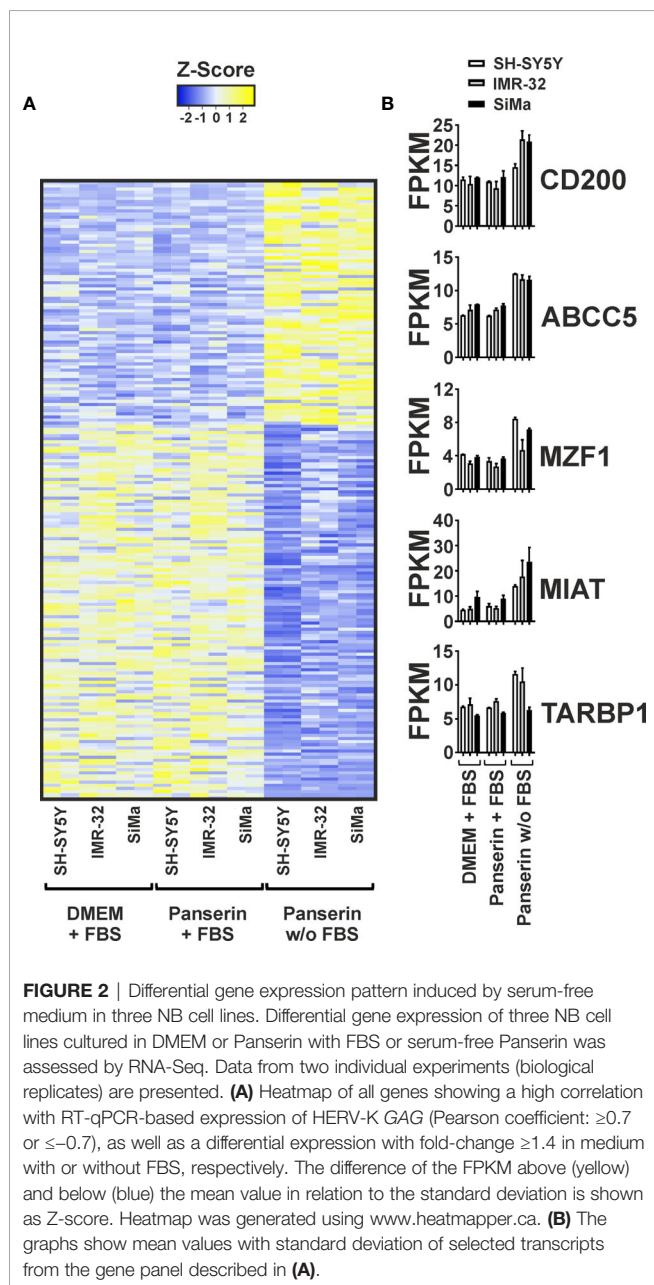


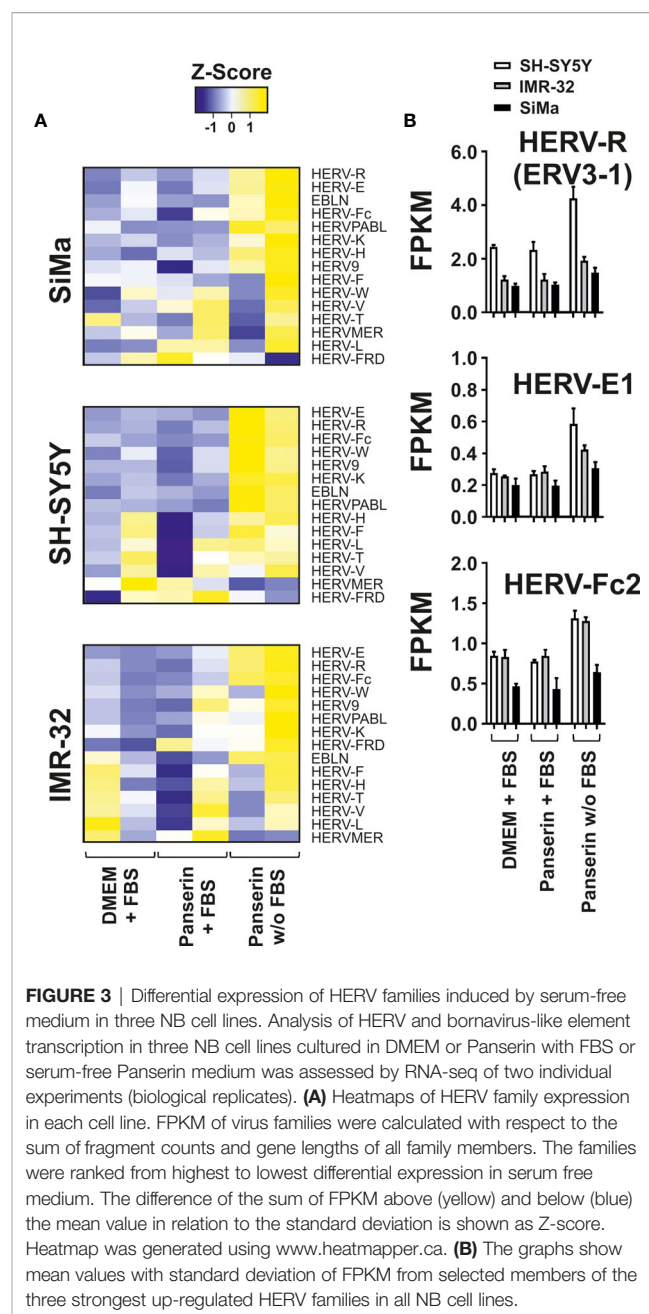
FIGURE 1 | Promotion of malignancy markers by medium-induced microenvironmental changes is accompanied by HERV induction in NB cell lines. Expression of proposed malignancy markers in NB and three selected HERV transcripts was assessed by RT-qPCR. Relative expression of the indicated genes was represented by $2^{-\Delta\Delta Ct}$ with normalization to HPRT1 and the overall median. The graphs show mean values and standard deviations of three individual experiments (biological replicates) determined in duplicates (technical replicates). Statistics: two-way ANOVA with Tukey test; **** $p < 0.0001$; *** $p < 0.001$; ** $p < 0.01$.



expression was most increased by factor 2.1 in SH-SY5Y cells and by factor 1.6 in IMR-32 cells. In SiMa cells, ERV3-1 was strongest upregulated with a fold change of 1.4 and here the highest expression of the bornavirus like-family was observed, too.

DISCUSSION

In the present study, we have investigated the expression of HERV as potential targets in NB cell lines during stem-cell medium-induced microenvironmental change by RT-qPCR and RNA-seq. For RT-qPCR analyses we initially focused on HERV-K due to its well-described relationship in a number of cancers including neural crest-derived tumors such as melanoma



(22, 39, 48–50). Our results suggest a strong correlation of HERV-K GAG with stressful cell culture conditions by serum-depleted stem cell medium in all three NB cell lines (**Figure 1**). In this context, studies on human pluripotent stem cells (PSCs) suggest HERV-K (HML-2) activation in early stem cell development (51, 52) and that the differentiation of PSCs into neuronal cells is promoted by silencing of its *ENV* (53). It is of particular interest, that Wang's group were not able to demonstrate similar results with GAG proteins. This might be a result of an only moderate HERV-K GAG activation in PSC-like cells, as we observed for SiMa cells after stem cell media induction. Instead, elevation was significant in SH-SY5Y cells ($p < 0.0001$) and IMR-32 cells ($p < 0.01$) where no

morphological changes were observed (**Figure 1** and **Supplementary Figure 2**).

Besides up-regulation of HERV-K GAG, enhanced expression of HERV-W1 ENV with significance in SH-SY5Y cells ($p < 0.001$) and to a lesser extent up-regulation of HERV-Fc1 ENV were observed as consequence of stem cell medium induction (**Figure 1**). In addition, virus transcriptome analyses revealed activation of three endogenous retrovirus elements: HERV-R (ERV3-1), HERV-E1 and HERV-Fc2 (**Figure 3**). HERV-R transcripts have broad expression in normal tissue and due to its overexpression in the first trimester of pregnancy an immunosuppressive function in the mother-fetus interaction was suggested (54, 55). ERV3-1 is the only copy of approximately 40 ERV3-like elements in the human genome that has a complete ORF for its ENV (56). Interestingly, the expression of this full-length ENV is associated with several tumor entities including colorectal (57), ovarian (58) and endometrial carcinoma. Of interest is that during endometrial carcinoma progression, ERV3-1 ENV is co-expressed with six other ENV (HERV-W1, HERV-T, HERV-Fc2, HERV-H1-3, HERV-V1, HERV-E1) and showed significantly increased expression in more undifferentiated grade 3 tumors compared to differentiated grade 1 tumors (59). In accordance with the results from endometrial carcinoma, elevated expression of HERV-E1, HERV-R, and also HERV-K were observed in ovarian cancer (58). Several reports suggest a putative pathogenic role in systemic lupus erythematosus as expression of provirus elements was found to be enhanced compared to healthy individuals and to correlate with disease progression (60–63). Altogether, this demonstrates the genetic variety of HERVs in the pathogenesis of autoimmune disorders and malignancies, even in the limited subset of NB cell lines shown here. HERV transcriptome analysis of tumor biopsy samples from NB patients might be helpful for identification of putative HERV targets that can be used for development of anti-HERV antibodies. Such antibodies might be tools for a more personalized and, at best, more effective therapy, as it is already established for *HER2* in breast cancer patients (64). The stem cell medium-induced element identified within our virus metagenome analysis, HERV-Fc2 ENV with location on chromosome 7q36 has not been investigated extensively in the past. Due to its activation in all three NB cell lines upon tumor microenvironmental change, we propose HERV-Fc2 ENV as a putative target in NB that should be further studied.

In RT-qPCR analyses, IMR-32 cells and SH-SY5Y cells had either a distinct MYCN (IMR-32 cells) or MYC (SH-SY5Y cells) positive phenotype, which has been pronounced under stem cell incubation significantly in SH-SY5Y cells ($p < 0.0001$). Another fact exemplifying the heterogeneity of NB was the CD133 positive character of the SiMa cell line and its medium-induced morphological change from loosely adherent monolayers to low proliferating grape-like cellular aggregates. Phenotype switching in SiMa cells was further accompanied by significant increase of CD133 levels assessed by RT-qPCR ($p < 0.0001$) and by RNA-seq with a fold change of 1.56. Altogether, this indicates that SiMa cells used in our study are so-called I-type NB (65). I-type cells were shown to be significantly more malignant than N- or S-type NB independent of MYCN amplification and suggested as cancer stem

cell population according to their CD133 positive background (66, 67). Besides these differences, expression of CD24, CD200 and ABCC5 were upregulated upon stem cell-promoting conditions with highly significant fold changes for CD200 ($p < 0.0001$) in all three NB cell lines and for CD24 ($p < 0.001$) and ABCC5 ($p < 0.001$) in SH-SY5Y cells (**Figure 1**). Since overexpression of CD200 was reported in a variety of human tumors including multiple myeloma (68), neuroendocrine tumors (69), melanoma (70, 71), ovarian cancer (72), and very recently also in more than 90 % of NB samples (38), high correlation of CD200 and HERV-K GAG for the studied NB cell lines ($r = 0.92$) might be of special interest (**Figure 2**). This raises the question, if CD200 is activated by HERV expression upon microenvironmental change or *vice versa* considering possible signaling pathways. In the case of an initial HERV overexpression by e.g. exogenous viruses (73–75) HERV proteins from almost complete ORF might induce clonal deletion of lymphocytes in a T cell receptor V-beta specific manner resembling superantigens (13, 76). The polyclonal expansion of T lymphocytes that has been previously shown for a HERV-W protein *in-vitro* (77), lead to secretion of cytokines and consequently upregulation of CD200 by activated T cells (34). Of interest, CD4 positive and CD8 positive T cells of CD200^{high} NB were shown to produce less interferon gamma and tumor necrosis factor alpha thereby inhibiting anti-tumor immunity (38). Nevertheless, controversial results have been reported according the significance and role of CD200 expression in cancer progression indicating a certain dependence on the tumor type (69, 78, 79). The three NB cell lines used in this study showed an increased CD200 expression upon medium-induced microenvironmental change, both at the RNA level and at the surface protein level (**Supplementary Figure 1**). Though CD24 was not included in the list of most differentially expressed genes (**Figure 2** and **Supplementary Table 1**) due to a fold change smaller than 1.4, transcriptome analysis confirms enhanced expression in Panserin medium. Previous studies reported CD24 as an inhibitor for neurite outgrowth in mice and that expression was related to the differentiation state in human NB suggesting an activation of CD24 in less differentiated tumor samples (80, 81). This might be of interest, since morphological changes with loss of dendritic branching was solely observed in SiMa cells after 72 h of serum-free media incubation (**Supplementary Figure 2**), but may indicate also ongoing genetic reprogramming in SH-SY5Y cells and IMR-32 cells. In this context it is interesting that stem-cell medium induced down regulation of ID1 and ID2, as well as VIM, which are typically expressed by neural crest cells (82, 83) (**Figure 2** and **Supplementary Table 2**). An overexpression of ID1 was associated with several cancers and cancer-associated pathways (84). However, the reduced expression of the ID1 and ID2 might be indicative for impaired proliferation in serum-depleted media that we observed at least in SiMa cells.

Furthermore, we observed overexpression of MIAT under stem-cell promoting conditions in all studied NB cell lines (**Figure 2B** and **Supplementary Table 1**). This nuclear lncRNA (NCBI accession no.: NR_003491) is widely expressed in endothelial cells, Müller glia and neurons, but dysregulation of MIAT is associated with various heart diseases and nervous system tumors, as it is involved in the maintenance of proper

microvascular and nervous function (85). Interestingly, silencing of MIAT was reported to correlate with down regulation of MYC leading to reduction of cell migration and promotion of basal apoptosis in the NB cell line SH-SY5Y (86). In our present study, the correlation of MYC and MIAT amplification seemed to be exclusive for SH-SY5Y cells, as expression of MYC was not detected in IMR-32 cells and SiMa cells (Figure 1). In contrast, differential expression analyses in stage 4 NB and stage 4S NB suggested that MIAT might be a “good survival lncRNA” which needs further investigation (87). Overexpression of transcription factor MZF1 detected by RNA-seq (Figure 2 and Supplementary Table 1) was in line with previous reports of MZF1 association with poor clinical outcome in different tumor entities [reviewed in (88)] and especially NB tumor cell progression through modulation of tumor environment by facilitating aerobic glycolysis in NB cell lines (89). Last but not least, co-activation of TARBP-1 and HERV transcripts might be of special interest. Initially identified to bind with HIV type-1 transactivation response RNA to activate long terminal repeat (LTR) expression in the presence or absence of the viral transactivator Tat (90), it is reasonable to hypothesize that TARBPs might be able to activate nuclear LTR transcription of endogenous proviruses and consequently promote expression of HERV proteins if they possess intact ORF.

In summary, NB are very heterogeneous tumors hampering the identification of robust biomarkers. Our results strongly suggest enhancement of malignancy markers by medium-induced tumor microenvironmental change in RT-qPCR and RNA-seq, which is accompanied by activation of HERV transcription in all studied NB cell lines. To our knowledge, this is the first time that HERV-R ENV (ERV3-1), HERV-E1 and HERV-Fc2 ENV were reported to be associated with NB and should be investigated in further studies especially regarding their prevalence in more undifferentiated tumor cells. In addition, significant increase of immune checkpoint molecule CD200 indicating and possible activation of immune escape mechanisms, as well as TARBP-1 co-activation with HERV needs to be further explored. The expression analysis of HERV elements in patient specimens might lead to identification of new therapeutic targets, especially regarding the ongoing efforts in the production of HERV-targeting drugs.

REFERENCES

1. Belshaw R, Pereira V, Katzourakis A, Talbot G, Paces J, Burt A, et al. Long-Term Reinfection of the Human Genome by Endogenous Retroviruses. *Proc Natl Acad Sci USA* (2004) 101:4894–9. doi: 10.1073/pnas.0307800101
2. Christensen T. Herts in Neuropathogenesis. *J Neuroimmune Pharmacol* (2010) 5:326–35. doi: 10.1007/s11481-010-9214-y
3. Griffiths DJ. Endogenous Retroviruses in the Human Genome Sequence. *Genome Biol* (2001) 2:REVIEWS1017. doi: 10.1186/gb-2001-2-6-reviews1017
4. Lander ES, Linton LM, Birren B, Nusbaum C, Zody MC, Baldwin J, et al. Initial Sequencing and Analysis of the Human Genome. *Nature* (2001) 409:860–921. doi: 10.1038/35057062
5. de Parseval N, Heidmann T. Human Endogenous Retroviruses: From Infectious Elements to Human Genes. *Cytogenet Genome Res* (2005) 110:318–32. doi: 10.1159/000084964
6. Gröger V, Wieland L, Naumann M, Meinecke AC, Meinhardt B, Rossner S, et al. Formation of HERV-K and HERV-Fc1 Envelope Family Members is Suppressed on Transcriptional and Translational Level. *Int J Mol Sci* (2020) 21:7855. doi: 10.3390/ijms21217855

DATA AVAILABILITY STATEMENT

The datasets presented in this study can be found in online repositories. The names of the repository/repositories and accession number(s) can be found below: NCBI Sequence Read Archive (SRA) (<https://www.ncbi.nlm.nih.gov/sra/>). Accession number: PRJNA684790.

AUTHOR CONTRIBUTIONS

Conceptualization: LW and MS. Methodology: LW, KE, and IV. Data curation: LW and MS. Visualization and original draft preparation: LW. Review and editing: LW, AK, GP, and MS. Supervision, resources, and project administration: AE, MK, and MS. All authors contributed to the article and approved the submitted version.

FUNDING

The work was supported by grant ZS/2018/12/96228 (to University of Halle) from European Regional Development Fund within the local program “Sachsen-Anhalt WISSENSCHAFT Schwerpunkte”. We acknowledge the financial support of the Open Access Publication Fund of the Martin Luther University Halle-Wittenberg.

ACKNOWLEDGMENTS

We thank Dr. Holtkötter for kind support of our study.

SUPPLEMENTARY MATERIAL

The Supplementary Material for this article can be found online at: <https://www.frontiersin.org/articles/10.3389/fonc.2021.637522/full#supplementary-material>

7. Denner J. Expression and Function of Endogenous Retroviruses in the Placenta. *APMIS* (2016) 124:31–43. doi: 10.1111/apm.12474
8. Mi S, Lee X, Li X, Veldman GM, Finnerty H, Racie L, et al. Syncytin is a Captive Retroviral Envelope Protein Involved in Human Placental Morphogenesis. *Nature* (2000) 403:785–9. doi: 10.1038/35001608
9. van Horssen J, van der Pol S, Nijland P, Amor S, Perron H. Human Endogenous Retrovirus W in Brain Lesions: Rationale for Targeted Therapy in Multiple Sclerosis. *Mult Scler Relat Disord* (2016) 8:11–8. doi: 10.1016/j.msard.2016.04.006
10. Balada E, Vilardell-Tarrés M, Ordi-Ros J. Implication of Human Endogenous Retroviruses in the Development of Autoimmune Diseases. *Int Rev Immunol* (2010) 29:351–70. doi: 10.3109/08830185.2010.485333
11. Gröger V, Cynis H. Human Endogenous Retroviruses and Their Putative Role in the Development of Autoimmune Disorders Such as Multiple Sclerosis. *Front Microbiol* (2018) 9:265. doi: 10.3389/fmicb.2018.00265
12. Avrameas S, Selmi C. Natural Autoantibodies in the Physiology and Pathophysiology of the Immune System. *J Autoimmun* (2013) 41:46–9. doi: 10.1016/j.jaut.2013.01.006
13. Küry P, Nath A, Créange A, Dolei A, Marche P, Gold J, et al. Human Endogenous Retroviruses in Neurological Diseases. *Trends Mol Med* (2018) 24:379–94. doi: 10.1016/j.molmed.2018.02.007

14. Laska MJ, Brudek T, Nissen KK, Christensen T, Møller-Larsen A, Petersen T, et al. Expression of HERV-Fc1, a Human Endogenous Retrovirus, is Increased in Patients With Active Multiple Sclerosis. *J Virol* (2012) 86:3713–22. doi: 10.1128/JVI.06723-11
15. Nexø BA, Villesen P, Nissen KK, Lindegaard HM, Rossing P, Petersen T, et al. Are Human Endogenous Retroviruses Triggers of Autoimmune Diseases? Unveiling Associations of Three Diseases and Viral Loci. *Immunol Res* (2016) 64:55–63. doi: 10.1007/s12026-015-8671-z
16. Benit L, Calteau A, Heidmann T. Characterization of the Low-Copy HERV-Fc Family: Evidence for Recent Integrations in Primates of Elements With Coding Envelope Genes. *Virology* (2003) 312:159–68. doi: 10.1016/s0042-6822(03)00163-6
17. Hohn O, Hanke K, Bannert N. Herv-K(HML-2), the Best Preserved Family of HERVs: Endogenization, Expression, and Implications in Health and Disease. *Front Oncol* (2013) 3:246. doi: 10.3389/fonc.2013.00246
18. Wildschutte JH, Williams ZH, Montesion M, Subramanian RP, Kidd JM, Coffin JM. Discovery of Unfixed Endogenous Retrovirus Insertions in Diverse Human Populations. *Proc Natl Acad Sci USA* (2016) 113:E2326–34. doi: 10.1073/pnas.1602336113
19. Garcia-Montojo M, Doucet-O'Hare T, Henderson L, Nath A. Human Endogenous Retrovirus-K (HML-2): A Comprehensive Review. *Crit Rev Microbiol* (2018) 44:715–38. doi: 10.1080/1040841X.2018.1501345
20. Herbst H, Sauter M, Mueller-Lantsch N. Expression of Human Endogenous Retrovirus K Elements in Germ Cell and Trophoblastic Tumors. *Am J Pathol* (1996) 149:1727–35.
21. Wang-Johanning F, Frost AR, Jian B, Epp L, Lu DW, Johanning GL. Quantitation of HERV-K Env Gene Expression and Splicing in Human Breast Cancer. *Oncogene* (2003) 22:1528–35. doi: 10.1038/sj.onc.1206241
22. Serafino A, Balestrieri E, Pierimarchi P, Matteucci C, Moroni G, Oricchio E, et al. The Activation of Human Endogenous Retrovirus K (Herv-K) is Implicated in Melanoma Cell Malignant Transformation. *Exp Cell Res* (2009) 315:849–62. doi: 10.1016/j.yexcr.2008.12.023
23. Downey RF, Sullivan FJ, Wang-Johanning F, Amsb S, Giles FJ, Glynn SA. Human Endogenous Retrovirus K and Cancer: Innocent Bystander or Tumorigenic Accomplice? *Int J Cancer* (2015) 137:1249–57. doi: 10.1002/ijc.29003
24. Giebler M, Staeger MS, Blaschmidt S, Ohm LI, Kraus M, Würfl P, et al. Elevated HERV-K Expression in Soft Tissue Sarcoma is Associated With Worsened Relapse-Free Survival. *Front Microbiol* (2018) 9:211. doi: 10.3389/fmicb.2018.00211
25. Barth M, Gröger V, Cynis H, Staeger MS. Identification of Human Endogenous Retrovirus Transcripts in Hodgkin Lymphoma Cells. *Mol Biol Rep* (2019) 46:1885–93. doi: 10.1007/s11033-019-04640-x
26. Maris JM. Recent Advances in Neuroblastoma. *N Engl J Med* (2010) 362:2202–11. doi: 10.1056/NEJMra0804577
27. Brodeur GM. Neuroblastoma: Biological Insights Into a Clinical Enigma. *Nat Rev Cancer* (2003) 3:203–16. doi: 10.1038/nrc1014
28. Zimmerman MW, Liu Y, He S, Durbin AD, Abraham BJ, Easton J, et al. MYC Drives a Subset of High-Risk Pediatric Neuroblastomas and is Activated Through Mechanisms Including Enhancer Hijacking and Focal Enhancer Amplification. *Cancer Discov* (2018) 8:320–35. doi: 10.1158/2159-8290.CD-17-0993
29. Matsuno R, Gifford AJ, Fang J, Warren M, Lukeis RE, Trahair T, et al. Rare MYC-amplified Neuroblastoma With Large Cell Histology. *Pediatr Dev Pathol* (2018) 21:461–6. doi: 10.1177/1093526617749670
30. Colon NC, Chung DH. Neuroblastoma. *Adv Pediatr* (2011) 58:297–311. doi: 10.1016/j.yapd.2011.03.011
31. Park JA, Cheung NV. Limitations and Opportunities for Immune Checkpoint Inhibitors in Pediatric Malignancies. *Cancer Treat Rev* (2017) 58:22–33. doi: 10.1016/j.ctrv.2017.05.006
32. Wedekind MF, Denton NL, Chen CY, Cripe TP. Pediatric Cancer Immunotherapy: Opportunities and Challenges. *Paediatr Drugs* (2018) 20:395–408. doi: 10.1007/s40272-018-0297-x
33. Nakagawara A, Li Y, Izumi H, Muramori K, Inada H, Nishi M. Neuroblastoma. *Jpn J Clin Oncol* (2018) 48:214–41. doi: 10.1093/jjco/hyx176
34. Liu JQ, Hu A, Zhu J, Yu J, Talebian F, Bai XF. Cd200-CD200R Pathway in the Regulation of Tumor Immune Microenvironment and Immunotherapy. *Adv Exp Med Biol* (2020) 1223:155–65. doi: 10.1007/978-3-030-35582-1_8
35. de Cremoux P, Jourdan-Da-Silva N, Couturier J, Tran-Perennou C, Schleiermacher G, Fehlbach P, et al. Role of Chemotherapy Resistance Genes in Outcome of Neuroblastoma. *Pediatr Blood Cancer* (2007) 48:311–7. doi: 10.1002/pbc.20853
36. Oue T, Yoneda A, Uehara S, Yamanaka H, Fukuzawa M. Increased Expression of Multidrug Resistance-Associated Genes After Chemotherapy in Pediatric Solid Malignancies. *J Pediatr Surg* (2009) 44:377–80. doi: 10.1016/j.jpedsurg.2008.10.088
37. Topcagic J, Feldman R, Ghazalpour A, Swensen J, Gatalica Z, Vranic S. Comprehensive Molecular Profiling of Advanced/Metastatic Olfactory Neuroblastomas. *PLoS One* (2018) 13:e0191244. doi: 10.1371/journal.pone.0191244
38. Xin C, Zhu J, Gu S, Yin M, Ma J, Pan C, et al. CD200 is Overexpressed in Neuroblastoma and Regulates Tumor Immune Microenvironment. *Cancer Immunol Immunother* (2020) 69:2333–43. doi: 10.1007/s00262-020-02589-6
39. Argaw-Denboba A, Balestrieri E, Serafino A, Cipriani C, Buccì I, Sorrentino R, et al. HERV-K Activation is Strictly Required to Sustain CD133+ Melanoma Cells With Stemness Features. *J Exp Clin Cancer Res* (2017) 36:20. doi: 10.1186/s13046-016-0485-x
40. Biedler JL, Helson L, Spengler BA. Morphology and Growth, Tumorigenicity, and Cytogenetics of Human Neuroblastoma Cells in Continuous Culture. *Cancer Res* (1973) 33:2643–52.
41. Tumulowicz JJ, Nichols WW, Cholon JJ, Greene AE. Definition of a Continuous Human Cell Line Derived From Neuroblastoma. *Cancer Res* (1970) 30:2110–8.
42. Marini P, MacLeod RA, Treuner C, Bruchelt G, Böhm W, Wolburg H, et al. SiMa, a New Neuroblastoma Cell Line Combining Poor Prognostic Cytogenetic Markers With High Adrenergic Differentiation. *Cancer Genet Cytogenet* (1999) 112:161–4. doi: 10.1016/s0165-4608(98)00269-6
43. Karimi A, Esmaili N, Ranjkesh M, Zolfaghari MA. Expression of Human Endogenous Retroviruses in Pemphigus Vulgaris Patients. *Mol Biol Rep* (2019) 46:6181–6. doi: 10.1007/s11033-019-05053-6
44. Livak KJ, Schmittgen TD. Analysis of Relative Gene Expression Data Using Real-Time Quantitative PCR and the 2(-Delta Delta C(T)) Method. *Methods* (2001) 25:402–8. doi: 10.1006/meth.2001.1262
45. Engel K, Wieland L, Krüger A, Volkmer I, Cynis H, Emmer A, et al. Identification of Differentially Expressed Human Endogenous Retrovirus Families in Human Leukemia and Lymphoma Cell Lines and Stem Cells. *Front Oncol* (2021) 11:637981. doi: 10.3389/fonc.2021.637981
46. Afgan E, Baker D, van den Beek M, Blankenberg D, Bouvier D, Čech M, et al. The Galaxy Platform for Accessible, Reproducible and Collaborative Biomedical Analyses: 2016 Update. *Nucleic Acids Res* (2016) 44(W1):W3–W10. doi: 10.1093/nar/gkw343
47. Liao Y, Smyth GK, Shi W. featureCounts: An Efficient General Purpose Program for Assigning Sequence Reads to Genomic Features. *Bioinformatics* (2014) 30:923–30. doi: 10.1093/bioinformatics/btt656
48. Büscher K, Trefzer U, Hofmann M, Sterry W, Kurth R, Denner J. Expression of Human Endogenous Retrovirus K in Melanomas and Melanoma Cell Lines. *Cancer Res* (2005) 65:4172–80. doi: 10.1158/0008-5472.CAN-04-2983
49. Hahn S, Ugurel S, Hanschmann KM, Strobel H, Tondera C, Schadendorf D, et al. Serological Response to Human Endogenous Retrovirus K in Melanoma Patients Correlates With Survival Probability. *AIDS Res Hum Retroviruses* (2008) 24:717–23. doi: 10.1089/aid.2007.0286
50. Curty G, Marston JL, de Mulder Rougvie M, Leal FE, Nixon DF, Soares MA. Human Endogenous Retrovirus K in Cancer: A Potential Biomarker and Immunotherapeutic Target. *Viruses* (2020) 12:726. doi: 10.3390/v12070726
51. Fuchs NV, Loewer S, Daley GQ, Izsvák Z, Löwer J, Löwer R. Human Endogenous Retrovirus K (Hml-2) RNA and Protein Expression is a Marker for Human Embryonic and Induced Pluripotent Stem Cells. *Retrovirology* (2013) 10:115. doi: 10.1186/1742-4690-10-115
52. Mareschi K, Montanari P, Rasmussen M, Galliano I, Daprà V, Adamini A, et al. Human Endogenous Retrovirus-H and K Expression in Human Mesenchymal Stem Cells as Potential Markers of Stemness. *Intervirology* (2019) 62(1):9–14. doi: 10.1159/000499185
53. Wang T, Medynets M, Johnson KR, Doucet-O'Hare T, DiSanza B, Li W, et al. Regulation of Stem Cell Function and Neuronal Differentiation by HERV-K Via mTOR Pathway. *Proc Natl Acad Sci USA* (2020) 117(30):17842–53. doi: 10.1073/pnas.2002427117
54. Holder BS, Tower CL, Abrahams VM, Aplin JD. Syncytin 1 in the Human Placenta. *Placenta* (2012) 33:460–6. doi: 10.1016/j.placenta.2012.02.012
55. Venables PJ, Brookes SM, Griffiths D, Weiss RA, Boyd MT. Abundance of an Endogenous Retroviral Envelope Protein in Placental Trophoblasts Suggests a Biological Function. *Virology* (1995) 211:589–92. doi: 10.1006/viro.1995.1442

56. Bustamante Rivera YY, Brütting C, Schmidt C, Volkmer I, Staeger MS. Endogenous Retrovirus 3 - History, Physiology, and Pathology. *Front Microbiol* (2017) 8:2691. doi: 10.3389/fmicb.2017.02691
57. Lee SH, Kang YJ, Jo JO, Ock MS, Baek KW, Eo J, et al. Elevation of Human ERV3-1 Env Protein Expression in Colorectal Cancer. *J Clin Pathol* (2014) 67:840-4. doi: 10.1136/jclinpath-2013-202089
58. Wang-Johanning F, Liu J, Rycaj K, Huang M, Tsai K, Rosen DG, et al. Expression of Multiple Human Endogenous Retrovirus Surface Envelope Proteins in Ovarian Cancer. *Int J Cancer* (2007) 120:81-90. doi: 10.1002/ijc.22256
59. Strissel PL, Ruebner M, Thiel F, Wachter D, Ekici AB, Wolf F, et al. Reactivation of Codogenic Endogenous Retroviral (ERV) Envelope Genes in Human Endometrial Carcinoma and Prestages: Emergence of New Molecular Targets. *Oncotarget* (2012) 3:1204-19. doi: 10.18632/oncotarget.679
60. Ogasawara H, Naito T, Kaneko H, Hishikawa T, Sekigawa I, Hashimoto H, et al. Quantitative Analyses of Messenger RNA of Human Endogenous Retrovirus in Patients With Systemic Lupus Erythematosus. *J Rheumatol* (2001) 28:533-8.
61. Piotrowski PC, Duriagin S, Jagodzinski PP. Expression of Human Endogenous Retrovirus Clone 4-1 may Correlate With Blood Plasma Concentration of Anti-U1 RNP and anti-Sm Nuclear Antibodies. *Clin Rheumatol* (2005) 24:620-4. doi: 10.1007/s10067-005-1123-8
62. Wu Z, Mei X, Zhao D, Sun Y, Song J, Pan W, et al. DNA Methylation Modulates HERV-E Expression in CD4+ T Cells From Systemic Lupus Erythematosus Patients. *J Dermatol Sci* (2015) 77:110-6. doi: 10.1016/j.jdermsci.2014.12.004
63. Wang X, Zhao C, Zhang C, Mei X, Song J, Sun Y, et al. Increased HERV-E Clone 4-1 Expression Contributes to DNA Hypomethylation and IL-17 Release From CD4+ T Cells Via miR-302d/MBD2 in Systemic Lupus Erythematosus. *Cell Commun Signal* (2019) 17:94. doi: 10.1186/s12964-019-0416-5
64. Meric-Bernstam F, Johnson AM, Dumbrava EEI, Raghav K, Balaji K, Bhatt M, et al. Advances in HER2-Targeted Therapy: Novel Agents and Opportunities Beyond Breast and Gastric Cancer. *Clin Cancer Res* (2019) 25(7):2033-41. doi: 10.1158/1078-0432.CCR-18-2275
65. Ross RA, Spengler BA, Doménech C, Porubcin M, Rettig WJ, Biedler JL. Human Neuroblastoma I-type Cells are Malignant Neural Crest Stem Cells. *Cell Growth Differ* (1995) 6:449-56.
66. Walton JD, Kattan DR, Thomas SK, Spengler BA, Guo HF, Biedler JL, et al. Characteristics of Stem Cells From Human Neuroblastoma Cell Lines and in Tumors. *Neoplasia* (2004) 6:838-45. doi: 10.1593/neo.04310
67. Kamijo T. Role of Stemness-Related Molecules in Neuroblastoma. *Pediatr Res* (2012) 71:511-5. doi: 10.1038/pr.2011.54
68. Moreaux J, Hose D, Reme T, Jourdan E, Hundemer M, Legouffe E, et al. CD200 is a New Prognostic Factor in Multiple Myeloma. *Blood* (2006) 108:4194-7. doi: 10.1182/blood-2006-06-029355
69. Love JE, Thompson K, Kilgore MR, Westerhoff M, Murphy CE, Papanicolaou-Sengos A, et al. CD200 Expression in Neuroendocrine Neoplasms. *Am J Clin Pathol* (2017) 148:236-42. doi: 10.1093/ajcp/axq071
70. Petermann KB, Rozenberg GI, Zedek D, Groben P, McKinnon K, Buehler C, et al. CD200 is Induced by ERK and is a Potential Therapeutic Target in Melanoma. *J Clin Invest* (2007) 117:3922-9. doi: 10.1172/JCI32163
71. Alapat D, Coviello-Malle J, Owens R, Qu P, Barlogie B, Shaughnessy JD, et al. Diagnostic Usefulness and Prognostic Impact of CD200 Expression in Lymphoid Malignancies and Plasma Cell Myeloma. *Am J Clin Pathol* (2012) 137:93-100. doi: 10.1309/AJCP59UORCYZEVQO
72. Siva A, Xin H, Qin F, Oltean D, Bowdish KS, Kretz-Rommel A. Immune Modulation by Melanoma and Ovarian Tumor Cells Through Expression of the Immunosuppressive Molecule CD200. *Cancer Immunol Immunother* (2008) 57:987-96. doi: 10.1007/s00262-007-0429-6
73. Sutkowski N, Chen G, Calderon G, Huber BT. Epstein-Barr Virus Latent Membrane Protein LMP-2A is Sufficient for Transactivation of the Human Endogenous Retrovirus HERV-K18 Superantigen. *J Virol* (2014) 78:7852-60. doi: 10.1128/JVI.78.14.7852-7860.2004
74. Nelläker C, Yao Y, Jones-Brando L, Mallet F, Yolken RH, Karlsson H. Transactivation of Elements in the Human Endogenous Retrovirus W Family by Viral Infection. *Retrovirology* (2006) 3:44. doi: 10.1186/1742-4690-3-44
75. Assinger A, Yaiw KC, Göttesdorfer I, Leib-Mösch C, Söderberg-Nauclér C. Human Cytomegalovirus (HCMV) Induces Human Endogenous Retrovirus (HERV) Transcription. *Retrovirology* (2013) 10:132. doi: 10.1186/1742-4690-10-132
76. Emmer A, Staeger MS, Kornhuber ME. The Retrovirus/Superantigen Hypothesis of Multiple Sclerosis. *Cell Mol Neurobiol* (2014) 34(8):1087-96. doi: 10.1007/s10571-014-0100-7
77. Perron H, Jouvin-Marche E, Michel M, Ounanian-Paraz A, Camelo S, Dumon A, et al. Multiple Sclerosis Retrovirus Particles and Recombinant Envelope Trigger an Abnormal Immune Response In Vitro, by Inducing Polyclonal Vbeta16 T-Lymphocyte Activation. *Virology* (2001) 287:321-32. doi: 10.1006/viro.2001.1045
78. Clark DA, Dhesy-Thind S, Ellis P, Ramsay J. The CD200-tolerance Signaling Molecule Associated With Pregnancy Success is Present in Patients With Early-Stage Breast Cancer But Does Not Favor Nodal Metastasis. *Am J Reprod Immunol* (2014) 72:435-9. doi: 10.1111/aji.1229
79. Erin N, Podnos A, Tanriover G, Duymuş Ö, Cote E, Khatri I, et al. Bidirectional Effect of CD200 on Breast Cancer Development and Metastasis, With Ultimate Outcome Determined by Tumor Aggressiveness and a Cancer-Induced Inflammatory Response. *Oncogene* (2015) 34:3860-70. doi: 10.1038/onc.2014.317
80. Poncet C, Frances V, Gristina R, Scheiner C, Pellissier JF, Figarella-Branger D. CD24, a Glycosylphosphatidylinositol-Anchored Molecules is Transiently Expressed During the Development of Human Central Nervous System and is a Marker of Human Neural Cell Lineage Tumors. *Acta Neuropathol* (1996) 91:400-8. doi: 10.1007/s004010050442
81. Shewan D, Calaora V, Nielsen P, Cohen J, Rougon G, Moreau H. mCD24, a Glycoprotein Transiently Expressed by Neurons, is an Inhibitor of Neurite Outgrowth. *J Neurosci* (1996) 16:2624-34. doi: 10.1523/JNEUROSCI.16-08-02624.1996
82. Ziller C, Dupin E, Brazeau P, Paulin D, Le Douarin NM. Early Segregation of a Neuronal Precursor Cell Line in the Neural Crest as Revealed by Culture in a Chemically Defined Medium. *Cell* (1983) 32:627-38. doi: 10.1016/0092-8674(83)90482-8
83. Löfstedt T, Jögi A, Sigvardsson M, Gradin K, Poellinger L, Pahlman S, et al. Induction of ID2 Expression by Hypoxia-Inducible factor-1: A Role in Dedifferentiation of Hypoxic Neuroblastoma Cells. *J Biol Chem* (2004) 279:39223-31. doi: 10.1074/jbc.M402904200
84. Zhao Z, Bo Z, Gong W, Guo Y. Inhibitor of Differentiation 1 (Id1) in Cancer and Cancer Therapy. *Int J Med Sci* (2020) 17:995-1005. doi: 10.7150/ijms.42805
85. Jiang Q, Shan K, Qun-Wang X, Zhou RM, Yang H, Liu C, et al. Long non-Coding RNA-MIAT Promotes Neurovascular Remodeling in the Eye and Brain. *Oncotarget* (2016) 7:49688-98. doi: 10.18632/oncotarget.10434
86. Bountali A, Tonge DP, Mourrada-Maarabouni M. RNA Sequencing Reveals a Key Role for the Long non-Coding RNA MIAT in Regulating Neuroblastoma and Glioblastoma Cell Fate. *Int J Biol Macromol* (2019) 130:878-91. doi: 10.1016/j.ijbiomac.2019.03.005
87. Meng X, Fang E, Zhao X, Feng J. Identification of Prognostic Long Noncoding RNAs Associated With Spontaneous Regression of Neuroblastoma. *Cancer Med* (2020) 9:3800-15. doi: 10.1002/cam4.3022
88. Brix DM, Bundgaard Clemmensen KK, Kallunki T. Zinc Finger Transcription Factor MZF1-A Specific Regulator of Cancer Invasion. *Cells* (2020) 9:223. doi: 10.3390/cells9010223
89. Fang E, Wang X, Wang J, Hu A, Song H, Yang F, et al. Therapeutic Targeting of YY1/MZF1 Axis by MZF1-uPEP Inhibits Aerobic Glycolysis and Neuroblastoma Progression. *Theranostics* (2020) 10:1555-71. doi: 10.7150/thno.37383
90. Kozak CA, Gatignol A, Graham K, Jeang KT, McBride OW. Genetic Mapping in Human and Mouse of the Locus Encoding TRBP, a Protein That Binds the TAR Region of the Human Immunodeficiency Virus (HIV-1). *Genomics* (1995) 25:66-72. doi: 10.1016/0888-7543(95)80110-8

Conflict of Interest: The authors declare that the research was conducted in the absence of any commercial or financial relationships that could be construed as a potential conflict of interest.

Copyright © 2021 Wieland, Engel, Volkmer, Krüger, Posern, Kornhuber, Staeger and Emmer. This is an open-access article distributed under the terms of the Creative Commons Attribution License (CC BY). The use, distribution or reproduction in other forums is permitted, provided the original author(s) and the copyright owner(s) are credited and that the original publication in this journal is cited, in accordance with accepted academic practice. No use, distribution or reproduction is permitted which does not comply with these terms.

Supplementary Material for

**Overexpression of Endogenous Retroviruses and Malignancy Markers
in Neuroblastoma Cell Lines by Medium-Induced Microenvironmental
Changes**

**Lisa Wieland, Kristina Engel, Ines Volkmer, Anna Krüger, Guido Posern, Malte E.
Kornhuber, Martin S. Staeger, Alexander Emmer**

This file contains:

- **Supplementary Table STab.1** **page 2**
- **Supplementary Table STab.2** **page 4**
- **Supplementary Figure SFig. 1** **page 7**
- **Supplementary Figure SFig. 2** **page 8**

1 Supplementary Tables

Supplementary Table STab.1. Up-regulated genes expressed in three NB cell lines after culture in serum-free stem cell medium. Up-regulated genes were identified by RNA-Seq. Genes are ranked from highest to lowest fold change of FPKM in serum-free medium in the same order as shown in Figure 2 of the manuscript.

Gene ID	Name	<i>fold change</i>
ENSG00000277311	RF02247	3.331
ENSG00000274520	RF02246	2.602
ENSG00000152377	SPOCK1	2.354
ENSG00000184194	GPR173	2.271
ENSG00000250067	YJEFN3	2.265
ENSG00000225783	MIAT	2.106
ENSG00000185615	PDIA2	2.071
ENSG00000232931	LINC00342	2.023
ENSG00000245849	RAD51-AS1	1.969
ENSG00000197093	GAL3ST4	1.961
ENSG00000155980	KIF5A	1.920
ENSG00000264112	AC015813.1	1.883
ENSG00000114796	KLHL24	1.874
ENSG00000099326	MZF1	1.872
ENSG00000171004	HS6ST2	1.837
ENSG00000267595	AC060780.3	1.827
ENSG00000101349	PAK5	1.794
ENSG00000267523	AC008735.2	1.736
ENSG00000144362	PHOSPHO2	1.720
ENSG00000272240	AC004908.1	1.719
ENSG00000144834	TAGLN3	1.713
ENSG00000267002	AC060780.1	1.707
ENSG00000244879	GABPB1-AS1	1.695
ENSG00000151376	ME3	1.693
ENSG00000215252	GOLGA8B	1.671
ENSG00000091972	CD200	1.666
ENSG00000250467	AC105389.3	1.657
ENSG00000263272	AC004148.2	1.654
ENSG00000215397	SCRT2	1.654
ENSG00000267254	AC020928.1	1.651
ENSG00000018236	CNTN1	1.610
ENSG00000146966	DENND2A	1.602
ENSG00000108309	RUNDC3A	1.592
ENSG00000149809	TM7SF2	1.591
ENSG00000124406	ATP8A1	1.586

ENSG00000158292	GPR153	1.583
ENSG00000162004	CCDC78	1.581
ENSG00000133134	BEX2	1.576
ENSG00000114770	ABCC5	1.568
ENSG00000105270	CLIP3	1.561
ENSG00000135596	MICAL1	1.554
ENSG00000182901	RGS7	1.554
ENSG00000131067	GGT7	1.554
ENSG00000129003	VPS13C	1.551
ENSG00000169231	THBS3	1.537
ENSG00000104899	AMH	1.537
ENSG00000224032	EPB41L4A-AS1	1.521
ENSG00000145198	VWA5B2	1.517
ENSG00000077264	PAK3	1.515
ENSG00000160271	RALGDS	1.511
ENSG00000250959	GLUD1P3	1.495
ENSG00000272301	AP002360.3	1.494
ENSG00000175265	GOLGA8A	1.491
ENSG00000169733	RFNG	1.488
ENSG00000220205	VAMP2	1.481
ENSG00000034677	RNF19A	1.474
ENSG00000254064	AC105206.2	1.467
ENSG00000054793	ATP9A	1.467
ENSG00000059588	TARBP1	1.464
ENSG00000171533	MAP6	1.452
ENSG00000120324	PCDHB10	1.452
ENSG00000102078	SLC25A14	1.447
ENSG00000139636	LMBR1L	1.447
ENSG00000188785	ZNF548	1.439
ENSG00000196123	KIAA0895L	1.439
ENSG00000166924	NYAP1	1.433
ENSG00000105443	CYTH2	1.432
ENSG00000131584	ACAP3	1.432
ENSG00000167363	FN3K	1.430
ENSG00000177410	ZFAS1	1.425
ENSG00000100167	SEPT3	1.424
ENSG00000155093	PTPRN2	1.421
ENSG00000183098	GPC6	1.414
ENSG00000212694	LINC01089	1.412
ENSG00000234338	AC073349.2	1.407
ENSG00000258682	AL132989.1	1.406
ENSG00000162687	KCNT2	1.404
ENSG00000033627	ATP6V0A1	1.402

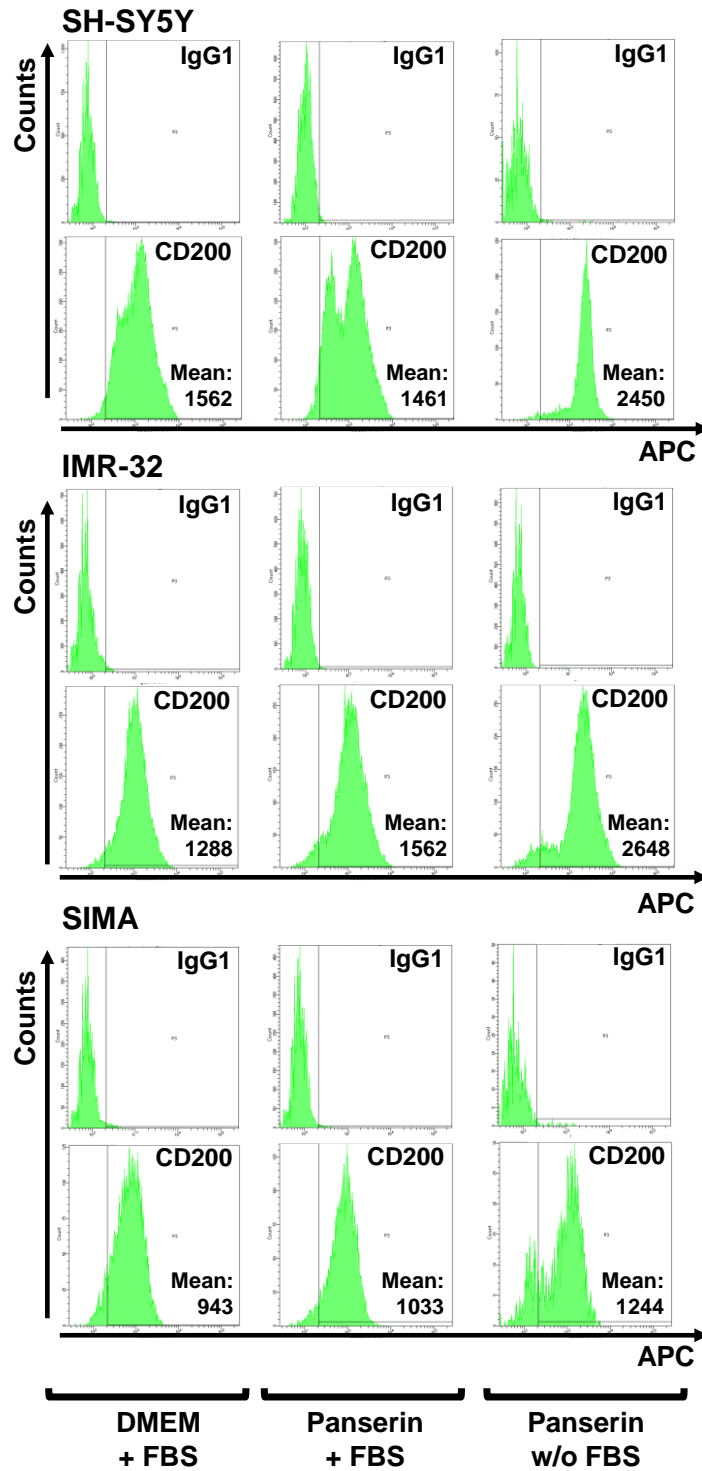
Supplementary Table STab.2. Down-regulated genes in NB cell lines after culture in serum-free medium. Down-regulated genes were identified by RNA-Seq. Genes are ranked from lowest to highest fold change of FPKM in serum-supplemented medium in the same order as in Figure 2 of the manuscript.

Gene ID	Name	<i>fold change</i>
ENSG00000130147	SH3BP4	1.401
ENSG00000172403	SYNPO2	1.403
ENSG00000089159	PXN	1.404
ENSG00000130347	RTN4IP1	1.404
ENSG00000108423	TUBD1	1.404
ENSG00000006576	PHTF2	1.408
ENSG00000100281	HMGXB4	1.408
ENSG00000173786	CNP	1.409
ENSG00000174177	CTU2	1.409
ENSG00000196498	NCOR2	1.409
ENSG00000104332	SFRP1	1.411
ENSG00000106628	POLD2	1.412
ENSG00000145386	CCNA2	1.416
ENSG00000104147	OIP5	1.417
ENSG00000086827	ZW10	1.421
ENSG00000126787	DLGAP5	1.421
ENSG00000111328	CDK2AP1	1.426
ENSG00000269958	AL049840.4	1.427
ENSG00000253954	HMGNI1P38	1.429
ENSG00000203760	CENPW	1.430
ENSG00000138448	ITGAV	1.431
ENSG00000080839	RBL1	1.433
ENSG00000165490	DDIAS	1.435
ENSG00000100162	CENPM	1.439
ENSG00000115129	TP53I3	1.442
ENSG00000115325	DOK1	1.447
ENSG00000188229	TUBB4B	1.452
ENSG00000117593	DARS2	1.455
ENSG00000119326	CTNNAL1	1.457
ENSG00000060656	PTPRU	1.460
ENSG00000116791	CRYZ	1.461
ENSG00000159055	MIS18A	1.464
ENSG00000144354	CDCA7	1.464
ENSG00000107816	LZTS2	1.465
ENSG00000030110	BAK1	1.467
ENSG00000174021	GNG5	1.467

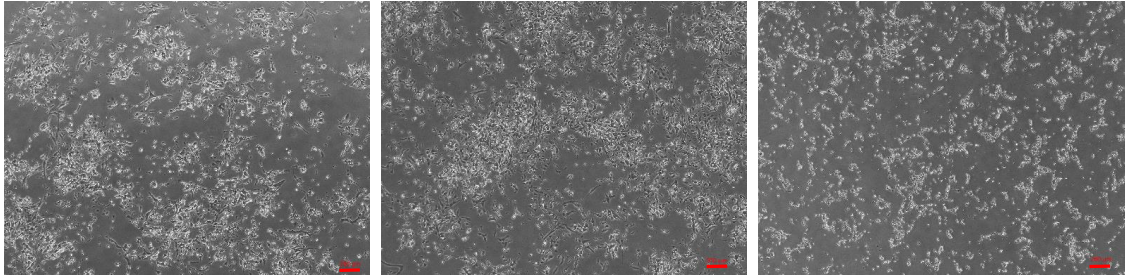
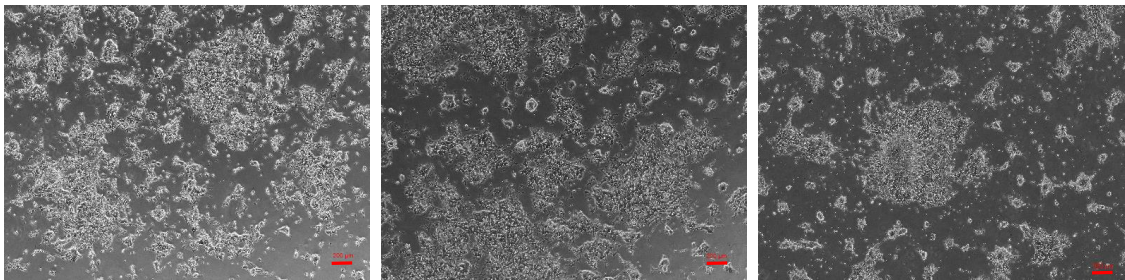
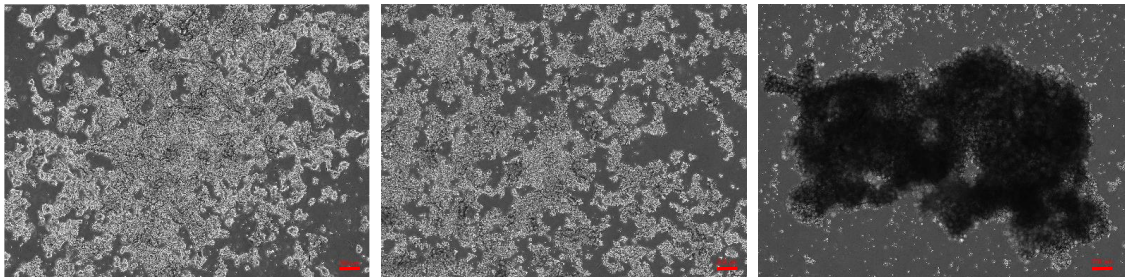
ENSG00000163629	PTPN13	1.468
ENSG00000117280	RAB29	1.470
ENSG00000173207	CKS1B	1.472
ENSG00000109390	NDUFC1	1.475
ENSG00000134569	LRP4	1.477
ENSG00000151503	NCAPD3	1.481
ENSG00000178999	AURKB	1.483
ENSG00000171241	SHCBP1	1.484
ENSG00000128228	SDF2L1	1.486
ENSG00000122756	CNTFR	1.495
ENSG00000102158	MAGT1	1.498
ENSG00000259917	HNRNPLP2	1.499
ENSG00000105968	H2AFV	1.500
ENSG00000153044	CENPH	1.511
ENSG00000106211	HSPB1	1.513
ENSG00000131873	CHSY1	1.521
ENSG00000105011	ASF1B	1.526
ENSG00000168078	PBK	1.530
ENSG00000197905	TEAD4	1.532
ENSG00000149929	HIRIP3	1.537
ENSG00000148219	ASTN2	1.561
ENSG00000149554	CHEK1	1.566
ENSG00000106105	GARS	1.566
ENSG00000187741	FANCA	1.568
ENSG00000090889	KIF4A	1.573
ENSG00000075188	NUP37	1.575
ENSG00000129173	E2F8	1.582
ENSG00000198860	TSEN15	1.582
ENSG00000254858	MPV17L2	1.585
ENSG00000066735	KIF26A	1.606
ENSG00000040275	SPDL1	1.612
ENSG00000072571	HMMR	1.619
ENSG00000125703	ATG4C	1.621
ENSG00000140545	MFGE8	1.636
ENSG00000136603	SKIL	1.637
ENSG00000149257	SERPINH1	1.646
ENSG00000165304	MELK	1.648
ENSG00000064042	LIMCH1	1.653
ENSG00000115163	CENPA	1.654
ENSG00000184260	HIST2H2AC	1.677
ENSG00000135862	LAMC1	1.689
ENSG00000162129	CLPB	1.689
ENSG00000173456	RNF26	1.699

ENSG00000183580	FBXL7	1.701
ENSG00000166002	SMCO4	1.704
ENSG00000072110	ACTN1	1.725
ENSG00000150961	SEC24D	1.727
ENSG00000125170	DOK4	1.730
ENSG00000140332	TLE3	1.736
ENSG00000268942	CKS1BP3	1.737
ENSG00000109790	KLHL5	1.743
ENSG00000114738	MAPKAPK3	1.746
ENSG00000164649	CDCA7L	1.751
ENSG00000129195	PIMREG	1.754
ENSG00000135736	CCDC102A	1.773
ENSG00000186350	RXRA	1.777
ENSG00000123473	STIL	1.786
ENSG00000185043	CIB1	1.800
ENSG00000144045	DQX1	1.811
ENSG00000168476	REEP4	1.844
ENSG00000153551	CMTM7	1.854
ENSG00000132423	COQ3	1.857
ENSG00000110108	TMEM109	1.873
ENSG00000163661	PTX3	1.961
ENSG00000175183	CSRP2	2.058
ENSG00000076356	PLXNA2	2.061
ENSG00000188486	H2AFX	2.075
ENSG00000095739	BAMBI	2.089
ENSG00000223764	AL645608.1	2.166
ENSG00000176014	TUBB6	2.195
ENSG00000179348	GATA2	2.251
ENSG00000115297	TLX2	2.255
ENSG00000101665	SMAD7	2.409
ENSG00000111145	ELK3	2.410
ENSG00000112559	MDFI	3.061
ENSG00000135111	TBX3	3.105
ENSG00000026025	VIM	3.167
ENSG00000107731	UNC5B	3.177
ENSG00000143320	CRABP2	3.328
ENSG00000168453	HR	3.855
ENSG00000064666	CNN2	6.016
ENSG00000115738	ID2	16.011
ENSG00000187634	SAMD11	24.625
ENSG00000125968	ID1	40.625

2 Supplementary Figures



Supplementary Figure 1. Regulation of CD200 surface protein expression in three NB cell lines by medium-induced microenvironmental changes by flow cytometry. The histograms of NB cells stained with CD200-APC antibodies or isotype controls are shown. The mean fluorescence intensities of APC-positive cells are included.

SH-SY5Y**IMR-32****SiMA**

**DMEM
+ FBS**

**Panserin
+ FBS**

**Panserin
w/o FBS**

Supplementary Figure 2. Morphological analyses of three NB cell lines upon medium-induced microenvironmental change. For SiMa cells, a phenotype switching from loosely-adherent monolayers to low proliferating grape-like cellular aggregates was observed. Phase contrast microscopy on a Keyence microscope BZ-X810 was used. The bar represents 200 μ m.

2.3. Epstein-Barr Virus-Induced Genes and Endogenous Retroviruses in Immortalized B Cells from Patients with Multiple Sclerosis

2.3.1. Zusammenfassung

Es wird angenommen, dass zur Entstehung der MS sowohl umweltbedingte Faktoren, als auch die genetische Prädisposition eine Rolle spielen. Die Infektion mit EBV gilt als Hauptrisikofaktor für die spätere Entwicklung von MS. HERVs stellen z. T. intrinsisch transponierbare Elemente in unserem Genom dar, die durch vielschichtige Regulationsmechanismen des Wirts kontrolliert werden und im Normalfall nicht oder nur schwach exprimiert sind. Jedoch können sie durch EBV aktiviert werden. Dies lässt die Vermutung zu, dass HERVs das fehlende Bindeglied zwischen einer einstigen Infektion mit EBV und dem späteren Auftreten von MS sein könnten. Das Ziel der Studie war es, differenzielle Gen- und HERV-Expressionsmuster in EBV-immortalisierten B-Zellen von MS-Patienten (MSLCL) und Kontrollen (coLCL) mit Hilfe von Transkriptomanalysen (RNAseq) und quantitativer PCR zu untersuchen. Dazu wurden B-Zellen aus PBMC *in vitro* mit EBV immortalisiert und sogenannte LCL erzeugt. Neben der menschlichen Genomversion GRCh38/hg38, wurde ein von unserer Gruppe designtes Virus-Transkriptom verwendet, um auch HERVs als mögliche Zielgene für MS oder krankheitsrelevante Risikofaktoren, z. B. die Schubrate, untersuchen zu können. Wir stellten fest, dass die Expression von EBNA-1 der lytischen Phase des EBV negativ mit dem Alter korrelierte, was zu einer erhöhten Expression in LCL von jüngeren PBMC-Spendern führte. Darüber hinaus war die Transkription von HERV-K (HML-2) *GAG* durch die Immortalisierung mit EBV verstärkt. Neben der bekannten Transaktivierung von HERV-K18 deuten unsere Transkriptomanalysen darauf hin, dass weitere sechs HERV-Loci in EBV-infizierten B-Zellen hochreguliert werden. Zudem wurden in MSLCL differenziell exprimierte Gene identifiziert, wozu u.a. mehrere HERV-K-Loci, ERVMER61-1 und ERV3-1 zählten, sowie auch Gene, die mit dem Auftreten von Schüben in Verbindung stehen könnten. Zusammenfassend konnten mittels der EBV-induzierten Proliferation potentielle Targets, u. a. auch HERVs, in MS-assoziierten B-Zelllinien identifiziert werden, die als Zielstrukturen für diagnostische oder prognostische Fragestellungen, wie z. B. das Schubrisiko, geeignet sein könnten.

2.3.2. Darlegung des Eigenanteils und Zitierung

Im Folgenden ist der experimentelle und schriftliche Eigenanteil aller Autoren prozentual angegeben und die Beteiligung mehrerer Personen an der Veröffentlichung durch einen Betreuer bestätigt.

Publikation III:

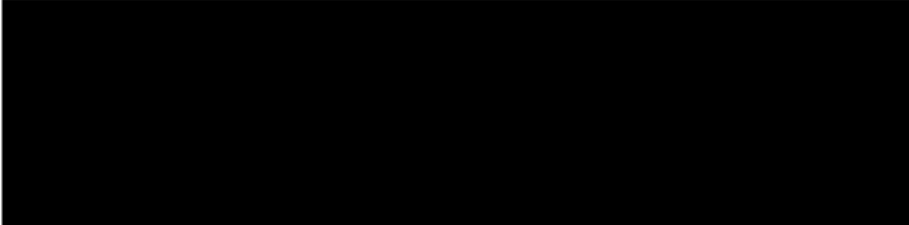
Wieland, L., Schwarz, T., Engel, K., Volkmer, I., Krüger, A., Tarabuko, A., Junghans, J., Kornhuber, M. E., Hoffmann, F., Staeger, M. S., & Emmer, A. (2022). Epstein-Barr Virus-Induced Genes and Endogenous Retroviruses in Immortalized B Cells from Patients with Multiple Sclerosis. *Cells*, 11(22), 3619. <https://doi.org/10.3390/cells11223619>

Tabelle 4: Übersicht zu den Beiträgen aller Autoren der Publikation III.

	Entwurf (Design)	Umsetzung (Implementation)	Auswertung (Analysis)	Schreiben (Writing)
Wieland, L.	10 %	35 %	70 %	70 %
Schwarz, T.		25 %		
Engel, K.			15 %	5 %
Volkmer, I.		10 %		
Krüger, A.		10 %		
Tarabuko, A.		5 %		
Junghans, J.		5 %		
Kornhuber, M. E.	10 %			5 %
Hoffmann, F.	10 %			5 %
Staeger, M. S.	40 %		15 %	10 %

Emmer, A.	30 %	10 %		5 %
------------------	------	------	--	-----

Datum: 15.03.2024



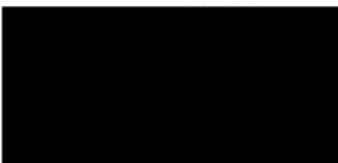
Lisa Wieland

Dr. med. Alexander Emmer

2.3.3. Bestätigung des Betreuers der Dissertation von Frau Lisa Wieland

Hiermit bestätige ich als Betreuer der o. g. Dissertation, dass die gemeinsame Arbeit mehrerer Personen an der Arbeit durch den Forschungsgegenstand gerechtfertigt ist.

Mit freundlichen Grüßen,





Dr. med. Alexander Emmer

Datum: 15.03.2024

Nachfolgend sind die Publikation und die supplementären Daten aufgeführt.

Article

Epstein-Barr Virus-Induced Genes and Endogenous Retroviruses in Immortalized B Cells from Patients with Multiple Sclerosis

Lisa Wieland ^{1,2}, Tommy Schwarz ¹, Kristina Engel ², Ines Volkmer ², Anna Krüger ², Alexander Tarabuko ¹, Jutta Junghans ³, Malte E. Kornhuber ¹, Frank Hoffmann ³, Martin S. Staege ^{2,*} and Alexander Emmer ¹

¹ Department of Neurology, Medical Faculty, Martin Luther University Halle-Wittenberg, 06120 Halle (Saale), Germany

² Department of Surgical and Conservative Pediatrics and Adolescent Medicine, Medical Faculty, Martin Luther University Halle-Wittenberg, 06120 Halle (Saale), Germany

³ Department of Neurology, Martha-Maria Hospital Halle-Dölau, 06120 Halle (Saale), Germany

* Correspondence: martin.staega@medizin.uni-halle.de; Tel.: +49-34-5557-7280

Abstract: The immune pathogenesis of multiple sclerosis (MS) is thought to be triggered by environmental factors in individuals with an unfavorable genetic predisposition. Epstein-Barr virus (EBV) infection is a major risk factor for subsequent development of MS. Human endogenous retroviruses (HERVs) can be activated by EBV, and might be a missing link between an initial EBV infection and the later onset of MS. In this study, we investigated differential gene expression patterns in EBV-immortalized lymphoblastoid B cell lines (LCL) from MS-affected individuals (MSLCL) and controls by using RNAseq and qRT-PCR. RNAseq data from LCL mapped to the human genome and a virtual virus metagenome were used to identify possible biomarkers for MS or disease-relevant risk factors, e.g., the relapse rate. We observed that lytic EBNA-1 transcripts seemed to be negatively correlated with age leading to an increased expression in LCL from younger PBMC donors. Further, HERV-K (HML-2) GAG was increased upon EBV-triggered immortalization. Besides the well-known transactivation of HERV-K18, our results suggest that another six HERV loci are up-regulated upon stimulation with EBV. We identified differentially expressed genes in MSLCL, e.g., several HERV-K loci, ERVMER61-1 and ERV3-1, as well as genes associated with relapses. In summary, EBV induces genes and HERV in LCL that might be suitable as biomarkers for MS or the relapse risk.

Keywords: multiple sclerosis; Epstein-Barr virus; lymphoblastoid cell lines; human endogenous retrovirus; biomarkers



Citation: Wieland, L.; Schwarz, T.; Engel, K.; Volkmer, I.; Krüger, A.; Tarabuko, A.; Junghans, J.; Kornhuber, M.E.; Hoffmann, F.; Staega, M.S.; et al. Epstein-Barr Virus-Induced Genes and Endogenous Retroviruses in Immortalized B Cells from Patients with Multiple Sclerosis. *Cells* **2022**, *11*, 3619. <https://doi.org/10.3390/cells11223619>

Academic Editors: Simona Rolla, Gabriele Di Sante and Alexander E. Kalyuzhny

Received: 15 September 2022

Accepted: 6 November 2022

Published: 15 November 2022

Publisher's Note: MDPI stays neutral with regard to jurisdictional claims in published maps and institutional affiliations.



Copyright: © 2022 by the authors. Licensee MDPI, Basel, Switzerland. This article is an open access article distributed under the terms and conditions of the Creative Commons Attribution (CC BY) license (<https://creativecommons.org/licenses/by/4.0/>).

1. Introduction

The Epstein-Barr virus (EBV) is the causative agent of infectious mononucleosis (IM), also known as Pfeiffer's glandular fever. After infection, the virus stays present latently in the B cell memory pool and persists in the human body over a lifetime, without triggering symptoms [1,2]. If the immune system is weakened, the virus-infected B cells can proliferate uncontrollably, and EBV can become a trigger for lymphoproliferative disorders [3,4]. Besides cancer, EBV infection is thought to be a major risk factor for the development of multiple sclerosis (MS), since seropositivity to EBV nuclear antigen (EBNA) epitopes or the viral capsid antigen (VCA) is more prevalent among MS-affected individuals than in controls [5–8]. A very recent report from MS cases among US military personnel suggests a 32-fold increased risk of MS and higher serum levels of neurofilament light chain, a biomarker of neuroaxonal degeneration, after EBV seroconversion [9]. Furthermore, similarities between the epidemiology of MS and a delayed EBV primary infection manifesting as IM were observed, including the latitude gradient and earlier onset in women than in men [10,11]. As a result, an IM diagnosis in adolescents and young adults has been

associated with a two- to fourfold increased risk of MS [12–15]. However, exposure to EBV alone is not sufficient to develop MS. A combination of environmental and genetic factors appears to be involved, resulting in the dysregulation of the immune system [16,17]. In the last decades, human endogenous retroviruses (HERVs) have increasingly been associated with nervous system disorders, e.g., based on the increased expression of different HERV loci in various cell types, tissues, and biological fluids from individuals with MS (reviewed in [18]). Further, the appearance of retrovirus-like particles in B cells from the cerebrospinal fluid (CSF) of an individual with MS supported the hypothesis of a putative role in the pathogenesis of MS [19]. HERVs represent stably integrated copies of exogenous viruses in the human genome that have been “endogenized” during evolution and are commonly inactivated [20]. Nevertheless, some HERVs still have relatively intact open reading frames, e.g., for envelope proteins, which can have immunostimulatory and pro-inflammatory properties like superantigens [21–23]. HERVs can be transactivated by EBV [24,25], suggesting that there may be a connection between EBV, HERVs and MS.

In this paper we aimed to study the influence of an EBV-driven proliferation on the gene expression in B cells from individuals with MS. We used the fact that EBV can immortalize B cells in vitro and generate so-called lymphoblastoid cell lines (LCL) [26,27]. Concerning B cells that have been observed in MS brain lesions of early and progressive phases of MS [28] and the development of successful B cell-depleting therapies in the relapsing-remitting and primary progressive forms of MS [29], these LCL might overcome some limitations of traditional murine models of MS that are mediated largely by pathogenic T cells. In this study, we wanted to investigate putative differential expression patterns in MS and controls. Therefore, multiple LCL from 32 individuals with MS and 10 controls were established and analyzed by RNAseq. As HERVs, and especially their protein coding regions (e.g., ENVs), are discussed in the pathogenesis of MS, we secondly aimed to investigate for differentially expressed HERV within our LCLs from MS and controls. We used a synthetic virus metagenome designed by our group to simultaneously compare the expression of more than a hundred HERVs, providing the most complete open-reading frames for their coding regions or even nearly complete proviral sequences by RNAseq analyses. Further, we focused on possible correlations of environmental and clinicopathological features with the activation of the EBV lytic and latent cycle, and selected HERV transcripts using RNAseq and quantitative reverse transcription-polymerase chain reaction (qRT-PCR). In this regard, we focused on two HERV-families, namely HERV-W and HERV-K, as they are frequently discussed to play a role in the pathogenesis of MS (reviewed in [30–32]). For the HERV-W family, we examined the envelope from ERVWE-1 on chromosome 7 (HERV-W1 ENV), and another envelope with a yet unknown genomic location named MS-associated retrovirus (MSRV ENV). For HERV-K, the group specific antigen (GAG) region was chosen as the target region, because it allows the detection of numerous members of the most biologically active HERV family without distinguishing between type 1 and type 2 HERV-K proviruses. In qRT-PCR analyses, we took advantage of this fact and used specific primers to detect multiple members of the HERV-K (HML-2) family based on their high sequence homology. Since this was not possible for RNAseq analyses, we investigated the expression of a HERV, which is also targeted by qRT-PCR, namely HERV-K4. To monitor the activation of EBV, we detected the major transcript expressed in LCL during latent cycle progression, called EBNA-2, as well as EBNA-1 starting at the F promoter site, which is used in the lytic EBV cycle [33–36].

2. Materials and Methods

2.1. Cell Lines and Cell Culture

Peripheral blood mononuclear cells (PBMCs) were isolated by density gradient centrifugation [37] from 10 controls and from 32 individuals with MS with informed consent and with approval by the ethics committee of the Martin Luther University Halle-Wittenberg (protocol code: 2015-89). Within our study cohort the mean age was 39.1 (range: 23–56), and approximately two-thirds (n = 21) were female. All individuals with MS had

a diagnosed relapsing–remitting course of MS when they joined the study. The mean duration of the disease was 7.3 years (range 0–21 years). The mean EDSS score was 2.9 (range: 1–5.5). For one individual with MS no EDSS assessment was possible. Of all the individuals with MS, 22 received therapies including treatment with natalizumab (n = 14), fingolimod (n = 3), alemtuzumab (n = 1), interferon beta-1a (n = 1), carbamazepine (n = 1), glatiramer acetate (n = 1) or dimethyl fumarate (n = 1) at the time of blood collection. Ten individuals with MS were not receiving disease-modifying therapies (DMT) at the time of blood collection. To generate LCL, PBMCs were resuspended in Panserin 401 medium (PAN-Biotech GmbH, Aidenbach, Germany) supplemented with penicillin-streptomycin (Life Technologies, Carlsbad, CA, USA). PBMC were seeded at a density of 3×10^5 cells per well in a 24-well plate. EBV-containing supernatant was collected from the B95.8 cell line and added at a ratio of 1:1 per well. Cells were incubated at 37 °C in a 5% CO₂ humidified atmosphere. After 2 weeks, the conditioned medium was replaced with fresh medium. Once a week the cells were fed with fresh medium. After 5–6 weeks, big lymphoblastoid colonies had grown and could be expanded. Typically, the cells were split twice a week, at a ratio of 1:2, and harvested for downstream experiments 4–5 weeks after the first split.

2.2. Flow Cytometry

Surface antigen expression was detected by flow cytometry. Cells were resuspended in ice-cold PBS with 2 mM EDTA and stained for 30 min at 4 °C using 5 µL of two-color antibody solutions αCD45-FITC/αCD14-PE, αCD3-FITC/αCD19-PE, αCD3-FITC/αHLA-DR-PE, or αIgG1-FITC/αIgG2a-PE from the BD Simultest IMK Plus reagent kit, single-color antibodies αCD23-PE or αIgG1-PE control (all from BD Biosciences, Franklin Lakes, NJ, USA). After washing with 1 mL PBS/EDTA solution, cells were analyzed on a LSRII cytometer using FACSDiva software version 8.0.1 (BD Biosciences, Franklin Lakes, NJ, USA).

2.3. RNA Extraction, cDNA Generation, and Quantitative Real-Time PCR

Total cellular RNA was isolated using the NucleoSpin RNA kit (Machery-Nagel GmbH & Co. KG, Düren, Germany) following the manufacturer's instructions. Transcription into cDNA was performed using 1 µg total RNA in 16 µL nuclease-free water and 4 µL qScript cDNA 5× SuperMix (QuantaBio, Beverly, MA, USA). For qRT-PCR, each reaction contained 0.5 µL of cDNA, 500 nM of forward and reverse primer, 5 µL of PowerUP SYBR Green 2× Master Mix (Applied Biosystems by Thermo Fisher Scientific, Waltham, MA, USA), and 4 µL of nuclease-free water. All primers are listed in Table 1.

Table 1. Primers used for quantitative real-time PCR.

Target	Exemplary Accession Number	Sequence of Forward (f) and Reverse (r) Primer (5'-3')
EBNA-1	V01555.2:62399-107964 [38]	f: GCTTTGCGAAAACGAAAGTG r: CCCCTCGTCAGACATGAT
EBNA-2	V01555.2:48888-49287 [39]	f: TCTGCTATGCGAATGCTTTG r: GAGGGTGCATTGATTGGTCT
HERV-K GAG	JN675025.1:1621-1787 [40]	f: GGCCATCAGAGTCTAAACCACG r: CTGACTTTCTGGGGGTGGCCG
HERV-W1 ENV	NM_014590.4:2206-2341 [41]	f: TGCTAACCGCTGAAAGAGGG r: CGAAGCTCCTCTGCTCTACG

The amplification protocol included an initial denaturation step at 95 °C for 10 min, followed by 40 cycles with denaturation at 95 °C for 15 s, primer annealing, amplification, and extension at 61 °C for 60 s. Two technical replicates were measured for each sample. LCL from the same PBMC donor were taken together and therefore served as biological replicates. A total of 30 PBMC and 94 LCL were analyzed from 32 individuals with MS, as well as 10 PBMC and 29 LCL from 10 controls. The analysis was performed using QuantStudio3 and QuantStudio Design and Analysis Software v.1.4.3 (Applied Biosystems by Thermo Fisher Scientific, Waltham, MA, USA). For copy number determination, standard

curves were prepared using dilutions from 10 ng to 10^{-11} ng of purified target DNA. The copy number was calculated with respect to the molecular weight of the target DNA amplicon (EBNA-1: 156.381 kDa; EBNA-2: 247.219 kDa; HERV-K GAG: 103.226 kDa; HERV-W1 ENV: 84.057 kDa) using the DNA Molecular Weight calculator at https://www.bioinformatics.org/sms2/dna_mw.html (accessed on 1 January 2020). Standard curves can be found in the supplement (Supplementary Figure S1).

2.4. RNAseq Analysis

Generation of RNAseq data was performed by Novogene UK Co., Ltd. (Cambridge, UK) using the Illumina Novaseq6000 system, and can be downloaded from the NCBI Short Read Archive (SRA) under BioProject PRJNA765133. All samples presented in this manuscript passed the quality control. The quality control report is provided in the supplement. A total of 16 PBMC and 79 LCL from 32 individuals with MS ($n_{\text{LCL}} = 59$ and $n_{\text{PBMC}} = 9$) and 10 controls ($n_{\text{LCL}} = 20$ and $n_{\text{PBMC}} = 7$) were analyzed. LCL from the same PBMC donor were taken together and therefore served as biological replicates. Additional RNAseq data from activated B cells were downloaded from SRA (BioProjects PRJNA397793 [42] and PRJNA702159 [43]). Quantification of overall HERV expression was performed as described [44] by using the Galaxy server [45] for Bowtie2 mapping and quantification by FeatureCounts [46]. Quantification of human transcriptome data was performed by Novogene UK Co., Ltd. (Cambridge, UK) using human genome version GRCh38/hg38. For all analyses, fragments per kilobase per million (FPKM) values were calculated to quantify and normalize the counted fragments with FeatureCounts, according to the transcript length and the total number of reads.

To identify differentially expressed genes, we determined the fold changes calculated from the median of one group divided by the 75th percentile of the other group. Heatmaps of strongest differentially expressed genes were performed using the heatmap webtool at <http://heatmapper.ca/expression/> (accessed on 1 August 2022). For all volcano plots, GraphPad Prism was used (version 8.3.0 for Windows, GraphPad Software, San Diego, CA, USA).

To study the influence of environmental factors and clinical parameters (as, e.g., the relapse rate), the paired-end reads of the sequence data were mapped to a small synthetic virus metagenome using Bowtie2 (Galaxy Version 2.4.2 + galaxy0) from the Galaxy platform [45] with default settings. We have added the fasta file of this genome, including selected sequences of housekeeping genes, endogenous and exogenous viruses, in the supplement (Viruses21B4.fasta). For quantification of gene expression from the BAM files, the mapped reads were counted using FeatureCounts (Galaxy Version 2.0.1 + galaxy2 [46]). The GTF file used for quantification (Viruses21B4.gtf) is provided in the supplement. We used the following settings: enable counting of fragments instead of reads (-p), only allowing fragments with both reads aligned (-B), enable both multi- and overlapping features (-M -O). This has the advantage, that the readthrough transcripts in the smaller exons (F/Q and U) can also be detected and would not only be counted, e.g., for the larger EBNA-1 K exon. This provides the highest probability of detecting all lytic EBNA-1 transcripts starting in the F/Q promoter region.

To identify MS biomarkers within our LCL model, differentially up-regulated genes in MS ($p < 0.05$) were identified, and for each gene the 16th highest FPKM value in MSLCL ($n = 59$) was determined. Subsequently, the genes that showed an expression below this threshold in all coLCL ($n = 20$) were identified. As a result, we obtained a list of genes that had an expression above a target-dependent threshold in at least 25% of MSLCL. This cut-off was never exceeded by any coLCL. To identify targets that correlated with the relapse rate in MS, we used MSLCL in at least duplicates from each seven individuals with ($n = 14$) and without relapses ($n = 15$) in the last two years matched by gender and the duration of disease ± 1 year. Due to the limited number of samples, we determined targets that had an expression above or below a cut-off value in at least 75% of the MSLCL from individuals with relapses using the 11th highest FPKM.

2.5. Statistics

For all statistical analyses, GraphPad Prism was used (version 8.3.0 for Windows, GraphPad Software, San Diego, CA, USA). Comparisons of two groups were performed using *t*-test. To compare more than two groups, a one-way ANOVA with Dunnett T3 post-hoc test was performed. Multiple comparison analyses were performed using two-way ANOVA, followed by Bonferroni multiple comparisons test. The *p* values are indicated by asterisks: **** $p < 0.0001$, *** $p < 0.001$, ** $p < 0.01$, * $p < 0.05$. To determine the specificity and the sensitivity of putative biomarkers, receiver operating characteristic (ROC) analyses were performed.

3. Results

3.1. The GAG Regions of HERV-K (HML-2) Loci Are Up-Regulated by EBV-Triggered Immortalization

We studied the expression of EBV and distinct HERVs, which are frequently suggested to play a role in the pathogenesis of MS. Therefore, we designed a small virus meta-genome including the sequence of EBNA-2 as well as EBNA-1 transcripts including the exons F/Q, U and K, as well as sequences from HERV-W and HERV-K family members. Regarding HERV-W family, we focused on the envelope from ERVWE-1 coding locus on chromosome 7 (HERV-W1 *ENV*) and another envelope with a yet unknown genomic location named MS-associated retrovirus (MSRV *ENV*). Further, we investigated the expression of a group-specific antigen (GAG) region of HERV-K4 belonging to the biologically most active HERV-K (HML-2) family. Besides RNAseq, we determined copy numbers of the same HERV-W1 *ENV*, EBNA-2 and lytic EBNA-1 transcripts by qRT-PCR, using a larger number of PBMC samples and multiple LCL per donor. In total, 40 PBMC and 123 LCL from 32 individuals with MS ($n_{LCL} = 94$ and $n_{PBMC} = 30$) and 10 controls ($n_{LCL} = 29$ and $n_{PBMC} = 10$) were analyzed. Of notice, expression of HERV-K GAG was studied using primers that detected not only GAG from HERV-K4, but also other members of the HERV-K (HML-2) family.

Comparing the expression in PBMC and LCL, we observed strong increase after EBV-triggered immortalization of both EBNA-2 ($p < 0.0001$) and lytic EBNA-1 ($p < 0.0001$) using RNAseq and qRT-PCR (Figure 1). No expression of the EBV transcripts was observed in any of the PBMC samples studied. In contrast, the expression of the HERVs analyzed could be detected in LCL and PBMC, though at low levels. In controls, HERV-W1 *ENV* showed higher expression in LCL than in PBMC with significant difference in qRT-PCR analyses. In individuals with MS, high HERV-W1 *ENV* levels were also observed in several PBMC samples without significant up-regulation in LCL. However, the overall mean expression was comparably elevated in LCL from both controls and individuals with MS. For MSRV *ENV*, the expression showed no significant changes after EBV-immortalization by RNAseq analyses. Further, the expression of HERV-K4 GAG showed no significant differences in PBMC and LCL from individuals with MS or controls. In qRT-PCR analyses targeting broad numbers of HERV-K (HML-2) family members due to their high sequence homology, HERV-K GAG transcription was up-regulated after EBV-induced immortalization of both MS ($p < 0.0001$) and control ($p < 0.01$) samples.

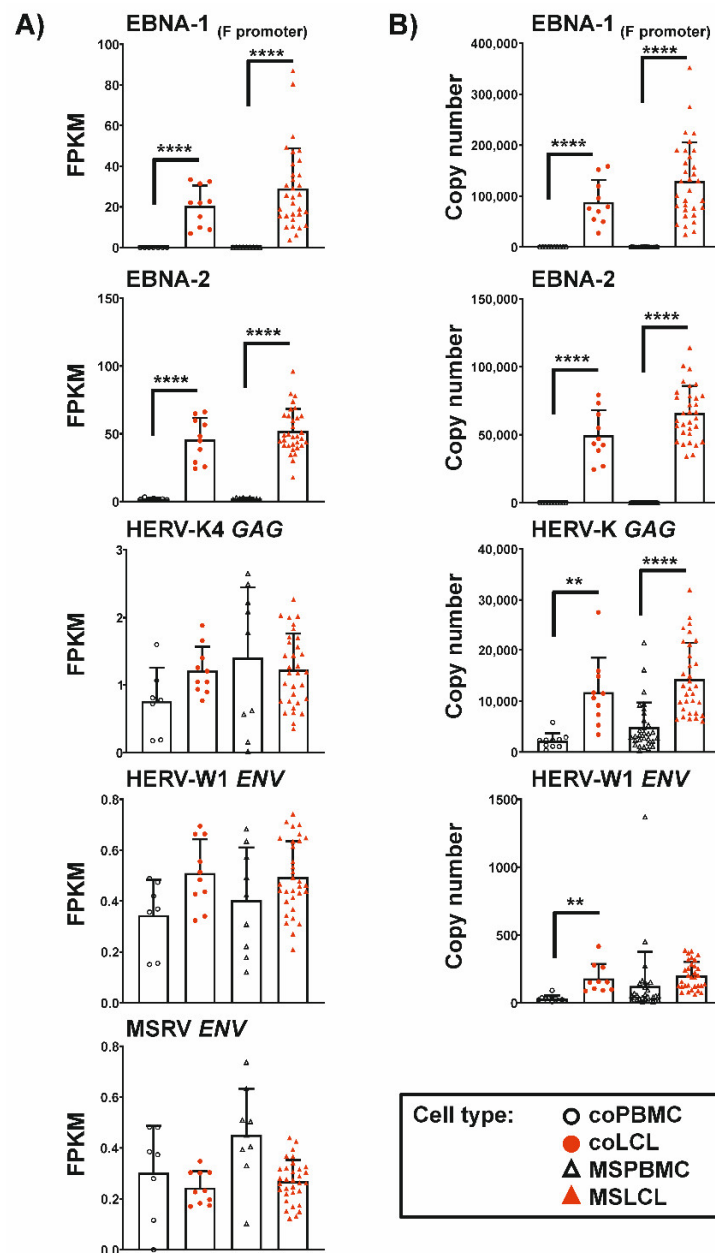


Figure 1. Comparison of EBV and HERV expression in PBMC and after EBV-triggered immortalization of B cells. The graphs show mean \pm SD of FPKM of RNAseq analyses (A) or copy numbers of qRT-PCR analyses (B). LCL from the same individual served as biological replicates. Statistics: One-way ANOVA with Dunnett T3 post-hoc test; **** $p < 0.0001$, ** $p < 0.01$.

3.2. Transcription of EBNA-1 from the Lytic Promoter Is Negatively Correlated with Age of PBMC Donors

Next, we investigated the influence of environmental risk factors and clinical parameters on the expression of the mentioned EBV and HERV targets in LCL from individuals with MS. We observed increased levels of lytic EBNA-1 transcripts ($p < 0.01$) in LCL from individuals with MS treated with natalizumab compared to those not receiving disease-modifying therapies (Table 2). The primers used for EBNA detect transcripts initiated at the F promoter that is used during EBV lytic cycle. Consequently, detection of EBNA-1 transcripts with these primers in LCL correlates well with the B cell-immortalization capacity of culture supernatants from these cells [38].

Table 2. Influence of environmental and clinicopathological factors on EBV and HERV expression in LCL from MS individuals. RNAseq data from EBNA-1, EBNA-2, HERV-K4 GAG, HERV-W1 ENV and MSR/V ENV were determined in a total of 59 LCL from 32 individuals with MS and presented as FPKM. LCL from the same individual served as biological replicates. Data are means \pm SD. Statistics: Two-way ANOVA with Bonferroni's posthoc test; p values < 0.05 from comparisons between the indicated groups (a: 1-2 relapses, b: no relapses; c natalizumab, d: no therapy) were indicated.

	EBNA-2	EBNA-1 F Promoter	HERV-K4 GAG	HERV-W1 ENV	MSRV ENV
GENDER					
Female (n = 21)	52.68 \pm 18.79	32.69 \pm 17.39	1.260 \pm 0.4868	0.5098 \pm 0.1336	0.2671 \pm 0.0825
Male (n = 11)	50.72 \pm 10.94	21.94 \pm 22.88	1.145 \pm 0.6285	0.4633 \pm 0.1589	0.2747 \pm 0.0856
SMOKING BEHAVIOR					
Smoker (n = 11)	58.75 \pm 35.12	28.17 \pm 24.38	1.275 \pm 0.6163	0.5157 \pm 0.1433	0.2326 \pm 0.0830
Non-Smoker (n = 21)	50.75 \pm 17.97	29.43 \pm 17.55	1.192 \pm 0.4969	0.4823 \pm 0.1435	0.2891 \pm 0.0768
VITAMIN D DEFICIENCY					
Deficient (n = 14)	50.27 \pm 21.30	31.28 \pm 20.28	1.303 \pm 0.4520	0.5074 \pm 0.1258	0.2613 \pm 0.0677
Non-Deficient (n = 7)	46.47 \pm 8.694	25.61 \pm 13.12	1.153 \pm 0.5582	0.4910 \pm 0.1539	0.2620 \pm 0.1024
Unknown (n = 11)	57.73 \pm 11.50	28.24 \pm 23.62	1.159 \pm 0.6399	0.4783 \pm 0.1649	0.2853 \pm 0.0913
AGE AT STUDY ENTRY					
Age 20–30 years (n = 6)	48.70 \pm 12.04	31.38 \pm 28.13	1.044 \pm 0.6815	0.4035 \pm 0.1595	0.2604 \pm 0.0483
Age 31–40 years (n = 12)	56.25 \pm 18.99	37.85 \pm 19.26	1.402 \pm 0.4946	0.5590 \pm 0.1213	0.3071 \pm 0.0801
Age 41–50 years (n = 8)	46.37 \pm 16.39	22.67 \pm 13.87	1.165 \pm 0.5178	0.4544 \pm 0.1427	0.2646 \pm 0.0794
Age 50–60 years (n = 6)	54.33 \pm 15.15	17.34 \pm 11.16	1.108 \pm 0.4931	0.5064 \pm 0.1266	0.2110 \pm 0.0951
DURATION OF DISEASE					
Time > 10 years (n = 11)	51.44 \pm 18.31	33.71 \pm 21.30	1.218 \pm 0.4479	0.5140 \pm 0.1233	0.2618 \pm 0.0986
Time \leq 10 years (n = 21)	52.30 \pm 15.70	26.52 \pm 18.99	1.222 \pm 0.5823	0.4832 \pm 0.1526	0.2739 \pm 0.0747
LIFETIME WITH DISEASE [†]					
Lifetime \geq 20% (n = 15)	51.66 \pm 16.37	35.64 \pm 23.88	1.282 \pm 0.5405	0.5238 \pm 0.1365	0.2726 \pm 0.0860
Lifetime < 20% (n = 17)	52.31 \pm 16.84	23.13 \pm 13.43	1.166 \pm 0.5357	0.4674 \pm 0.1455	0.2672 \pm 0.0814
RELAPSES IN THE LAST 2 YEARS					
Relapses > 2 (n = 7)	46.51 \pm 15.05	27.71 \pm 13.08	1.250 \pm 0.5834	0.4629 \pm 0.1424	0.2389 \pm 0.0421
Relapses 1–2 (n = 17)	49.06 \pm 13.71	22.35 \pm 14.34 ^a	1.041 \pm 0.4737	0.4471 \pm 0.1205	0.2722 \pm 0.0903
Relapse free (n = 8)	63.09 \pm 19.20	44.24 \pm 27.20 ^b	1.577 \pm 0.4753	0.6201 \pm 0.1192	0.2914 \pm 0.0912
p value		^a vs. ^b : $p < 0.01$			
DISEASE-MODIFYING THERAPIES (DMT)					
Natalizumab (n = 14)	49.40 \pm 19.73	37.24 \pm 21.63 ^c	1.578 \pm 0.3895	0.5632 \pm 0.0361	0.2742 \pm 0.0816
No DMT (n = 10)	56.70 \pm 13.53	15.79 \pm 10.82 ^d	0.8971 \pm 0.5186	0.4036 \pm 0.1593	0.2671 \pm 0.0794
Other therapies [‡] (n = 8)	50.70 \pm 13.38	31.06 \pm 17.93	0.9989 \pm 0.4087	0.4852 \pm 0.1046	0.2652 \pm 0.0971
p value		^c vs. ^d : $p < 0.01$			
EXPANDED DISABILITY STATUS SCALE (EDSS)					
EDSS 1.0–1.5 (n = 6)	48.13 \pm 26.23	44.34 \pm 33.14	1.252 \pm 0.6962	0.4987 \pm 0.1757	0.3046 \pm 0.0996
EDSS 2.0–2.5 (n = 11)	55.21 \pm 11.88	28.68 \pm 14.78	1.211 \pm 0.5583	0.4981 \pm 0.1516	0.2803 \pm 0.0668
EDSS 3.0–3.5 (n = 6)	53.58 \pm 18.80	21.98 \pm 15.75	1.137 \pm 0.4647	0.4841 \pm 0.1660	0.2963 \pm 0.0741
EDSS 4.0–5.5 (n = 8)	50.27 \pm 14.00	24.88 \pm 12.94	1.277 \pm 0.5465	0.4984 \pm 0.1188	0.2132 \pm 0.0835

[†] Calculated from duration of disease divided by age at study entry. [‡] Interferon beta-1a, carbamazepine, alemtuzumab, glatiramer acetate, dimethyl fumarate, fingolimod (n = 3).

Of interest, EBNA-1 transcripts were increased ($p < 0.01$) in individuals without relapses compared to individuals with one or two relapses in the last two years. Further, EBNA-1 expression was 1.7-fold higher in individuals with low disability scores (EDSS < 2), although this increase was not significant. Interestingly, the expression of EBNA-1 was

negatively correlated with age ($r = -0.36$). Using qRT-PCR analyses, we could not observe significant differences in the relapse rate, the treatment with natalizumab or the EDSS score, but EBNA-1 expression also tended to be higher in individuals without or with minimal disabilities compared to those with higher EDSS scores (Supplementary Table S1). The difference in EBNA-1 between the younger to the elder MS subgroups could be confirmed ($p < 0.001$ and $p < 0.0001$) using qRT-PCR analyses in 94 LCL from 32 individuals with MS. In addition, we detected higher expression of both EBNA2 ($p < 0.05$) and EBNA1 transcripts ($p < 0.05$) in MSLCL compared to controls. Further, the up-regulation of all EBV and HERV transcripts by qRT-PCR was more pronounced in MSLCL established from female donors compared to gender-matched controls, while no difference in expression could be detected in the male counterparts (Supplementary Figure S2). However, these differences in EBV and HERV expression with gender were not significant in RNAseq analyses (Supplementary Figure S3). For HERV-K GAG, differences in gene expression might be explained by targeting more than one distinct transcript due to the high similarity within the HERV-K family. For all additional investigated environmental sequence features and clinical parameters, no significant changes in expression were observed.

3.3. Differential Expression Pattern in Human Transcriptome in LCL from MS-Derived Samples and Controls

Mapping against the human genome version GRCh38/hg38 showed that gene expression profiles of PBMCs and LCL are distinctly different, as expected. Well-known EBV-induced genes like EB13 and CD70 were up-regulated 150- to 160-fold ($p < 0.0001$), in both coLCL and MSLCL. Furthermore, cytokines related to cell growth checkpoints, e.g., CCL22 and CCL25, were observed in the LCL (Supplementary Table S2). In PBMCs, genes that are mainly expressed by T lymphocytes, like CD3D (fold change: 503.1) and CD7 (fold change: 599.9), or monocytes, such as CD14 (fold change: 1610.9), were among the 100 most up-regulated genes compared to the LCL as pure B cell lines verified by flow cytometry (Supplementary Figure S4). In contrast, the overall gene expression pattern was highly similar in the comparison of MSLCL and coLCL, resulting in a limited number of differentially expressed genes (Figure 2). Notably, an ERV element of the medium reiteration frequency (MER) family, ERVMER61-1, was included within the 20 up-regulated genes (fold change > 1.5 , $p < 0.05$) in MSLCL. Furthermore, *REEDL1*, *RNU7-20P*, *RF00012* (member of U3 snoRNA family), *MT-TQ*, *DLG-AS1* and *MPL* were increased most significantly in MSLCL (STab. 3). In coLCL, 39 genes were found to be up-regulated (fold change > 1.5 , $p < 0.05$). The decidual protein induced by progesterone 1 autophagy regulator (*DEP1*) was increased most significantly in coLCL compared to MSLCL, which might suggest higher activation of autophagy mediated by oxidative stress [47]. Furthermore, beta-secretase 2 (*BACE2*) which cleaves the amyloid precursor protein (APP) in the A β domain, preventing A β generation, e.g., in Alzheimer's disease [48], as well as *RHOV*, *CTH*, *ANK1*, *HEP1L1*, *DTX1*, *DHX9P1*, *TNFSF11* and *AC018738.1* showed strongest evidence of differential expressions in controls (Supplementary Table S4).

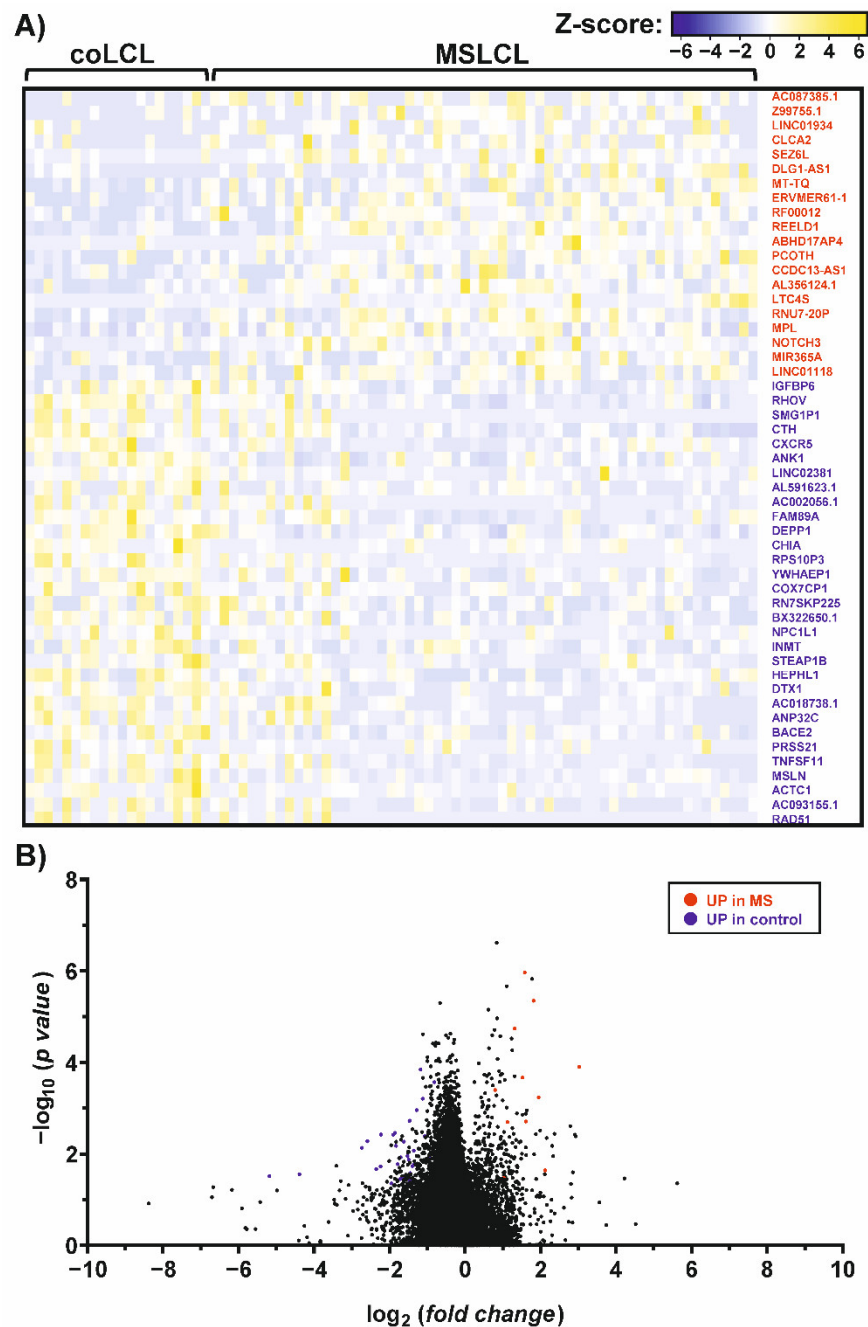


Figure 2. Differential gene expression patterns in individuals with MS and controls, assessed by RNAseq analysis. The graphs represent a heatmap (A) and a volcano plot (B) of differentially expressed genes (fold change > 1.5, $p < 0.05$) in MS and controls. Up-regulated genes in MS (red) and controls (blue) were indicated and ranked from highest to lowest fold change in MSLCL. For this analysis, a total of 20 LCL established from controls (coLCL) and 59 LCL from individuals with MS (MSLCL) were used. Human genome version GRCh38/hg38 was used for RNAseq read mapping. Fold changes and statistical significances were listed in the supplement (Supplementary Tables S3 and S4).

3.4. Up-Regulation of Distinct HERV-K Loci and ERV3-1 in LCL from MS-Derived Samples

To investigate the increase in HERVs in LCL and especially in MS samples, we mapped the reads against a synthetic virus metagenome including more than 100 individual HERV sequences [44]. As also exogenous viruses, like EBV, were included in this mapping process, we observed a distinct increase in EBNA-1 in LCL compared to PBMCs as expected. Among the differentially expressed HERV elements, HERV-K18, was most increased with a fold

change of 2.1. Additionally, six HERV elements were found to be up-regulated after the EBV-triggered immortalization of B cells (Supplementary Table S5): three HERV-K elements located at chromosome 1q21.3 (JN675012.1), 12q24.11 (JN675069.1) and 22q11.23 (JN675088.1), as well as HERV-KC4 (X80240.1), HERV-9 (X57147.1) and HERV-W5 (AC117456.6:51035-52536). Interestingly, the up-regulation of these HERVs can be observed in B cell receptor (BCR) and CD40-stimulated B cells [42], but not in B cells stimulated by phorbol myristate acetate (PMA) [43] (Supplementary Figure S5), suggesting activation of HERVs in B cells by stimulation of the BCR/CD40, which are pathways used by EBV for immortalization. Comparing MS and controls, we observed only six HERVs that showed an increased expression in MSLCL (Figure 3). Of interest, five of these HERVs belong to the HERV-K family: ERVK3-1 (NC_000019: 58305374-58315657), HERV-K11 and three elements located at chromosome 19p12a (JN675076.1), 3p12.3 (JN675019.1) and 1q32.2 (JN675016.1). Furthermore, ERV3-1 (NC_000007.14: 64990356-65006687) belonging to the HERV-R family was up-regulated most significantly in MSLCL (Supplementary Table S6). In contrast, no HERV sequence was significantly up-regulated in LCL from controls.

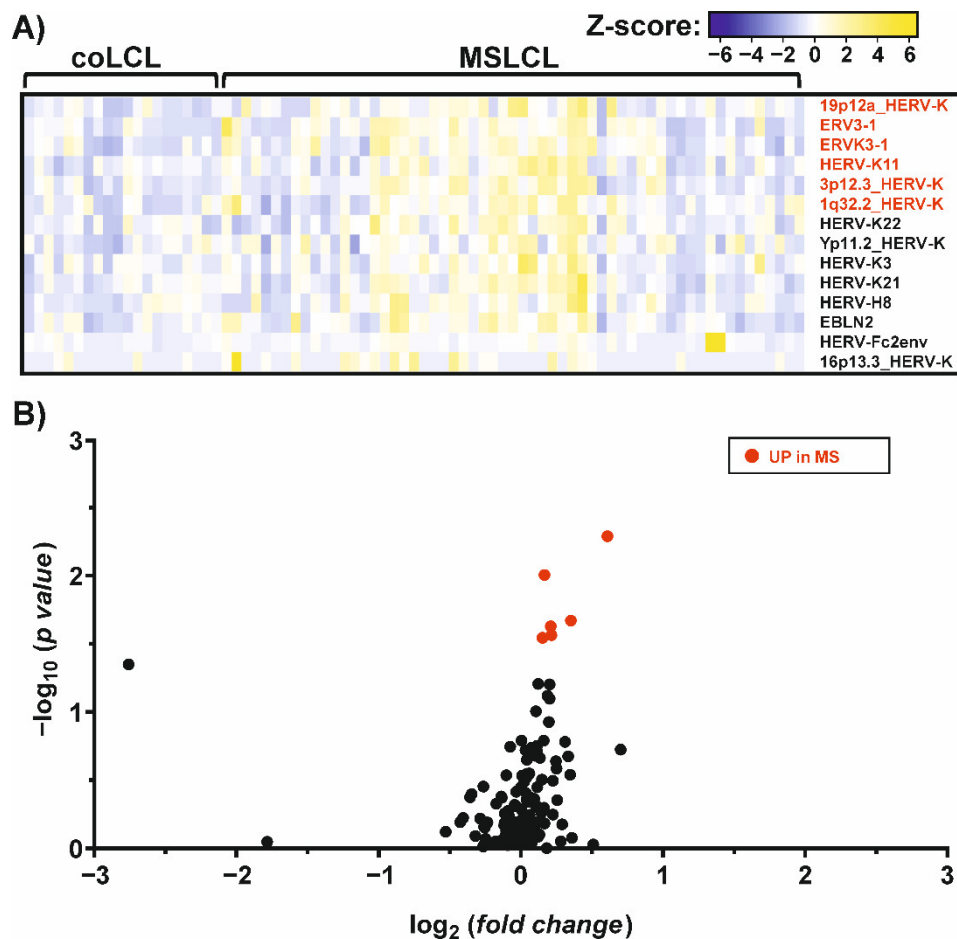


Figure 3. Differential expression of endogenous virus elements in MS and controls, assessed by RNAseq analysis. The graphs represent a heatmap (A) and a volcano plot (B) of differentially expressed genes ($p < 0.05$) in MS and controls. Up-regulated genes (fold change > 1) in MS (red) were indicated and ranked from highest to lowest fold change in MSLCL. None of the ERVs analyzed were found to be significantly up-regulated in control samples. For this analysis, a total of 20 LCL established from controls (coLCL) and 59 LCL from individuals with MS (MSLCL) were used. A synthetic virus metagenome was used for RNAseq read mapping. Fold changes and statistical significances were listed in the supplement (Supplementary Table S6).

3.5. Discovery of Gene Panels for MS and Relapse Risk Using RNAseq Data from LCL

To identify target genes that might be used as possible MS biomarkers, we analyzed the previously mentioned RNAseq data mapped against the human genome GRCh38/hg38, and the synthetic virus transcriptome for genes that were highly expressed at least in subgroups of MSLCL but not in coLCL. Among all up-regulated genes in MSLCL, we observed 35 genes showing a high expression level in at least 25% of the MSLCL which was never exceeded by any coLCL (Table 3).

Table 3. Genes with higher expression in MSLCL samples. All genes with an increased expression according to RNAseq analysis in at least 25% of MS samples, never exceeded by any control (co) were listed. The AUC \pm SE were determined and the FPKM at 100% specificity was taken as the cut-off value for predicting MS. Statistics: *p* values from unpaired *t*-test were adjusted by multiple correction using Bonferroni–Dunn method. The false discovery rate (FDR) was calculated by Benjamini–Hochberg method. Genes were ranked according to their adjusted *p* value.

Name	Mean (co) n = 20 [FPKM]	Mean (MS) n = 59 [FPKM]	<i>p</i> Value	Adjusted <i>p</i> Value (Bonferroni–Dunn)	FDR <i>q</i> Value (Benjamini–Hochberg)	AUC \pm SE	Cut-Off [FPKM] at 100% Specificity
MT-TY	24.09	55.71	0.00003	0.0011	0.0006	0.790 \pm 0.056	67.83
MT-TC	146.6	417.2	0.00004	0.0013	0.0006	0.847 \pm 0.046	355.7
AL669831.1	0.1678	0.2549	0.00005	0.0017	0.0006	0.800 \pm 0.052	0.277
MT-TE	4.012	9.250	0.00007	0.0024	0.0006	0.790 \pm 0.053	10.39
LINC01529	0.0394	0.1054	0.00010	0.0034	0.0006	0.797 \pm 0.052	0.119
AL365273.1	1.442	2.960	0.00010	0.0034	0.0006	0.773 \pm 0.058	3.426
SNORA79B	0.2844	0.7127	0.00019	0.0065	0.0009	0.800 \pm 0.053	0.807
MIR34AHG	0.4675	0.9528	0.00033	0.0116	0.0014	0.743 \pm 0.062	1.189
ENTPD1-AS1	0.3070	0.5408	0.00037	0.0129	0.0014	0.761 \pm 0.059	0.622
MFSD14C	0.7940	1.0780	0.00039	0.0137	0.0014	0.748 \pm 0.060	1.263
RNU7-20P	0.2588	0.7819	0.00071	0.0247	0.0022	0.780 \pm 0.055	1.016
REELD1	0.0213	0.0683	0.00076	0.0265	0.0022	0.791 \pm 0.053	0.081
MT-TG	6.905	14.600	0.00088	0.0307	0.0022	0.734 \pm 0.062	19.16
GABARAP	0.2457	0.5464	0.00088	0.0308	0.0022	0.757 \pm 0.059	0.616
SNORD20	0.6918	1.5220	0.00107	0.0375	0.0025	0.747 \pm 0.060	2.164
AL669831.3	0.0185	0.0411	0.00178	0.0622	0.0039	0.729 \pm 0.063	0.049
RF00012	0.0564	0.1735	0.00219	0.0766	0.0045	0.775 \pm 0.055	0.217
MPL	0.0084	0.0188	0.00234	0.0817	0.0045	0.726 \pm 0.060	0.024
FAM89B	0.5908	0.8061	0.00743	0.2599	0.0137	0.701 \pm 0.060	0.946
AC006001.3	0.5246	0.6044	0.00847	0.2963	0.0141	0.721 \pm 0.058	0.657
EBF2	0.0007	0.0024	0.00849	0.2970	0.0141	0.696 \pm 0.059	0.004
CFAP73	0.0359	0.0552	0.00998	0.3491	0.0159	0.699 \pm 0.062	0.063
LINC01118	0.0050	0.0120	0.01080	0.3781	0.0164	0.682 \pm 0.060	0.016
HERV-K 3p12.3	0.1862	0.2447	0.01254	0.4390	0.0177	0.637 \pm 0.061	0.334
DLG1-AS1	0.0023	0.0103	0.01262	0.4416	0.0177	0.664 \pm 0.063	0.016
DIAPH2-AS1	0.0130	0.0321	0.01402	0.4908	0.0189	0.713 \pm 0.059	0.033
RPL41P1	133.8	317.3	0.01642	0.5746	0.0212	0.675 \pm 0.062	276.9
MIR3150BHG	0.0372	0.1018	0.01693	0.5924	0.0212	0.680 \pm 0.059	0.102
TLL7-IT1	0.0022	0.0109	0.02014	0.7048	0.0243	0.704 \pm 0.059	0.009
RNU6-32P	0.0636	0.1835	0.02500	0.8751	0.0292	0.670 \pm 0.062	0.273
GOLGA6L4	0.0004	0.0041	0.02800	0.9798	0.0316	0.736 \pm 0.055	0.002
HIST2H2AC	0.8899	1.21	0.06537	>0.999999	0.0654	0.606 \pm 0.065	1.379
C3P1	0.0014	0.0045	0.02933	>0.999999	0.0321	0.659 \pm 0.062	0.005
MIR221	0.4966	0.9103	0.03409	>0.999999	0.0351	0.614 \pm 0.064	1.158
HERV-K11	0.2805	0.3140	0.03055	>0.999999	0.0324	0.683 \pm 0.064	0.303

We observed that one MSLCL did not show increased expression above the cut-off for any of these genes. However, this MSLCL had a duplicate LCL from the same subject (MSLCL-030) which did show increased expression above the cut-off for 8 of the 35 genes. Variability was also observed within the LCL from other subjects, suggesting that the usage of multiple LCL from one donor yields more powerful gene expression analyses (Supplementary Table S7). Using LCL duplicates, all 32 individuals with MS were identified with increased expression even for the smaller 15 gene panel, which we have chosen using multiple comparison analysis from all 35 targets (adjusted *p* < 0.05). The ROC curve

from this smaller MS gene panel confirmed the high predictive power with an AUC of 0.972 ± 0.018 (Figure 4).

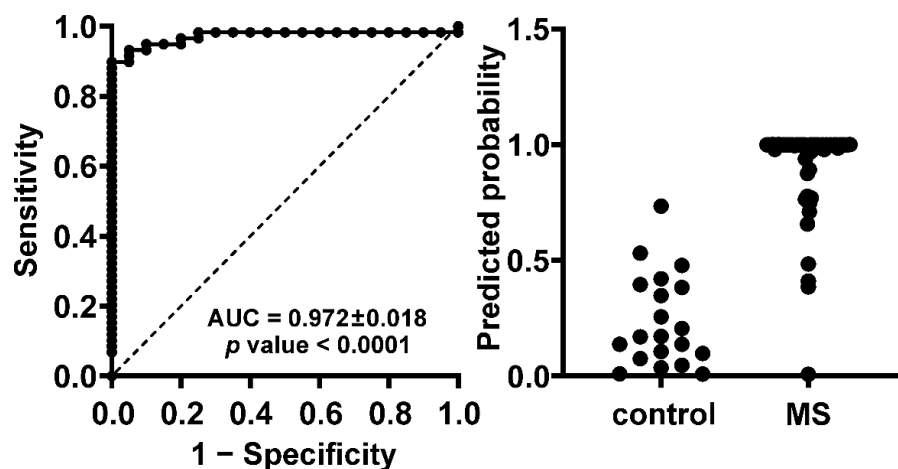


Figure 4. A panel of 15 target genes has high predictive power distinguishing between MS and control samples. RNAseq data of 20 LCL from 10 controls and 59 LCL from 32 individuals with MS were analyzed. The presented ROC curve and prediction probability were performed within a multiple logistic regression analysis using GraphPad PRISM 8.3.0. The 15 genes included for this analysis are listed in Table 3 with adjusted p values below 0.05. For ROC curve analysis, area under the curve (AUC) \pm SE is indicated. A positive predictive power of 100% could be achieved using a classification cut-off at 0.75, suggesting no false positive predictions and a correct identification of about 88% of MSLCL.

Second, we analyzed for targets that were correlated with the relapse rate in MS. Therefore, we used LCL from each 7 MS individuals with and without relapses matched by gender and duration of the disease ± 1 year. We identified two genes above and six genes below ($p < 0.05$) a target-specific threshold in at least 75% of the LCL from individuals with relapses (Table 4). All individual ROC curves from the MS risk targets and the genes correlating with relapse rate can be found in the supplement (Supplementary Figures S6 and S7).

Table 4. Genes that correlated with relapse rate in LCL from individuals with MS. Each 7 MS individuals with or without relapses in the last 2 years were compared. They were matched by gender and the duration of disease ± 1 year. LCL from these individuals were at least analyzed in duplicates by RNAseq. All genes with an exclusively up- or downregulated expression in at least 75% of MS samples with relapses in the last 2 years were listed. The AUC \pm SE were determined and the FPKM at 100% specificity was taken as the cut-off value for predicting relapses. Statistics: p values from unpaired t -test were adjusted by multiple correction using Bonferroni–Dunn method. The false discovery rate (FDR) was calculated by Benjamini–Hochberg method. Genes were ranked according to their adjusted p value.

Name	Mean MS with Relapses in the Last 2 Years n = 14 [FPKM]	Mean MS w/o Relapses in the Last 2 Years n = 15 [FPKM]	p Value	Adjusted p Value (Bonferroni–Dunn)	FDR q Value (Benjamini–Hochberg)	AUC \pm SE	Cut-Off [FPKM] at 100% Specificity
<u>UP</u>							
AK7	0.550	0.228	0.0001	0.0007	0.0004	0.895 ± 0.062	0.188
BX664727.3	0.0123	0.0004	0.0012	0.0105	0.0017	0.957 ± 0.043	0.006
<u>DOWN</u>							
ZNF302	1.904	2.942	0.0000	0.0003	0.0003	0.943 ± 0.041	2.237
PM20D2	1.224	2.598	0.0005	0.0046	0.0015	0.924 ± 0.053	1.410
ZNF283	0.293	0.471	0.0008	0.0068	0.0017	0.905 ± 0.059	0.347
DHFRP1	6.004	12.360	0.0009	0.0084	0.0017	0.871 ± 0.073	8.061
XKR9	0.037	0.085	0.0015	0.0135	0.0019	0.876 ± 0.071	0.044
ZNF195	1.658	2.670	0.0017	0.0153	0.0019	0.867 ± 0.075	1.787
TCERG1	4.837	6.280	0.0133	0.1195	0.0133	0.871 ± 0.078	4.994

4. Discussion

In the present study, we investigated differential gene expression patterns in MS and controls after EBV infection of B cells, as EBV infection is a major risk factor for the subsequent development of MS [5–15]. To investigate the influence of environmental risk factors and clinical parameters, we studied selected EBV and HERV targets in LCL by RNAseq and qRT-PCR. For lytic EBNA-1, we observed differential expression with certain parameters investigated. Using RNAseq, EBNA-1 showed up-regulation in MSLCL from individuals treated with natalizumab compared to those not receiving disease-modifying therapies, and in individuals without relapses compared to individuals with one to two relapses in the last two years. However, both results regarding the relapse rate or the DMT could not be confirmed using qRT-PCR method (Supplementary Table S1, Supplementary Figure S9 and S10). Additionally, our results from qRT-PCR suggested an up-regulation of EBNA-1, EBNA-2 and HERV-K GAG expression, which was more pronounced in LCL from female individuals with MS. Differential expression of HERV-K4 GAG was not detected by RNAseq analysis. Quantification of reads that mapped exclusively to the HERV-K4 region that was also amplified by PCR showed higher similarity with the qRT-PCR results (Supplementary Figure S8). For lytic EBNA transcripts we observed approximate reduction in expression levels by half from the youngest to the oldest group in both RNAseq and qRT-PCR analyses. While beneficial effects of vitamin D supplementation on inflammation in MS have been frequently observed [49,50], the contribution of vitamin D deficiency to MS risk, or its association with EBV in MS, is still elusive, and commonly conflicting results can be found in the literature [51,52]. According to the data presented, no significant differences in the studied EBV and HERV genes between deficient and non-deficient individuals could be observed in both, qRT-PCR and RNAseq analyses. However, the study presented here was limited to a single point in time of PBMC extraction. To confirm a relationship of EBV transcription and vitamin D deficiency in MS, we propose further investigation on EBV expression and the vitamin D titer at the stage of deficiency, and within time after successful vitamin D supplementation in LCL from individuals with MS and controls, as an interplay between EBV, HERVs and vitamin D seems at least plausible [53,54]. In this scenario, higher vitamin D titer after supplementation might result in reduced EBNA levels in EBV-immortalized B cells. For EBNA-2, the inverse correlation could be explained by overlapping DNA binding sites with the vitamin D receptor that would outcompete EBNA-2 at high vitamin D levels and vice versa [55]. Consequently, the transactivation of HERVs as putative EBV-triggered drivers in the pathogenesis of MS should be affected by lower EBV levels.

Regarding HERVs that can be transactivated by EBV, we observed an increase in HERV-K18 expression by up to 2.1-fold upon EBV-triggered immortalization. This result was not unexpected, as the Huber's group has previously studied the mechanism of an EBV-triggered transactivation of HERV-K18. On resting B cells, EBV glycoprotein gp350 binds to CD21, and therefore leads to the activation of HERV-K18 ENV protein coding for a superantigen that strongly stimulates a large number of T cells [24,56,57]. In addition, we found that activation of HERV-K18 is not limited to the coding region of the ENV, as we observed an equal distribution of reads across the complete proviral sequence (data not shown).

On the other hand, the results for the expression pattern from HERV-W1 ENV and MSRV were more ambiguous. From the literature, one might expect that the expression of both MSRV ENV and HERV-W1 ENV RNA is up-regulated in B cells and monocytes after exposure to the EBV glycoprotein, gp350, that had been found to transactivate the ENV of HERV-K18 [58,59]. In our study, we used complete EBV from the B95.8 cell lines instead of gp350. However, we observed an increase in HERV-W1 ENV in controls after EBV-induced immortalization by qPCR, analyzing higher numbers of PBMC and multiple LCL per donor. This might be explained by high HERV-W1 ENV levels in PBMCs from several individuals with MS, which is supported by similar results from other studies suggesting an overall higher frequency of circulating HERV-W in individuals with MS [58,60]. Based on our data,

we observed a tendency for higher HERV-W1 *ENV* expression which was not significant in PBMC of individuals with MS, but no up-regulation of MSR *ENV* in LCL, although an increase in HERV-K18 and six other HERV loci occurred upon EBV-immortalization via CD40/BCR-receptor signaling pathway. Of interest, HERV-W5, belonging to the HERV-W family, was one of these EBV-activated HERV genes.

In the present study, we observed up-regulation of ERVMER61-1, several loci from HERV-K family and ERV3-1 exclusively in MSLCL. So far, the ERV3-1 element, belonging to the HERV-R family, was found to be differentially expressed in PBMCs from individuals with MS and controls [61] but none of the investigated *ENV* allelic forms were associated with MS [62]. The ERVMER61-1 was previously analyzed as a putative candidate lncRNAs in subtypes of breast cancer [63] and hepatocellular carcinoma (HCC), where it was thought to be included in a prognostic signature of dysregulated RNAs in HCC [64]. Of note, expression of these HERV loci did not show a dependency on age or gender (Supplementary Figures S11 and S12). Since the differences between MSLCL and coLCL were subtle, it should be discussed to what extent the expression level of HERVs alone is crucial in the pathogenesis of MS. HERVs are intrinsic transposable elements, which are capable of modulating their integration site within or near to genes. By disruption or promotion of co-localized genes, e.g., critical immune factors, the existence of full or partial HERV provirus sequences might have an impact itself [65,66]. As a result, HERV transcription is under constant surveillance by multilayered regulatory mechanisms of the host. This balance between the persistence of HERV expression and the host immune protection might be very subtle, especially in the case of HERV activation as a first line of antiviral defense counteracting infections with exogenous (retro-)viruses [67]. In the case of HERV glycoprotein expression, this mechanism of molecular mimicry could also accidentally trigger other proteins with similarity in sequence that are principal targets of an autoimmune response, as it has been suggested for myelin and viral peptides from EBV and HERV *ENV* via binding to the MS risk factor HLA class II DR2b [68]. Recently, cross-reactive antibodies against EBNA-1 and the glial antigen GlialCAM have been found in the CSF of individuals with MS [69]. In addition, the EBV-specific T cell repertoire in individuals with MS seems to be expanded [70], and EBV-specific CD8-positive T-cells are frequently observed in the CSF and in brain tissue at sites of white matter lesions and the meninges in MS [71,72]. These observations suggest ongoing EBV (re-)activation that might challenge the immune homeostasis directly or by transactivation of HERVs. Besides the antiviral defense, HERVs seem to be involved in the maintenance of the pluripotency of stem cells [44] and are activated at specific developmental stages during embryogenesis and pregnancy, which also challenges the mentioned host–virus balance [73]. In summary, HERVs are able to regulate the host genes' activity in several ways and at different expression levels. For future analyses, the HERV loci here identified should be considered as putative MS risk factors by, e.g., RNAseq analyses in a larger cohort. Considering the high variability in gene expression, we recommend including multiple LCL from each subject. Further, we suggest matching of MS and control samples by age and gender due to the tendencies we observed in the present study. A very recent report also found a slightly higher seroprevalence of EBNA-1 antibodies in females [74]. Finally, the expression of ERV3-1 should be also investigated on the protein level, as specific antibodies are available.

Besides HERV elements as candidate MS biomarkers, we identified a gene panel consisting of 15 targets that were highly expressed in at least 25% of our MS samples and could perfectly distinguish between our LCL from individuals with MS and the healthy controls, which never exceeded the given cut-off values for any target. Further, the same approach using multiple LCL from the same donor was used to explore targets that correlated with relapse risk. Despite a limited number of MS samples matched by gender and disease duration, we identified eight targets discriminating between our individuals with and without relapses. Of course, these data are preliminary and have to be examined with a larger number of samples, but this can be achieved through further collection and sharing of RNAseq data from LCL as we did in the SRA database from NCBI.

5. Conclusions

The collection of RNAseq data is increasing, and disease-associated biomarker panels might be a helpful diagnostic tool for more-extensive and individualized disease monitoring, as deep genomic analyses are becoming ever faster and less expensive. In this manuscript, we have presented a strategy for using common RNAseq analysis techniques to identify target genes that might be suitable as biomarkers for MS, or risk factors such as the relapse rate in an EBV-mediated B cell approach. Furthermore, our data suggest an EBV-triggered transactivation of HERVs with differential expression of ERVMER61-1, ERV3-1, and copies from the HERV-K (HML-2) family in LCL from individuals with MS.

Supplementary Materials: The following materials are available online at <https://www.mdpi.com/article/10.3390/cells11223619/s1>: Supplementary Figure S1: Standard curves relating the copy number of target genes to the cycle threshold (CT) measured by qRT-PCR. Supplementary Figure S2: Transcriptional activation of EBV and HERVs in MSLCL is pronounced in LCL generated from female donors (qRT-PCR). Supplementary Figure S3: Expression of EBV and HERVs in LCL from female and male PBMC donors (RNAseq). Supplementary Figure S4: Characterization of LCL from MS individuals (MSLCL) and control donors (coLCL) by flow cytometry. Supplementary Figure S5: The activation of HERV can be triggered through CD40 and B cell receptor (BCR)-signaling but not by phorbol myristate acetate (PMA) in B cells. Supplementary Figure S6: ROC curves of identified MS biomarkers. Supplementary Figure S7: ROC curves of targets that correlated with relapse rate in MS. Supplementary Figure S8: Comparison of HERV-K GAG expression in PBMC and EBV-immortalized B cells (RNAseq analysis). Supplementary Figure S9: Expression of EBV and HERVs in LCL from individuals with MS regarding disease-modifying therapy (DMT). Supplementary Figure S10: Expression of EBV and HERVs in LCL from individuals with MS regarding relapse rate. Supplementary Figure S11: Expression of HERVs up-regulated in MS regarding age of the individuals. Supplementary Figure S12: Expression of HERVs up-regulated in MS regarding gender of the individuals. Supplementary Table S1: Influence of environmental and clinicopathological factors on EBV and HERV expression in LCL from MS individuals. Supplementary Table S2: Strongest up-regulated genes in LCL. Supplementary Table S3: Strongest up-regulated genes in MSLCL. Supplementary Table S4: Strongest up-regulated genes in coLCL. Supplementary Table S5: Strongest up-regulated viral transcripts in LCL. Supplementary Table S6: Strongest up-regulated viral transcripts in MS-derived LCL. Supplementary Table S7: Variability of gene expression in LCL replicates from the same PBMC donor.

Author Contributions: Conceptualization, L.W., M.S.S. and A.E.; Data curation, L.W.; Funding acquisition, M.S.S. and A.E.; Investigation, L.W. and T.S.; Methodology, L.W., T.S., K.E., I.V.; Project administration, M.S.S. and A.E.; Resources, A.T., J.J., M.E.K., F.H. and A.E.; Supervision, M.S.S. and A.E.; Visualization, L.W. and M.S.S.; Writing—original draft, L.W.; Writing—review and editing, L.W., K.E., A.K., M.E.K., F.H., M.S.S. and A.E. All authors have read and agreed to the published version of the manuscript.

Funding: The work was supported by grant ZS/2018/12/96228 (to the University of Halle) from the European Regional Development Fund under the local program “Sachsen-Anhalt WISSENSCHAFT Schwerpunkte”.

Institutional Review Board Statement: The study was conducted according to the guidelines of the Declaration of Helsinki and approved by the Institutional Ethics Committee of the Martin-Luther-University Halle-Wittenberg (protocol code: 2015-89).

Informed Consent Statement: Informed consent was obtained from all subjects involved in the study.

Data Availability Statement: The datasets generated for this study can be found in the NCBI Sequence Read Archive (BioProject PRJNA765133) at <https://www.ncbi.nlm.nih.gov/sra> (accessed on 1 November 2022).

Acknowledgments: The authors wish to thank Holtkötter for his contribution and helpful support of our study. We also thank the Novartis Pharma GmbH for their financial support.

Conflicts of Interest: The authors declare that the research was conducted in the absence of any commercial or financial relationships that could be construed as potential conflicts of interest. The funders had no role in the design of the study; in the collection, analyses, or interpretation of data; in the writing of the manuscript; or in the decision to publish the results.

References

1. Tischendorf, P.; Shramek, G.J.; Balagtas, R.C.; Deinhardt, F.; Knospe, W.H.; Noble, G.R.; Maynard, J.E. Development and persistence of immunity to Epstein-Barr virus in man. *J. Infect. Dis.* **1970**, *122*, 401–409. [[CrossRef](#)] [[PubMed](#)]
2. Warner, H.B.; Carp, R.I. Multiple sclerosis and Epstein-Barr virus. *Lancet* **1981**, *2*, 1290. [[CrossRef](#)]
3. Flavell, K.J.; Murray, P.G. Hodgkin's disease and the Epstein-Barr virus. *Mol. Pathol.* **2000**, *53*, 262–269. [[CrossRef](#)] [[PubMed](#)]
4. Brady, G.; MacArthur, G.J.; Farrell, P.J. Epstein-Barr virus and Burkitt lymphoma. *J. Clin. Pathol.* **2007**, *60*, 1397–1402. [[CrossRef](#)] [[PubMed](#)]
5. Munch, M.; Riisom, K.; Christensen, T.; Møller-Larsen, A.; Haahr, S. The significance of Epstein-Barr virus seropositivity in multiple sclerosis patients? *Acta Neurol. Scand.* **1998**, *97*, 171–174. [[CrossRef](#)] [[PubMed](#)]
6. Alotaibi, S.; Kennedy, J.; Tellier, R.; Stephens, D.; Banwell, B. Epstein-Barr virus in pediatric multiple sclerosis. *JAMA* **2004**, *291*, 1875–1879. [[CrossRef](#)]
7. Pohl, D.; Krone, B.; Rostasy, K.; Kahler, E.; Brunner, E.; Lehnert, M.; Wagner, H.J.; Gärtner, J.; Hanefeld, F. High seroprevalence of Epstein-Barr virus in children with multiple sclerosis. *Neurology* **2006**, *67*, 2063–2065. [[CrossRef](#)]
8. Pandit, L.; Malli, C.; D'Cunha, A.; Shetty, R.; Singhal, B. Association of Epstein-Barr virus infection with multiple sclerosis in India. *J. Neurol. Sci.* **2013**, *325*, 86–89. [[CrossRef](#)]
9. Bjornevik, K.; Cortese, M.; Healy, B.C.; Kuhle, J.; Mina, M.J.; Leng, Y.; Elledge, S.J.; Niebuhr, D.W.; Scher, A.I.; Munger, K.L.; et al. Longitudinal analysis reveals high prevalence of Epstein-Barr virus associated with multiple sclerosis. *Science* **2022**, *375*, 296–301. [[CrossRef](#)]
10. Haahr, S.; Höllsberg, P. Multiple sclerosis is linked to Epstein-Barr virus infection. *Rev. Med. Virol.* **2006**, *16*, 297–310. [[CrossRef](#)]
11. Ascherio, A.; Munger, K.L. Environmental risk factors for multiple sclerosis. Part I: The role of infection. *Ann. Neurol.* **2007**, *61*, 288–299. [[CrossRef](#)]
12. Goldacre, M.J.; Wotton, C.J.; Seagroatt, V.; Yeates, D. Multiple sclerosis after infectious mononucleosis: Record linkage study. *J. Epidemiol. Community Health* **2004**, *58*, 1032–1035. [[CrossRef](#)]
13. Haahr, S.; Plesner, A.M.; Vestergaard, B.F.; Höllsberg, P. A role of late Epstein-Barr virus infection in multiple sclerosis. *Acta Neurol. Scand.* **2004**, *109*, 270–275. [[CrossRef](#)]
14. Thacker, E.L.; Mirzaei, F.; Ascherio, A. Infectious mononucleosis and risk for multiple sclerosis: A meta-analysis. *Ann. Neurol.* **2006**, *59*, 499–503. [[CrossRef](#)]
15. Sheik-Ali, S. Infectious mononucleosis and multiple sclerosis—Updated review on associated risk. *Mult. Scler. Relat. Disord.* **2017**, *14*, 56–59. [[CrossRef](#)]
16. Bar-Or, A.; Pender, M.P.; Khanna, R.; Steinman, L.; Hartung, H.P.; Maniar, T.; Croze, E.; Aftab, B.T.; Giovannoni, G.; Joshi, M.A. Epstein-Barr Virus in multiple sclerosis: Theory and emerging immunotherapies. *Trends Mol. Med.* **2020**, *26*, 296–310. [[CrossRef](#)]
17. Jacobs, B.M.; Giovannoni, G.; Cuzick, J.; Dobson, R. Systematic review and meta-analysis of the association between Epstein-Barr virus, multiple sclerosis and other risk factors. *Mult. Scler.* **2020**, *26*, 1281–1297. [[CrossRef](#)]
18. Gröger, V.; Emmer, A.; Staeger, M.S.; Cynis, H. Endogenous retroviruses in nervous system disorders. *Pharmaceuticals* **2021**, *14*, 70. [[CrossRef](#)]
19. Haahr, S.; Sommerlund, M.; Møller-Larsen, A.; Nielsen, R.; Hansen, H.J. Just another dubious virus in cells from a patient with multiple sclerosis? *Lancet* **1991**, *337*, 863–864. [[CrossRef](#)]
20. De Parseval, N.; Heidmann, T. Human endogenous retroviruses: From infectious elements to human genes. *Cytogenet. Genome Res.* **2005**, *110*, 318–332. [[CrossRef](#)]
21. Conrad, B.; Weissmahr, R.N.; Böni, J.; Arcari, R.; Schüpbach, J.; Mach, B. A human endogenous retroviral superantigen as candidate autoimmune gene in type I diabetes. *Cell* **1997**, *90*, 303–313. [[CrossRef](#)]
22. Stauffer, Y.; Marguerat, S.; Meylan, F.; Ucla, C.; Sutkowski, N.; Huber, B.; Pelet, T.; Conrad, B. Interferon-alpha-induced endogenous superantigen. A model linking environment and autoimmunity. *Immunity* **2001**, *15*, 591–601. [[CrossRef](#)]
23. Emmer, A.; Staeger, M.S.; Kornhuber, M.E. The retrovirus/superantigen hypothesis of multiple sclerosis. *Cell. Mol. Neurobiol.* **2014**, *34*, 1087–1096. [[CrossRef](#)] [[PubMed](#)]
24. Sutkowski, N.; Conrad, B.; Thorley-Lawson, D.A.; Huber, B.T. Epstein-Barr virus transactivates the human endogenous retrovirus HERV-K18 that encodes a superantigen. *Immunity* **2001**, *15*, 579–589. [[CrossRef](#)]
25. Bergallo, M.; Pinon, M.; Galliano, I.; Montanari, P.; Daprà, V.; Gambarino, S.; Calvo, P.L. Epstein Barr virus induces HERV-K and HERV-W expression in pediatrics liver transplant recipients? *Minerva Pediatr.* **2020**, *72*, 145–148. [[CrossRef](#)]
26. Küppers, R. B cells under influence: Transformation of B cells by Epstein-Barr virus. *Nat. Rev. Immunol.* **2003**, *3*, 801–812. [[CrossRef](#)]
27. Thorley-Lawson, D.A.; Gross, A. Persistence of the Epstein-Barr virus and the origins of associated lymphomas. *N. Engl. J. Med.* **2004**, *350*, 1328–1337. [[CrossRef](#)]

28. Lassmann, H. Pathogenic mechanisms associated with different clinical courses of multiple sclerosis. *Front. Immunol.* **2019**, *9*, 3116. [[CrossRef](#)]
29. Greenfield, A.L.; Hauser, S.L. B-cell Therapy for multiple sclerosis: Entering an era. *Ann. Neurol.* **2018**, *83*, 13–26. [[CrossRef](#)]
30. Dolei, A. The aliens inside us: HERV-W endogenous retroviruses and multiple sclerosis. *Mult. Scler.* **2018**, *24*, 42–47. [[CrossRef](#)]
31. Pérez-Pérez, S.; Domínguez-Mozo, M.I.; García-Martínez, M.Á.; Ballester-González, R.; Nieto-Gañán, I.; Arroyo, R.; Alvarez-Lafuente, R. Epstein-Barr virus load correlates with multiple sclerosis-associated retrovirus envelope expression. *Biomedicines* **2022**, *10*, 387. [[CrossRef](#)]
32. Ilse, V.; Scholz, R.; Wermann, M.; Naumann, M.; Staege, M.S.; Roßner, S.; Cynis, H. Immunogenicity of the envelope surface unit of human endogenous retrovirus K18 in mice. *Int. J. Mol. Sci.* **2022**, *23*, 8330. [[CrossRef](#)]
33. Lear, A.L.; Rowe, M.; Kurilla, M.G.; Lee, S.; Henderson, S.; Kieff, E.; Rickinson, A.B. The Epstein-Barr virus (EBV) nuclear antigen 1 BamHI F promoter is activated on entry of EBV-transformed B cells into the lytic cycle. *J. Virol.* **1992**, *66*, 7461–7468. [[CrossRef](#)]
34. Schaefer, B.C.; Strominger, J.L.; Speck, S.H. The Epstein-Barr virus BamHI F promoter is an early lytic promoter: Lack of correlation with EBNA 1 gene transcription in group 1 Burkitt's lymphoma cell lines. *J. Virology* **1995**, *69*, 5039–5047. [[CrossRef](#)]
35. Brink, A.A.; Meijer, C.J.; Nicholls, J.M.; Middeldorp, J.M.; van den Brule, A.J. Activity of the EBNA1 promoter associated with lytic replication (Fp) in Epstein-Barr virus associated disorders. *Mol. Pathol.* **2001**, *54*, 98–102. [[CrossRef](#)]
36. Pajic, A.; Polack, A.; Staege, M.S.; Spitkovsky, D.; Baier, B.; Bornkamm, G.W.; Laux, G. Elevated expression of c-myc in lymphoblastoid cells does not support an Epstein-Barr virus latency III-to-I switch. *J. Gen. Virol.* **2001**, *82*, 3051–3055. [[CrossRef](#)]
37. Foell, J.L.; Volkmer, I.; Giersberg, C.; Kornhuber, M.; Horneff, G.; Staege, M.S. Loss of detectability of Charcot-Leyden crystal protein transcripts in blood cells after treatment with dimethyl sulfoxide. *J. Immunol. Methods* **2008**, *339*, 99–103. [[CrossRef](#)]
38. Bernig, T.; Richter, N.; Volkmer, I.; Staege, M.S. Functional analysis and molecular characterization of spontaneously outgrown human lymphoblastoid cell lines. *Mol. Biol. Rep.* **2014**, *41*, 6995–7007. [[CrossRef](#)]
39. Hoennscheidt, C.; Max, D.; Richter, N.; Staege, M.S. Expression of CD4 on Epstein-Barr virus-immortalized B cells. *Scand. J. Immunol.* **2009**, *70*, 216–225. [[CrossRef](#)]
40. Giebler, M.; Staege, M.S.; Blauschmidt, S.; Ohm, L.I.; Kraus, M.; Würzl, P.; Taubert, H.; Greither, T. Elevated HERV-K Expression in soft tissue sarcoma is associated with worsened relapse-free survival. *Front. Microbiol.* **2018**, *9*, 211. [[CrossRef](#)]
41. Karimi, A.; Esmaili, N.; Ranjkesh, M.; Zolfaghari, M.A. Expression of human endogenous retroviruses in pemphigus vulgaris patients. *Mol. Biol. Rep.* **2019**, *46*, 6181–6186. [[CrossRef](#)]
42. Hipp, N.; Symington, H.; Pastoret, C.; Caron, G.; Monvoisin, C.; Tarte, K.; Fest, T.; Delaloy, C. IL-2 imprints human naive B cell fate towards plasma cell through ERK/ELK1-mediated BACH2 repression. *Nat. Commun.* **2017**, *8*, 1443. [[CrossRef](#)]
43. Lévy, R.; Langlais, D.; Béziat, V.; Rapaport, F.; Rao, G.; Lazarov, T.; Bourgey, M.; Zhou, Y.J.; Briand, C.; Moriya, K.; et al. Inherited human c-Rel deficiency disrupts myeloid and lymphoid immunity to multiple infectious agents. *J. Clin. Investig.* **2021**, *131*, e150143. [[CrossRef](#)]
44. Engel, K.; Wieland, L.; Krüger, A.; Volkmer, I.; Cynis, H.; Emmer, A.; Staege, M.S. Identification of Differentially expressed human endogenous retrovirus families in human leukemia and lymphoma cell lines and stem cells. *Front. Oncol.* **2021**, *11*, 637981. [[CrossRef](#)]
45. Afgan, E.; Baker, D.; van den Beek, M.; Blankenberg, D.; Bouvier, D.; Čech, M.; Chilton, J.; Clements, D.; Coraor, N.; Eberhard, C.; et al. The Galaxy platform for accessible, reproducible and collaborative biomedical analyses: 2016 update. *Nucleic Acids Res.* **2016**, *44*, W3–W10. [[CrossRef](#)]
46. Liao, Y.; Smyth, G.K.; Shi, W. Feature counts: An efficient general purpose program for assigning sequence reads to genomic features. *Bioinformatics* **2014**, *30*, 923–930. [[CrossRef](#)] [[PubMed](#)]
47. Stepp, M.W.; Folz, R.J.; Yu, J.; Zelko, I.N. The c10orf10 gene product is a new link between oxidative stress and autophagy. *Biochim. Biophys. Acta* **2014**, *1843*, 1076–1088. [[CrossRef](#)] [[PubMed](#)]
48. Sun, X.; He, G.; Song, W. BACE2, as a novel APP theta-secretase, is not responsible for the pathogenesis of Alzheimer's disease in Down syndrome. *FASEB J.* **2006**, *20*, 1369–1376. [[CrossRef](#)] [[PubMed](#)]
49. Cortese, M.; Munger, K.L.; Martínez-Lapiscina, E.H.; Barro, C.; Edan, G.; Freedman, M.S.; Hartung, H.P.; Montalbán, X.; Foley, F.W.; Penner, I.K.; et al. BENEFIT Study Group. Vitamin D, smoking, EBV, and long-term cognitive performance in MS: 11-year follow-up of BENEFIT. *Neurology* **2020**, *94*, e1950–e1960. [[CrossRef](#)]
50. Pierrot-Deseilligny, C.; Souberbielle, J.C. Vitamin D and multiple sclerosis: An update. *Mult. Scler. Rel. Disord.* **2017**, *14*, 35–45. [[CrossRef](#)]
51. Salzer, J.; Nyström, M.; Hallmans, G.; Stenlund, H.; Wadell, G.; Sundström, P. Epstein-Barr virus antibodies and vitamin D in prospective multiple sclerosis biobank samples. *Mult. Scler.* **2013**, *19*, 1587–1591. [[CrossRef](#)]
52. Décard, B.F.; von Ahsen, N.; Grunwald, T.; Streit, F.; Stroet, A.; Niggemeier, P.; Schottstedt, V.; Riggert, J.; Gold, R.; Chan, A. Low vitamin D and elevated immunoreactivity against Epstein-Barr virus before first clinical manifestation of multiple sclerosis. *J. Neurol. Neurosurg. Psychiatry* **2012**, *83*, 1170–1173. [[CrossRef](#)]
53. Brütting, C.; Stangl, G.I.; Staege, M.S. Vitamin D, Epstein-Barr virus, and endogenous retroviruses in multiple sclerosis—Facts and hypotheses. *J. Integr. Neurosci.* **2021**, *20*, 233–238. [[CrossRef](#)]
54. Latifi, T.; Zebardast, A.; Marashi, S.M. The role of human endogenous retroviruses (HERVs) in multiple sclerosis and the plausible interplay between HERVs, Epstein-Barr virus infection, and vitamin D. *Mult. Scler. Rel. Disord.* **2022**, *57*, 103318. [[CrossRef](#)]

55. Ricigliano, V.A.; Handel, A.E.; Sandve, G.K.; Annibaldi, V.; Ristori, G.; Mechelli, R.; Cader, M.Z.; Salvetti, M. EBNA2 binds to genomic intervals associated with multiple sclerosis and overlaps with vitamin D receptor occupancy. *PLoS ONE* **2015**, *10*, e0119605. [[CrossRef](#)]
56. Sutkowski, N.; Chen, G.; Calderon, G.; Huber, B.T. Epstein-Barr virus latent membrane protein LMP-2A is sufficient for transactivation of the human endogenous retrovirus HERV-K18 superantigen. *J. Virol.* **2004**, *78*, 7852–7860. [[CrossRef](#)]
57. Hsiao, F.C.; Lin, M.; Tai, A.; Chen, G.; Huber, B.T. Cutting edge: Epstein-Barr virus transactivates the HERV-K18 superantigen by docking to the human complement receptor 2 (CD21) on primary B cells. *J. Immunol.* **2006**, *177*, 2056–2060. [[CrossRef](#)]
58. Mameli, G.; Astone, V.; Arru, G.; Marconi, S.; Lovato, L.; Serra, C.; Sotgiu, S.; Bonetti, B.; Dolei, A. Brains and peripheral blood mononuclear cells of multiple sclerosis (MS) patients hyperexpress MS-associated retrovirus/HERV-W endogenous retrovirus, but not Human herpesvirus 6. *J. Gen. Virol.* **2007**, *88*, 264–274. [[CrossRef](#)]
59. Mameli, G.; Poddighe, L.; Mei, A.; Uleri, E.; Sotgiu, S.; Serra, C.; Manetti, R.; Dolei, A. Expression and activation by Epstein Barr virus of human endogenous retroviruses-W in blood cells and astrocytes: Inference for multiple sclerosis. *PLoS ONE* **2012**, *7*, e44991. [[CrossRef](#)]
60. Garcia-Montojo, M.; Rodriguez-Martin, E.; Ramos-Mozo, P.; Ortega-Madueño, I.; Dominguez-Mozo, M.I.; Arias-Leal, A.; García-Martínez, M.Á.; Casanova, I.; Galan, V.; Arroyo, R.; et al. Syncytin-1/HERV-W envelope is an early activation marker of leukocytes and is upregulated in multiple sclerosis patients. *Eur. J. Immunol.* **2020**, *50*, 685–694. [[CrossRef](#)]
61. Rasmussen, H.B.; Geny, C.; Deforges, L.; Perron, H.; Tourtelotte, W.; Heltberg, A.; Clausen, J. Expression of endogenous retroviruses in blood mononuclear cells and brain tissue from multiple sclerosis patients. *Mult. Scler.* **1995**, *1*, 82–87. [[CrossRef](#)] [[PubMed](#)]
62. Rasmussen, H.B.; Heltberg, A.; Lisby, G.; Clausen, J. Three allelic forms of the human endogenous retrovirus, ERV3, and their frequencies in multiple sclerosis patients and healthy individuals. *Autoimmunity* **1996**, *23*, 111–117. [[CrossRef](#)] [[PubMed](#)]
63. Liu, Z.; Mi, M.; Li, X.; Zheng, X.; Wu, G.; Zhang, L. lncRNA OSTN-AS1 may represent a novel immune-related prognostic marker for triple-negative breast cancer based on integrated analysis of a ceRNA network. *Front. Genet.* **2019**, *10*, 850. [[CrossRef](#)] [[PubMed](#)]
64. Liao, X.; Wang, X.; Huang, K.; Han, C.; Deng, J.; Yu, T.; Yang, C.; Huang, R.; Liu, X.; Yu, L.; et al. Integrated analysis of competing endogenous RNA network revealing potential prognostic biomarkers of hepatocellular carcinoma. *J. Cancer* **2019**, *10*, 3267–3283. [[CrossRef](#)] [[PubMed](#)]
65. Samuelson, L.C.; Wiebauer, K.; Snow, C.M.; Meisler, M.H. Retroviral and pseudogene insertion sites reveal the lineage of human salivary and pancreatic amylase genes from a single gene during primate evolution. *Mol. Cell. Biol.* **1990**, *10*, 2513–2520. [[CrossRef](#)]
66. Kamp, C.; Hirschmann, P.; Voss, H.; Huellen, K.; Vogt, P.H. Two long homologous retroviral sequence blocks in proximal Yq11 cause AZFa microdeletions as a result of intrachromosomal recombination events. *Hum. Mol. Genet.* **2000**, *9*, 2563–2572. [[CrossRef](#)]
67. Grandi, N.; Tramontano, E. Human endogenous retroviruses are ancient acquired elements still shaping innate immune responses. *Front. Immunol.* **2018**, *9*, 2039. [[CrossRef](#)]
68. Ramasamy, R.; Mohammed, F.; Meier, U.C. HLA DR2b-binding peptides from human endogenous retrovirus envelope, Epstein-Barr virus and brain proteins in the context of molecular mimicry in multiple sclerosis. *Immunol. Lett.* **2020**, *217*, 15–24. [[CrossRef](#)]
69. Lanz, T.V.; Brewer, R.C.; Ho, P.P.; Moon, J.S.; Jude, K.M.; Fernandez, D.; Fernandes, R.A.; Gomez, A.M.; Nadj, G.S.; Bartley, C.M.; et al. Clonally expanded B cells in multiple sclerosis bind EBV EBNA1 and GialCAM. *Nature* **2022**, *603*, 321–327. [[CrossRef](#)]
70. Schneider-Hohendorf, T.; Gerdes, L.A.; Pignolet, B.; Gittelman, R.; Ostkamp, P.; Rubelt, F.; Raposo, C.; Tackenberg, B.; Riepenhausen, M.; Janoschka, C.; et al. Broader Epstein-Barr virus-specific T cell receptor repertoire in patients with multiple sclerosis. *J. Exp. Med.* **2022**, *219*, e20220650. [[CrossRef](#)]
71. Serafini, B.; Rosicarelli, B.; Veroni, C.; Mazzola, G.A.; Aloisi, F. Epstein-Barr virus-specific CD8 T cells selectively infiltrate the brain in multiple sclerosis and interact locally with virus-infected cells: Clue for a virus-driven immunopathological mechanism. *J. Virol.* **2019**, *93*, e00980-19. [[CrossRef](#)]
72. Veroni, C.; Aloisi, F. The CD8 T cell-Epstein-Barr virus-B cell triologue: A central issue in multiple sclerosis pathogenesis. *Front. Immunol.* **2021**, *12*, 665718. [[CrossRef](#)]
73. Fu, B.; Ma, H.; Liu, D. Endogenous retroviruses function as gene expression regulatory elements during mammalian pre-implantation embryo development. *Int. J. Mol. Sci.* **2019**, *20*, 790. [[CrossRef](#)]
74. Mentzer, A.J.; Brenner, N.; Allen, N.; Littlejohns, T.J.; Chong, A.Y.; Cortes, A.; Almond, R.; Hill, M.; Sheard, S.; McVean, G.; et al. Identification of host-pathogen-disease relationships using a scalable multiplex serology platform in UK Biobank. *Nat. Commun.* **2022**, *13*, 1818. [[CrossRef](#)]

Supplementary materials

Epstein–Barr Virus-Induced Genes and Endogenous Retroviruses in Immortalized B Cells from Patients with Multiple Sclerosis

Lisa Wieland ^{1,2}, Tommy Schwarz ¹, Kristina Engel ², Ines Volkmer ², Anna Krüger ², Alexander Tarabuko ¹, Jutta Junghans ³, Malte E. Kornhuber ¹, Frank Hoffmann ³, Martin S. Staege ^{2,*} and Alexander Emmer ¹

¹ Department of Neurology, Medical Faculty, Martin Luther University Halle-Wittenberg, 06120 Halle (Saale), Germany

² Department of Surgical and Conservative Pediatrics and Adolescent Medicine, Medical Faculty, Martin Luther University Halle-Wittenberg, 06120 Halle (Saale), Germany

³ Department of Neurology, Martha-Maria Hospital Halle-Dölau, 06120 Halle (Saale), Germany

* Correspondence: martin.staege@medizin.uni-halle.de; Tel.: +49-34-5557-7280

This file contains:

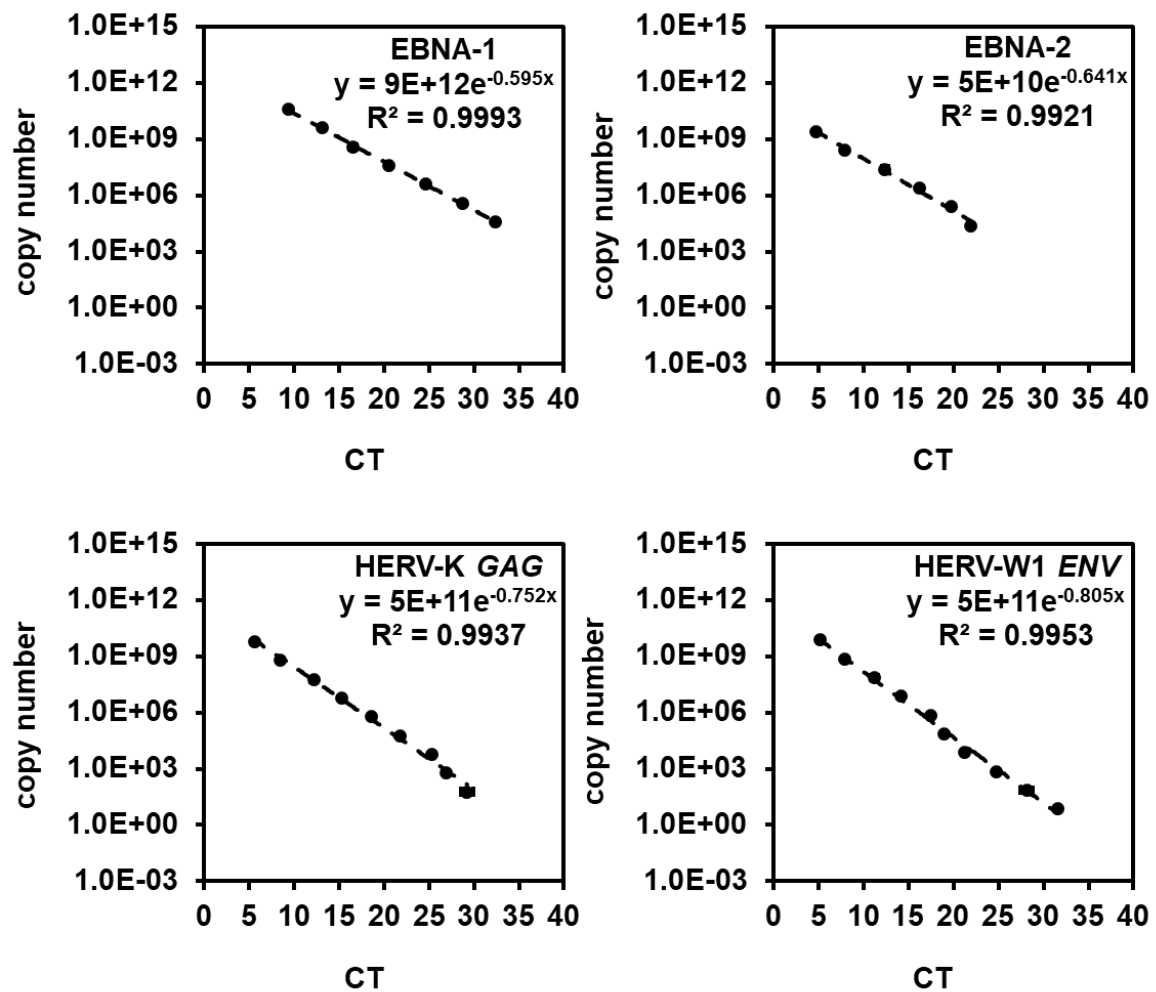
Supplementary Figures

Supplementary Figure S1
Supplementary Figure S2
Supplementary Figure S3
Supplementary Figure S4
Supplementary Figure S5
Supplementary Figure S6
Supplementary Figure S7
Supplementary Figure S8
Supplementary Figure S9
Supplementary Figure S10
Supplementary Figure S11
Supplementary Figure S12

Supplementary Tables

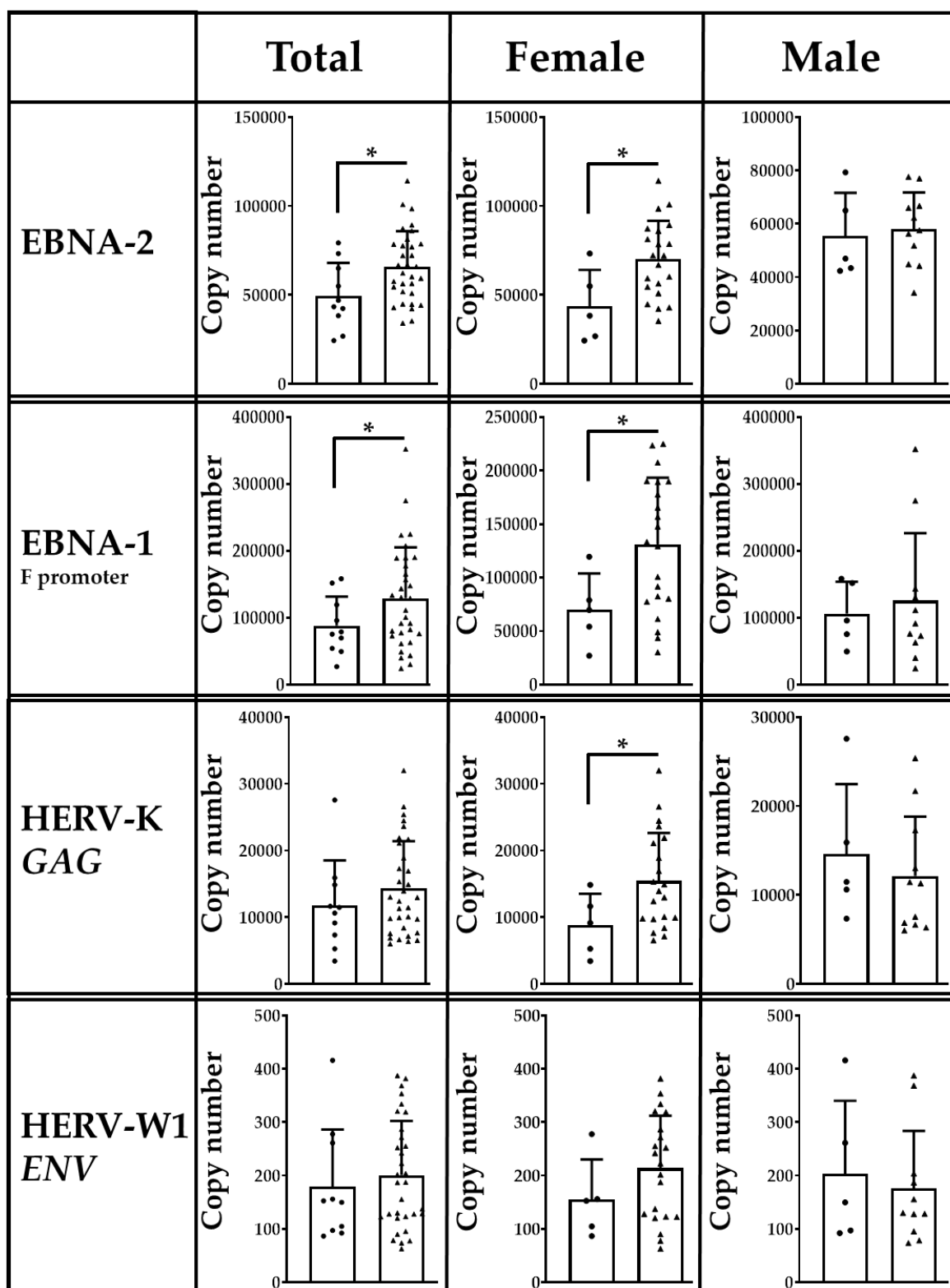
Supplementary Table S1
Supplementary Table S2
Supplementary Table S3
Supplementary Table S4
Supplementary Table S5
Supplementary Table S6
Supplementary Table S7

Supplementary Figures



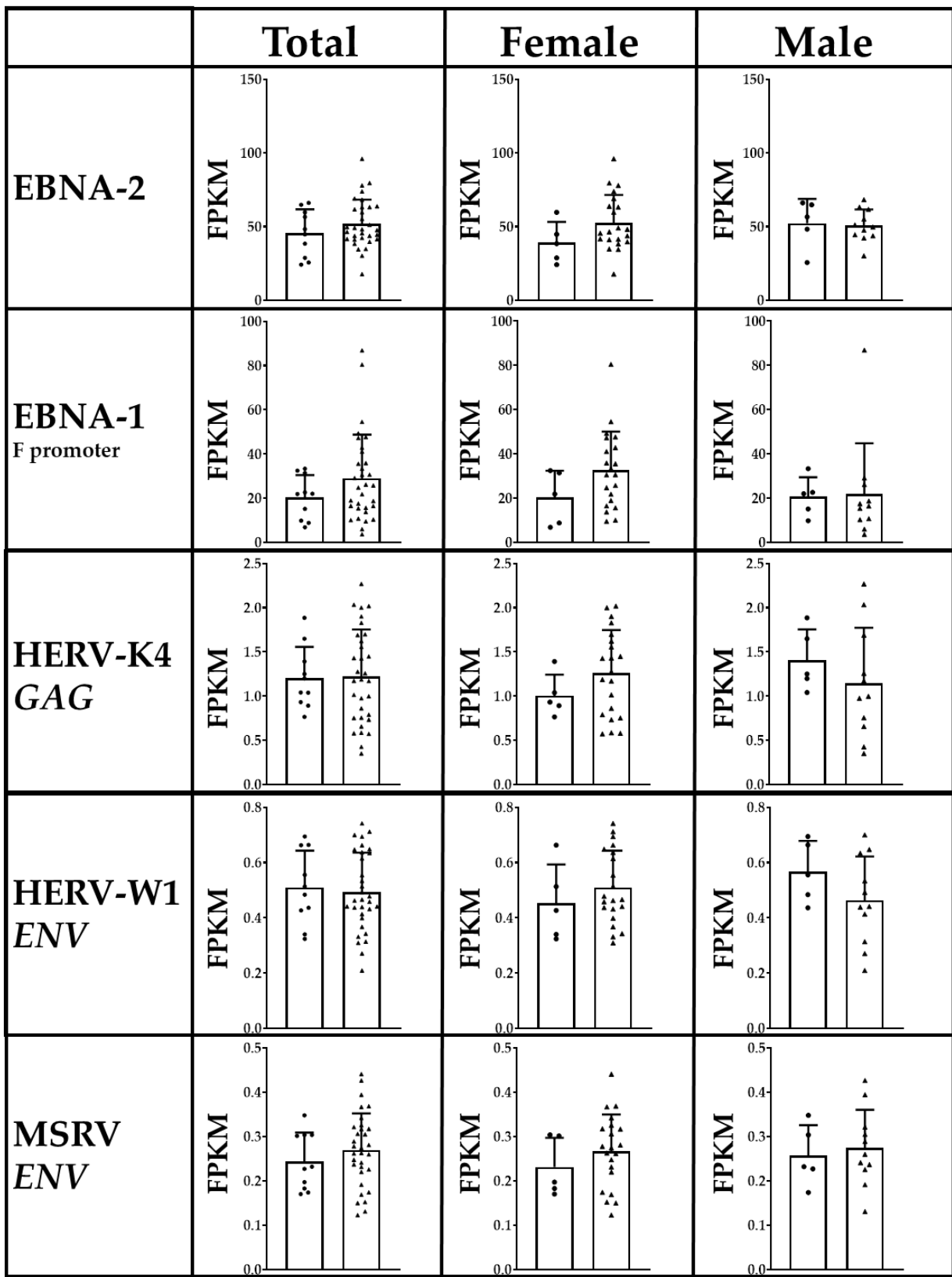
Supplementary Figure S1. Standard curves relating the copy number of target genes to the cycle threshold (CT) measured by qRT-PCR. For each target, dilution series from 10 ng to 1×10^{-11} ng of purified DNA were performed in triplicates. The graphs represent means \pm SD of data points belonging to the linear dynamic range (dashed line).

Cell type: ● coLCL ▲ MSLCL

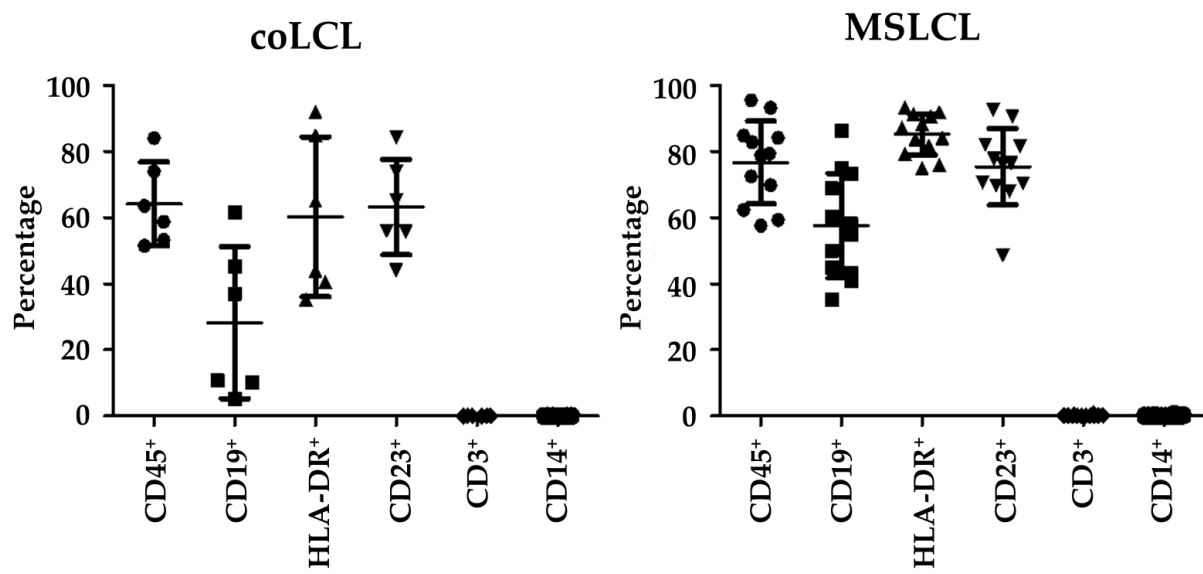


Supplementary Figure S2. Transcriptional activation of EBV and HERVs in MSLCL is pronounced in LCL generated from female donors (qRT-PCR). The graphs show means \pm SD of 94 LCL from 32 individuals with MS and 29 LCL from 10 controls analyzed by qRT-PCR. Copy numbers were determined by standard curves for individual target genes. Multiple LCL from the same donor served as biological replicates. The copy numbers from these LCL are also included in Figure 1B of the manuscript. Statistics: Welch's t-test; * $p < 0.05$.

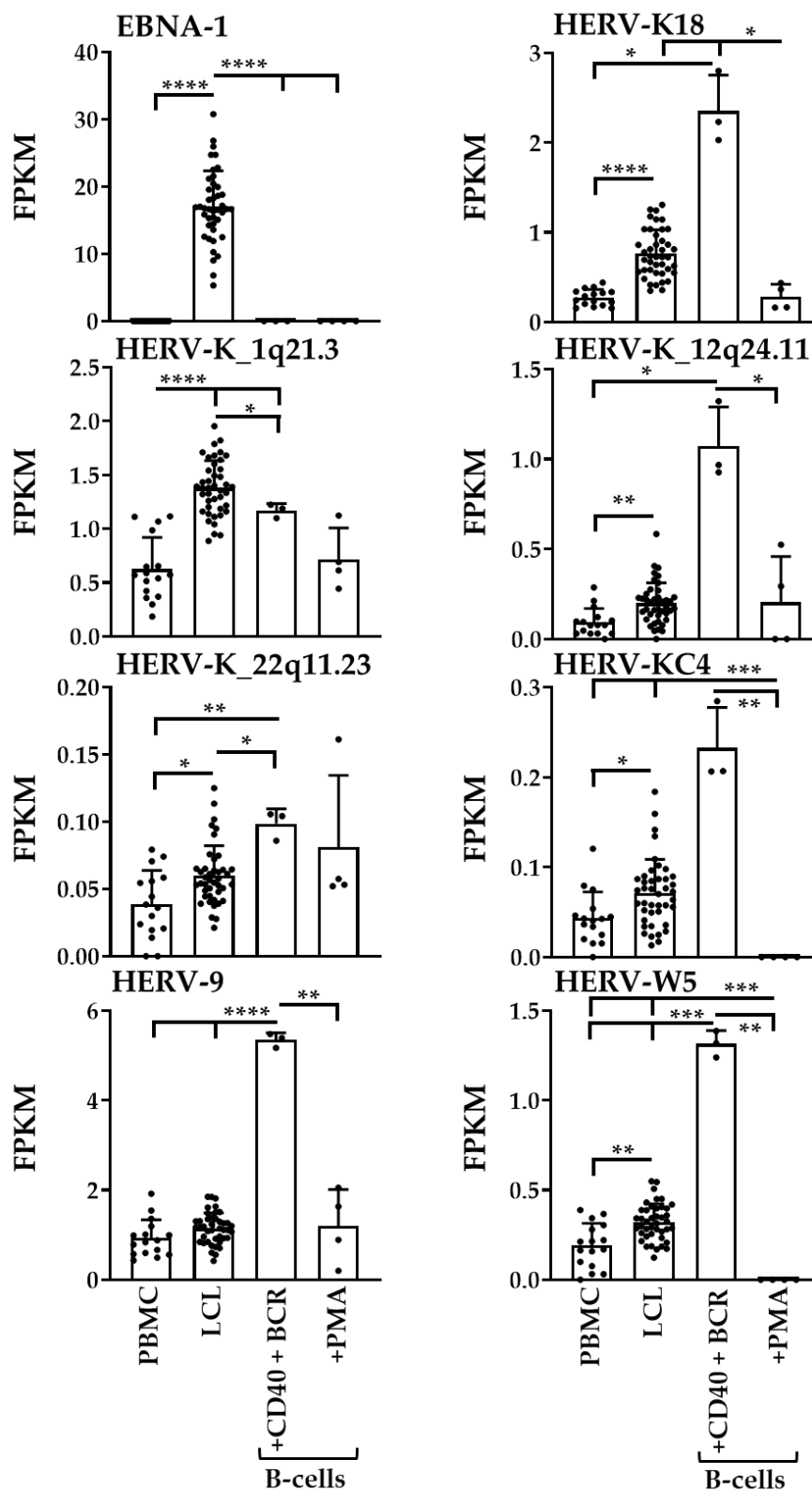
Cell type: ● coLCL ▲ MSLCL



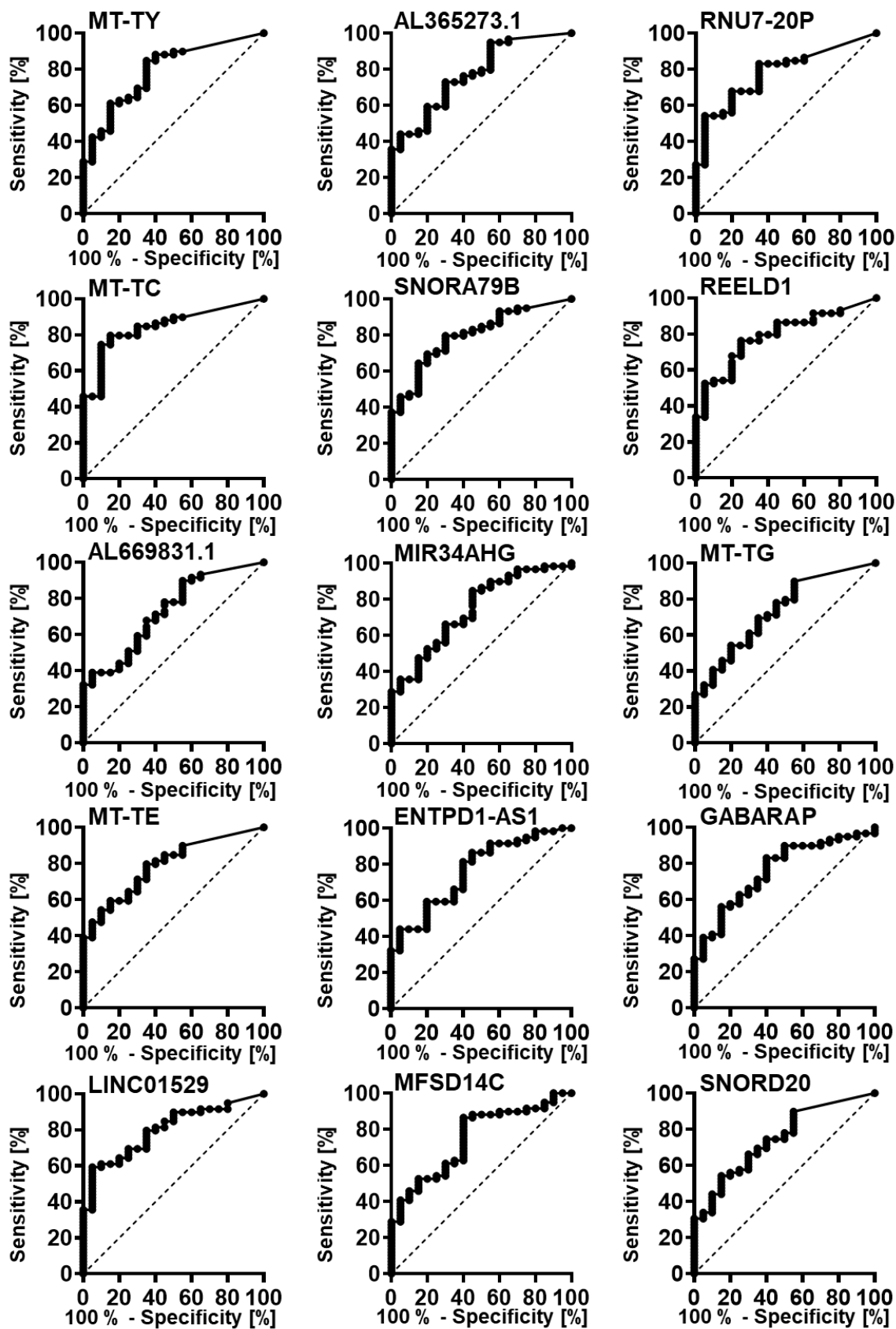
Supplementary Figure S3. Expression of EBV and HERVs in LCL from female and male PBMC donors (RNAseq). The graphs show means±SD of 59 LCL from 32 individuals with MS and 20 LCL from 10 controls analyzed by RNAseq. Multiple LCL from the same donor served as biological replicates. The RNAseq data from these LCL are also included in Figure 1A of the manuscript.



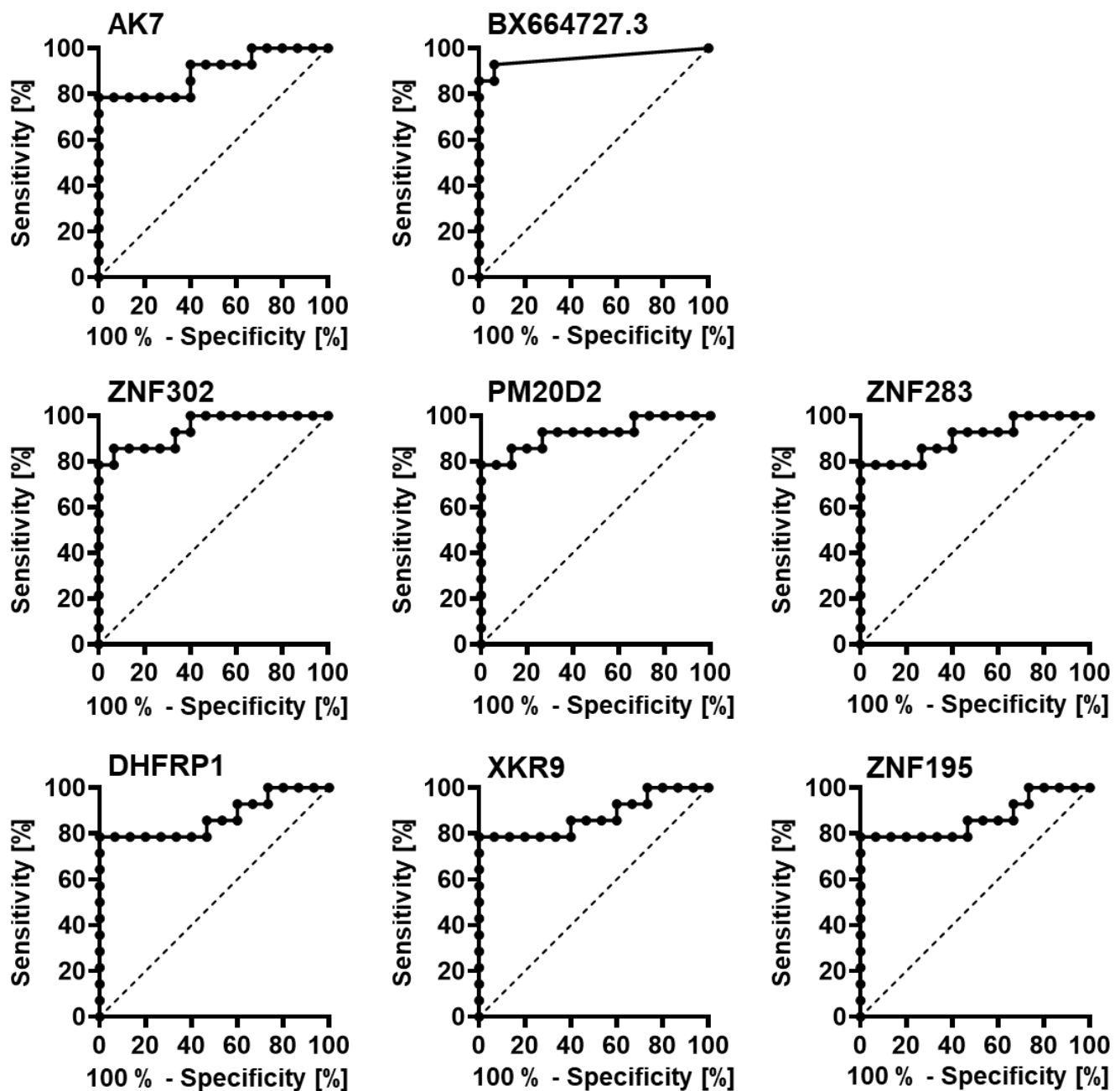
Supplementary Figure S4. Characterization of LCL from MS individuals (MSLCL) and control donors (coLCL) by flow cytometry. The graphs represent means \pm SD of the percentage of positive cells from all living cells. All tested coLCL and MSLCL showed expression of CD45, CD19, CD23, and HLA-DR. The presence of T-lymphocytes (CD3), as well as monocytes (CD14) was excluded.



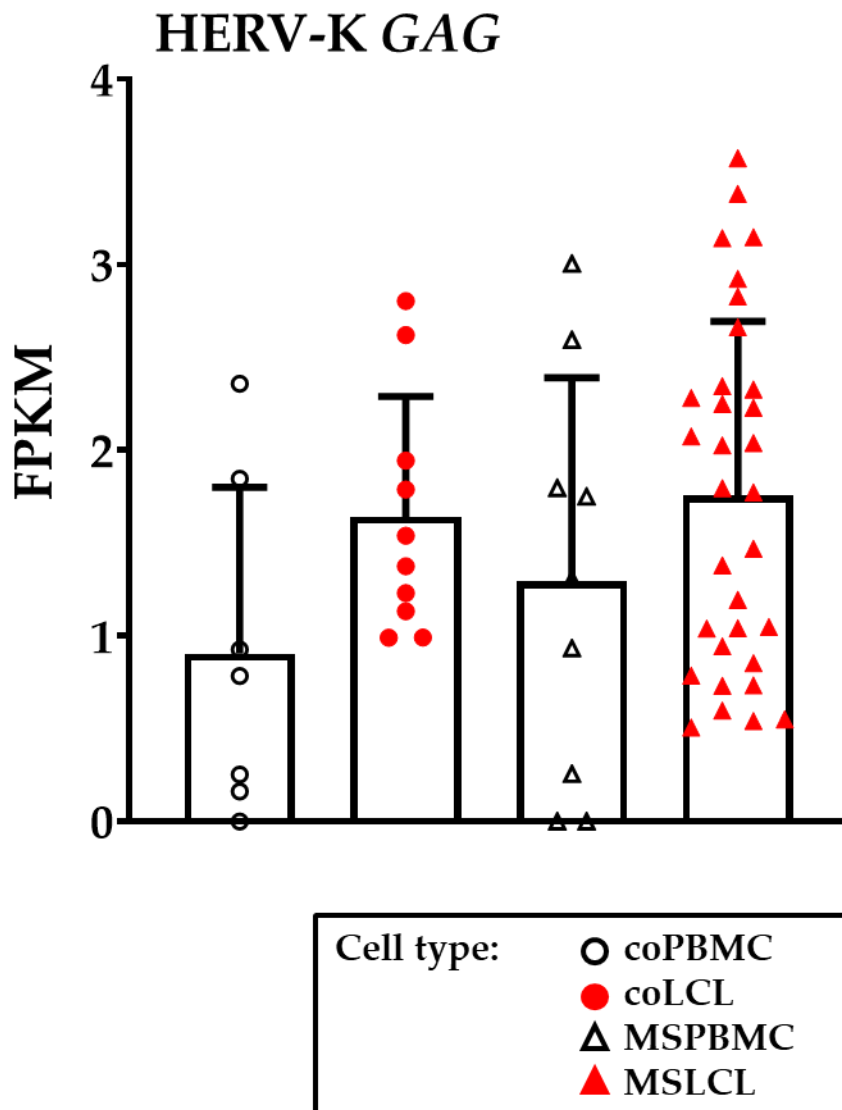
Supplementary Figure S5. The activation of HERV can be triggered through CD40 and B cell receptor (BCR)-signaling but not by phorbol myristate acetate (PMA) in B cells. The graphs show means±SD of FPKM from all PBMC (n = 16) and LCL (n = 42) in comparison to B cells stimulated with CD40 and BCR or PMA, respectively. The data from PBMC and LCL are the same as shown in Figure 1 of the manuscript. The presented HERV were selected according to their differential expression in PBMC and LCL as shown in the supplement (Supplementary Table S5). Statistics: one-way ANOVA with Dunnett T3 post-hoc test; ****p < 0.0001, ***p < 0.001, **p < 0.01, *p < 0.05.



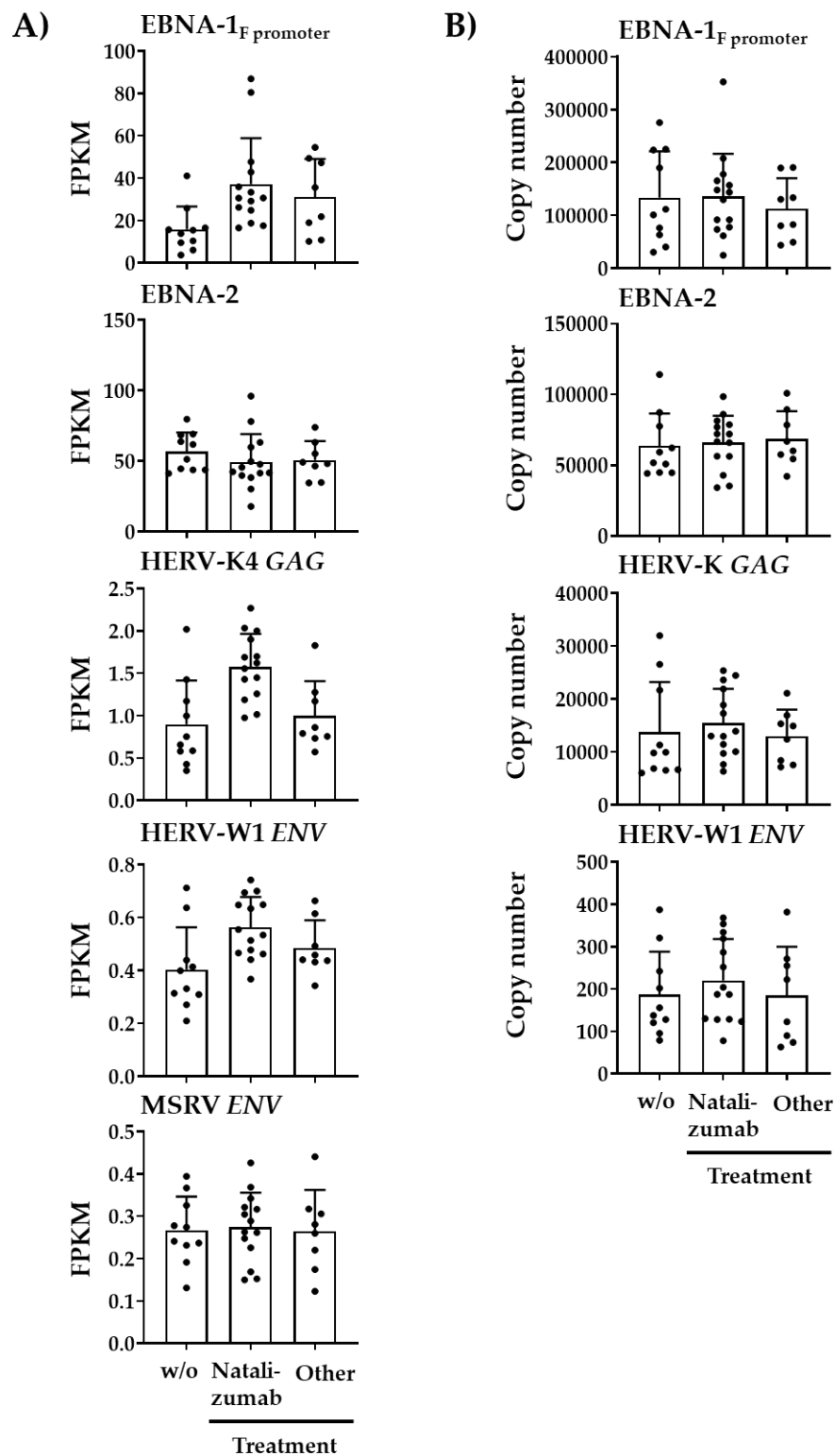
Supplementary Figure S6. ROC curves of identified MS biomarkers. Target genes were determined by RNAseq analyses of LCL as described in the manuscript. The ROC curve analyses were performed by GraphPad PRISM software version 8.3.0. The AUC of 0.5 is indicated by a dashed line.



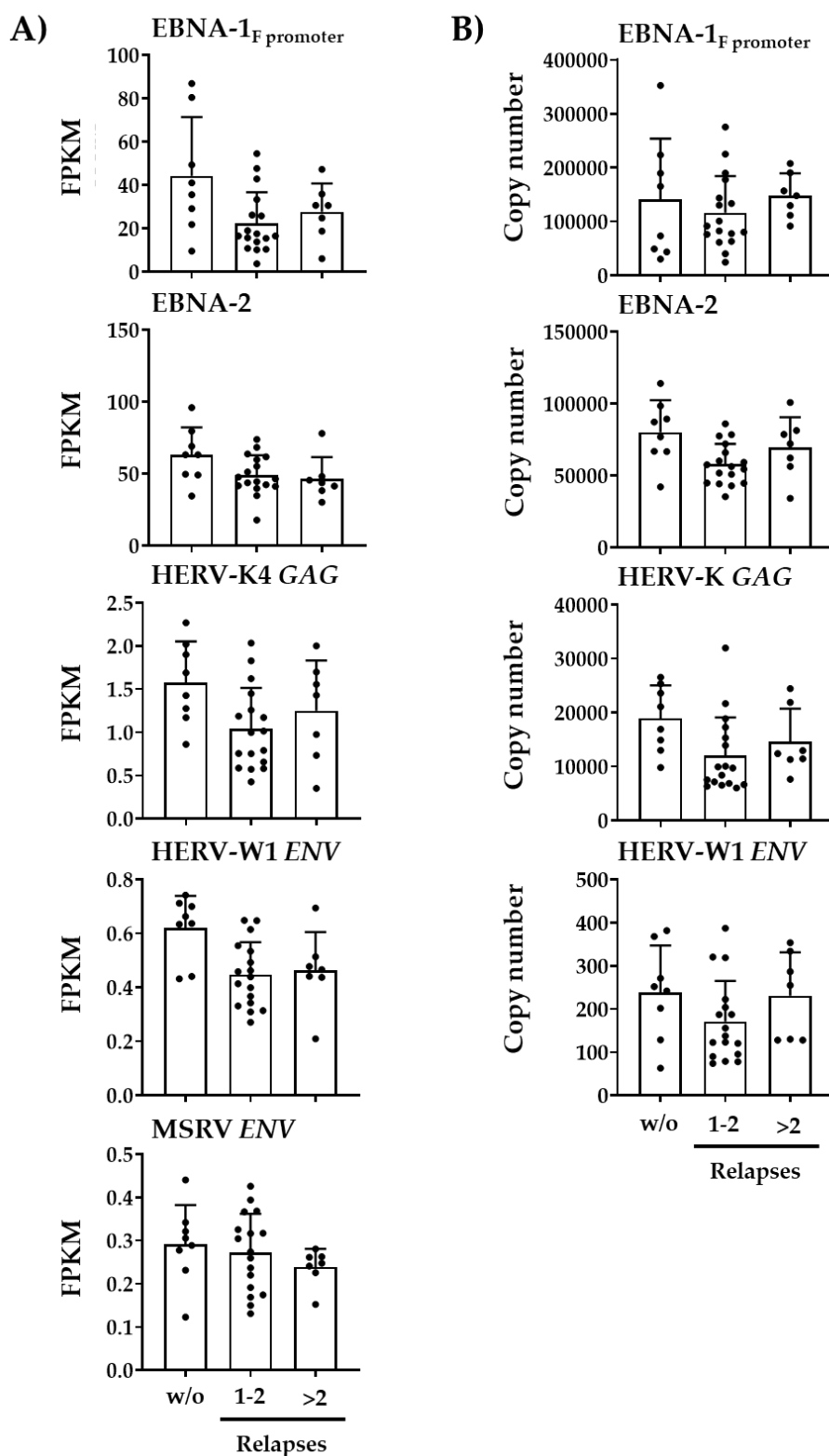
Supplementary Figure S7. ROC curves of targets that correlated with relapse rate in MS. Target genes were determined by RNAseq analyses of LCL as described in the manuscript. The ROC curve analyses were performed by GraphPad PRISM software version 8.3.0. The AUC of 0.5 is indicated by a dashed line.



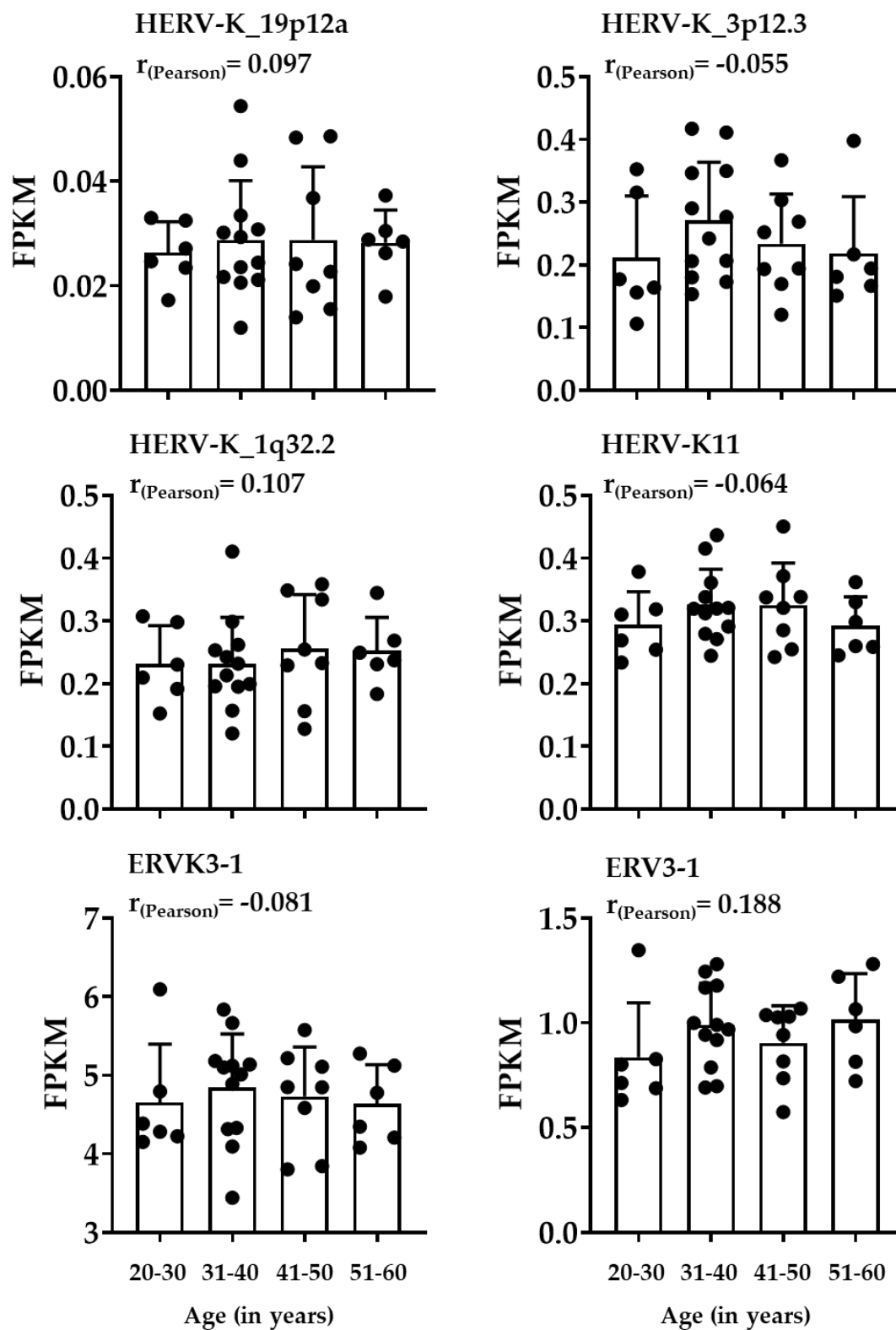
Supplementary Figure S8. Comparison of HERV-K GAG expression in PBMC and EBV-immortalized B cells (RNAseq analysis). Only reads that mapped to the region of the HERV-K4 GAG sequence that was the target for amplification by qRT-PCR were counted. Multiple LCL from the same donor served as biological replicates.



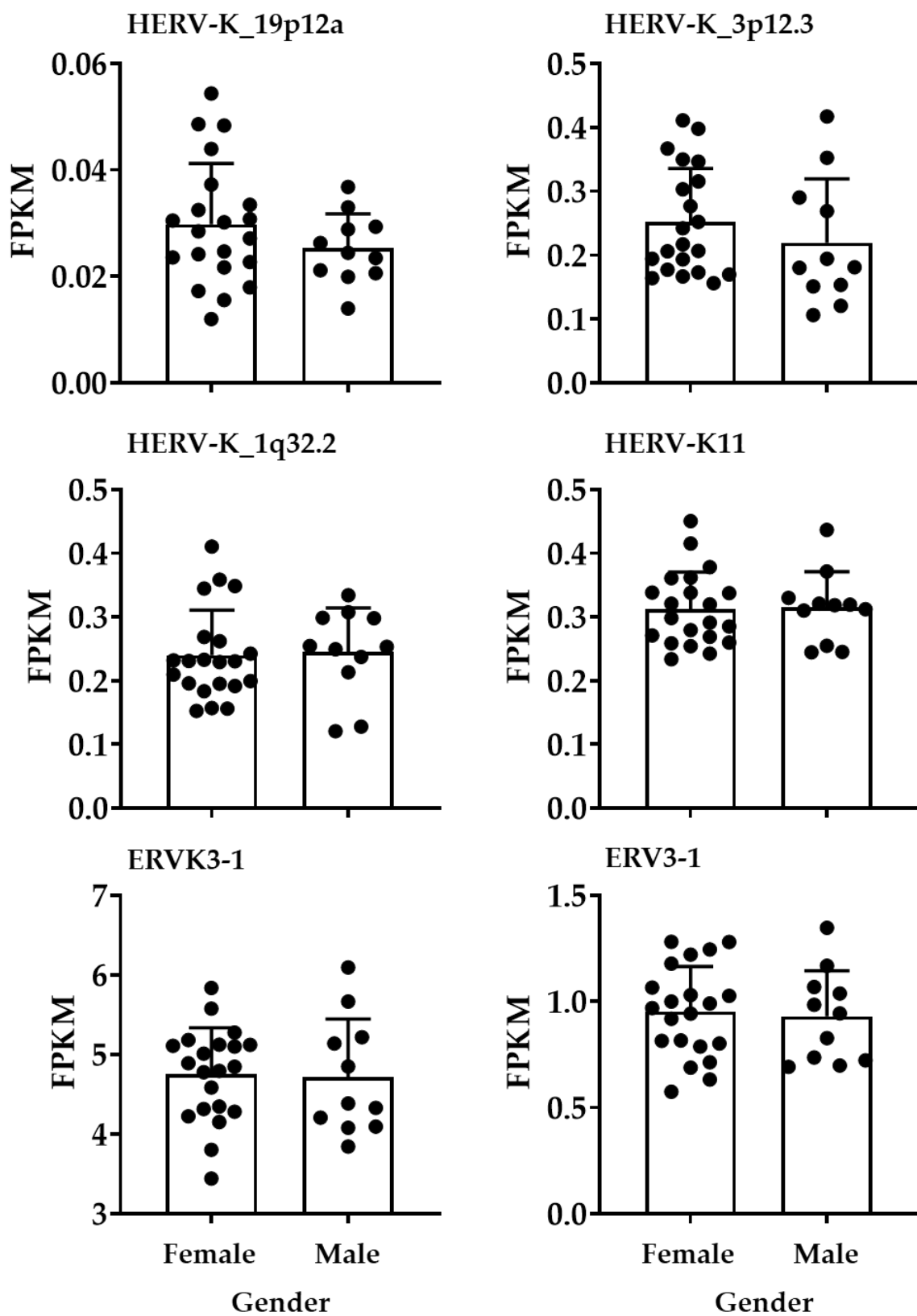
Supplementary Figure S9. Expression of EBV and HERVs in LCL from individuals with MS regarding disease-modifying therapy. The graphs show means±SD of 59 LCL from 32 individuals with MS by A) RNAseq or B) qRT-PCR. Multiple LCL from the same donor served as biological replicates. Twenty-two of all individuals with MS received therapy with natalizumab (n=14) or other drugs (n=8). These drugs include fingolimod (n=3), alemtuzumab (n=1), interferon beta-1a (n=1), carbamazepine (n=1), glatiramer acetate (n=1) and dimethyl fumarate (n=1). Ten individuals with MS were not receiving disease-modifying-therapies at the time of blood collection. Statistical significances were calculated using a two-way ANOVA with Bonferroni’s posthoc test and are presented in Table 2 of the manuscript (RNAseq) or in Table S1 of the supplement (qRT-PCR).



Supplementary Figure S10. Expression of EBV and HERVs in LCL from individuals with MS regarding relapse rate. The graphs show means±SD of 59 LCL from 32 individuals with MS by A) RNAseq or B) qRT-PCR. Multiple LCL from the same donor served as biological replicates. Eight of all individuals with MS were relapse-free, seventeen had one or two relapses and seven had more than two relapses within the last two years at the time of blood collection. Statistical significances were calculated using a two-way ANOVA with Bonferroni’s posthoc test and indicated in Table 2 of the manuscript (RNAseq) or in Table S1 of the supplement (qRT-PCR).



Supplementary Figure S11. Expression of HERVs up-regulated in MS regarding age of the individuals. The graphs show means \pm SD of 59 LCL from 32 individuals with MS analyzed by RNAseq. Multiple LCL from the same donor served as biological replicates. The correlation of HERV expression with age was indicated by Pearson's correlation coefficient. The increase of these HERV loci in MS compared to controls is presented in Figure 3 of the manuscript.



Supplementary Figure S12. Expression of HERVs up-regulated in MS regarding gender of the individuals. The graphs show means \pm SD of 59 LCL from 32 individuals with MS analyzed by RNAseq. Multiple LCL from the same donor served as biological replicates. The increase of these HERV loci in MS compared to controls is presented in Figure 3 of the manuscript.

Supplementary Tables

Supplementary Table S1. Influence of environmental and clinicopathological factors on EBV and HERV expression in LCL from MS individuals. Copies from the indicated transcripts were determined in 94 LCL from 32 individuals with MS by qRT-PCR. LCL from the same individual served as biological replicates. Data are means±SD. The RNAseq analysis from a part of the same LCL is shown in Table 2 of the manuscript. Statistics: Two-way ANOVA with Bonferroni's posthoc test; *p* values < 0.05 were indicated.

	EBNA-2	EBNA-1 F promoter	HERV-K GAG	HERV-W1 ENV
GENDER				
Female (n=21)	70101±21531	131151±62245	15438±7189	213.7±98.32
Male (n=11)	58031±13684	125605±101008	12142±6668	176.0±107.7
SMOKING BEHAVIOR				
Smoker (n=11)	66940±12583	145965±91374	15308±6932	241.0±113.6
Non-Smoker (n=21)	65435±23017	120486±67660	13780±7278	179.6±90.39
VITAMIN D DEFICIENCY				
Deficient (n=14)	65782±24946	125928±66590	14874±8025	187.2±83.19
Non-Deficient (n=7)	71167±20332	102789±64349	15401±6136	244.8±81.62
Unknown (n=11)	62850±11526	150302±93442	12884±6771	190.0±131.3
AGE AT STUDY ENTRY				
Age 20-30 years (n=6)	62030±12589	222036±89983 ^a	15431±8463	248.2±133.6
Age 31-40 years (n=12)	69903±21808	113316±59994 ^b	14402±2265	207.0±101.8
Age 41-50 years (n=8)	60179±24279	115278±54312 ^c	13733±6161	150.4±63.96
Age 50-60 years (n=6)	69671±16828	86932±48996 ^d	13750±6978	208.0±103.2
<i>P</i> value		^a vs ^c : <i>P</i> < 0.001 ^a vs ^{b,d} : <i>P</i> < 0.0001		
DURATION OF DISEASE				
Time >10 years (n=11)	64598±21900	108458±54903	13823±5208	166.7±97.80
Time ≤10 years (n=21)	66661±19195	140133±84365	14558±8005	101.1±22.07
LIFETIME WITH DISEASE[†]				
Lifetime ≥20 % (n=15)	68080±22778	138272±86110	15056±6546	186.9±99.91
Lifetime ≥20 % (n=15)	68080±22778	138272±86110	15056±6546	186.9±99.91
RELAPSE RATE IN 2 YEARS				
Relapses >2 (n=7)	69405±21157	147896±41391	14587±6154	230.7±100.6
Relapses 1-2 (n=17)	57808±14217	116103±67960	12020±7094	170.7±94.51
Relapse free (n=8)	80238±22142	140852±112828	18917±6152	238.5±108.9
DISEASE-MODIFYING THERAPIES (DMT)				
Natalizumab (n=14)	65958±19054	135784±80586	15475±6442	219.9±98.11
No DMT (n=10)	63708±22871	133550±87457	13736±9458	186.6±101.5
Others [‡] (n=8)	68748±19477	112420±57850	12971±5008	184.9±115.1
EXPANDED DISABILITY STATUS SCALE (EDSS)				
EDSS 1.0-1.5 (n=6)	64092±21320	161319±104042	19190±9539	200.6±130.6
EDSS 2.0-2.5 (n=11)	73013±21177	162466±76976	14518±7374	221.0±114.1
EDSS 3.0-3.5 (n=6)	64328±21781	96535±48275	12004±4131	174.1±83.88
EDSS 4.0-5.5 (n=8)	61494±16376	95184±42677	13112±5570	198.6±91.19

[†] Calculated from duration of disease divided by age at study entry

[‡] Interferon beta-1a, carbamazepine, alemtuzumab, glatiramer acetate, dimethyl fumarate, fingolimod (n=3)

Supplementary Table S2. Strongest up-regulated genes in LCL. The expression in 79 LCL and 16 PBMC was compared by RNAseq analysis. Genes were filtered for $p < 0.0001$ from Student's t-test, fold change > 100 and ranked from highest to lowest fold change in LCL. Means \pm SD of EB13 and CD70 in LCL and PBMC were shown in Figure 2 of the manuscript.

Name	Gene ID	Gene length	Fold change	P value
RPS18P12	ENSG00000230897	459	1845.695	3.64E-17
AL080243.2	ENSG00000237214	582	1521.000	8.27E-19
AL355032.1	ENSG00000241494	438	1325.957	4.92E-17
TUBBP2	ENSG00000214222	411	1203.464	3.28E-18
TUBBP1	ENSG00000127589	1646	963.355	2.66E-19
COX20P2	ENSG00000235013	358	735.251	6.25E-21
C6orf223	ENSG00000181577	3917	476.062	2.21E-34
RPL35P1	ENSG00000237991	370	464.138	2.42E-26
RF00154	ENSG00000222937	70	457.162	1.63E-24
AICDA	ENSG00000111732	3115	419.816	4.84E-18
CCL22	ENSG00000102962	2929	409.837	3.18E-10
WDR83OS	ENSG00000105583	2656	406.278	1.93E-30
UBE2V1P2	ENSG00000214192	440	397.900	1.52E-26
LINC01055	ENSG00000235366	1721	358.118	3.73E-26
AC011495.1	ENSG00000243829	584	339.879	6.41E-19
PIEZO2	ENSG00000154864	14796	317.221	8.87E-21
TSPAN12	ENSG00000106025	3368	278.091	5.92E-17
PBX2P1	ENSG00000244171	1291	266.579	4.60E-19
LIPH	ENSG00000163898	4122	244.040	1.76E-34
UCHL1	ENSG00000154277	2282	233.756	3.63E-16
PRR18	ENSG00000176381	3149	217.639	5.10E-17
TBXT	ENSG00000164458	2629	210.461	3.11E-08
CREB3L1	ENSG00000157613	4037	207.154	1.57E-22
KCNN3	ENSG00000143603	13598	205.670	7.51E-37
AL365434.1	ENSG00000225519	380	202.237	4.60E-20
SCD	ENSG00000099194	5362	190.252	3.28E-41
EIF5AP4	ENSG00000234743	465	187.840	1.15E-28
DHFRP1	ENSG00000188985	559	184.358	2.10E-22
NAALADL2-AS2	ENSG00000226779	1038	182.651	3.98E-07
AC005674.1	ENSG00000250413	459	176.468	2.64E-18
SLC12A8	ENSG00000221955	5586	175.928	1.95E-25
PTP4A1	ENSG00000112245	5996	171.767	6.16E-24
AC010343.1	ENSG00000240376	629	169.230	3.40E-18
EBI3	ENSG00000105246	1284	166.358	4.11E-27
CMA1	ENSG00000092009	937	159.748	1.75E-16
RPL38P4	ENSG00000250562	214	159.214	2.09E-28
ASCL1	ENSG00000139352	2472	157.791	4.66E-09
CD70	ENSG00000125726	1532	153.499	6.55E-37

DSG2	ENSG00000046604	6190	151.716	1.30E-24
ENTPD2	ENSG00000054179	2633	149.833	2.64E-12
RPS20P14	ENSG00000223803	360	149.346	2.31E-25
CLIC1P1	ENSG00000231313	724	148.516	1.87E-18
CLDN14	ENSG00000159261	2853	140.856	3.96E-27
GCSHP5	ENSG00000224837	522	138.391	2.72E-23
AC116347.1	ENSG00000238000	720	135.091	1.33E-24
SUMO2P6	ENSG00000249031	288	134.499	6.28E-23
AL109918.1	ENSG00000216775	3821	134.221	1.92E-25
MYL12BP2	ENSG00000227765	512	134.049	3.59E-19
PIR	ENSG00000087842	2512	133.566	2.92E-29
LAMP3	ENSG00000078081	3816	131.781	1.69E-29
SERBP1P1	ENSG00000213740	1160	130.691	4.42E-28
MIR138-1	ENSG00000207954	99	128.875	6.48E-19
RHOV	ENSG00000104140	1705	128.789	6.35E-20
STC2	ENSG00000113739	6128	121.871	5.79E-12
NUSAP1	ENSG00000137804	2875	119.434	3.72E-24
HNRNPKP4	ENSG00000243547	1386	118.948	3.04E-28
AC016734.1	ENSG00000228305	654	116.305	2.41E-26
TMOD1	ENSG00000136842	3708	114.141	2.85E-32
BHLHE22	ENSG00000180828	3262	109.369	4.36E-08
LGALS14	ENSG00000006659	1079	107.848	1.49E-15
CCL25	ENSG00000131142	989	102.408	2.31E-18
MAP1B	ENSG00000131711	12630	101.623	7.63E-22

Supplementary Table S3. Strongest up-regulated genes in MSLCL. The expression in 20 coLCL and 59 MSLCL was compared by RNAseq analysis. Genes were filtered for $p < 0.05$ from Student's t-test, fold change > 1.5 and ranked from highest to lowest fold change in MSLCL.

Name	Gene ID	Gene length	Fold change	P value
AC087385.1	ENSG00000240163	312	4.7733	0.0239
Z99755.1	ENSG00000238153	380	3.9157	0.0045
LINC01934	ENSG00000234663	14668	3.7429	0.0477
CLCA2	ENSG00000137975	4496	3.7421	0.0322
SEZ6L	ENSG00000100095	7149	3.2999	0.0069
DLG1-AS1	ENSG00000227375	1694	3.0632	0.0002
MT-TQ	ENSG00000210107	72	2.3671	0.0002
ERVMER61-1	ENSG00000230426	10142	2.2245	0.0001
RF00012	ENSG00000221044	204	2.0735	1.81E-05
REELD1	ENSG00000250673	2260	1.9752	1.08E-06
ABHD17AP4	ENSG00000229107	909	1.9349	0.0228
PCOTH	ENSG00000205861	1200	1.9214	0.0032
CCDC13-AS1	ENSG00000173811	2164	1.7574	0.0020
AL356124.1	ENSG00000226149	864	1.7018	0.0006
LTC4S	ENSG00000213316	1192	1.6733	0.0010
RNU7-20P	ENSG00000251712	62	1.6365	4.47E-06
MPL	ENSG00000117400	2212	1.6161	0.0002
NOTCH3	ENSG00000074181	9394	1.6144	0.0020
MIR365A	ENSG00000207725	110	1.5450	0.0331
LINC01118	ENSG00000222005	2267	1.5317	0.0004

Supplementary Table S4. Strongest up-regulated genes in coLCL. The expression in 20 coLCL and 59 MSLCL was compared by RNAseq analysis. Genes were filtered for $p < 0.05$ from Student's *t*-test, fold change > 1.5 and ranked from highest to lowest fold change in coLCL. The heatmap of these genes is shown in Figure 2 of the manuscript.

Name	Gene ID	Gene length	Fold change	<i>P</i> value
RAD51	ENSG00000051180	3046	3.2257	0.0187
AC093155.1	ENSG00000225568	826	2.5951	0.0053
ARPC3P5	ENSG00000214027	534	2.4604	0.0219
ACTC1	ENSG00000159251	4639	2.4297	0.0215
MSLN	ENSG00000102854	2560	2.3196	0.0074
C16orf46	ENSG00000166455	2376	2.2051	0.0128
TNFSF11	ENSG00000219451	428	1.9708	0.0035
C4orf36	ENSG00000163633	2100	1.9332	0.0103
AL354702.1	ENSG00000215895	1960	1.9142	0.0098
PRSS21	ENSG0000007038	1967	1.8912	0.0280
BACE2	ENSG00000182240	9619	1.8450	0.0038
ANP32C	ENSG00000248546	705	1.8374	0.0119
DHX9P1	ENSG00000228002	3076	1.8113	0.0021
AC018738.1	ENSG00000237039	210	1.7672	0.0038
DTX1	ENSG00000135144	4387	1.7585	0.0019
HEPHL1	ENSG00000181333	5345	1.7306	0.0019
STEAP1B	ENSG00000105889	2316	1.6934	0.0391
INMT	ENSG00000241644	3376	1.6817	0.0085
AC093616.1	ENSG00000234231	2070	1.6741	0.0266
NPC1L1	ENSG00000015520	5252	1.6429	0.0441
BX322650.1	ENSG00000183171	2143	1.6424	0.0067
RN7SKP225	ENSG00000222337	352	1.6397	0.0354
COX7CP1	ENSG00000235957	192	1.6042	0.0132
YWHAEP1	ENSG00000169418	5003	1.6004	0.0054
RPS10P3	ENSG00000217716	494	1.5987	0.0041
CHIA	ENSG00000134216	4632	1.5948	0.0305
RPL3P2	ENSG00000227939	1203	1.5937	0.0089
IGHV1-69	ENSG00000211973	412	1.5787	0.0491
DEPP1	ENSG00000165507	2979	1.5715	0.0001
FAM89A	ENSG00000182118	2394	1.5678	0.0263
AC002056.1	ENSG00000213683	760	1.5673	0.0111
AL591623.1	ENSG00000225300	1960	1.5655	0.0168
LINC02381	ENSG00000250742	2310	1.5613	0.0350
ANK1	ENSG00000029534	10797	1.5341	0.0011
CXCR5	ENSG00000160683	4431	1.5297	0.0171
CTH	ENSG00000213763	1123	1.5297	0.0006
SMG1P1	ENSG00000237296	7046	1.5104	0.0127
RHOV	ENSG00000074416	10102	1.5033	0.0003

IGFBP6	ENSG00000167779	1279	1.5023	0.0184
---------------	-----------------	------	--------	--------

Supplementary Table S5. Strongest up-regulated viral transcripts in LCL. The expression in 79 LCL and 16 PBMC was compared by RNAseq analysis. Genes were filtered for $p < 0.05$ from Student's t-test. Fold change > 1 and ranked from highest to lowest fold change in LCL.

Name	Exemplary accession number	Gene length	Fold change	P value
EBNA-1	NC_007605	1926	1692.747	4.00E-44
HERV-K18	JN675013.1	9232	2.132	1.35E-20
1q21.3_HERV-K	JN675012.1	3091	1.849	3.98E-09
12q24.11_HERV-K	JN675069.1	1485	1.564	0.0002
HERV-KC4	X80240.1	6369	1.332	0.0038
HERV-9	X57147.1	3918	1.119	0.0393
HERV-W5	AC117456.6: 51035-52536	1502	1.075	0.0008
22q11.23_HERV-K	JN675088.1	8859	1.038	0.0030

Supplementary Table S6. Strongest up-regulated viral transcripts in MS-derived LCL. The expression in 59 MSLCL and 20 coLCL was compared by RNAseq analysis. Genes were filtered for $p < 0.05$ value from Student's t-test, fold change > 1 and ranked from highest to lowest fold change in MSLCL. The heatmap of these genes is shown in Figure 3 of the manuscript.

Name	Exemplary accession number	Gene length	Fold change	P value
19p12a_HERV-K	JN675076.1	9382	1.1989	0.0008
ERV3-1	NC_000007.14:64990356-65006687	16332	1.1046	0.0008
ERVK3-1	NC_000019: 58305374-58315657	10284	1.0352	0.0015
HERV-K11	JN675025.1	9180	1.0285	0.0038
3p12.3_HERV-K	JN675019.1	8686	1.0070	0.0024
1q32.2_HERV-K	JN675016.1	4213	1.0045	0.0054

Supplementary Table S7. Variability of gene expression in LCL replicates from the same PBMC donor. The sum of genes above the cut-off values listed in Table 3 of the manuscript was calculated. The sum of genes from (a) all 35 genes or (b) 15 genes proposed from them for a biomarker panel is presented for all MS individuals. Individuals without a second LCL replicate were stated as not available (n.a.).

Donor	(a) Sum of genes above <i>cut-off</i> from 35 genes		(b) Sum of genes above <i>cut-off</i> from 15 genes	
	LCL replicate 1	LCL replicate 2	LCL replicate 1	LCL replicate 2
MS-001	9	15	2	5
MS-002	6	3	0	2
MS-003	3	2	1	1
MS-006	8	4	2	1
MS-008	19	7	6	1
MS-009	7	n.a.	4	n.a.
MS-010	4	10	1	5
MS-011	13	n.a.	6	n.a.
MS-012	16	21	8	11
MS-013	14	15	5	4
MS-014	9	16	4	9
MS-015	3	8	1	2
MS-016	19	18	9	10
MS-017	4	n.a.	2	n.a.
MS-018	13	25	6	10
MS-019	11	16	6	6
MS-020	22	16	11	9
MS-021	11	16	5	5
MS-022	16	22	7	8
MS-023	26	17	11	8
MS-026	11	19	2	7
MS-027	5	5	4	1
MS-028	11	12	6	4
MS-029	9	n.a.	4	n.a.
MS-030	8	0	3	0
MS-031	4	6	1	1
MS-032	13	3	8	3
MS-033	5	n.a.	2	n.a.
MS-038	8	15	5	8
MS-039	22	15	10	6
MS-040	7	16	3	8
MS-041	13	n.a.	7	n.a.

3. Diskussion

Zu Beginn der Arbeit sollte die Proteinexpression und -reifung ausgewählter HERV ENV untersucht werden. Zur stärkeren Aktivierung der Proteinsynthese wurden die nativen HERV-Sequenzen einer Kodon-Optimierung unterzogen, wobei der verwendete Algorithmus neben der Kodon-Präferenz auch den GC-Gehalt oder das Vorhandensein RNA-destabilisierender Elemente berücksichtigte.

3.1. Kodon-Optimierung überwindet die limitierte Proteinsynthese nativer ENV *in vitro* und führt zur Akkumulation überexprimierter ENV im ER

Wie in Publikation I dargestellt wurde, war die Proteinexpression der nativen ENV von HERV-Fc1, -K113 und -K18 *in vitro* stark limitiert und konnte mittels der Kodon-Optimierung um das 150-fache (HERV-K113) und das 290-fache (HERV-Fc1) gesteigert werden. Hierbei wurden mit Ausnahme von HERV-K18 die untersuchten ENV als glykosylierte Vorläuferproteine beobachtet. Das ENV von HERV-K18 konnte erst nach Kodon-Optimierung, sowie der Rekonstruktion einer Signalpeptidsequenz, welche durch eine 292 bp-Deletion im *POL-ENV*-Bereich bei Typ-1-Proviren der HERV (HML-2)-Familie verloren gegangen ist (18), ebenfalls als glykosyliertes Vorläuferprotein (coK18*) im Western Blot dargestellt werden.

Mittels Immunfluoreszenzfärbung konnte die Lokalisierung der ENV von HERV-K18, -Fc1 und -K113 im ER nachgewiesen werden. Für HERV-K113 konnte zudem eine teilweise Überlappung der Fluoreszenzsignale des trans-Golgi-Netzwerk-Markers und ENV beobachtet werden. Dies erscheint aufgrund der im Western Blot nachgewiesenen TM-Untereinheit des ENV (MW: 35-40 kDa) plausibel, da die Spaltung des ENV-Vorläuferproteins in SU und TM durch Furin-Proteasen, die im Golgi-Apparat aktiv sind, erfolgt (209, 210). Anhand vorangegangener Arbeiten war eine schwache Expression des ENV von HERV-K113 an der Zelloberfläche zu erwarten (211), jedoch konnten wir keines der untersuchten ENV an der Zelloberfläche nachweisen. Erst nach Permeabilisierung der transfizierten HEK293-Zellen konnte die Expression der kodon-optimierten ENV von HERV-K18 und HERV-K113 mittels Durchflusszytometrie detektiert werden. Eine Unzugänglichkeit des Epitops für den verwendeten Antikörper können wir mit hoher Wahrscheinlichkeit ausschließen, da frühere Berichte für den Nachweis von HERV-K ENV an der Zelloberfläche denselben Antikörper verwendeten (211, 212). Zusammenfassend lassen unsere Untersuchungen den Rückschluss zu, dass die Überexpression von ENV mittels Kodon-Optimierung zu einer Anreicherung von ENV im ER führt. In Einklang hiermit führte die Expression von coK113, sowie K18/coK18 zur Induktion von Genen (*sXBP1*, *DDIT3*), die im Zuge der Signaltransduktion durch fehlgefaltete Proteine im ER aktiviert werden. Das Fehlen eines effizienten intrazellulären Transports könnte im Falle von HERV-K18 auf eine defekte

Signalsequenz oder eine geringe Ausbeute an gespaltenem Vorläuferprotein, wie sie für das Kodon-optimierte ENV des HERV-K113 gezeigt wurde, zurückzuführen sein. Da weitestgehend unklar ist, inwieweit die Expression ruhender proviraler Sequenzen im menschlichen Genom reaktiviert werden kann, lassen unsere Beobachtungen von insbesondere Kodon-optimierten ENV jedoch keine konkreten Rückschlüsse auf deren physiologische Relevanz zu.

3.2. Seltene Nukleotidtripletts haben einen negativen Effekt auf die Expression des ENV von HERV-K113 in Säugerzellen und im zellfreien System

Bei Betrachtung der Nukleotidsequenz des ENV von HERV-K113 war auffällig, dass die Mehrzahl der durch die Kodon-Optimierung betroffenen Nukleotidtripletts für Leucin (CUA und UUA) oder Valin (GUA) kodieren, was auf eine begrenzte Verfügbarkeit geeigneter tRNAs für die Tripletts der Wildtypsequenz hindeuten könnte. In Publikation I konnte beobachtet werden, dass die schrittweise Wiedereinführung der seltenen Leucin-Kodone zur Verminderung der ENV-Expression von K113 in allen getesteten Zelllinien führte. Die Verwendung von seltenen Leucin-Kodonen allein hatte keinen Einfluss auf die Expression von ENV in der untersuchten Affenzelllinie COS-7. Hier beobachteten wir eine Abnahme des Proteingehalts nach Einführung seltener Valin-Kodone (mutcoK113*GUA: 3-fach; mutcoK113*GUA*CUA*UUA: 5,6-fach).

Die limitierte Proteinsynthese ließ sich auch in einem zellfreien Expressionssystem darstellen. Hierbei zeigten alle ENV-Varianten mit seltenen Leucin- und Valintripletts eine vergleichbar starke Abnahme des Expressionsniveaus. Interessanterweise konnte im zellfreien System das native ENV neben dem Kodon-optimierten ENV im Western Blot nachgewiesen werden, wenn gleiche Mengen an Proteinlysate geladen wurden. Bei der Expression in Säugerzellen war hierzu bislang eine Reduktion der geladenen Gesamtproteinmenge mit Kodon-optimierten ENV, z. B. um mindestens das 100-fache für coK113 in HEK293-Zellen, notwendig. Der verminderte Expressionsunterschied im zellfreien System (ca. 6-fach) deutet auf eine stärkere Proteinausbeute an nativem ENV hin, welche auf die zellfreie Translation selbst bzw. eine geeignetere tRNA-Zusammensetzung im nicht-menschlichen Retikulozyten-Lysat des verwendeten *in vitro* Translationssystems zurückzuführen sein könnte. Zwischen nativen und allen Kodon-optimierten ENV-Varianten wurde eine Diskrepanz an *in vitro* synthetisierter mRNA (ca. 1,4-fach) trotz gleicher Mengen an eingesetzter Vektor-DNA beobachtet, was neben dem negativen Einfluss der zellulären Translationsmaschinerie, auf eine zusätzlich ineffizientere Transkription des nativen ENV von HERV-K113 hinzuweisen scheint.

3.3. Mögliche Bedeutung der mRNA-Sekundärstruktur für die Synthese nativer HERV-Proteine

In der Konsequenz sollte nachfolgend eine Analyse der mRNA-Sekundärstruktur erfolgen, da die Kodon-Zusammensetzung die mRNA-Stabilität direkt beeinflusst (213). Die nähere Betrachtung der mRNA-Sekundärstruktur erfolgte mittels *in-silico*-Vorhersagen des *mfold* Web-Servers (<http://www.unafold.org/mfold/applications/rna-folding-form.php>), dessen Algorithmus eine Auswahl an möglichen mRNA-Modellierungen präsentiert (214). Beim Vergleich der thermodynamisch günstigen Modelle wiesen die untersuchten nativen *ENV* gegenüber den Kodon-optimierten Sequenzen jeweils eine höhere minimale freie Energie vor, was auf eine höhere thermodynamische Stabilität der mRNA hindeutet. Hinsichtlich der Translationseffizienz spielen jedoch vor allem die Länge und Struktur regulatorischer Stammschleifen eine bedeutsame Rolle (215), da sie durch die reverse Transkriptase übersprungen werden können, was einen frühen Abbruch der cDNA-Synthese und verkürzte Transkripte zur Folge haben kann (216, 217). Als eine mögliche Begründung für die sterisch ungünstigeren mRNA-Sekundärstruktur-Modelle der nativen *ENV* wäre denkbar, dass im Laufe der Evolution durch Mutationen und rekombinatorische Ereignisse solche Änderungen der Nukleotidabfolge akkumulierten, die eine effizientere Regulierung und Hemmung der Translation ermöglichten. Im Gegensatz dazu können mobile Elemente und insbesondere Viren bestimmte Bereiche mit stabilen mRNA-Sekundärstrukturelementen, wie Stammschleifen und Pseudoknoten, zur Favorisierung einer gewollten Verschiebung des Leserahmens (*programmed ribosomal frameshifting*, PRF) nutzen, um weitere Genprodukte von derselben mRNA ablesen zu lassen (218, 219). Für HIV-1 konnte gezeigt werden, dass eine derartige PRF um -1 Nukleotid (-1PRF) im Bereich der *GAG-POL* auftritt, um neben dem strukturellen Kapsidprotein (GAG), auch virale Enzyme (GAG-POL) bereitstellen zu können. Entscheidend für die Leserahmenverschiebung ist ein kurzes Sequenzmotiv (*slippery site*) in Kombination mit einer in Leserichtung nachfolgenden stabilen mRNA-Sekundärstruktur (220-223). Interessanterweise kodiert die 7-Nukleotid lange *slippery site* der *GAG-POL* mRNA, UUUUUUA, für die Aminosäuren Phenylalanin (UUU) und Leucin (UUA), wobei die Abundanz der für Leucin passenden tRNA direkt über die Wahl des Leserahmens bzw. dessen Verschiebung entscheidend ist (224). Korniy *et al.* konnten demonstrieren, dass mit zunehmender tRNA^{Leu(UUA)}-Konzentration die -1PRF-Effizienz zunahm. Physiologisch könnte dies auch für eine Aktivierung nativer HERV-Sequenzen von Bedeutung sein, wenn sich der tRNA-Pool in einem bestimmten Zelltyp (225, 226) oder durch äußere Faktoren, wie Zellstress (227, 228) oder eine Virusinfektion (229, 230), zu Gunsten der seltenen Nukleotidtripletts ändert. In den meisten Fällen würde dies zu einer effizienteren Translation der nativen Sequenz führen, wie wir sie im Sinne der verwendeten Kodon-Optimierung imitierten. Ähnlich zum HIV-1, könnten zudem PRF-Mechanismen in überlappenden Sequenzbereichen die Expression von Genen begünstigen, die insbesondere im späteren Lebenszyklus zur Reifung und

dem Virus-Zusammenbau notwendig sind. Im Hinblick auf die Anhäufung der seltenen Leucintripletts für das HERV-K113, wobei das Kodon UUA allein in der ENV-Sequenz 23-mal auftritt, erscheint die Relevanz eines dynamischen Pools an tRNA^{Leu(UUA)} auf die Translationseffizienz plausibel und sollte in weiterführenden Studien näher untersucht werden.

3.4. Induktion eines HERV-K/CD133-positiven Phänotyps in SiMa-Zellen und weiterer, bekannter Malignitätsmarker in NB-Zelllinien durch Kultivierung in Serum-depletiertem Stammzell-Medium

Nachfolgend wollten wir den potentiellen Einfluss der Mikroumgebung auf die Aktivität von HERV-Elementen näher untersuchen. Wie in Publikation II beschrieben, haben wir hierzu drei NB-Zelllinien in Standardmedium, sowie vor und nach Serumdepletion in Stammzell-Medium kultiviert und die Genexpression mittels RNAseq und qRT-PCR untersucht. Frühere Berichte wiesen darauf hin, dass eine stärkere HERV-Expression in weniger differenzierten Zellen auftritt (231-233), sowie Melanomzellen einen distinkten HERV-K/CD133-positiven Phänotyp unter Stammzell-fördernden Bedingungen entwickeln (198). Dies ist von besonderem Interesse, da Melanome Tumore sind, dessen Zellen ursprünglich aus der Neuralleiste stammen, wie es auch für NB zutrifft. Unsere Ergebnisse deuten auf eine stärkere Aktivierung von HERV-K GAG in Serum-depletiertem Stammzell-Medium hin, wobei die Induktion am stärksten in den Zelllinien SH-SY5Y (ca. 5-fach, $p < 0,0001$) und IMR-32 (ca. 3-fach, $p < 0,01$) und nur moderat in SiMa-Zellen (ca. 2-fach, n. s.) war. Dahingegen konnten wir ausschließlich in SiMa-Zellen einen CD133-positiven Phänotyp beobachten, der durch die Stammzell-Medium-Behandlung weiter zunahm (ca. 1,6-fach, $p < 0,0001$) und mit einer morphologischen Veränderung von locker anhaftenden Zellen zu schwach proliferierenden, traubenartigen Suspensionszellen einherging. Ähnliche Änderungen in der Morphologie wurden auch von Serafino *et al.* im Zusammenhang mit einer verstärkten Expression des Stammzellmarkers CD133 in Melanom-Zelllinien beobachtet. Andere Studien schrieben diesem NB-Phänotyp, der auch I-Typ genannt wird, als mögliche Population von Tumorstammzellen ein höheres malignes Potential zu (234, 235). Bemerkenswerterweise konnte kein Zusammenhang für I-Typ-Zellen und der Amplifikation bzw. Überexpression des Onkogens *MYCN* beobachtet werden (236), welches klassischerweise als prognostischer Marker für maligne NB dient (237, 238). Im Einklang mit diesen Beobachtungen, wurde *MYCN* in den untersuchten SiMa-Zellen zwar robust exprimiert, zeigte in Folge der Inkubation in Stammzell-Medium jedoch keine erhöhte Aktivität. Für IMR-32-Zellen war ein Anstieg in Folge der Kultivierung in Serum-freiem Stammzell-Medium erkennbar (ca. 1,6-fach, n. s.). Die SH-SY5Y-Zellen zeichneten sich durch Expression des verwandten Proto-Onkogens *MYC* aus, die sich durch Kultivierung in Serum-freiem Stammzellmedium deutlich erhöhte (ca. 5-fach, $p < 0,0001$). Diese hohe Heterogenität in der Morphologie und der exprimierten

Malignitätsmarker ist für NB charakteristisch, weshalb die Identifizierung genetischer Schlüsselmechanismen und therapeutisch relevanter Zielgene umso bedeutsamer ist (195, 239).

Mittels RNAseq-Analysen konnten wir Gene identifizieren, die in allen drei Zelllinien nach Serumdepletion in Stammzell-Medium einheitlich hoch- bzw. herunterreguliert ($|Fold\ change| > 1$, $p < 0,05$) waren. Nachfolgend wurde für diese differenziell exprimierten Gene (DEGs) der Korrelationskoeffizient nach Pearson ($R_{Pearson}$) mit den $2^{(-ddCT)}$ -Werten von HERV-K GAG berechnet, um eine nähere Eingrenzung der für uns potentiell interessanten Gene zu erzielen ($|R_{Pearson}| > 0,7$). Die stärkste Herabregulierung, in Folge der Serumdepletion in Stammzell-Medium, beobachteten wir u.a. für *ID1* (*Fold change*: 40,625) und *ID2* (*Fold change*: 16,011), die typischerweise von Zellen mit Ursprung aus der Neuralleiste exprimiert werden (240-242). Die Familie der *Inhibitor of differentiation/DNA binding* (ID)-Proteine ist häufig bei fortgeschrittenen, malignen Erkrankungen dereguliert (243-245), da sie zu grundlegenden Tumor-fördernden Mechanismen, wie De-Differenzierung, Verstärkung der Proliferation, Erhöhung der Invasivität und Angiogenese, beiträgt (246-248). Im Kontext mit der Pathogenese des NB wird angenommen, dass ID2 als direktes Target von MYCN rekrutiert wird, um die Tumor-hemmende Funktion des Retinoblastom (Rb)-Proteins zu umgehen und die Zellproliferation zu erhöhen (249, 250). Zudem scheint die Expression von ID2 und MYCN mit einer ungünstigen Prognose in NB zu korrelieren (251). Ähnlich zu ID2, wird eine Überexpression von ID1 mit verschiedenen Krebsarten und Tumor-fördernden Prozessen assoziiert, wobei u. a. eine starke Korrelation zu MYC-abhängigen Signalwegen und Faktoren angenommen wird, die an der epithelial-mesenchymalen Transition (EMT) von Zellen beteiligt sind (252). Interessanterweise lassen unsere Beobachtungen auf eine negative Korrelation von *MYC* bzw. *MYCN* und *ID1*, sowie *ID2* unter Serumdepletion schließen. Die verringerte Expression von *ID1* und *ID2* der NB-Zellen im Serum-freien Stammzell-Medium könnte auf die beeinträchtigte Proliferation zurückzuführen sein, wie wir sie zumindest für SiMa-Zellen nach Serumdepletion beobachteten. Unklar ist, inwiefern die Abnahme von ID1 und ID2 einen direkten Einfluss auf die Zelldifferenzierung hat. Zwar gibt es Hinweise darauf, dass ein Anstieg von ID2 in NB-Zellen stärker mit Genexpressionsmustern von sympathischen Vorläuferzellen der Neuralleiste, als neuroendokrinen Markern korreliert, wobei dieser Zusammenhang nicht eindeutig für SH-SY5Y-Zellen gezeigt werden konnte (253). Zudem legen zahlreiche Berichte nahe, dass anderen Faktoren, wie z. B. SOX10, FOXD3, Mitglieder der SNAIL-Familie von Transkriptionsfaktoren, sowie auch ID3, eine bedeutsamere Rolle bei der Aufrechterhaltung des Stammzell-Charakters von Zellen aus der Neuralleiste zuzuschreiben ist (254-259). Zusammenfassend konnten wir in NB-Zellen keine Genexpressionsmuster nachweisen, die einen undifferenzierten Zellstatus nach Kultivierung in Serum-freiem Stammzell-Medium bestätigen oder widerlegen würden.

3.5. Aktivierung des Immuncheckpunkt-Moleküls CD200 und Identifizierung ko-exprimierter HERV-Loci mittels Virus-Metagenomanalysen unter Stammzell-fördernden Bedingungen

Von Interesse ist, dass eine Zunahme von CD200 in Folge der Kultivierung in Serum-freiem Stammzell-Medium (*Fold change*: 1,666) zu beobachten war, welche sich mittels qRT-PCR und durchflusszytometrische Analyse in allen untersuchten Zelllinien bestätigen ließ. CD200 ist ein immunregulatorischer Zelloberflächenligand, welcher in einer Vielzahl von Geweben und Zelltypen, sowie auch B- und T-Lymphozyten exprimiert wird (260, 261). CD200 wird eine Tumor-fördernde Rolle zugeschrieben, da die Bindung von CD200 an seinen Rezeptor (CD200R) einen wichtigen Mechanismus zur Regulation der Immunantwort darstellt, wobei die Interaktion des CD200R an Antigen-präsentierenden Zellen (APCs) mit CD200 einen immunsuppressiven Effekt hat (262-264). Darüber hinaus wurde eine Überexpression von CD200 im Zusammenhang verschiedener Krebsentitäten beobachtet (265-270). Jedoch gibt es auch kontroverse Berichte über die Bedeutung und Rolle der CD200-Expression bei der Krebsentstehung, die auf eine gewisse Abhängigkeit vom Tumortyp hindeuten (266, 271, 272). Im Kontext mit der CD200-Expression im NB konnten Xin *et al.* zeigen, dass CD4- und CD8-T-Lymphozyten von NB mit einer starken CD200-Expression weniger pro-inflammatorische Faktoren, wie IFN γ oder TNF α , produzierten, was die Antitumor-Immunität der T-Zellen hemmt (270). Interessanterweise korrelierte die Aktivierung von CD200 mit der Transkription von HERV-K *GAG* ($R_{\text{Pearson}} >0,92$) in den von uns untersuchten NB-Zelllinien. Vor dem Hintergrund, dass HERVs als Expressionsverstärkende Elemente (67, 68) agieren und HERV-Insertionen im Speziellen zur Verstärkung IFN-induzierter Gene beitragen können (69), sowie HERV-Proteinen selbst immunsuppressive Eigenschaften zugesprochen werden (73, 77-79), könnte diese Beobachtung auf eine höhere Immuntoleranz von Krebszellen unter Stammzell-fördernden Bedingungen hinweisen (199).

Ein weiteres Ziel dieser Arbeit war die Identifizierung distinkter HERV-Loci, die potentiell als diagnostische oder therapeutische Zielstrukturen zukünftig relevant sein könnten. Zur effizienteren Identifizierung aktivierter HERVs mittels RNAseq verwendeten wir ein von uns designtes Virusgenom, welches u.a. 115 individuelle HERV mit nahezu vollständigen *GAG*, *POL* und *ENV* aus 14 HERV-Familien enthält. Die Expressionsstärke (gemessen als *Fragments Per Kilobase per Million reads*, FPKM) einer HERV-Familie wurde hierbei mittels der Anzahl aller Fragmente und der Summe der Genlängen aller Familienmitglieder berechnet. Wir beobachteten einen Anstieg der Expression für rund die Hälfte der HERV-Familien in NB-Zellen unter Kultivierung in Serum-freiem Stammzell-Medium, obwohl die Expressionsstärke insgesamt eher gering war. Am stärksten war hierbei die Expression von drei HERVs aus den Familien HERV-R (ERV3-1), HERV-E (HERV-E1, Alias HERV-E4-1) und HERV-Fc (HERV-Fc2 *ENV*) für alle untersuchten NB-Zelllinien in Folge der Serumdepletion. Zu ERV3-1 (7q11.21; NCBI accession

no.: NC_000007.14:64990356-65006687) ist anzumerken, dass es die einzige Kopie von etwa 40 ERV3-ähnlichen Elementen im menschlichen Genom ist, die einen vollständigen ORF für ihr ENV besitzt (273). Interessanterweise wird die Expression dieses ENV mit verschiedenen Tumorentitäten in Verbindung gebracht, darunter Kolorektal- (274), Ovarial- (93) und Endometriumkarzinom (275). Strissel *et al.* beobachteten, dass während der Progression des Endometriumkarzinoms ERV3-1 ENV mit sechs anderen ENV (HERV-W1, HERV-T, HERV-Fc2, HERV-H1-3, HERV-V1, HERV-E1) ko-exprimiert wird und eine signifikant erhöhte Expression in mehr undifferenzierten Tumoren des Grades 3 im Vergleich zu differenzierten Tumoren des Grades 1 aufweist. In Einklang damit, steht die Ko-Expression von ERV3-1 ENV, HERV-Fc2 ENV und HERV-E1 unter Stammzell-fördernden Bedingungen in allen hier untersuchten NB-Zellen, sowie ein Anstieg von HERV-W1 ENV in SH-SY5Y-Zellen (ca. 4-fach, $p < 0,001$) und ein deutlich undifferenzierter, Stammzell-ähnlicher Phänotyp in SiMa-Zellen. Ähnlich zu den zahlreichen Kopien des ERV3-1, sind 50 Kopien des HERV-E1 an 30 Integrationsorten des menschlichen Genoms bekannt (276). Obwohl das untersuchte HERV-E1 (17q11.2; NCBI accession no.: AB062274.1) nicht für ein komplett vollständiges ENV kodiert (277), konnte das ENV in diversen Tumorgeweben mittels Antikörper nachgewiesen werden (93, 278-280). Interessanterweise legen die Untersuchungen von Wang-Johanning *et al.* aus 2007 ebenfalls eine Ko-Expression mehrerer HERV-Proteine, HERV-K, HERV-E und ERV3-1, im Ovarialkarzinom nahe. Bis auf die Untersuchungen im Endometriumkarzinom, ist zur Proteinexpression des HERV-Fc2 ENV, das auf Chromosom 7q36 lokalisiert ist (NCBI accession no.: AC073236.8:162447-165176), bislang nur wenig bekannt. Zur Recherche verwendeten wir neben der bekannten Literatur-Datenbank *PubMed Central* (<https://www.ncbi.nlm.nih.gov/pmc/>), u.a. auch die kürzlich veröffentlichte Datenbank *CancerHERVdb* (<https://erikstricker.shinyapps.io/cancerHERVdb/>). Diese übersichtliche, frei zugängliche Datenbank beinhaltet eine interaktive Zusammenfassung veröffentlichter Publikationen im Zusammenhang von HERVs und diversen Tumorentitäten, die vierteljährlich seitens der Autoren aktualisiert wird (281). Anhand dieser Datenbank konnten zwei weitere Berichte für die Expression von HERV-Fc2-Transkripten in Tumorerkrankungen gefunden werden (282, 283), wobei ausschließlich Buslei *et al.* das von uns beobachtete HERV-Fc2 ENV in ihrer Studie untersuchten. Die Autoren beobachteten die Expression diverser HERV-ENV in verschiedenen Subtypen des Hypophysenadenoms (*pituitary adenoma*, PA), wobei die ENV von HERV-Fc2, ERV3-1 und HERV-T in allen 92 PA-Geweben signifikant höher exprimiert waren als in den nicht-tumorösen PA-Vorläuferzellen.

Im Vergleich zu unserem beobachteten Anstieg von HERV-K GAG mittels qRT-PCR war die Expression der HERV-K-Familie in den untersuchten NB-Linien nach Serumdepletion eher schwach. Jedoch stellt dies nicht zwingend einen Widerspruch dar, da die Diskrepanz sehr wahrscheinlich auf die verschiedene Zusammensetzung der jeweils untersuchten HERV-Loci

zurückzuführen ist. So wurde mittels qRT-PCR ausschließlich die Amplifikation von HERV-K GAG untersucht, wohingegen die RNAseq-Analyse die Expression nahezu vollständiger HERV-K-Sequenzen, inklusive GAG, POL, ENV und LTR-Bereiche, berücksichtigt. Damit einhergehend beschränkte sich die Anzahl der in unserem Virus-Metagenom annotierten HERV-K auf insgesamt 92 Loci mit (nahezu) vollständigen ORF, obwohl im menschlichen Genom mehr als 100 Kopien der HERV-K (HML-2) Familie enthalten sind. Bei näherer Betrachtung einzelner HERV-K-Familienmitglieder mittels RNAseq konnten wir zwei distinkte HERV-K Loci beobachten, die in allen drei NB-Zelllinien in Folge der Serumdepletion stärker exprimiert waren ($|Fold\ change| > 1$, $p < 0,05$): HERV-K 14q11.2 (Alias HERV-K71; NCBI accession no.: JN675071.1) und HERV-K 4p16.1b (Alias HERV-K50c; NCBI accession no.: JN675027.1). Eine Studie beobachtete eine Anreicherung ungespleißter mRNA des HERV-K-Loci 4p16.1b im Zytoplasma in Folge eines *in vitro* exprimierten HIV-1 Rev-Proteins, wobei unklar ist, inwiefern Rev zum Export der HERV-K mRNA aus dem Zytoplasma aufgrund des trunkierten 3'LTR-Bereichs beitragen kann (284). Unseres Wissens nach sind diese HERV-K-Kopien darüber hinaus nicht näher im Kontext maligner Erkrankungen untersucht. Zusammenfassend deuten die Ergebnisse unserer und zahlreicher weiterer Berichte auf eine Ko-Expression verschiedener HERV-Loci, insbesondere HERV ENV, im Zusammenhang mit malignen Tumoren hin. Die Unterschiede in den beobachteten HERV-Elementen könnten möglicherweise auf eine distinkte Signatur der jeweiligen Entitäten zurückzuführen sein und sollten in weiterführenden Studien mit einem großen *Panel* an Tumorproben näher untersucht werden.

3.6. Virus-Metagenomanalysen führen zur Identifizierung aktivierter HERV-Loci über den B-Zell-Rezeptor/CD40-Signalweg in EBV-immortalisierten B-Zelllinien

Neben der Expression in verschiedenen Tumorentitäten, wurden HERVs in den letzten Jahrzehnten zunehmend mit inflammatorischen Erkrankungen des ZNS in Verbindung gebracht (82, 127, 130, 131, 133-136, 138). Basierend auf der erhöhten HERV-Expression in diversen Zelltypen, Geweben und biologischen Flüssigkeiten von Patient:innen wird insbesondere eine mögliche Beteiligung an der Pathogenese der MS vermutet (85, 86, 89, 91, 92, 96, 123, 145). Es hat sich gezeigt, dass HERV-Elemente durch exogene Viren, wie das EBV, transaktiviert werden können (120, 121, 126). Zudem gilt eine Infektion mit EBV als bedeutsamer Risikofaktor für die spätere Entwicklung von MS (161, 162, 164), weshalb re-aktivierte HERV ein potentielles Bindeglied in diesem Zusammenhang darstellen könnten (137, 138, 141, 166, 169, 285). Im Rahmen der dritten Veröffentlichung sollte daher der Einfluss einer EBV-gesteuerten Proliferation auf die Genexpression in Personen mit MS und gesunden Kontrollen analysiert werden. Wir nutzten die EBV-spezifische Eigenschaft der latenten Infektion und

Immortalisierung von B-Zellen *in vitro*, um stabil wachsenden B-Zelllinien aus PBMC zu etablieren und hinsichtlich differenzieller Genexpressionsmuster zwischen MS-assoziierten und Kontroll-LCL untersuchen zu können. In Anbetracht der Tatsache, dass B-Zellen in MS-Gehirnläsionen der frühen und progredienten Phasen der MS beobachtet wurden (286) und B-Zell-depletierende Therapien bei Patient:innen mit RRMS und PPMS gute Resultate erzielen (287-289), könnte unser gewähltes B-Zell-Modell neue nützliche Erkenntnisse liefern, da die traditionellen Mausmodelle der MS weitestgehend auf die pathogene T-Zellantwort beschränkt sind (290). Für die Genexpressionsanalysen wurden alle LCLs innerhalb eines definierten Zeitraums von 10-11 Wochen nach Immortalisierung geerntet, was in etwa 10 Passagen entspricht, um mögliche Verzerrungen durch ein unterschiedliches Zellalter (291, 292) zu minimieren. Zur Identifizierung aktivierter HERV-Loci verwendeten wir wiederum unser designtes Virus-Metagenom. Wie in Publikation III gezeigt, stellten wir einen Anstieg der Expression von HERV-K18 (ca. 2,1-fach) durch die EBV-medierte Immortalisierung in allen LCL fest, wobei eine gleichmäßige Verteilung der gelesenen *Reads* über die gesamte provirale Sequenz stattfand. Dies lässt vermuten, dass die Aktivierung nicht allein auf die kodierende Region des ENV beschränkt ist, wie aus früheren Berichten in Folge der Stimulation mit dem gp350 Glykoprotein des EBV hervorgeht (120, 293). Neben HERV-K18 waren sechs weitere HERV-Loci nach Immortalisierung mittels EBV höher exprimiert, wozu drei HERV-K-Kopien auf Chromosom 1q21.3 (NCBI accession no.: JN675012.1), 12q24.11 (NCBI accession no.: JN675069.1) und 22q11.23 (NCBI accession no.: JN675088.1), sowie HERV-KC4 (NCBI accession no.: X80240.1), HERV-9 (NCBI accession no.: X57147.1), und HERV-W5 (NCBI accession no.: AC117456.6:51035-52536) zählen. Erwähnenswert ist, dass wir die Aktivierung dieser identifizierten HERVs ebenfalls in B-Zell-Rezeptor (BCR)- und CD40-stimulierten B-Zellen beobachten konnten. EBV nutzt genau diese Signalwege zur Stimulation der B-Zellen (294). Hierbei trägt aktiviertes CD40 entscheidend zur Proliferation und Immunglobulin-Sekretion von B-Zellen bei (295). Im Gegenteil dazu waren diese HERV-Loci nicht stärker in B-Zellen exprimiert, die mittels anderer Zellwachstums-fördernden Substanzen, wie z. B. Phorbolmyristat-Acetat (PMA), stimuliert wurden.

3.7. Immortalisierung mittels EBV führt ausschließlich in MS-assoziierten LCL zur Induktion distinkter HERV-Loci

Hinsichtlich differenziell exprimierter HERVs, war ein Anstieg von ERVMER61-1 (1q31.3; NCBI accession no.: AL357559.16: 123186-125823), den HERV-K-Loci 19p12a (NCBI accession no.: JN675076.1), 3p12.3 (NCBI accession no.: JN675019.1), 1q32.2 (NCBI accession no.: JN675016.1), sowie HERV-K11 (3q27.2, NCBI accession no.: JN675025.1), ERVK3-1 (19q13.43; NCBI accession no.: NC_000019: 58305374-58315657), und ERV3-1 ausschließlich

in MS-assoziierten LCL zu beobachten. Eine Abhängigkeit vom Alter oder Geschlecht der PBMC-Donner konnten wir ausschließen. Interessanterweise wurde in einer anderen Studie ebenfalls eine differenzielle Expression von ERV3-1 in PBMCs von MS-Patienten und Kontrollpersonen festgestellt (296). Jedoch konnte in einer nachfolgenden Arbeit derselben Gruppe keine der untersuchten ENV-Allelformen mit MS in Verbindung gebracht werden (297). Die Expression der weiteren sechs HERV-Elemente ist bislang nicht im Kontext neurodegenerativer Erkrankungen des ZNS diskutiert worden. Nachfolgend soll daher der derzeitige Kenntnisstand zu den genannten Loci und der Pathogenese anderer Entitäten kurz zusammengefasst werden.

Aus einer phylogenetischen Stammbaumanalyse von HML-6 Sequenzen geht hervor, dass mindestens zwei provirale Loci für intakte HERV-Proteine kodieren (298), wozu das ERVK3-1, als auch ein ENV gehört, das verstärkt in Melanomen detektiert und deshalb HERV-K-MEL genannt wird (299). Das ERVK3-1 weist eine ubiquitäre Expression in diversen Geweben, u. a. auch im Gehirn, auf (300), wobei ein 2,4-facher Anstieg in Lungen-Adenokarzinomen (301) und in einem Zellmodell unter hypoxischer und Zytokin-vermittelter Induktion von Nierenschäden beobachtet wurde (302). Interessanterweise wurde eine Überexpression des ENV von ERVK3-1 in Glioblastom (GBM)-Zelllinien mittels qPCR und *in-situ*-Hybridisierung von RNA beobachtet, welche zudem mit einer schlechteren Überlebensrate in GBM-Patient:innen korrelierte (303). Des Weiteren ist ein Fall einer myeloproliferativen Stammzellerkrankung beschrieben, bei der eine Translokation der Chromosomen 19q13.3 und 8q12 zur Fusion des ERVK3-1 und des Fibroblasten-Wachstumsfaktor-Rezeptor 1 (FGFR1)-Gens führte, welche die konstitutive Aktivierung des Zellwachstums förderte (304, 305). Das ERVMER61-1 wurde als mutmaßlicher lncRNA-Kandidat in Subtypen von Brustkrebs (306) und hepatozellulärem Karzinom (HCC) identifiziert, wobei es für eine prognostischen Signatur dysregulierter RNAs in HCC vorgeschlagen wurde (307). Die vier weiteren Loci gehören zu vollständigen bzw. nahezu vollständigen Provirussequenzen der HERV-K (HML-2)-Familie (308), welche die jüngste und biologisch aktivste HERV-Familie darstellt (197). Das HERV-K11 (Alias: HERV-K50b) zählt zu den in jüngerer Zeit integrierten Proviren, deren Expression auf den Menschen beschränkt ist, wobei die Integrationszeit auf in etwa zwei Millionen Jahre geschätzt wird (309). Aus einer Studie zur Charakterisierung von Polymorphismen ging hervor, dass in allen 18 getesteten Personen Polymorphismen für HERV-K11 vorlagen, diese jedoch weder alters- noch geschlechtsspezifisch waren (310). Eine familienspezifische Signatur kann aufgrund fehlender Informationen über Verwandtschaftsverhältnisse der Proband:innen nicht ausgeschlossen werden. In RNAseq-Analysen mit annotierten Provirussequenzen von ca. 90 HERV-K-Familienmitgliedern wurde eine gesteigerte Expression von fünf HERV-K-Loci, u. a. auch HERV-K11, in Leberkarzinomen beobachtet (311). Die für die differenzielle Expression verantwortlichen, abgelesenen Regionen waren nicht auf die ORFs von *GAG* oder *POL* zurückzuführen, sondern beschränkte sich fast

ausschließlich auf den 3'LTR-Bereich (312). Das HERV-K auf Chromosom 3p12.3 wurde als eine von fünf HERV-K (HML-2)-Provirussequenzen mittels RNAseq und qRT-PCR in Lymphozyten des peripheren Blutes (PBLs) nachgewiesen, die in Anwesenheit des HIV-1 Tat-Proteins verstärkt (ca. 78-fach gegenüber der Vergleichskontrolle) exprimiert wurden (313). HIV-1 und HERVs kodieren als Retroviren ähnliche Proteine, so dass Tat, als effektiver Transaktivator des HIV-1 Promotors, möglicherweise auch an LTR-Bereiche von HERVs binden und in der Konsequenz zur Aktivierung von HERVs und nachgeschalteten Genen führen könnte (314). Die HERV-K Loci auf Chromosom 19p12a und Chromosom 1q32.2 sind bislang nicht näher untersucht und es sind keine Berichte hinsichtlich einer differenziellen Expression veröffentlicht worden. Die Integrationszeit auf 19p12a wird auf 29,71 bis 54,79 Millionen Jahre geschätzt (315).

Obwohl lediglich in MS-assoziierten B-Zelllinien eine stärkere Expression von HERVs beobachtet wurde, waren die Unterschiede in der Expressionsstärke zwischen LCL von Personen mit MS und gesunden Kontrollen gering. Jedoch ist unklar, inwieweit die Höhe des Expressionsniveaus von HERVs entscheidend für die Aktivierung potentiell nachgeschalteter Signalwege ist. Möglicherweise ist das Gleichgewicht zwischen der persistierenden HERV-Expression und einer Aktivierung, die z. B. als antiviraler Abwehrmechanismus dient (316), sehr subtil. In diesem Zusammenhang ist es von besonderem Interesse, dass keine unserer untersuchten HERV-Kopien in den Kontrollen stärker, als in MS-assoziierten LCL, exprimiert war. Im Falle der Expression von HERV-Proteinen könnten insbesondere ENV unbeabsichtigt zur Aktivierung einer Immunantwort gegen Proteine mit ähnlicher Sequenz beitragen, welche Hauptziele einer Autoimmunreaktion darstellen. *In-silico* Analysen von Myelinproteinen und den drei ENV von HERV-W1, HERV-FRD und MSR/V lassen einen möglichen Rückschluss auf diesen Mechanismus der molekularen Mimikry zu, wobei die stärkste Homologie für einen 13 Aminosäure-langen Abschnitt des Myelin-Oligodendrozytenproteins (MOG) und HERV-W1 ENV (Alias: Syncytin-1) beobachtet wurde (143). In einer späteren Arbeit derselben Gruppe konnte neben der Sequenz-Verwandtschaft der HERV ENV und MOG die Bindung an Moleküle des HLA-DR2b gezeigt werden (317), dessen HLA-DRB1-Allele als genetische Hochrisikofaktor für MS gelten (318, 319).

Interessanterweise legt eine von Morandi *et al.* durchgeführte Meta-Analyse von 12 Studien ebenfalls einen starken Zusammenhang zwischen MSR/V/HERV-W *POL* und *ENV* und MS nahe (96). Im Rahmen unserer Analysen stellten wir keine signifikanten Unterschiede für die Expression der *ENV* von HERV-W1 oder MSR/V (NCBI-Genbank-Nr.: AF331500) in Zellen von MS-Patient:innen und Kontrollen fest. Interessanterweise gehörte eine andere HERV-W-Kopie, das HERV-W5, in Folge der Immortalisierung mittels EBV zu den am stärksten aktivierten Transkripten. Ein Anstieg des HERV-W1 *ENV* war nach EBV-vermittelter Immortalisierung der B-Zellen mittels qRT-PCR zu beobachten, jedoch war dieser nur in den LCL von Kontrollen

signifikant. Dies ist sehr wahrscheinlich auf die hohe Expression von HERV-W1 *ENV* in PBMCs mehrerer MS-Patienten zurückzuführen, was durch ähnliche Ergebnisse aus anderen Studien unterstützt wird, die auf eine insgesamt höhere Häufigkeit von zirkulierendem HERV-W bei MS-Patienten hindeuten (92, 320). In der Vergangenheit wurde auch in anderen Berichten keine Assoziation zwischen MS und einer verstärkten Expression von HERV-W (95, 321) bzw. keine erhöhte Immunantwort gegen HERV-W/MSRV-Antikörper in MS-Patient:innen beobachtet (94). Eine mögliche Ursache dieser abweichenden Beobachtungen zum Auftreten von HERV-W bzw. MSRV in MS, liegt in der komplexen genomischen Verteilung von HERV-W-Elementen im menschlichen Genom (95, 322), welche oftmals die Vergleichbarkeit von Studien erschwert, wenn unzureichend Angaben zum untersuchten HERV-Loci gemacht werden. Hierbei ist auch anzumerken, dass der genomische Integrationsort des beschriebenen MSRV *ENV* bislang unbekannt ist (323-325). Für die Expression des MSRV *ENV* wird eine Rekombination verschiedener HERV-W *ENV*-Transkripte vermutet (322), wobei eine Anzahl von mindestens sechs Loci angenommen wird (17). Zusätzlich könnten HERV-W-Kopien, die sich noch nicht in der breiten Population fest im Genom fixiert haben und bisher nur in bestimmten geografischen Regionen etabliert sind (326-328), zu abweichenden Beobachtungen beitragen. Für zukünftige Studien ist daher die Entwicklung von Strategien notwendig, die zur Identifizierung unfixierter HERV-Kopien beitragen, um u. a. auch somatische Gen-Umlagerungen und krankheitsspezifische Integrationsorte aufspüren zu können. Als Limitation unserer Studie ist die Isolation der PBMC zu nennen, die auf einen Zeitpunkt nach Diagnosestellung begrenzt war, sodass wir hinsichtlich einer möglichen Relevanz, von insbesondere HERV-W1- und MSRV-Transkripten als diagnostischer Frühmarker, keine Aussage treffen können. Zusammenfassend lassen unsere Beobachtungen eher darauf schließen, dass HERV-W5, aber nicht HERV-W1 und MSRV zu den Loci gehören, die präferiert durch EBV transaktiviert werden. Alternativ zum EBV wird das humane Herpesvirus 6 (HHV-6) als potentieller Transaktivator von HERV-W-Loci diskutiert (329, 330). Aufgrund des begrenzten Umfangs dieser Arbeit konnte auf eine potentielle Aktivierung von HERVs durch weitere exogene Viren, wie z. B. das HHV-6 oder das HIV-1, nicht näher eingegangen werden.

3.8. Darstellung potentiell prädiktiver Gen-Panel für die MS und deren krankheitsrelevante Faktoren mittels differenzieller Genexpressionsmuster in EBV-immortalisierten B-Zelllinien

Eine weitere Fragestellung der vorliegenden Arbeit war, inwiefern ein differenzielles Genexpressionsmuster in EBV-infizierten B-Zellen von MS-Patient:innen und Kontrollen beobachtet werden kann oder bestimmte Zielgene zur Identifizierung der MS-assoziierten LCL genutzt werden können. Übereinstimmend mit unseren Beobachtungen zur HERV-Expression,

war nur eine limitierte Anzahl von 59 Genen differenziell zwischen LCL von MS-Patient:innen und Kontrollen exprimiert ($|Fold\ change| > 1,5$; $p < 0,05$), was auf ein eher homogenes Genexpressionsmuster in den analysierten EBV-infizierten Zellen hinweist. Interessanterweise beobachteten wir darunter differenziell regulierte Gene, die eine starke Überexpression in einem Teil der MSLCL zeigten. Wie in Publikation III dargestellt, konnten 35 Gene und HERVs identifiziert werden, die in mindestens 25 % (15 von 59) der MSLCL eine hohe Expression vorwiesen, welche von keiner coLCL übertroffen wurde. Hierbei gehörte eine MSLCL bei keinem der 35 identifizierten Gene zu den oberen 25 %, wohingegen dies für acht Gene bei einer zweiten Linie desselben Spenders zutraf. Dies weist auf eine gewisse Heterogenität innerhalb der LCL eines Spenders hin, weshalb bei der Verwendung mehrerer LCL pro Spender eine höhere Aussagekraft für die Identifizierung differenzieller Expressionsmuster anzunehmen ist. Mit Hilfe von LCL-Duplikaten je Spender konnte so eine kleine Gruppe von 15 Genen identifiziert werden, welche in mindestens einem Viertel aller MSLCL überexprimiert war und eine perfekte Diskriminierung zwischen MS-Patient:innen und Kontrollen zuließ. Die Betrachtung aller Linien ergab eine korrekte Zuordnung von 88 % der MSLCL (52 von 59), ohne dass eine falsch positive Vorhersage für die Kontrollen getroffen wurde. Anhand dieser Beobachtung stellte sich nachfolgend die Frage, inwieweit eine ähnliche Auswahl an Genen für die Vorhersage eines krankheitsrelevanten Risikofaktors, wie beispielsweise der Schubrate, identifiziert werden kann. Hierzu nutzten wir die Genexpressionsanalysen der LCLs von je sieben MS-Patient:innen mit bzw. ohne Schübe in den letzten zwei Jahren. Die MS-Patient:innen wurden basierend auf ihrem Geschlecht, sowie der Krankheitsdauer ± 1 Jahr gepaart, um eine Verzerrungen aufgrund der limitierten Stichprobenanzahl bestmöglich zu minimieren. Innerhalb der differenziell exprimierten Gene, konnten acht Gene mit einer exklusiv hohen oder niedrigen Expression in mehr als 75 % der Schub-assoziierten MSLCL (11 von 14) identifiziert werden. Mittels der Verwendung von LCL-Duplikaten je Spender, konnte für das *Panel* aus zwei hoch- und sechs herunter-regulierten Genen eine ideale Unterscheidung der MS-Patient:innen mit und ohne Schübe gezeigt werden.

3.9. Mögliche Bedeutung *in vitro* exprimierter EBV-Genprodukte im Zusammenhang mit Umwelt-bedingten und klinischen Parametern in der MS

Der Fokus auf das EBV als exogenen Treiber einer späteren Entwicklung von MS ist, neben der Transaktivierung intrinsischer Gene viralen Ursprungs, auf seine eigene Virusreplikation und die durch EBV-Antigene ausgelöste Immunreaktion zurückzuführen. So weisen zahlreiche Berichte auf die Präsenz EBV-infizierter B-Zellen in aktiven Hirnläsionen in der MS hin (331-334). Mit Hinblick auf eine EBV-Serokonversion von über 90 % aller Menschen vor ihrem 30. Lebensjahr (335-337), ist jedoch fraglich, was ausschlaggebende Faktoren für die Entwicklung der MS sind,

woran aktuell 2,8 Millionen Menschen weltweit erkrankt sind (171). Zur Untersuchung dieser Frage, haben wir die Expression von EBNA-1 und EBNA-2, die während der lytischen bzw. latenten Phase des EBV transkribiert werden, im Zusammenhang verschiedener klinischer Parameter, sowie den am stärksten diskutierten Risikofaktoren in den aus PBMCs etablierten LCL unserer MS-Patient:innen analysiert. Nachfolgend sollen die in Publikation III dargelegten Beobachtungen im Kontext der aktuellen Literatur näher eingeordnet und diskutiert werden. Für unsere EBV-immortalisierten LCL war eine höhere Expression von lytischem EBNA-1, sowie EBNA-2 in MS-assoziierten Linien mittels qRT-PCR zu beobachten ($p < 0,05$). Auch frühere Berichte weisen auf eine stärker ausgelöste Immunantwort durch zirkulierendes EBV (338-340) oder in Folge einer Infektion mit EBV hin, wobei z. B. höhere Antikörpertiter gegen Epitope des EBV bereits Jahre vor einem Ausbruch der MS im Serum der Patient:innen detektiert werden können (164, 341-343). Zudem wurde in einer anderen Arbeit mit etablierten LCL von Patient:innen mit dem Louis-Bar-Syndrom, einer seltenen erblichen neurodegenerativen Erkrankung, keine differenzielle Expression der EBV-Latenzgene nachgewiesen (344), was auch für eine spezifische Beteiligung in der Pathogenese der MS spricht. Für die Überexpression der EBV-Gene stellten wir geschlechtsspezifische Unterschiede fest. Innerhalb der männlichen Kohorte waren keine Unterschiede in der Expression beider EBV-Transkripte zwischen MS- und Kontrollgruppe zu sehen, wohingegen die Diskrepanz zur Kontrollgruppe in weiblichen Probandinnen deutlich ausgeprägt war (EBNA-1: 1,8-fach; EBNA-2: 1,6-fach; je $p < 0,05$). Interessanterweise deutet eine Studie aus Großbritannien von über 9000 Proband:innen auf eine generell höhere EBV-Seroprävalenz bei Frauen hin (345), was hinsichtlich der höheren Frequenz weiblicher MS-Patientinnen von Bedeutung sein könnte (171). In der Vergangenheit wurden auch Rauchen (346), sowie ein niedriger Vitamin-D-Spiegel (347-349), als mögliche Risikofaktoren in der MS diskutiert. Unsere Beobachtungen liefern keine Indizien für den Einfluss dieser Faktoren auf die Expression von EBV- und HERV-Transkripten zum Zeitpunkt der Analyse in LCL. Um eine Aussage hinsichtlich der potentiellen Auswirkung auf die Krankheitsprogression treffen zu können, wäre wiederum eine längerfristige Begleitung der Patient:innen notwendig. Hierbei wäre die Untersuchung der EBV- und HERV-Expression durch eine Blutabnahme innerhalb routinemäßiger Kontrolltermine denkbar. Zudem wäre die Erfassung des Vitamin-D-Titers zu diesen Zeitpunkten nötig, um insbesondere Aufschluss über die EBV-Aktivität in Phasen des Vitamin-D-Mangels und der Substituierung zu erhalten, da ein möglicher Zusammenhang weiterhin als plausibel erscheint (350, 351). Des Weiteren wird in der MS eine ineffizientere oder dysfunktionale Immunantwort auf zirkulierendes EBV angenommen (352, 353). Diese Auffassung wird gestützt durch die Beobachtung, dass in MS die Höhe des Anti-EBNA1 IgG-Titer invers mit der Frequenz EBV-spezifischer CD8⁺-T-Zellen korreliert (354), wohingegen bei gesunden Personen eine positive Korrelation festgestellt wurde (355). In diesem Kontext ist bemerkenswert, dass wir eine negative Korrelation der EBNA-1 Expression in LCL

mit zunehmendem Alter der PBMC-Spender:innen mittels RNAseq und qRT-PCR beobachteten, so dass die Expression in der ältesten Patientengruppe (50-60 Jahre) in etwa halb so hoch, als in der jüngsten Gruppe (20-30 Jahre) war. Obgleich dieser Unterschied nicht signifikant war, könnte dies auf eine abnehmende Kontrolle der Virusaktivität mit zunehmendem Alter hinweisen. Klassischerweise wird die gegen EBV-gerichtete Immunantwort durch CD8+-T-Zellen getrieben, welche auch *in vitro* durch die Anwesenheit von LCLs in PBMC beobachtet werden kann (352). Cencioni *et al.* beobachteten eine Verminderung der zytotoxischen Aktivität dieser EBV-spezifischen CD8⁺-CD57⁺-T-Zellpopulation ausschließlich bei MS-Patient:innen mit stabilen, schubfreien Krankheitsverläufen. In diesem Zusammenhang könnte der von uns beobachtete Anstieg von EBNA-1 in LCL von Personen, die die letzten zwei Jahre keine Schübe hatten (vgl. zu 1-2 Schübe: 2-fach, $p < 0,01$), auf eine zunehmende lytische Virusaktivität des EBV, als auch auf eine möglicherweise verminderte Immunabwehr durch einen erschöpften T-Zell-Phänotyp in der stabilen Krankheitsphase der MS zurückzuführen sein. Es ist denkbar, dass ein vorangegangenes Schubereignis möglicherweise zur Erschöpfung der EBV-spezifischen T-Zellen beiträgt, wobei eine Erholung dieser Zellen nicht oder nur sehr langsam stattfindet, wodurch das EBV in der Zwischenzeit uneingeschränkt zirkulieren kann. Es wurde gezeigt, dass die Expansion EBV-infizierter Zellen *in vitro* durch IFN γ -produzierende CD8+-CD57+-T-Zellen gehemmt werden kann (356), was die Wiederherstellung der zytotoxischen Immunabwehr als therapeutisch wünschenswert erscheinen lässt. In Bezug darauf wurde beobachtet, dass die Erschöpfung EBV-spezifischer T-Zellen in Phasen ohne Krankheitsaktivität durch die Behandlung mit Glatirameracetat bei RRMS-Patient:tinnen z. T. reversibel war (357). Fraglich ist, inwiefern sich die Aktivierung EBV-spezifischer T-Zellen auf das generelle Entzündungsgeschehen in Patient:innen auswirken und ggf. die Schubrate beeinflussen würde. Diesbezüglich wurden in der genannten Arbeit von Guerrara *et al.* keine Anzeichen einer voranschreitenden Krankheitsaktivität in der Glatirameracetat-behandelten Patientengruppe (n = 35) festgestellt, wohingegen es bei ca. 20 % der unbehandelten RRMS-Patient:innen (8 von 39) zu Auffälligkeiten im MRT oder in der klinischen Darstellung im Beobachtungszeitraum von einem Jahr kam. Zudem deuten Phase-III-Studien darauf hin, dass sich die Behandlung mit Glatirameracetat (Handelsname: Copaxone®, Clift®) generell positiv auf die Schubrate auswirkt. So wurde über einen Zeitraum von zwei Jahren eine Schubraten-Reduktion in RRMS-Patient:innen gegenüber der Placebo-Gruppe (358), sowie eine Verlängerung des Zeitfensters vor einem erneuten Schubereignis beim klinisch isolierten Syndrom (engl.: *clinically isolated syndrome*, CIS) (359), welches sich häufig als erste schubartige Episode vor dem Übergang zu einer diagnostizierten MS manifestiert (360), beobachtet. Für die PPMS oder SPMS ist der Einsatz von Glatirameracetat nicht zugelassen, was ebenfalls auf seine spezifische Wirksamkeit in stabilen Krankheitsphasen und bei Patient:innen mit geringen neurologischen Einschränkungen hinweist.

Neben der Wiederherstellung der zytotoxischen Aktivität gegenüber EBV, ist die Eindämmung der EBV-Replikation als therapeutische Zielstellung potentiell relevant. In diesem Kontext ist das Immunsuppressivum Teriflunomid zu nennen, das in der Behandlung von RRMS (361, 362) und dem CIS (363) eingesetzt wird. Abseits der Hemmung der Zellproliferation mittels Blockierung der *de novo*-Synthese von Pyrimidinen, zeigte Teriflunomid eine antivirale „*off-target*“-Wirkung auf die Replikation diverser Viren (364-367). Für das EBV wurde eine Reduktion der detektierbaren DNA-Menge im Speichel von Patient:innen (368) nachgewiesen, als auch eine anti-proliferative Wirkung durch Überexpression des latenten Membranprotein 1 (LMP1), sowie die Aktivierung apoptotischer Signalwege durch den Tumorsuppressor p53 in EBV-immortalisierten B-Zellen *in vitro* beobachtet (367). Zudem wurde in einer spanischen Studie eine Abnahme der viralen Antikörpertiter nach 6-monatiger Behandlung mit Teriflunomid beobachtet, wobei insbesondere die Patient:innen mit den initial höchsten Anti-EBNA-1-Titern nach zwei Jahren gute klinische Verläufe ohne eine nachweisliche Krankheitsprogression, in Form von Schüben, Gadolinium-positiven- oder T2-Läsionen oder im Grad der körperlichen Einschränkungen, zeigten (369, 370). Hinsichtlich dieser Studienkohorte von ca. 100 RRMS-Patient:innen ist anzumerken, dass u.a. der durchschnittliche Grad an körperlichen Einschränkungen nach EDSS gering ($\bar{X} < 2$) war, sowie kaum Schübe ($\bar{X} = 1$) in den letzten zwei Jahren vor Studienbeginn verzeichnet wurden. Interessanterweise detektierten wir in unseren RRMS-Patient:innen mit den niedrigsten EDSS ($n = 6$) die höchste Expression an lytischem EBNA-1, wobei die Unterschiede um das 1,5 bis 2-Fache zu den Gruppen mit höheren EDSS (≥ 2) nicht signifikant waren. Aufgrund unserer vergleichbar kleinen Anzahl an Studienteilnehmenden von 32 RRMS-Patient:innen und den aktuell in Deutschland verfügbaren 18 Medikamenten zur Erkrankungs-modifizierenden Therapie (engl. *disease modifying therapy*, DMT) für die RRMS (371) konnte lediglich für die DMT mit Natalizumab ($n = 14$) eine statistisch sinnvolle Stichprobengröße erzielt werden.

Natalizumab, ein Integrin-Rezeptor-Antagonist, zählt zu den Präparaten, die gemessen an der Schubratenreduktion, zur höchsten Wirksamkeitskategorie gehören und wird im Normalfall bei Patient:innen mit ungünstigen Prognosefaktoren, wie einem hohen EDSS, neuen Hirnläsionen oder einer hohen Schubrate eingesetzt (371-373). Im Allgemeinen wird der Einsatz von DMTs für Personen mit einer neu-diagnostizierten RRMS stark diskutiert (374-376), auch weil Präparate der höchsten Wirksamkeitsstufe in der Vergangenheit vielversprechende Ergebnisse erzielten (377-380). Im Hinblick auf einen möglichen Einfluss auf die Aktivität des EBV konnte keine (381, 382) oder nur eine moderate Abnahme (383) der Antikörpertiter gegen EBV-Antigene beobachtet werden. Nichts desto trotz kann ein potentieller Zusammenhang nicht gänzlich ausgeschlossen werden, da ein Fall einer massiven letalen Krankheitsprogression nach Absetzen der Natalizumab-Behandlung bekannt ist, wobei eine hohe Frequenz an EBV-infizierten B-Zellen und EBV-assoziierten CD8⁺-T-Zellinfiltraten in intrazerebralen Hirnregionen und auch aktiven

Läsionsherden festgestellt wurde (384). Unsere Beobachtungen weisen nicht auf einen Rückgang der EBV-Aktivität in Natalizumab-behandelten Personen hin, da für die Expression von EBNA-2 keine Unterschiede und für das lytische Transkript des EBNA-1 sogar eine höhere Expression (2,35-fach, $p < 0,01$) verglichen zu unseren Patient:innen außerhalb einer DMT detektiert wurde. Hierbei ist unklar, ob die Expression von EBNA-1 in Folge der Natalizumab-Behandlung zunahm oder eine unvermindert hohe Aktivität der lytischen Phase des EBV seit Therapiebeginn bestand. Abschließend lassen unsere beobachteten Unterschiede der lytischen EBNA-1-Expression keinen konkreten Rückschluss auf eine prognostische Relevanz der untersuchten klinischen Parameter, wie Schubrate oder EDSS, zu. Hierzu wäre eine längerfristige Begleitung der Patient:innen vor, während und nach Abschluss der DMT notwendig. In Summe deuten die Beobachtungen jedoch stark auf eine mögliche Relevanz klinischer Parameter auf die Chancen eines Therapieerfolgs bzw. der Gefahr eines Therapieversagens bestimmter DMTs hin. Wie für Teriflunomid bereits dargelegt, korrelieren ein hoher anti-EBNA-1-IgG-Titer, sowie ein geringer Behinderungsgrad und ein nahezu schubfreier Krankheitsverlauf vor Therapiebeginn mit klinisch besseren Endresultaten. Eine ähnliche Schlussfolgerung bezüglich eines schubfreien Krankheitsverlaufs könnte für die erfolgreiche Wiederherstellung einer zytotoxischen EBV-spezifischen T-Zellpopulation mit Glatirameracetat bei RRMS getroffen werden. Zur Abwägung des Einsatzes von Natalizumab weist eine Studie darauf hin, dass (I) eine höhere Chance auf einen positiven Krankheitsverlauf für Personen besteht, die einen niedrigen EBNA-1-IgG-Titer und eine maximal mäßiggradige Einschränkung ohne Gehbehinderung (EDSS < 3) bei Behandlungsstart vorwiesen, sowie (II) ein prozentual höheres Therapieversagen bei initial hohen EBV-Antikörpertitern und einem EDSS über 3 (31,8 %) bzw. über 4 (60 %) zu befürchten sei (385).

4. Zusammenfassung und Ausblick

In den letzten 30 Jahren wurden die Expression von HERV-Transkripten und -Proteinen zunehmend im Zusammenhang der Pathogenese von Tumor- oder Autoimmunerkrankungen diskutiert. Jedoch ist die Identifizierung distinkter HERV-Loci mit diagnostischer oder therapeutischer Relevanz durch die genomische Verbreitung zahlreicher HERV-Kopien derselben Familie und größtenteils fehlender Annotationen in verfügbaren Versionen des menschlichen Genoms erschwert. Darüber hinaus ist weitestgehend unklar, inwieweit potentielle Transaktivatoren zur Überwindung der limitierten Proteinexpression nativer HERVs beitragen und welche intrazellulären Konsequenzen mit einer effizienten Translation einhergehen können.

Nachfolgend sind die wichtigsten Ergebnisse der für die Dissertation relevanten Publikationen zusammengefasst.

- I) In Publikation I wurde eine limitierte Expression drei nativer HERV ENV *in vitro* gezeigt, welche mittels einer Kodon-Optimierung der Sequenz deutlich gesteigert und alle ENV als glykosylierte Vorläuferproteine im Western Blot dargestellt werden konnten. Anzumerken ist, dass für die vollständige Glykosylierung des ENVs von HERV-K18 zudem die Rekonstruktion einer Signalpeptidsequenz notwendig war. Darüber hinaus war die Darstellung der Kodon-optimierten ENV ebenfalls mittels Immunfluoreszenz- und durchflusszytometrischer Analyse möglich, wobei wir eine Lokalisation im ER, sowie teilweise im Golgi-Apparat für das ENV von HERV-K113, beobachteten. Jedoch konnten wir keines der untersuchten ENV an der Zelloberfläche nachweisen. In Einklang mit der Akkumulation der überexprimierten ENV im ER, wurde die Induktion von Genen mittels qRT-PCR beobachtet, die im Zuge der Signaltransduktion durch fehlgefaltete Proteine im ER aktiviert werden. Unsere Ergebnisse deuten auf das Fehlen eines effizienten intrazellulären Transports hin, welche für HERV-K18 auf eine defekte Signalsequenz, sowie eine geringe Ausbeute an gespaltenem Vorläuferprotein, wie sie für das Kodon-optimierte ENV des HERV-K113 gezeigt wurde, zurückzuführen sein könnte. Neben der ineffizienten, zellulären Proteinsynthese beobachteten wir geringere Transkriptmengen für das native ENV von HERV-K113 im zellfreien Expressionssystem. Als mögliche Ursachen wurde auf eine höhere Stabilität der *in-silico* RNA-Sekundärstrukturmodelle aller nativen ENV-Sequenzen, sowie den Einfluss seltener Leucin-Triplets und die Relevanz eines dynamischen Pools an tRNA^{Leu(UUA)} auf die Translationseffizienz des ENVs von HERV-K113 hingewiesen.
- II) In Publikation II konnte der Nutzen des von uns etablierten „Virus-Metagenoms“ demonstriert werden. Auf Basis dieser Sammlung bekannter viraler Sequenzen, können zukünftig auch bereits bestehende RNA-Sequenzierungsdatensätze

vielfältiger Entitäten auf die Expression von insbesondere HERV-Sequenzen mit nahezu vollständigen Leserahmen untersucht werden. Dies trägt zur effizienteren Identifizierung potentiell diagnostisch oder therapeutisch relevanter HERV-Elemente bei, was bislang durch fehlende Annotationen in den herkömmlichen Genom-Versionen nicht gewährleistet werden konnte. Anhand von drei NB-Zelllinien konnte die Induktion der *ENVs* von ERV3-1 und HERV-Fc2, sowie HERV-E1- und HERV-K (HML-2)-Transkripten nach Kultivierung in Serum-depletiertem Stammzell-Medium nachgewiesen werden. Die Ko-Expression dieser distinkten HERVs korrelierte mit der Aktivierung bekannter NB-Malignitätsmarker, wie *MYC* oder *MYCN* und CD133, obwohl diese sehr heterogen in den untersuchten NB-Linien exprimiert waren. In Übereinstimmung dazu, konnte ausschließlich in SiMa-Zellen ein HERV-K/CD133-positiver Phänotyp beobachtet werden, der von einer morphologischen Veränderung der Zellen von locker anhaftenden Zellen zu schwach proliferierenden, traubenartigen Suspensionszellen, begleitet wurde. Zudem konnte eine Induktion des Immuncheckpunkt-Moleküls CD200 in Folge der Medium-induzierten Veränderung auf RNA- und auch Proteinebene mittels durchflusszytometrischer Analysen in allen NB-Zelllinien nachgewiesen werden. Unsere Beobachtungen könnten auf einen Mechanismus zur Steigerung der Immuntoleranz in der Tumorperipherie von NB hinweisen, wobei unklar ist, inwiefern CD200 die Expression der nachgewiesenen HERVs in einer Stammzell-fördernden Mikroumgebung begünstigen kann oder umgekehrt.

- III) Der Einfluss einer EBV-gesteuerten Proliferation auf die Genexpression in Personen mit MS und gesunden Kontrollen wurde in der dritten Publikation behandelt. Grundlegend wurden differenzielle Genexpressionsmuster in EBV-immortalisierten B-Zelllinien, sowie die Expression ausgewählter EBV-Transkripte und HERVs analysiert, da eine Re-Aktivierung von HERVs durch EBV als mögliches Bindeglied für die Pathogenese der MS diskutiert wird. Die EBV-vermittelte Immortalisierung der B-Zellen führte zu einer stärkeren Expression von lytischem EBNA-1, sowie EBNA-2 in MS-assoziierten LCL, wobei der Unterschied zu den Kontrollen innerhalb der weiblichen Studien-Kohorte deutlich ausgeprägter war und bezüglich der höheren Prädisposition von Frauen in der MS relevant sein könnte. Hinsichtlich der klinischen Parameter beobachteten wir eine höhere Expression von EBNA-1 in LCL von MS-Patient:innen mit schubfreien Verläufen in den letzten zwei Jahren, was auf eine verminderte Immunabwehr gegen die lytische Virusreplikation des EBV in der stabilen Krankheitsphase der MS hindeuten könnte. Eine hohe Expression des EBNA-1 wurde in MS-Patient:innen unter Natalizumab-Behandlung gegenüber Patient:innen außerhalb einer DMT festgestellt, wobei unklar ist, ob eine stärkere

Expression bereits vor Behandlungsbeginn vorlag bzw. Natalizumab einen Einfluss auf den lytischen Replikationszyklus des EBV hat. Eine längerfristige Begleitung der Patient:innen könnte nähere Rückschlüsse auf eine prognostische Relevanz der EBNA-1 Expression geben. Mit Hilfe unseres vorgestellten Virus-Transkriptoms konnten wir eine Induktion von HERV-K18 und sechs weiteren HERV-Loci in den LCLs über den BCR/CD40-Signalweg nachweisen. Trotz eines überwiegend homogenen Expressionsmusters innerhalb aller untersuchten LCLs waren ERVMER61-1, ERV3-1, sowie vier Mitglieder der HERV-K-Familie ausschließlich in MS-assoziierten LCL stärker exprimiert. Wir konnten keine signifikanten Unterschiede für die Expression der ENV von HERV-W1 oder MSR1 in unseren LCLs detektieren, was darauf hinweist, dass sie nicht zu den Loci gehören, die präferiert durch EBV transaktiviert werden. Eine mögliche Relevanz als diagnostischer Frühmarker erscheint aufgrund der höheren Frequenz auch in einigen unserer PBMCs von MS-Patient:innen zumindest plausibel. Im Hinblick auf weitere prädiktive Genexpressionsmuster wurde eine Gruppe von Genen beobachtet, die in mindestens einem Viertel aller MS-assoziierten LCLs exklusiv überexprimiert waren. Unter Berücksichtigung von LCL-Duplikaten je Person konnten 15 Gene identifiziert werden, die eine perfekte Unterscheidung unserer MS- und Kontrollgruppe zuließ. Hinsichtlich der Vorhersagekraft jeder einzelner Zelllinie wurden 52 von 59 der MS-assoziierten LCL, was in etwa 88 % entspricht, korrekt zugeordnet, wobei keine Kontrolle falsch positiv erkannt wurde. Analog dazu, wurde eine Gruppe von acht DEGs identifiziert, die mit dem Schub-Risiko innerhalb unserer MS-Patient:innen korrelierte und eine korrekte Zuordnung der LCLs von Patient:innen mit bzw. ohne Schübe in den letzten zwei Jahren erlaubte. Zur besseren Abschätzung der Relevanz dieser Auswahl an potentiell prädiktiven Genen sind weiterführende Studien mit verblindeten Testgruppen aus LCLs von MS-Patient:innen, Kontrollen, sowie anderen neurodegenerativen Erkrankungen notwendig.

Abschließend lässt sich sagen, dass im Rahmen der vorliegenden Arbeit die Expression von HERVs als potentiell diagnostisch und therapeutisch relevante Zielstrukturen untersucht wurde. Hierbei wurde die limitierte Proteinexpression ausgewählter HERV ENV *in vitro* gezeigt, sowie die Konsequenzen einer verbesserten Translation der nativen Sequenz, welche im Sinne der verwendeten Kodon-Optimierung imitiert wurde, auf die intrazelluläre Proteinreifung und -lokalisation untersucht. Zudem wurde ein von uns etabliertes, auf Sequenzierungsdaten-basierendes *Mapping*-Verfahren zur effizienteren Identifizierung exprimierter Transkripte viralen Ursprungs in RNA-Isolaten maligner und neurodegenerativer Entitäten demonstriert. So konnte in NB-Zelllinien eine Ko-Expression fünf distinkter HERV mit ORFs in Protein-kodierenden Bereichen, den NB-Malignitätsmarkern *MYC*, *MYCN* und *CD133*, sowie dem Immunchekpunkt-

Molekül CD200 unter einer Medium-induzierten Stammzell-fördernden Umgebung nachgewiesen werden. Mittels EBV-immortalisierter B-Zelllinien konnten eine ausschließlich in MS-assoziierten LCL stattfindende Induktion von ERVMER61-1, ERV3-1, sowie vier Mitgliedern der HERV-K-Familie nachgewiesen werden, wobei die Transaktivierung diverser HERV-Loci durch EBV über den BCR/CD40-Signalweg erfolgte. Zudem wurden Gen-Panel identifiziert, die mit der Expression bzw. dem Schub-Risiko in unseren MS-assoziierten LCLs korrelierten, wobei sich eine potentiell diagnostische Relevanz zukünftig erst beweisen muss.

Um einen Ausblick auf weiterführende Arbeiten zu geben, sind im Folgenden zwei Konzeptideen aufgeführt, die als Ausgangspunkte für zukünftige Projekte dienen könnten.

Um die pathologischen Konsequenzen der HERV-Expression in NB näher zu untersuchen, könnten mit Hilfe unseres Virus-Metagenoms differenzielle Expressionsanalysen von Tumorproben durchgeführt werden. Zur effizienten und Ressourcen-schonenden Umsetzung könnten hierzu bereits öffentlich verfügbare RNA-Sequenzierungsdatensätze der NCBI SRA-Datenbank, wie z. B. eine Sammlung von fast 100 NB-Tumoren (BioProject Nr.: PRJNA752570) aus einer publizierten Arbeit (386), genutzt werden. Anhand dieser Tumorproben wären Analysen hinsichtlich einer möglichen Korrelation differenziell exprimierter HERVs und klinisch relevanter Parameter wie dem Tumorgrad (1-4S), der Amplifikation von *MYCN* oder der Überlebensrate möglich. Darüber hinaus wäre von Interesse, ob ein direkter Zusammenhang für die Expression von CD200 und den nachgewiesenen HERVs im dargestellten NB-Zellmodell besteht. Unter Verwendung CD200-depletierter NB-Zellen könnte beispielsweise gezeigt werden, inwieweit eine Aktivierung der HERV-Loci nach Kultivierung in Serum-freien Stammzell-Medium erfolgen kann. Eine shRNA- bzw. siRNA- oder CRISPR/Cas9-vermittelte Depletion von CD200 wäre aufgrund der robusten Oberflächenexpression in den verwendeten NB-Zelllinien gut überprüfbar. Zudem könnte eine funktionelle Charakterisierung der molekularbiologischen Konsequenzen einer induzierten oder unterdrückten Expression von CD200 *in vitro* näheren Aufschluss zur Relevanz in der Pathogenese von NB geben. Beispielhaft seien hierzu Untersuchungen zum Proliferations- und Migrationsverhalten, sowie zur Resistenz gegenüber Chemotherapeutika genannt.

Ein weiterer denkbarer Ansatz wäre eine Ausweitung der Untersuchung zur EBV-vermittelten Proliferation in immortalisierten B-Zelllinien von MS-Patient:innen, um offene Fragen aus der im Rahmen der Arbeit durchgeführten explorativen Studie aufklären zu können. Zum einen könnte ein verblindetes Test-Set neu-etablierter LCLs von Patient:innen mit MS und anderen neurodegenerativen Erkrankungen, sowie Kontrollen näheren Aufschluss zur Aussagekraft unserer hier identifizierten Gen-Panel geben. Des Weiteren ist als größte Limitation der vorliegenden Arbeit die einmalige PBMC-Isolation und Etablierung von LCLs zu nennen, die insbesondere konkrete Rückschlüsse der detektierten EBV- und HERV-Aktivität auf

krankheitsrelevante Parameter erschweren. Beispielhaft würde eine längerfristige Begleitung von MS-Patient:innen inklusive PBMC-Isolation und LCL-Etablierung die Analyse der EBV- und HERV-Aktivität zu Zeitpunkten vor, während und nach Abschluss einer DMT oder Vitamin-D-Supplementierung zulassen. Möglicherweise könnten diese zukünftigen Erkenntnisse zur Optimierung einer individuell geeigneten Wahl der DMT für Patient:innen beitragen, wie sie hier bereits beispielhaft für den Einsatz von Glatirameracetat und Teriflunomid diskutiert wurden. Darüber hinaus wäre von Interesse, inwiefern die HERV-Aktivität während einer B-Zell-depletierenden Therapie oder einer Behandlung mit RT-inhibierenden Virustatika, z. B. Tenofovir (387), beeinflusst wird.

5. Literaturverzeichnis

- (1) Lander, E. S., Linton, L. M., Birren, B., Nusbaum, C., Zody, M. C., Baldwin, J., Devon, K., Dewar, K., Doyle, M., FitzHugh, W., Funke, R., Gage, D., Harris, K., Heaford, A., Howland, J., Kann, L., Lehoczy, J., LeVine, R., McEwan, P., McKernan, K., Meldrim, J., Mesirov, J. P., Miranda, C., Morris, W., Naylor, J., Raymond, C., Rosetti, M., Santos, R., Sheridan, A., Sougnez, C., Stange-Thomann, Y., Stojanovic, N., Subramanian, A., Wyman, D., Rogers, J., Sulston, J., Ainscough, R., Beck, S., Bentley, D., Burton, J., Clee, C., Carter, N., Coulson, A., Deadman, R., Deloukas, P., Dunham, A., Dunham, I., Durbin, R., French, L., Grafham, D., Gregory, S., Hubbard, T., Humphray, S., Hunt, A., Jones, M., Lloyd, C., McMurray, A., Matthews, L., Mercer, S., Milne, S., Mullikin, J. C., Mungall, A., Plumb, R., Ross, M., Shownkeen, R., Sims, S., Waterston, R. H., Wilson, R. K., Hillier, L. W., McPherson, J. D., Marra, M. A., Mardis, E. R., Fulton, L. A., Chinwalla, A. T., Pepin, K. H., Gish, W. R., Chissoe, S. L., Wendl, M. C., Delehaunty, K. D., Miner, T. L., Delehaunty, A., Kramer, J. B., Cook, L. L., Fulton, R. S., Johnson, D. L., Minx, P. J., Clifton, S. W., Hawkins, T., Branscomb, E., Predki, P., Richardson, P., Wenning, S., Slezak, T., Doggett, N., Cheng, J. F., Olsen, A., Lucas, S., Elkin, C., Uberbacher, E., Frazier, M., Gibbs, R. A., Muzny, D. M., Scherer, S. E., Bouck, J. B., Sodergren, E. J., Worley, K. C., Rives, C. M., Gorrell, J. H., Metzker, M. L., Naylor, S. L., Kucherlapati, R. S., Nelson, D. L., Weinstock, G. M., Sakaki, Y., Fujiyama, A., Hattori, M., Yada, T., Toyoda, A., Itoh, T., Kawagoe, C., Watanabe, H., Totoki, Y., Taylor, T., Weissenbach, J., Heilig, R., Saurin, W., Artiguenave, F., Brottier, P., Bruls, T., Pelletier, E., Robert, C., Wincker, P., Smith, D. R., Doucette-Stamm, L., Rubenfield, M., Weinstock, K., Lee, H. M., Dubois, J., Rosenthal, A., Platzer, M., Nyakatura, G., Taudien, S., Rump, A., Yang, H., Yu, J., Wang, J., Huang, G., Gu, J., Hood, L., Rowen, L., Madan, A., Qin, S., Davis, R. W., Federspiel, N. A., Abola, A. P., Proctor, M. J., Myers, R. M., Schmutz, J., Dickson, M., Grimwood, J., Cox, D. R., Olson, M. V., Kaul, R., Raymond, C., Shimizu, N., Kawasaki, K., Minoshima, S., Evans, G. A., Athanasiou, M., Schultz, R., Roe, B. A., Chen, F., Pan, H., Ramser, J., Lehrach, H., Reinhardt, R., McCombie, W. R., de la Bastide, M., Dedhia, N., Blöcker, H., Hornischer, K., Nordsiek, G., Agarwala, R., Aravind, L., Bailey, J. A., Bateman, A., Batzoglu, S., Birney, E., Bork, P., Brown, D. G., Burge, C. B., Cerutti, L., Chen, H. C., Church, D., Clamp, M., Copley, R. R., Doerks, T., Eddy, S. R., Eichler, E. E., Furey, T. S., Galagan, J., Gilbert, J. G., Harmon, C., Hayashizaki, Y., Haussler, D., Hermjakob, H., Hokamp, K., Jang, W., Johnson, L. S., Jones, T. A., Kasif, S., Kasprzyk, A., Kennedy, S., Kent, W. J., Kitts, P., Koonin, E. V., Korf, I., Kulp, D., Lancet, D., Lowe, T. M., McLysaght, A., Mikkelsen, T., Moran, J. V., Mulder, N., Pollara, V. J., Ponting, C. P., Schuler, G., Schultz, J., Slater, G., Smit, A. F., Stupka, E., Szustakowki, J., Thierry-Mieg, D., Thierry-Mieg, J., Wagner, L., Wallis, J., Wheeler, R., Williams, A., Wolf, Y. I., Wolfe, K. H., Yang, S. P., Yeh, R. F., Collins, F., Guyer, M. S., Peterson, J., Felsenfeld, A.,

- Wetterstrand, K. A., Patrinos, A., Morgan, M. J., de Jong, P., Catanese, J. J., Osoegawa, K., Shizuya, H., Choi, S., Chen, Y. J., Szustakowki, J., & International Human Genome Sequencing Consortium (2001). Initial sequencing and analysis of the human genome. *Nature*, 409(6822), 860–921. <https://doi.org/10.1038/35057062>
- (2) Chakravarti A. (2001). To a future of genetic medicine. *Nature*, 409(6822), 822–823. <https://doi.org/10.1038/35057281>
- (3) Zuckerkandl E. (2002). Why so many noncoding nucleotides? The eukaryote genome as an epigenetic machine. *Genetica*, 115(1), 105–129. <https://doi.org/10.1023/a:1016080316076>
- (4) Ling, H., Vincent, K., Pichler, M., Fodde, R., Berindan-Neagoe, I., Slack, F. J., & Calin, G. A. (2015). Junk DNA and the long non-coding RNA twist in cancer genetics. *Oncogene*, 34(39), 5003–5011. <https://doi.org/10.1038/onc.2014.456>
- (5) Palazzo, A. F., & Koonin, E. V. (2020). Functional Long Non-coding RNAs Evolve from Junk Transcripts. *Cell*, 183(5), 1151–1161. <https://doi.org/10.1016/j.cell.2020.09.047>
- (6) Venter, J. C., Adams, M. D., Myers, E. W., Li, P. W., Mural, R. J., Sutton, G. G., Smith, H. O., Yandell, M., Evans, C. A., Holt, R. A., Gocayne, J. D., Amanatides, P., Ballew, R. M., Huson, D. H., Wortman, J. R., Zhang, Q., Kodira, C. D., Zheng, X. H., Chen, L., Skupski, M., Subramanian, G., Thomas, P. D., Zhang, J., Gabor Miklos, G. L., Nelson, C., Broder, S., Clark, A. G., Nadeau, J., McKusick, V. A., Zinder, N., Levine, A. J., Roberts, R. J., Simon, M., Slayman, C., Hunkapiller, M., Bolanos, R., Delcher, A., Dew, I., Fasulo, D., Flanigan, M., Florea, L., Halpern, A., Hannenhalli, S., Kravitz, S., Levy, S., Mobarry, C., Reinert, K., Remington, K., Abu-Threideh, J., Beasley, E., Biddick, K., Bonazzi, V., Brandon, R., Cargill, M., Chandramouliswaran, I., Charlab, R., Chaturvedi, K., Deng, Z., Di Francesco, V., Dunn, P., Eilbeck, K., Evangelista, C., Gabrielian, A. E., Gan, W., Ge, W., Gong, F., Gu, Z., Guan, P., Heiman, T. J., Higgins, M. E., Ji, R. R., Ke, Z., Ketchum, K. A., Lai, Z., Lei, Y., Li, Z., Li, J., Liang, Y., Lin, X., Lu, F., Merkulov, G. V., Milshina, N., Moore, H. M., Naik, A. K., Narayan, V. A., Neelam, B., Nuskern, D., Rusch, D. B., Salzberg, S., Shao, W., Shue, B., Sun, J., Wang, Z., Wang, A., Wang, X., Wang, J., Wei, M., Wides, R., Xiao, C., Yan, C., Yao, A., Ye, J., Zhan, M., Zhang, W., Zhang, H., Zhao, Q., Zheng, L., Zhong, F., Zhong, W., Zhu, S., Zhao, S., Gilbert, D., Baumhueter, S., Spier, G., Carter, C., Cravchik, A., Woodage, T., Ali, F., An, H., Awe, A., Baldwin, D., Baden, H., Barnstead, M., Barrow, I., Beeson, K., Busam, D., Carver, A., Center, A., Cheng, M. L., Curry, L., Danaher, S., Davenport, L., Desilets, R., Dietz, S., Dodson, K., Doup, L., Ferriera, S., Garg, N., Gluecksmann, A., Hart, B., Haynes, J., Haynes, C., Heiner, C., Hladun, S., Hostin, D., Houck, J., Howland, T., Ibegwam, C., Johnson, J., Kalush, F., Kline, L., Koduru, S., Love, A., Mann, F., May, D., McCawley, S., McIntosh, T., McMullen, I., Moy, M., Moy, L., Murphy, B., Nelson, K., Pfannkoch, C., Pratts, E., Puri, V., Qureshi, H., Reardon, M., Rodriguez, R., Rogers, Y. H., Romblad, D., Ruhfel, B., Scott, R., Sitter, C., Smallwood, M., Stewart, E., Strong, R., Suh,

- E., Thomas, R., Tint, N. N., Tse, S., Vech, C., Wang, G., Wetter, J., Williams, S., Williams, M., Windsor, S., Winn-Deen, E., Wolfe, K., Zaveri, J., Zaveri, K., Abril, J. F., Guigó, R., Campbell, M. J., Sjolander, K. V., Karlak, B., Kejariwal, A., Mi, H., Lazareva, B., Hatton, T., Narechania, A., Diemer, K., Muruganujan, A., Guo, N., Sato, S., Bafna, V., Istrail, S., Lippert, R., Schwartz, R., Walenz, B., Yooseph, S., Allen, D., Basu, A., Baxendale, J., Blick, L., Caminha, M., Cames-Stine, J., Caulk, P., Chiang, Y. H., Coyne, M., Dahlke, C., Deslattes Mays, A., Dombroski, M., Donnelly, M., Ely, D., Esparham, S., Fosler, C., Gire, H., Glanowski, S., Glasser, K., Glodek, A., Gorokhov, M., Graham, K., Gropman, B., Harris, M., Heil, J., Henderson, S., Hoover, J., Jennings, D., Jordan, C., Jordan, J., Kasha, J., Kagan, L., Kraft, C., Levitsky, A., Lewis, M., Liu, X., Lopez, J., Ma, D., Majoros, W., McDaniel, J., Murphy, S., Newman, M., Nguyen, T., Nguyen, N., Nodell, M., Pan, S., Peck, J., Peterson, M., Rowe, W., Sanders, R., Scott, J., Simpson, M., Smith, T., Sprague, A., Stockwell, T., Turner, R., Venter, E., Wang, M., Wen, M., Wu, D., Wu, M., Xia, A., Zandieh, A., Zhu, X. (2001). The sequence of the human genome. *Science (New York, N.Y.)*, 291(5507), 1304–1351. <https://doi.org/10.1126/science.1058040>
- (7) McClintock, B. (1956). Controlling elements and the gene. *Cold Spring Harbor symposia on quantitative biology*, 21, 197–216. <https://doi.org/10.1101/sqb.1956.021.01.017>
- (8) Finnegan D. J. (1989). Eukaryotic transposable elements and genome evolution. *Trends in genetics : TIG*, 5(4), 103–107. [https://doi.org/10.1016/0168-9525\(89\)90039-5](https://doi.org/10.1016/0168-9525(89)90039-5)
- (9) Wells, J. N., & Feschotte, C. (2020). A Field Guide to Eukaryotic Transposable Elements. *Annual review of genetics*, 54, 539–561. <https://doi.org/10.1146/annurev-genet-040620-022145>
- (10) Wicker, T., Sabot, F., Hua-Van, A., Bennetzen, J. L., Capy, P., Chalhoub, B., Flavell, A., Leroy, P., Morgante, M., Panaud, O., Paux, E., SanMiguel, P., & Schulman, A. H. (2007). A unified classification system for eukaryotic transposable elements. *Nature reviews. Genetics*, 8(12), 973–982. <https://doi.org/10.1038/nrg2165>
- (11) Piégu, B., Bire, S., Arensburger, P., & Bigot, Y. (2015). A survey of transposable element classification systems--a call for a fundamental update to meet the challenge of their diversity and complexity. *Molecular phylogenetics and evolution*, 86, 90–109. <https://doi.org/10.1016/j.ympev.2015.03.009>
- (12) Cordaux, R., & Batzer, M. A. (2009). The impact of retrotransposons on human genome evolution. *Nature reviews. Genetics*, 10(10), 691–703. <https://doi.org/10.1038/nrg2640>
- (13) Belancio, V. P., Hedges, D. J., & Deininger, P. (2008). Mammalian non-LTR retrotransposons: for better or worse, in sickness and in health. *Genome research*, 18(3), 343–358. <https://doi.org/10.1101/gr.5558208>
- (14) Belshaw, R., Pereira, V., Katzourakis, A., Talbot, G., Paces, J., Burt, A., & Tristem, M. (2004). Long-term reinfection of the human genome by endogenous retroviruses.

- Proceedings of the National Academy of Sciences of the United States of America*, 101(14), 4894–4899. <https://doi.org/10.1073/pnas.0307800101>
- (15) Lindemann, D., Steffen, I., & Pöhlmann, S. (2013). Cellular entry of retroviruses. *Advances in experimental medicine and biology*, 790, 128–149. https://doi.org/10.1007/978-1-4614-7651-1_7
- (16) Grandi, N., & Tramontano, E. (2018). HERV Envelope Proteins: Physiological Role and Pathogenic Potential in Cancer and Autoimmunity. *Frontiers in microbiology*, 9, 462. <https://doi.org/10.3389/fmicb.2018.00462>
- (17) Grandi, N., Cadeddu, M., Blomberg, J., & Tramontano, E. (2016). Contribution of type W human endogenous retroviruses to the human genome: characterization of HERV-W proviral insertions and processed pseudogenes. *Retrovirology*, 13(1), 67. <https://doi.org/10.1186/s12977-016-0301-x>
- (18) Bannert, N., & Kurth, R. (2004). Retroelements and the human genome: new perspectives on an old relation. *Proceedings of the National Academy of Sciences of the United States of America*, 101 Suppl 2(Suppl 2), 14572–14579. <https://doi.org/10.1073/pnas.0404838101>
- (19) Mayer, J., Blomberg, J., & Seal, R. L. (2011). A revised nomenclature for transcribed human endogenous retroviral loci. *Mobile DNA*, 2(1), 7. <https://doi.org/10.1186/1759-8753-2-7>
- (20) Gifford, R. J., Blomberg, J., Coffin, J. M., Fan, H., Heidmann, T., Mayer, J., Stoye, J., Tristem, M., & Johnson, W. E. (2018). Nomenclature for endogenous retrovirus (ERV) loci. *Retrovirology*, 15(1), 59. <https://doi.org/10.1186/s12977-018-0442-1>
- (21) Hanke, K., Hohn, O., & Bannert, N. (2016). HERV-K(HML-2), a seemingly silent subtenant - but still waters run deep. *APMIS : acta pathologica, microbiologica, et immunologica Scandinavica*, 124(1-2), 67–87. <https://doi.org/10.1111/apm.12475>
- (22) de Parseval, N., & Heidmann, T. (2005). Human endogenous retroviruses: from infectious elements to human genes. *Cytogenetic and genome research*, 110(1-4), 318–332. <https://doi.org/10.1159/000084964>
- (23) Young, G. R., Stoye, J. P., & Kassiotis, G. (2013). Are human endogenous retroviruses pathogenic? An approach to testing the hypothesis. *BioEssays : news and reviews in molecular, cellular and developmental biology*, 35(9), 794–803. <https://doi.org/10.1002/bies.201300049>
- (24) Jansz, N., & Faulkner, G. J. (2021). Endogenous retroviruses in the origins and treatment of cancer. *Genome biology*, 22(1), 147. <https://doi.org/10.1186/s13059-021-02357-4>
- (25) Nelson, P. N., Hooley, P., Roden, D., Davari Ejtehadi, H., Rylance, P., Warren, P., Martin, J., Murray, P. G., & Molecular Immunology Research Group (2004). Human endogenous retroviruses: transposable elements with potential?. *Clinical and experimental immunology*, 138(1), 1–9. <https://doi.org/10.1111/j.1365-2249.2004.02592.x>

- (26) Rowe, H. M., & Trono, D. (2011). Dynamic control of endogenous retroviruses during development. *Virology*, *411*(2), 273–287. <https://doi.org/10.1016/j.virol.2010.12.007>
- (27) Hurst, T. P., & Magiorkinis, G. (2017). Epigenetic Control of Human Endogenous Retrovirus Expression: Focus on Regulation of Long-Terminal Repeats (LTRs). *Viruses*, *9*(6), 130. <https://doi.org/10.3390/v9060130>
- (28) Hendrich, B., & Bird, A. (1998). Identification and characterization of a family of mammalian methyl-CpG binding proteins. *Molecular and cellular biology*, *18*(11), 6538–6547. <https://doi.org/10.1128/MCB.18.11.6538>
- (29) Matsui, T., Leung, D., Miyashita, H., Maksakova, I. A., Miyachi, H., Kimura, H., Tachibana, M., Lorincz, M. C., & Shinkai, Y. (2010). Proviral silencing in embryonic stem cells requires the histone methyltransferase ESET. *Nature*, *464*(7290), 927–931. <https://doi.org/10.1038/nature08858>
- (30) Wolf, D., & Goff, S. P. (2007). TRIM28 mediates primer binding site-targeted silencing of murine leukemia virus in embryonic cells. *Cell*, *131*(1), 46–57. <https://doi.org/10.1016/j.cell.2007.07.026>
- (31) Wolf, D., & Goff, S. P. (2009). Embryonic stem cells use ZFP809 to silence retroviral DNAs. *Nature*, *458*(7242), 1201–1204. <https://doi.org/10.1038/nature07844>
- (32) Rowe, H. M., Friedli, M., Offner, S., Verp, S., Mesnard, D., Marquis, J., Aktas, T., & Trono, D. (2013). De novo DNA methylation of endogenous retroviruses is shaped by KRAB-ZFPs/KAP1 and ESET. *Development (Cambridge, England)*, *140*(3), 519–529. <https://doi.org/10.1242/dev.087585>
- (33) Geis, F. K., & Goff, S. P. (2020). Silencing and Transcriptional Regulation of Endogenous Retroviruses: An Overview. *Viruses*, *12*(8), 884. <https://doi.org/10.3390/v12080884>
- (34) Karimi, M. M., Goyal, P., Maksakova, I. A., Bilenky, M., Leung, D., Tang, J. X., Shinkai, Y., Mager, D. L., Jones, S., Hirst, M., & Lorincz, M. C. (2011). DNA methylation and SETDB1/H3K9me3 regulate predominantly distinct sets of genes, retroelements, and chimeric transcripts in mESCs. *Cell stem cell*, *8*(6), 676–687. <https://doi.org/10.1016/j.stem.2011.04.004>
- (35) Liu, S., Brind'Amour, J., Karimi, M. M., Shirane, K., Bogutz, A., Lefebvre, L., Sasaki, H., Shinkai, Y., & Lorincz, M. C. (2014). Setdb1 is required for germline development and silencing of H3K9me3-marked endogenous retroviruses in primordial germ cells. *Genes & development*, *28*(18), 2041–2055. <https://doi.org/10.1101/gad.244848.114>
- (36) Rowe, H. M., Jakobsson, J., Mesnard, D., Rougemont, J., Reynard, S., Aktas, T., Maillard, P. V., Layard-Liesching, H., Verp, S., Marquis, J., Spitz, F., Constam, D. B., & Trono, D. (2010). KAP1 controls endogenous retroviruses in embryonic stem cells. *Nature*, *463*(7278), 237–240. <https://doi.org/10.1038/nature08674>

- (37) Kraus, B., Mönk, B., Sliva, K., & Schnierle, B. S. (2012). Expression of human endogenous retrovirus-K coincides with that of micro-RNA-663 and -638 in germ-cell tumor cells. *Anticancer research*, 32(11), 4797–4804.
- (38) Hakim, S. T., Alsayari, M., McLean, D. C., Saleem, S., Addanki, K. C., Aggarwal, M., Mahalingam, K., & Bagasra, O. (2008). A large number of the human microRNAs target lentiviruses, retroviruses, and endogenous retroviruses. *Biochemical and biophysical research communications*, 369(2), 357–362. <https://doi.org/10.1016/j.bbrc.2008.02.025>
- (39) Iwasaki, Y. W., Siomi, M. C., & Siomi, H. (2015). PIWI-Interacting RNA: Its Biogenesis and Functions. *Annual review of biochemistry*, 84, 405–433. <https://doi.org/10.1146/annurev-biochem-060614-034258>
- (40) Peng, J. C., & Lin, H. (2013). Beyond transposons: the epigenetic and somatic functions of the Piwi-piRNA mechanism. *Current opinion in cell biology*, 25(2), 190–194. <https://doi.org/10.1016/j.ceb.2013.01.010>
- (41) Zheng, Y. H., Jeang, K. T., & Tokunaga, K. (2012). Host restriction factors in retroviral infection: promises in virus-host interaction. *Retrovirology*, 9, 112. <https://doi.org/10.1186/1742-4690-9-112>
- (42) Refsland, E. W., & Harris, R. S. (2013). The APOBEC3 family of retroelement restriction factors. *Current topics in microbiology and immunology*, 371, 1–27. https://doi.org/10.1007/978-3-642-37765-5_1
- (43) Bishop, K. N., Holmes, R. K., & Malim, M. H. (2006). Antiviral potency of APOBEC proteins does not correlate with cytidine deamination. *Journal of virology*, 80(17), 8450–8458. <https://doi.org/10.1128/JVI.00839-06>
- (44) Bishop, K. N., Verma, M., Kim, E. Y., Wolinsky, S. M., & Malim, M. H. (2008). APOBEC3G inhibits elongation of HIV-1 reverse transcripts. *PLoS pathogens*, 4(12), e1000231. <https://doi.org/10.1371/journal.ppat.1000231>
- (45) Lee, Y. N., Malim, M. H., & Bieniasz, P. D. (2008). Hypermutation of an ancient human retrovirus by APOBEC3G. *Journal of virology*, 82(17), 8762–8770. <https://doi.org/10.1128/JVI.00751-08>
- (46) Bhardwaj, N., Montesion, M., Roy, F., & Coffin, J. M. (2015). Differential expression of HERV-K (HML-2) proviruses in cells and virions of the teratocarcinoma cell line Tera-1. *Viruses*, 7(3), 939–968. <https://doi.org/10.3390/v7030939>
- (47) Chertova, E., Chertov, O., Coren, L. V., Roser, J. D., Trubey, C. M., Bess, J. W., Jr, Sowder, R. C., 2nd, Barsov, E., Hood, B. L., Fisher, R. J., Nagashima, K., Conrads, T. P., Veenstra, T. D., Lifson, J. D., & Ott, D. E. (2006). Proteomic and biochemical analysis of purified human immunodeficiency virus type 1 produced from infected monocyte-derived macrophages. *Journal of virology*, 80(18), 9039–9052. <https://doi.org/10.1128/JVI.01013-06>

- (48) Burdick, R., Smith, J. L., Chaipan, C., Friew, Y., Chen, J., Venkatachari, N. J., Delviks-Frankenberry, K. A., Hu, W. S., & Pathak, V. K. (2010). P body-associated protein Mov10 inhibits HIV-1 replication at multiple stages. *Journal of virology*, *84*(19), 10241–10253. <https://doi.org/10.1128/JVI.00585-10>
- (49) Furtak, V., Mulky, A., Rawlings, S. A., Kozhaya, L., Lee, K., Kewalramani, V. N., & Unutmaz, D. (2010). Perturbation of the P-body component Mov10 inhibits HIV-1 infectivity. *PloS one*, *5*(2), e9081. <https://doi.org/10.1371/journal.pone.0009081>
- (50) Arjan-Odedra, S., Swanson, C. M., Sherer, N. M., Wolinsky, S. M., & Malim, M. H. (2012). Endogenous MOV10 inhibits the retrotransposition of endogenous retroelements but not the replication of exogenous retroviruses. *Retrovirology*, *9*, 53. <https://doi.org/10.1186/1742-4690-9-53>
- (51) Limjoco, T. I., Dickie, P., Ikeda, H., & Silver, J. (1993). Transgenic Fv-4 mice resistant to Friend virus. *Journal of virology*, *67*(7), 4163–4168. <https://doi.org/10.1128/JVI.67.7.4163-4168.1993>
- (52) Armezzani, A., Varela, M., Spencer, T. E., Palmarini, M., & Arnaud, F. (2014). "Ménage à Trois": the evolutionary interplay between JSRV, enJSRVs and domestic sheep. *Viruses*, *6*(12), 4926–4945. <https://doi.org/10.3390/v6124926>
- (53) Rolland, A., Jouvin-Marche, E., Viret, C., Faure, M., Perron, H., & Marche, P. N. (2006). The envelope protein of a human endogenous retrovirus-W family activates innate immunity through CD14/TLR4 and promotes Th1-like responses. *Journal of immunology (Baltimore, Md. : 1950)*, *176*(12), 7636–7644. <https://doi.org/10.4049/jimmunol.176.12.7636>
- (54) Kim, H., Yang, E., Lee, J., Kim, S. H., Shin, J. S., Park, J. Y., Choi, S. J., Kim, S. J., & Choi, I. H. (2008). Double-stranded RNA mediates interferon regulatory factor 3 activation and interleukin-6 production by engaging Toll-like receptor 3 in human brain astrocytes. *Immunology*, *124*(4), 480–488. <https://doi.org/10.1111/j.1365-2567.2007.02799.x>
- (55) Kremer, D., Schichel, T., Förster, M., Tzekova, N., Bernard, C., van der Valk, P., van Horssen, J., Hartung, H. P., Perron, H., & Küry, P. (2013). Human endogenous retrovirus type W envelope protein inhibits oligodendroglial precursor cell differentiation. *Annals of neurology*, *74*(5), 721–732. <https://doi.org/10.1002/ana.23970>
- (56) Zhou, Y., Wang, X., Liu, M., Hu, Q., Song, L., Ye, L., Zhou, D., & Ho, W. (2010). A critical function of toll-like receptor-3 in the induction of anti-human immunodeficiency virus activities in macrophages. *Immunology*, *131*(1), 40–49. <https://doi.org/10.1111/j.1365-2567.2010.03270.x>
- (57) Lester, S. N., & Li, K. (2014). Toll-like receptors in antiviral innate immunity. *Journal of molecular biology*, *426*(6), 1246–1264. <https://doi.org/10.1016/j.jmb.2013.11.024>
- (58) Garrison, K. E., Jones, R. B., Meiklejohn, D. A., Anwar, N., Ndhlovu, L. C., Chapman, J. M., Erickson, A. L., Agrawal, A., Spotts, G., Hecht, F. M., Rakoff-Nahoum, S., Lenz, J.,

- Ostrowski, M. A., & Nixon, D. F. (2007). T cell responses to human endogenous retroviruses in HIV-1 infection. *PLoS pathogens*, 3(11), e165. <https://doi.org/10.1371/journal.ppat.0030165>
- (59) Jones, R. B., Garrison, K. E., Mujib, S., Mihajlovic, V., Aidarus, N., Hunter, D. V., Martin, E., John, V. M., Zhan, W., Faruk, N. F., Gyenes, G., Sheppard, N. C., Priumboom-Brees, I. M., Goodwin, D. A., Chen, L., Rieger, M., Muscat-King, S., Loudon, P. T., Stanley, C., Holditch, S. J., Wong, J. C., Clayton, K., Duan, E., Song, H., Xu, Y., SenGupta, D., Tandon, R., Sacha, J. B., Brockman, M. A., Benko, E., Kovacs, C., Nixon, D. F., & Ostrowski, M. A. (2012). HERV-K-specific T cells eliminate diverse HIV-1/2 and SIV primary isolates. *The Journal of clinical investigation*, 122(12), 4473–4489. <https://doi.org/10.1172/JCI64560>
- (60) Michaud, H. A., de Mulder, M., SenGupta, D., Deeks, S. G., Martin, J. N., Pilcher, C. D., Hecht, F. M., Sacha, J. B., & Nixon, D. F. (2014). Trans-activation, post-transcriptional maturation, and induction of antibodies to HERV-K (HML-2) envelope transmembrane protein in HIV-1 infection. *Retrovirology*, 11, 10. <https://doi.org/10.1186/1742-4690-11-10>
- (61) Monde, K., Terasawa, H., Nakano, Y., Soheilian, F., Nagashima, K., Maeda, Y., & Ono, A. (2017). Molecular mechanisms by which HERV-K Gag interferes with HIV-1 Gag assembly and particle infectivity. *Retrovirology*, 14(1), 27. <https://doi.org/10.1186/s12977-017-0351-8>
- (62) Mantovani, F., Kitsou, K., & Magiorkinis, G. (2024). HERVs: Expression Control Mechanisms and Interactions in Diseases and Human Immunodeficiency Virus Infection. *Genes*, 15(2), 192. <https://doi.org/10.3390/genes15020192>
- (63) Contreras-Galindo, R., Kaplan, M. H., Contreras-Galindo, A. C., Gonzalez-Hernandez, M. J., Ferlenghi, I., Giusti, F., Lorenzo, E., Gitlin, S. D., Dosik, M. H., Yamamura, Y., & Markovitz, D. M. (2012). Characterization of human endogenous retroviral elements in the blood of HIV-1-infected individuals. *Journal of virology*, 86(1), 262–276. <https://doi.org/10.1128/JVI.00602-11>
- (64) Young, G. R., Terry, S. N., Manganaro, L., Cuesta-Dominguez, A., Deikus, G., Bernal-Rubio, D., Campisi, L., Fernandez-Sesma, A., Sebra, R., Simon, V., & Mulder, L. C. F. (2017). HIV-1 Infection of Primary CD4+ T Cells Regulates the Expression of Specific Human Endogenous Retrovirus HERV-K (HML-2) Elements. *Journal of virology*, 92(1), e01507-17. <https://doi.org/10.1128/JVI.01507-17>
- (65) Gonzalez-Hernandez, M. J., Swanson, M. D., Contreras-Galindo, R., Cookinham, S., King, S. R., Noel, R. J., Jr, Kaplan, M. H., & Markovitz, D. M. (2012). Expression of human endogenous retrovirus type K (HML-2) is activated by the Tat protein of HIV-1. *Journal of virology*, 86(15), 7790–7805. <https://doi.org/10.1128/JVI.07215-11>
- (66) O'Carroll, I. P., Fan, L., Kroupa, T., McShane, E. K., Theodore, C., Yates, E. A., Kondrup, B., Ding, J., Martin, T. S., Rein, A., & Wang, Y. X. (2020). Structural Mimicry Drives HIV-

- 1 Rev-Mediated HERV-K Expression. *Journal of molecular biology*, 432(24), 166711. <https://doi.org/10.1016/j.jmb.2020.11.010>
- (67) Russ, E., & Iordanskiy, S. (2023). Endogenous Retroviruses as Modulators of Innate Immunity. *Pathogens (Basel, Switzerland)*, 12(2), 162. <https://doi.org/10.3390/pathogens12020162>
- (68) Ruda, V. M., Akopov, S. B., Trubetskoy, D. O., Manuylov, N. L., Vetchinova, A. S., Zavalova, L. L., Nikolaev, L. G., & Sverdlov, E. D. (2004). Tissue specificity of enhancer and promoter activities of a HERV-K(HML-2) LTR. *Virus research*, 104(1), 11–16. <https://doi.org/10.1016/j.virusres.2004.02.036>
- (69) Chuong, E. B., Elde, N. C., & Feschotte, C. (2016). Regulatory evolution of innate immunity through co-option of endogenous retroviruses. *Science (New York, N.Y.)*, 351(6277), 1083–1087. <https://doi.org/10.1126/science.aad5497>
- (70) Laviaille, C., Cornelis, G., Dupressoir, A., Esnault, C., Heidmann, O., Vernochet, C., & Heidmann, T. (2013). Paleovirology of 'syncytins', retroviral env genes exapted for a role in placentation. *Philosophical transactions of the Royal Society of London. Series B, Biological sciences*, 368(1626), 20120507. <https://doi.org/10.1098/rstb.2012.0507>
- (71) Dupressoir, A., Laviaille, C., & Heidmann, T. (2012). From ancestral infectious retroviruses to bona fide cellular genes: role of the captured syncytins in placentation. *Placenta*, 33(9), 663–671. <https://doi.org/10.1016/j.placenta.2012.05.005>
- (72) Roberts, R. M., Ezashi, T., Schulz, L. C., Sugimoto, J., Schust, D. J., Khan, T., & Zhou, J. (2021). Syncytins expressed in human placental trophoblast. *Placenta*, 113, 8–14. <https://doi.org/10.1016/j.placenta.2021.01.006>
- (73) Lv, H., Han, J., Liu, J., Zheng, J., Zhong, D., & Liu, R. (2014). ISDTool 2.0: a computational model for predicting immunosuppressive domain of retroviruses. *Journal of theoretical biology*, 360, 78–82. <https://doi.org/10.1016/j.jtbi.2014.06.033>
- (74) Denner J. (2016). Expression and function of endogenous retroviruses in the placenta. *APMIS : acta pathologica, microbiologica, et immunologica Scandinavica*, 124(1-2), 31–43. <https://doi.org/10.1111/apm.12474>
- (75) Cianciolo, G. J., Copeland, T. D., Oroszlan, S., & Snyderman, R. (1985). Inhibition of lymphocyte proliferation by a synthetic peptide homologous to retroviral envelope proteins. *Science (New York, N.Y.)*, 230(4724), 453–455. <https://doi.org/10.1126/science.2996136>
- (76) Haraguchi, S., Good, R. A., James-Yarish, M., Cianciolo, G. J., & Day, N. K. (1995). Differential modulation of Th1- and Th2-related cytokine mRNA expression by a synthetic peptide homologous to a conserved domain within retroviral envelope protein. *Proceedings of the National Academy of Sciences of the United States of America*, 92(8), 3611–3615. <https://doi.org/10.1073/pnas.92.8.3611>

- (77) Nelson, M., Nelson, D. S., Cianciolo, G. J., & Snyderman, R. (1989). Effects of CKS-17, a synthetic retroviral envelope peptide, on cell-mediated immunity in vivo: immunosuppression, immunogenicity, and relation to immunosuppressive tumor products. *Cancer immunology, immunotherapy* : *CII*, 30(2), 113–118. <https://doi.org/10.1007/BF01665962>
- (78) Cianciolo, G. J., & Pizzo, S. V. (2012). Anti-inflammatory and vasoprotective activity of a retroviral-derived peptide, homologous to human endogenous retroviruses: endothelial cell effects. *PloS one*, 7(12), e52693. <https://doi.org/10.1371/journal.pone.0052693>
- (79) Mangeney, M., Renard, M., Schlecht-Louf, G., Bouallaga, I., Heidmann, O., Letzelter, C., Richaud, A., Ducos, B., & Heidmann, T. (2007). Placental syncytins: Genetic disjunction between the fusogenic and immunosuppressive activity of retroviral envelope proteins. *Proceedings of the National Academy of Sciences of the United States of America*, 104(51), 20534–20539. <https://doi.org/10.1073/pnas.0707873105>
- (80) Bahrami, S., Gryz, E. A., Graversen, J. H., Troldborg, A., Stengaard Pedersen, K., & Laska, M. J. (2018). Immunomodulating peptides derived from different human endogenous retroviruses (HERVs) show dissimilar impact on pathogenesis of a multiple sclerosis animal disease model. *Clinical immunology (Orlando, Fla.)*, 191, 37–43. <https://doi.org/10.1016/j.clim.2018.03.007>
- (81) Gonzalez-Cao, M., Iduma, P., Karachaliou, N., Santarpia, M., Blanco, J., & Rosell, R. (2016). Human endogenous retroviruses and cancer. *Cancer biology & medicine*, 13(4), 483–488. <https://doi.org/10.20892/j.issn.2095-3941.2016.0080>
- (82) Gröger, V., & Cynis, H. (2018). Human Endogenous Retroviruses and Their Putative Role in the Development of Autoimmune Disorders Such as Multiple Sclerosis. *Frontiers in microbiology*, 9, 265. <https://doi.org/10.3389/fmicb.2018.00265>
- (83) Staage, M. S., & Emmer, A. (2018). Editorial: Endogenous Viral Elements-Links Between Autoimmunity and Cancer?. *Frontiers in microbiology*, 9, 3171. <https://doi.org/10.3389/fmicb.2018.03171>
- (84) Stricker, E., Peckham-Gregory, E. C., & Scheurer, M. E. (2023). HERVs and Cancer-A Comprehensive Review of the Relationship of Human Endogenous Retroviruses and Human Cancers. *Biomedicines*, 11(3), 936. <https://doi.org/10.3390/biomedicines11030936>
- (85) Laska, M. J., Brudek, T., Nissen, K. K., Christensen, T., Møller-Larsen, A., Petersen, T., & Nexø, B. A. (2012). Expression of HERV-Fc1, a human endogenous retrovirus, is increased in patients with active multiple sclerosis. *Journal of virology*, 86(7), 3713–3722. <https://doi.org/10.1128/JVI.06723-11>
- (86) Garcia-Montojo, M., Dominguez-Mozo, M., Arias-Leal, A., Garcia-Martinez, Á., De las Heras, V., Casanova, I., Faucard, R., Gehin, N., Madeira, A., Arroyo, R., Curtin, F., Alvarez-Lafuente, R., & Perron, H. (2013). The DNA copy number of human endogenous retrovirus-

- W (MSRV-type) is increased in multiple sclerosis patients and is influenced by gender and disease severity. *PLoS one*, 8(1), e53623. <https://doi.org/10.1371/journal.pone.0053623>
- (87) Büscher, K., Trefzer, U., Hofmann, M., Sterry, W., Kurth, R., & Denner, J. (2005). Expression of human endogenous retrovirus K in melanomas and melanoma cell lines. *Cancer research*, 65(10), 4172–4180. <https://doi.org/10.1158/0008-5472.CAN-04-2983>
- (88) Steele, A. J., Al-Chalabi, A., Ferrante, K., Cudkowicz, M. E., Brown, R. H., Jr, & Garson, J. A. (2005). Detection of serum reverse transcriptase activity in patients with ALS and unaffected blood relatives. *Neurology*, 64(3), 454–458. <https://doi.org/10.1212/01.WNL.0000150899.76130.71>
- (89) Sotgiu, S., Mameli, G., Serra, C., Zarbo, I. R., Arru, G., & Dolei, A. (2010). Multiple sclerosis-associated retrovirus and progressive disability of multiple sclerosis. *Multiple sclerosis (Houndmills, Basingstoke, England)*, 16(10), 1248–1251. <https://doi.org/10.1177/1352458510376956>
- (90) Steiner, J. P., Bachani, M., Malik, N., DeMarino, C., Li, W., Sampson, K., Lee, M. H., Kowalak, J., Bhaskar, M., Doucet-O'Hare, T., Garcia-Montojo, M., Cowen, M., Smith, B., Reoma, L. B., Medina, J., Brunel, J., Pierquin, J., Charvet, B., Perron, H., & Nath, A. (2022). Human Endogenous Retrovirus K Envelope in Spinal Fluid of Amyotrophic Lateral Sclerosis Is Toxic. *Annals of neurology*, 92(4), 545–561. <https://doi.org/10.1002/ana.26452>
- (91) Perron, H., Lazarini, F., Ruprecht, K., Péchoux-Longin, C., Seilhean, D., Sazdovitch, V., Créange, A., Battail-Poirot, N., Sibai, G., Santoro, L., Jolivet, M., Darlix, J. L., Rieckmann, P., Arzberger, T., Hauw, J. J., & Lassmann, H. (2005). Human endogenous retrovirus (HERV)-W ENV and GAG proteins: physiological expression in human brain and pathophysiological modulation in multiple sclerosis lesions. *Journal of neurovirology*, 11(1), 23–33. <https://doi.org/10.1080/13550280590901741>
- (92) Mameli, G., Astone, V., Arru, G., Marconi, S., Lovato, L., Serra, C., Sotgiu, S., Bonetti, B., & Dolei, A. (2007). Brains and peripheral blood mononuclear cells of multiple sclerosis (MS) patients hyperexpress MS-associated retrovirus/HERV-W endogenous retrovirus, but not Human herpesvirus 6. *The Journal of general virology*, 88(Pt 1), 264–274. <https://doi.org/10.1099/vir.0.81890-0>
- (93) Wang-Johanning, F., Liu, J., Rycaj, K., Huang, M., Tsai, K., Rosen, D. G., Chen, D. T., Lu, D. W., Barnhart, K. F., & Johanning, G. L. (2007). Expression of multiple human endogenous retrovirus surface envelope proteins in ovarian cancer. *International journal of cancer*, 120(1), 81–90. <https://doi.org/10.1002/ijc.22256>
- (94) Ruprecht, K., Gronen, F., Sauter, M., Best, B., Rieckmann, P., & Mueller-Lantsch, N. (2008). Lack of immune responses against multiple sclerosis-associated retrovirus/human endogenous retrovirus W in patients with multiple sclerosis. *Journal of neurovirology*, 14(2), 143–151. <https://doi.org/10.1080/13550280801958922>

- (95) Schmitt, K., Richter, C., Backes, C., Meese, E., Ruprecht, K., & Mayer, J. (2013). Comprehensive analysis of human endogenous retrovirus group HERV-W locus transcription in multiple sclerosis brain lesions by high-throughput amplicon sequencing. *Journal of virology*, 87(24), 13837–13852. <https://doi.org/10.1128/JVI.02388-13>
- (96) Morandi, E., Tanasescu, R., Tarlinton, R. E., Constantinescu, C. S., Zhang, W., Tench, C., & Gran, B. (2017). The association between human endogenous retroviruses and multiple sclerosis: A systematic review and meta-analysis. *PloS one*, 12(2), e0172415. <https://doi.org/10.1371/journal.pone.0172415>
- (97) Avrameas, S., Alexopoulos, H., & Moutsopoulos, H. M. (2018). Natural Autoantibodies: An Undersung Hero of the Immune System and Autoimmune Disorders-A Point of View. *Frontiers in immunology*, 9, 1320. <https://doi.org/10.3389/fimmu.2018.01320>
- (98) Matoušková, M., Blazková, J., Pajer, P., Pavlíček, A., & Hejnar, J. (2006). CpG methylation suppresses transcriptional activity of human syncytin-1 in non-placental tissues. *Experimental cell research*, 312(7), 1011–1020. <https://doi.org/10.1016/j.yexcr.2005.12.010>
- (99) Grow, E. J., Flynn, R. A., Chavez, S. L., Bayless, N. L., Wossidlo, M., Wesche, D. J., Martin, L., Ware, C. B., Blish, C. A., Chang, H. Y., Pera, R. A., & Wysocka, J. (2015). Intrinsic retroviral reactivation in human preimplantation embryos and pluripotent cells. *Nature*, 522(7555), 221–225. <https://doi.org/10.1038/nature14308>
- (100) Mueller, T., Hantsch, C., Volkmer, I., & Staeger, M. S. (2018). Differentiation-Dependent Regulation of Human Endogenous Retrovirus K Sequences and Neighboring Genes in Germ Cell Tumor Cells. *Frontiers in microbiology*, 9, 1253. <https://doi.org/10.3389/fmicb.2018.01253>
- (101) Jones, M. J., Goodman, S. J., & Kobor, M. S. (2015). DNA methylation and healthy human aging. *Aging cell*, 14(6), 924–932. <https://doi.org/10.1111/acer.12349>
- (102) Tan, Q., Heijmans, B. T., Hjelmborg, J. V., Soerensen, M., Christensen, K., & Christiansen, L. (2016). Epigenetic drift in the aging genome: a ten-year follow-up in an elderly twin cohort. *International journal of epidemiology*, 45(4), 1146–1158. <https://doi.org/10.1093/ije/dyw132>
- (103) Cardelli, M., Doorn, R. V., Larcher, L., Donato, M. D., Piacenza, F., Pierpaoli, E., Giacconi, R., Malavolta, M., Rachakonda, S., Gruis, N. A., Molven, A., Andresen, P. A., Pjanova, D., van den Oord, J. J., Provinciali, M., Nagore, E., & Kumar, R. (2020). Association of HERV-K and LINE-1 hypomethylation with reduced disease-free survival in melanoma patients. *Epigenomics*, 12(19), 1689–1706. <https://doi.org/10.2217/epi-2020-0127>
- (104) de Cubas, A. A., Dunker, W., Zaninovich, A., Hongo, R. A., Bhatia, A., Panda, A., Beckermann, K. E., Bhanot, G., Ganesan, S., Karijolic, J., & Rathmell, W. K. (2020). DNA hypomethylation promotes transposable element expression and activation of immune

- signaling in renal cell cancer. *JCI insight*, 5(11), e137569. <https://doi.org/10.1172/jci.insight.137569>
- (105) Di Giorgio, E., & Xodo, L. E. (2022). Endogenous Retroviruses (ERVs): Does RLR (RIG-I-Like Receptors)-MAVS Pathway Directly Control Senescence and Aging as a Consequence of ERV De-Repression?. *Frontiers in immunology*, 13, 917998. <https://doi.org/10.3389/fimmu.2022.917998>
- (106) Liu, X., Liu, Z., Wu, Z., Ren, J., Fan, Y., Sun, L., Cao, G., Niu, Y., Zhang, B., Ji, Q., Jiang, X., Wang, C., Wang, Q., Ji, Z., Li, L., Esteban, C. R., Yan, K., Li, W., Cai, Y., Wang, S., Zheng, A., Zhang, Y. E., Tan, S., Cai, Y., Song, M., Lu, F., Tang, F., Ji, W., Zhou, Q., Belmonte, J. C. I., Zhang, W., Qu, J., Liu, G. H. (2023). Resurrection of endogenous retroviruses during aging reinforces senescence. *Cell*, 186(2), 287–304.e26. <https://doi.org/10.1016/j.cell.2022.12.017>
- (107) Reiche, J., Pauli, G., & Ellerbrok, H. (2010). Differential expression of human endogenous retrovirus K transcripts in primary human melanocytes and melanoma cell lines after UV irradiation. *Melanoma research*, 20(5), 435–440. <https://doi.org/10.1097/CMR.0b013e32833c1b5d>
- (108) Lee, J. R., Ahn, K., Kim, Y. J., Jung, Y. D., & Kim, H. S. (2012). Radiation-induced human endogenous retrovirus (HERV)-R env gene expression by epigenetic control. *Radiation research*, 178(5), 379–384. <https://doi.org/10.1667/RR2888.1>
- (109) Kelleher, C. A., Wilkinson, D. A., Freeman, J. D., Mager, D. L., & Gelfand, E. W. (1996). Expression of novel-transposon-containing mRNAs in human T cells. *The Journal of general virology*, 77 (Pt 5), 1101–1110. <https://doi.org/10.1099/0022-1317-77-5-1101>
- (110) Johnston, J. B., Silva, C., Holden, J., Warren, K. G., Clark, A. W., & Power, C. (2001). Monocyte activation and differentiation augment human endogenous retrovirus expression: implications for inflammatory brain diseases. *Annals of neurology*, 50(4), 434–442. <https://doi.org/10.1002/ana.1131>
- (111) Diem, O., Schäffner, M., Seifarth, W., & Leib-Mösch, C. (2012). Influence of antipsychotic drugs on human endogenous retrovirus (HERV) transcription in brain cells. *PloS one*, 7(1), e30054. <https://doi.org/10.1371/journal.pone.0030054>
- (112) Liu, C., Chen, Y., Li, S., Yu, H., Zeng, J., Wang, X., & Zhu, F. (2013). Activation of elements in HERV-W family by caffeine and aspirin. *Virus genes*, 47(2), 219–227. <https://doi.org/10.1007/s11262-013-0939-6>
- (113) Mommert, M., Tabone, O., Oriol, G., Cerrato, E., Guichard, A., Naville, M., Fournier, P., Volff, J. N., Pachot, A., Monneret, G., Venet, F., Brengel-Pesce, K., Textoris, J., & Mallet, F. (2018). LTR-retrotransposon transcriptome modulation in response to endotoxin-induced stress in PBMCs. *BMC genomics*, 19(1), 522. <https://doi.org/10.1186/s12864-018-4901-9>

- (114) Wang-Johanning, F., Frost, A. R., Jian, B., Epp, L., Lu, D. W., & Johanning, G. L. (2003). Quantitation of HERV-K env gene expression and splicing in human breast cancer. *Oncogene*, 22(10), 1528–1535. <https://doi.org/10.1038/sj.onc.1206241>
- (115) Golan, M., Hizi, A., Resau, J. H., Yaal-Hahoshen, N., Reichman, H., Keydar, I., & Tsarfaty, I. (2008). Human endogenous retrovirus (HERV-K) reverse transcriptase as a breast cancer prognostic marker. *Neoplasia (New York, N.Y.)*, 10(6), 521–533. <https://doi.org/10.1593/neo.07986>
- (116) Nguyen, T. D., Davis, J., Eugenio, R. A., & Liu, Y. (2019). Female Sex Hormones Activate Human Endogenous Retrovirus Type K Through the OCT4 Transcription Factor in T47D Breast Cancer Cells. *AIDS research and human retroviruses*, 35(3), 348–356. <https://doi.org/10.1089/AID.2018.0173>
- (117) Larsson, E., Venables, P., Andersson, A. C., Fan, W., Rigby, S., Botling, J., Oberg, F., Cohen, M., & Nilsson, K. (1997). Tissue and differentiation specific expression on the endogenous retrovirus ERV3 (HERV-R) in normal human tissues and during induced monocytic differentiation in the U-937 cell line. *Leukemia*, 11 Suppl 3, 142–144.
- (118) Liu, M., Ohtani, H., Zhou, W., Ørskov, A. D., Charlet, J., Zhang, Y. W., Shen, H., Baylin, S. B., Liang, G., Grønbaek, K., & Jones, P. A. (2016). Vitamin C increases viral mimicry induced by 5-aza-2'-deoxycytidine. *Proceedings of the National Academy of Sciences of the United States of America*, 113(37), 10238–10244. <https://doi.org/10.1073/pnas.1612262113>
- (119) Stauffer, Y., Marguerat, S., Meylan, F., Ucla, C., Sutkowski, N., Huber, B., Pelet, T., & Conrad, B. (2001). Interferon-alpha-induced endogenous superantigen. a model linking environment and autoimmunity. *Immunity*, 15(4), 591–601. [https://doi.org/10.1016/s1074-7613\(01\)00212-6](https://doi.org/10.1016/s1074-7613(01)00212-6)
- (120) Sutkowski, N., Conrad, B., Thorley-Lawson, D. A., & Huber, B. T. (2001). Epstein-Barr virus transactivates the human endogenous retrovirus HERV-K18 that encodes a superantigen. *Immunity*, 15(4), 579–589. [https://doi.org/10.1016/s1074-7613\(01\)00210-2](https://doi.org/10.1016/s1074-7613(01)00210-2)
- (121) Sutkowski, N., Chen, G., Calderon, G., & Huber, B. T. (2004). Epstein-Barr virus latent membrane protein LMP-2A is sufficient for transactivation of the human endogenous retrovirus HERV-K18 superantigen. *Journal of virology*, 78(14), 7852–7860. <https://doi.org/10.1128/JVI.78.14.7852-7860.2004>
- (122) Nellåker, C., Yao, Y., Jones-Brando, L., Mallet, F., Yolken, R. H., & Karlsson, H. (2006). Transactivation of elements in the human endogenous retrovirus W family by viral infection. *Retrovirology*, 3, 44. <https://doi.org/10.1186/1742-4690-3-44>
- (123) Brudek, T., Lühdorf, P., Christensen, T., Hansen, H. J., & Møller-Larsen, A. (2007). Activation of endogenous retrovirus reverse transcriptase in multiple sclerosis patient lymphocytes by inactivated HSV-1, HHV-6 and VZV. *Journal of neuroimmunology*, 187(1-2), 147–155. <https://doi.org/10.1016/j.jneuroim.2007.04.003>

- (124) Contreras-Galindo, R., López, P., Vélez, R., & Yamamura, Y. (2007). HIV-1 infection increases the expression of human endogenous retroviruses type K (HERV-K) in vitro. *AIDS research and human retroviruses*, 23(1), 116–122. <https://doi.org/10.1089/aid.2006.0117>
- (125) Toufaily, C., Landry, S., Leib-Mosch, C., Rassart, E., & Barbeau, B. (2011). Activation of LTRs from different human endogenous retrovirus (HERV) families by the HTLV-1 tax protein and T-cell activators. *Viruses*, 3(11), 2146–2159. <https://doi.org/10.3390/v3112146>
- (126) Mameli, G., Poddighe, L., Mei, A., Uleri, E., Sotgiu, S., Serra, C., Manetti, R., & Dolei, A. (2012). Expression and activation by Epstein Barr virus of human endogenous retroviruses-W in blood cells and astrocytes: inference for multiple sclerosis. *PloS one*, 7(9), e44991. <https://doi.org/10.1371/journal.pone.0044991>
- (127) Charvet, B., Reynaud, J. M., Gourru-Lesimple, G., Perron, H., Marche, P. N., & Horvat, B. (2018). Induction of Proinflammatory Multiple Sclerosis-Associated Retrovirus Envelope Protein by Human Herpesvirus-6A and CD46 Receptor Engagement. *Frontiers in immunology*, 9, 2803. <https://doi.org/10.3389/fimmu.2018.02803>
- (128) Sicat, J., Sutkowski, N., & Huber, B. T. (2005). Expression of human endogenous retrovirus HERV-K18 superantigen is elevated in juvenile rheumatoid arthritis. *The Journal of rheumatology*, 32(9), 1821–1831.
- (129) Erre, G. L., Mameli, G., Cossu, D., Muzzeddu, B., Piras, C., Paccagnini, D., Passiu, G., & Sechi, L. A. (2015). Increased Epstein-Barr Virus DNA Load and Antibodies Against EBNA1 and EA in Sardinian Patients with Rheumatoid Arthritis. *Viral immunology*, 28(7), 385–390. <https://doi.org/10.1089/vim.2015.0035>
- (130) Mameli, G., Erre, G. L., Caggiu, E., Mura, S., Cossu, D., Bo, M., Cadoni, M. L., Piras, A., Mundula, N., Colombo, E., Buscetta, G., Passiu, G., & Sechi, L. A. (2017). Identification of a HERV-K env surface peptide highly recognized in Rheumatoid Arthritis (RA) patients: a cross-sectional case-control study. *Clinical and experimental immunology*, 189(1), 127–131. <https://doi.org/10.1111/cei.12964>
- (131) Jasemi, S., Erre, G. L., Cadoni, M. L., Bo, M., & Sechi, L. A. (2021). Humoral Response to Microbial Biomarkers in Rheumatoid Arthritis Patients. *Journal of clinical medicine*, 10(21), 5153. <https://doi.org/10.3390/jcm10215153>
- (132) Aygun, D., Kuskucu, M. A., Sahin, S., Adrovic, A., Barut, K., Yıldız, M., Sharifova, S., Midilli, K., Cokugras, H., Camcioglu, Y., & Kasapcopur, O. (2020). Epstein-Barr virus, cytomegalovirus and BK polyomavirus burden in juvenile systemic lupus erythematosus: correlation with clinical and laboratory indices of disease activity. *Lupus*, 29(10), 1263–1269. <https://doi.org/10.1177/0961203320940029>
- (133) Quaglia, M., Merlotti, G., De Andrea, M., Borgogna, C., & Cantaluppi, V. (2021). Viral Infections and Systemic Lupus Erythematosus: New Players in an Old Story. *Viruses*, 13(2), 277. <https://doi.org/10.3390/v13020277>

- (134) Iwata, S., & Tanaka, Y. (2022). Association of Viral Infection With the Development and Pathogenesis of Systemic Lupus Erythematosus. *Frontiers in medicine*, 9, 849120. <https://doi.org/10.3389/fmed.2022.849120>
- (135) Jones, A. R., Iacoangeli, A., Adey, B. N., Bowles, H., Shatunov, A., Troakes, C., Garson, J. A., McCormick, A. L., & Al-Chalabi, A. (2021). A HML6 endogenous retrovirus on chromosome 3 is upregulated in amyotrophic lateral sclerosis motor cortex. *Scientific reports*, 11(1), 14283. <https://doi.org/10.1038/s41598-021-93742-3>
- (136) Li, W., Pandya, D., Pasternack, N., Garcia-Montojo, M., Henderson, L., Kozak, C. A., & Nath, A. (2022). Retroviral Elements in Pathophysiology and as Therapeutic Targets for Amyotrophic Lateral Sclerosis. *Neurotherapeutics : the journal of the American Society for Experimental NeuroTherapeutics*, 19(4), 1085–1101. <https://doi.org/10.1007/s13311-022-01233-8>
- (137) Meier, U. C., Cipian, R. C., Karimi, A., Ramasamy, R., & Middeldorp, J. M. (2021). Cumulative Roles for Epstein-Barr Virus, Human Endogenous Retroviruses, and Human Herpes Virus-6 in Driving an Inflammatory Cascade Underlying MS Pathogenesis. *Frontiers in immunology*, 12, 757302. <https://doi.org/10.3389/fimmu.2021.757302>
- (138) Pérez-Pérez, S., Domínguez-Mozo, M. I., García-Martínez, M. Á., Ballester-González, R., Nieto-Gañán, I., Arroyo, R., & Alvarez-Lafuente, R. (2022). Epstein-Barr Virus Load Correlates with Multiple Sclerosis-Associated Retrovirus Envelope Expression. *Biomedicines*, 10(2), 387. <https://doi.org/10.3390/biomedicines10020387>
- (139) Trela, M., Nelson, P. N., & Rylance, P. B. (2016). The role of molecular mimicry and other factors in the association of Human Endogenous Retroviruses and autoimmunity. *APMIS : acta pathologica, microbiologica, et immunologica Scandinavica*, 124(1-2), 88–104. <https://doi.org/10.1111/apm.12487>
- (140) Emmer, A., Staege, M. S., & Kornhuber, M. E. (2014). The retrovirus/superantigen hypothesis of multiple sclerosis. *Cellular and molecular neurobiology*, 34(8), 1087–1096. <https://doi.org/10.1007/s10571-014-0100-7>
- (141) Küry, P., Nath, A., Créange, A., Dolei, A., Marche, P., Gold, J., Giovannoni, G., Hartung, H. P., & Perron, H. (2018). Human Endogenous Retroviruses in Neurological Diseases. *Trends in molecular medicine*, 24(4), 379–394. <https://doi.org/10.1016/j.molmed.2018.02.007>
- (142) Oldstone M. B. (2014). Molecular mimicry: its evolution from concept to mechanism as a cause of autoimmune diseases. *Monoclonal antibodies in immunodiagnosis and immunotherapy*, 33(3), 158–165. <https://doi.org/10.1089/mab.2013.0090>
- (143) Ramasamy, R., Joseph, B., & Whittall, T. (2017). Potential molecular mimicry between the human endogenous retrovirus W family envelope proteins and myelin proteins in multiple sclerosis. *Immunology letters*, 183, 79–85. <https://doi.org/10.1016/j.imlet.2017.02.003>

- (144) de Luca, V., Martins Higa, A., Malta Romano, C., Pimenta Mambrini, G., Peroni, L. A., Trivinho-Strixino, F., & Lima Leite, F. (2019). Cross-reactivity between myelin oligodendrocyte glycoprotein and human endogenous retrovirus W protein: nanotechnological evidence for the potential trigger of multiple sclerosis. *Micron (Oxford, England : 1993)*, *120*, 66–73. <https://doi.org/10.1016/j.micron.2019.02.005>
- (145) Herve, C. A., Lugli, E. B., Brand, A., Griffiths, D. J., & Venables, P. J. (2002). Autoantibodies to human endogenous retrovirus-K are frequently detected in health and disease and react with multiple epitopes. *Clinical and experimental immunology*, *128*(1), 75–82. <https://doi.org/10.1046/j.1365-2249.2002.01735.x>
- (146) Nelson, P. N., Roden, D., Nevill, A., Freimanis, G. L., Trela, M., Ejtehadi, H. D., Bowman, S., Axford, J., Veitch, A. M., Tugnet, N., & Rylance, P. B. (2014). Rheumatoid arthritis is associated with IgG antibodies to human endogenous retrovirus gag matrix: a potential pathogenic mechanism of disease?. *The Journal of rheumatology*, *41*(10), 1952–1960. <https://doi.org/10.3899/jrheum.130502>
- (147) Wan, X., Thomas, J. W., & Unanue, E. R. (2016). Class-switched anti-insulin antibodies originate from unconventional antigen presentation in multiple lymphoid sites. *The Journal of experimental medicine*, *213*(6), 967–978. <https://doi.org/10.1084/jem.20151869>
- (148) Murphy, K., & Weaver, C. (2018). Die Entstehung von Antigenrezeptoren in Lymphocyten. *Janeway Immunologie*, 221–271. https://doi.org/10.1007/978-3-662-56004-4_5
- (149) Jiang, J., Natarajan, K., & Margulies, D. H. (2019). MHC Molecules, T cell Receptors, Natural Killer Cell Receptors, and Viral Immuno-evasins-Key Elements of Adaptive and Innate Immunity. *Advances in experimental medicine and biology*, *1172*, 21–62. https://doi.org/10.1007/978-981-13-9367-9_2
- (150) Jardetzky, T. S., Brown, J. H., Gorga, J. C., Stern, L. J., Urban, R. G., Chi, Y. I., Stauffer, C., Strominger, J. L., & Wiley, D. C. (1994). Three-dimensional structure of a human class II histocompatibility molecule complexed with superantigen. *Nature*, *368*(6473), 711–718. <https://doi.org/10.1038/368711a0>
- (151) Solanki, L. S., Srivastava, N., & Singh, S. (2008). Superantigens: a brief review with special emphasis on dermatologic diseases. *Dermatology online journal*, *14*(2), 3.
- (152) Kozono, H., Parker, D., White, J., Marrack, P., & Kappler, J. (1995). Multiple binding sites for bacterial superantigens on soluble class II MHC molecules. *Immunity*, *3*(2), 187–196. [https://doi.org/10.1016/1074-7613\(95\)90088-8](https://doi.org/10.1016/1074-7613(95)90088-8)
- (153) Wen, R., Cole, G. A., Surman, S., Blackman, M. A., & Woodland, D. L. (1996). Major histocompatibility complex class II-associated peptides control the presentation of bacterial superantigens to T cells. *The Journal of experimental medicine*, *183*(3), 1083–1092. <https://doi.org/10.1084/jem.183.3.1083>

- (154) Kim, K. S., Jacob, N., & Stohl, W. (2003). In vitro and in vivo T cell oligoclonality following chronic stimulation with staphylococcal superantigens. *Clinical immunology (Orlando, Fla.)*, 108(3), 182–189. [https://doi.org/10.1016/s1521-6616\(03\)00167-0](https://doi.org/10.1016/s1521-6616(03)00167-0)
- (155) Tai, A. K., Lin, M., Chang, F., Chen, G., Hsiao, F., Sutkowski, N., & Huber, B. T. (2006). Murine Vbeta3+ and Vbeta7+ T cell subsets are specific targets for the HERV-K18 Env superantigen. *Journal of immunology (Baltimore, Md. : 1950)*, 177(5), 3178–3184. <https://doi.org/10.4049/jimmunol.177.5.3178>
- (156) Klamann, L. D., & Thorley-Lawson, D. A. (1995). Characterization of the CD48 gene demonstrates a positive element that is specific to Epstein-Barr virus-immortalized B-cell lines and contains an essential NF-kappa B site. *Journal of virology*, 69(2), 871–881. <https://doi.org/10.1128/JVI.69.2.871-881.1995>
- (157) Tischendorf, P., Shramek, G. J., Balagtas, R. C., Deinhardt, F., Knospe, W. H., Noble, G. R., & Maynard, J. E. (1970). Development and persistence of immunity to Epstein-Barr virus in man. *The Journal of infectious diseases*, 122(5), 401–409. <https://doi.org/10.1093/infdis/122.5.401>
- (158) Warner, H. B., & Carp, R. I. (1981). Multiple sclerosis and Epstein-Barr virus. *Lancet (London, England)*, 2(8258), 1290. [https://doi.org/10.1016/s0140-6736\(81\)91527-0](https://doi.org/10.1016/s0140-6736(81)91527-0)
- (159) Flavell, K. J., & Murray, P. G. (2000). Hodgkin's disease and the Epstein-Barr virus. *Molecular pathology : MP*, 53(5), 262–269. <https://doi.org/10.1136/mp.53.5.262>
- (160) Brady, G., Macarthur, G. J., & Farrell, P. J. (2008). Epstein-Barr virus and Burkitt lymphoma. *Postgraduate medical journal*, 84(993), 372–377. <https://doi.org/10.1136/jcp.2007.047977>
- (161) Goldacre, M. J., Wotton, C. J., Seagroatt, V., & Yeates, D. (2004). Multiple sclerosis after infectious mononucleosis: record linkage study. *Journal of epidemiology and community health*, 58(12), 1032–1035. <https://doi.org/10.1136/jech.2003.018366>
- (162) Thacker, E. L., Mirzaei, F., & Ascherio, A. (2006). Infectious mononucleosis and risk for multiple sclerosis: a meta-analysis. *Annals of neurology*, 59(3), 499–503. <https://doi.org/10.1002/ana.20820>
- (163) Sheik-Ali S. (2017). Infectious mononucleosis and multiple sclerosis - Updated review on associated risk. *Multiple sclerosis and related disorders*, 14, 56–59. <https://doi.org/10.1016/j.msard.2017.02.019>
- (164) Bjornevik, K., Cortese, M., Healy, B. C., Kuhle, J., Mina, M. J., Leng, Y., Elledge, S. J., Niebuhr, D. W., Scher, A. I., Munger, K. L., & Ascherio, A. (2022). Longitudinal analysis reveals high prevalence of Epstein-Barr virus associated with multiple sclerosis. *Science (New York, N.Y.)*, 375(6578), 296–301. <https://doi.org/10.1126/science.abj8222>

- (165) Sutkowski, N., Palkama, T., Ciurli, C., Sekaly, R. P., Thorley-Lawson, D. A., & Huber, B. T. (1996). An Epstein-Barr virus-associated superantigen. *The Journal of experimental medicine*, 184(3), 971–980. <https://doi.org/10.1084/jem.184.3.971>
- (166) Tai, A. K., O'Reilly, E. J., Alroy, K. A., Simon, K. C., Munger, K. L., Huber, B. T., & Ascherio, A. (2008). Human endogenous retrovirus-K18 Env as a risk factor in multiple sclerosis. *Multiple sclerosis (Houndmills, Basingstoke, England)*, 14(9), 1175–1180. <https://doi.org/10.1177/1352458508094641>
- (167) de la Hera, B., Varadé, J., García-Montojo, M., Lamas, J. R., de la Encarnación, A., Arroyo, R., Fernández-Gutiérrez, B., Alvarez-Lafuente, R., & Urcelay, E. (2013). Role of the human endogenous retrovirus HERV-K18 in autoimmune disease susceptibility: study in the Spanish population and meta-analysis. *PloS one*, 8(4), e62090. <https://doi.org/10.1371/journal.pone.0062090>
- (168) García-Montojo, M., de la Hera, B., Varadé, J., de la Encarnación, A., Camacho, I., Domínguez-Mozo, M., Árias-Leal, A., García-Martínez, A., Casanova, I., Izquierdo, G., Lucas, M., Fedetz, M., Alcina, A., Arroyo, R., Matesanz, F., Urcelay, E., & Alvarez-Lafuente, R. (2014). HERV-W polymorphism in chromosome X is associated with multiple sclerosis risk and with differential expression of MSR.V. *Retrovirology*, 11, 2. <https://doi.org/10.1186/1742-4690-11-2>
- (169) Dolei A. (2018). The aliens inside us: HERV-W endogenous retroviruses and multiple sclerosis. *Multiple sclerosis (Houndmills, Basingstoke, England)*, 24(1), 42–47. <https://doi.org/10.1177/1352458517737370>
- (170) Perron, H., Jouvin-Marche, E., Michel, M., Ounanian-Paraz, A., Camelo, S., Dumon, A., Jolivet-Reynaud, C., Marcel, F., Souillet, Y., Borel, E., Gebuhrer, L., Santoro, L., Marcel, S., Seigneurin, J. M., Marche, P. N., & Lafon, M. (2001). Multiple sclerosis retrovirus particles and recombinant envelope trigger an abnormal immune response in vitro, by inducing polyclonal Vbeta16 T-lymphocyte activation. *Virology*, 287(2), 321–332. <https://doi.org/10.1006/viro.2001.1045>
- (171) Walton, C., King, R., Rechtman, L., Kaye, W., Leray, E., Marrie, R. A., Robertson, N., La Rocca, N., Uitdehaag, B., van der Mei, I., Wallin, M., Helme, A., Angood Napier, C., Rijke, N., & Baneke, P. (2020). Rising prevalence of multiple sclerosis worldwide: Insights from the Atlas of MS, third edition. *Multiple sclerosis (Houndmills, Basingstoke, England)*, 26(14), 1816–1821. <https://doi.org/10.1177/1352458520970841>
- (172) Okuda, D. T., Mowry, E. M., Beheshtian, A., Waubant, E., Baranzini, S. E., Goodin, D. S., Hauser, S. L., & Pelletier, D. (2009). Incidental MRI anomalies suggestive of multiple sclerosis: the radiologically isolated syndrome. *Neurology*, 72(9), 800–805. <https://doi.org/10.1212/01.wnl.0000335764.14513.1a>

- (173) Hosseiny, M., Newsome, S. D., & Yousem, D. M. (2020). Radiologically Isolated Syndrome: A Review for Neuroradiologists. *AJNR. American journal of neuroradiology*, 41(9), 1542–1549. <https://doi.org/10.3174/ajnr.A6649>
- (174) de Vries, H. E., Kuiper, J., de Boer, A. G., Van Berkel, T. J., & Breimer, D. D. (1997). The blood-brain barrier in neuroinflammatory diseases. *Pharmacological reviews*, 49(2), 143–155.
- (175) Minagar, A., & Alexander, J. S. (2003). Blood-brain barrier disruption in multiple sclerosis. *Multiple sclerosis (Houndmills, Basingstoke, England)*, 9(6), 540–549. <https://doi.org/10.1191/1352458503ms965oa>
- (176) Kuhlmann, T., Lingfeld, G., Bitsch, A., Schuchardt, J., & Brück, W. (2002). Acute axonal damage in multiple sclerosis is most extensive in early disease stages and decreases over time. *Brain : a journal of neurology*, 125(Pt 10), 2202–2212. <https://doi.org/10.1093/brain/awf235>
- (177) Maida, E., & Lavorgna, L. (2023). Multiple Sclerosis: Diagnosis, Management, and Future Opportunities. *Journal of clinical medicine*, 12(14), 4558. <https://doi.org/10.3390/jcm12144558>
- (178) van Horssen, J., van der Pol, S., Nijland, P., Amor, S., & Perron, H. (2016). Human endogenous retrovirus W in brain lesions: Rationale for targeted therapy in multiple sclerosis. *Multiple sclerosis and related disorders*, 8, 11–18. <https://doi.org/10.1016/j.msard.2016.04.006>
- (179) Perron, H., Germi, R., Bernard, C., Garcia-Montojo, M., Deluen, C., Farinelli, L., Faucard, R., Veas, F., Stefan, I., Fabriek, B. O., Van-Horssen, J., Van-der-Valk, P., Gerdil, C., Mancuso, R., Saresella, M., Clerici, M., Marcel, S., Creange, A., Cavaretta, R., Caputo, D., Arru, G., Morand, P., Lang, A. B., Sotgiu, S., Ruprecht, K., Rieckmann, P., Villoslada, P., Chofflon, M., Boucraut, J., Pelletier, J., Hartung, H. P. (2012). Human endogenous retrovirus type W envelope expression in blood and brain cells provides new insights into multiple sclerosis disease. *Multiple sclerosis (Houndmills, Basingstoke, England)*, 18(12), 1721–1736. <https://doi.org/10.1177/1352458512441381>
- (180) Madeira, A., Burgelin, I., Perron, H., Curtin, F., Lang, A. B., & Faucard, R. (2016). MSRV envelope protein is a potent, endogenous and pathogenic agonist of human toll-like receptor 4: Relevance of GNBAC1 in multiple sclerosis treatment. *Journal of neuroimmunology*, 291, 29–38. <https://doi.org/10.1016/j.jneuroim.2015.12.006>
- (181) Kremer, D., Gruchot, J., Weyers, V., Oldemeier, L., Göttle, P., Healy, L., Ho Jang, J., Kang T Xu, Y., Volsko, C., Dutta, R., Trapp, B. D., Perron, H., Hartung, H. P., & Küry, P. (2019). pHERV-W envelope protein fuels microglial cell-dependent damage of myelinated axons in multiple sclerosis. *Proceedings of the National Academy of Sciences of the United States of America*, 116(30), 15216–15225. <https://doi.org/10.1073/pnas.1901283116>

- (182) Hartung, H. P., Derfuss, T., Cree, B. A., Sormani, M. P., Selmaj, K., Stutters, J., Prados, F., MacManus, D., Schneble, H. M., Lambert, E., Porchet, H., Glanzman, R., Warne, D., Curtin, F., Kornmann, G., Buffet, B., Kremer, D., Küry, P., Leppert, D., Rückle, T., & Barkhof, F. (2022). Efficacy and safety of temelimab in multiple sclerosis: Results of a randomized phase 2b and extension study. *Multiple sclerosis (Houndmills, Basingstoke, England)*, 28(3), 429–440. <https://doi.org/10.1177/13524585211024997>
- (183) Ruprecht, K., Mayer, J., Sauter, M., Roemer, K., & Mueller-Lantsch, N. (2008). Endogenous retroviruses and cancer. *Cellular and molecular life sciences : CMLS*, 65(21), 3366–3382. <https://doi.org/10.1007/s00018-008-8496-1>
- (184) Borovski, T., De Sousa E Melo, F., Vermeulen, L., & Medema, J. P. (2011). Cancer stem cell niche: the place to be. *Cancer research*, 71(3), 634–639. <https://doi.org/10.1158/0008-5472.CAN-10-3220>
- (185) Bruttel, V. S., & Wischhusen, J. (2014). Cancer stem cell immunology: key to understanding tumorigenesis and tumor immune escape?. *Frontiers in immunology*, 5, 360. <https://doi.org/10.3389/fimmu.2014.00360>
- (186) Colak, S., & Medema, J. P. (2014). Cancer stem cells--important players in tumor therapy resistance. *The FEBS journal*, 281(21), 4779–4791. <https://doi.org/10.1111/febs.13023>
- (187) Cabrera, M. C., Hollingsworth, R. E., & Hurt, E. M. (2015). Cancer stem cell plasticity and tumor hierarchy. *World journal of stem cells*, 7(1), 27–36. <https://doi.org/10.4252/wjsc.v7.i1.27>
- (188) Nassar, D., & Blanpain, C. (2016). Cancer Stem Cells: Basic Concepts and Therapeutic Implications. *Annual review of pathology*, 11, 47–76. <https://doi.org/10.1146/annurev-pathol-012615-044438>
- (189) Aponte, P. M., & Caicedo, A. (2017). Stemness in Cancer: Stem Cells, Cancer Stem Cells, and Their Microenvironment. *Stem cells international*, 2017, 5619472. <https://doi.org/10.1155/2017/5619472>
- (190) Aramini, B., Masciale, V., Grisendi, G., Bertolini, F., Maur, M., Guaitoli, G., Chrystel, I., Morandi, U., Stella, F., Dominici, M., & Haider, K. H. (2022). Dissecting Tumor Growth: The Role of Cancer Stem Cells in Drug Resistance and Recurrence. *Cancers*, 14(4), 976. <https://doi.org/10.3390/cancers14040976>
- (191) Nairuz, T., Mahmud, Z., Manik, R. K., & Kabir, Y. (2023). Cancer stem cells: an insight into the development of metastatic tumors and therapy resistance. *Stem cell reviews and reports*, 19(6), 1577–1595. <https://doi.org/10.1007/s12015-023-10529-x>
- (192) Argaw-Denboba, A., Balestrieri, E., Serafino, A., Cipriani, C., Bucci, I., Sorrentino, R., Sciamanna, I., Gambacurta, A., Sinibaldi-Vallebona, P., & Matteucci, C. (2017). HERV-K activation is strictly required to sustain CD133+ melanoma cells with stemness features.

- Journal of experimental & clinical cancer research* : CR, 36(1), 20.
<https://doi.org/10.1186/s13046-016-0485-x>
- (193) Maris J. M. (2010). Recent advances in neuroblastoma. *The New England journal of medicine*, 362(23), 2202–2211. <https://doi.org/10.1056/NEJMra0804577>
- (194) Colon, N. C., & Chung, D. H. (2011). Neuroblastoma. *Advances in pediatrics*, 58(1), 297–311. <https://doi.org/10.1016/j.yapd.2011.03.011>
- (195) Park, J. A., & Cheung, N. V. (2017). Limitations and opportunities for immune checkpoint inhibitors in pediatric malignancies. *Cancer treatment reviews*, 58, 22–33. <https://doi.org/10.1016/j.ctrv.2017.05.006>
- (196) Wedekind, M. F., Denton, N. L., Chen, C. Y., & Cripe, T. P. (2018). Pediatric Cancer Immunotherapy: Opportunities and Challenges. *Paediatric drugs*, 20(5), 395–408. <https://doi.org/10.1007/s40272-018-0297-x>
- (197) Tongyoo, P., Avihingsanon, Y., Prom-On, S., Mutirangura, A., Mhuantong, W., & Hirankarn, N. (2017). EnHERV: Enrichment analysis of specific human endogenous retrovirus patterns and their neighboring genes. *PloS one*, 12(5), e0177119. <https://doi.org/10.1371/journal.pone.0177119>
- (198) Serafino, A., Balestrieri, E., Pierimarchi, P., Matteucci, C., Moroni, G., Oricchio, E., Rasi, G., Mastino, A., Spadafora, C., Garaci, E., & Vallebona, P. S. (2009). The activation of human endogenous retrovirus K (HERV-K) is implicated in melanoma cell malignant transformation. *Experimental cell research*, 315(5), 849–862. <https://doi.org/10.1016/j.yexcr.2008.12.023>
- (199) Balestrieri, E., Argaw-Denboba, A., Gambacurta, A., Cipriani, C., Bei, R., Serafino, A., Sinibaldi-Vallebona, P., & Matteucci, C. (2018). Human Endogenous Retrovirus K in the Crosstalk Between Cancer Cells Microenvironment and Plasticity: A New Perspective for Combination Therapy. *Frontiers in microbiology*, 9, 1448. <https://doi.org/10.3389/fmicb.2018.01448>
- (200) Zhou, F., Krishnamurthy, J., Wei, Y., Li, M., Hunt, K., Johannang, G. L., Cooper, L. J., & Wang-Johanning, F. (2015). Chimeric antigen receptor T cells targeting HERV-K inhibit breast cancer and its metastasis through downregulation of Ras. *Oncoimmunology*, 4(11), e1047582. <https://doi.org/10.1080/2162402X.2015.1047582>
- (201) Krishnamurthy, J., Rabinovich, B. A., Mi, T., Switzer, K. C., Olivares, S., Maiti, S. N., Plummer, J. B., Singh, H., Kumaresan, P. R., Huls, H. M., Wang-Johanning, F., & Cooper, L. J. (2015). Genetic Engineering of T Cells to Target HERV-K, an Ancient Retrovirus on Melanoma. *Clinical cancer research : an official journal of the American Association for Cancer Research*, 21(14), 3241–3251. <https://doi.org/10.1158/1078-0432.CCR-14-3197>
- (202) Yan, Q., Wu, X., Zhou, P., Zhou, Y., Li, X., Liu, Z., Tan, H., Yao, W., Xia, Y., & Zhu, F. (2022). HERV-W Envelope Triggers Abnormal Dopaminergic Neuron Process through

- DRD2/PP2A/AKT1/GSK3 for Schizophrenia Risk. *Viruses*, 14(1), 145. <https://doi.org/10.3390/v14010145>
- (203) Masuda, Y., Ishihara, R., Murakami, Y., Watanabe, S., Asao, Y., Gotoh, N., Kasamatsu, T., Takei, H., Kobayashi, N., Saitoh, T., Murakami, H., & Handa, H. (2023). Clinical significance of human endogenous retrovirus K (HERV-K) in multiple myeloma progression. *International journal of hematology*, 117(4), 563–577. <https://doi.org/10.1007/s12185-022-03513-7>
- (204) Engel, K., Wieland, L., Krüger, A., Volkmer, I., Cynis, H., Emmer, A., & Staeger, M. S. (2021). Identification of Differentially Expressed Human Endogenous Retrovirus Families in Human Leukemia and Lymphoma Cell Lines and Stem Cells. *Frontiers in oncology*, 11, 637981. <https://doi.org/10.3389/fonc.2021.637981>
- (205) Lu, X., Yuan, Q., Zhang, C., Wang, S., & Wei, W. (2023). Predicting the immune microenvironment and prognosis with a anoikis - related signature in breast cancer. *Frontiers in oncology*, 13, 1149193. <https://doi.org/10.3389/fonc.2023.1149193>
- (206) He, E., Shi, B., Liu, Z., Chang, K., Zhao, H., Zhao, W., & Cui, H. (2023). Identification of the molecular subtypes and construction of risk models in neuroblastoma. *Scientific reports*, 13(1), 11790. <https://doi.org/10.1038/s41598-023-35401-3>
- (207) Clara, J. A., Monge, C., Yang, Y., & Takebe, N. (2020). Targeting signalling pathways and the immune microenvironment of cancer stem cells - a clinical update. *Nature reviews. Clinical oncology*, 17(4), 204–232. <https://doi.org/10.1038/s41571-019-0293-2>
- (208) Bénit, L., Calteau, A., & Heidmann, T. (2003). Characterization of the low-copy HERV-Fc family: evidence for recent integrations in primates of elements with coding envelope genes. *Virology*, 312(1), 159–168. [https://doi.org/10.1016/s0042-6822\(03\)00163-6](https://doi.org/10.1016/s0042-6822(03)00163-6)
- (209) Henrich, S., Cameron, A., Bourenkov, G. P., Kiefersauer, R., Huber, R., Lindberg, I., Bode, W., & Than, M. E. (2003). The crystal structure of the proprotein processing proteinase furin explains its stringent specificity. *Nature structural biology*, 10(7), 520–526. <https://doi.org/10.1038/nsb941>
- (210) Apte, S., & Sanders, D. A. (2010). Effects of retroviral envelope-protein cleavage upon trafficking, incorporation, and membrane fusion. *Virology*, 405(1), 214–224. <https://doi.org/10.1016/j.virol.2010.06.004>
- (211) Dewannieux, M., Blaise, S., & Heidmann, T. (2005). Identification of a functional envelope protein from the HERV-K family of human endogenous retroviruses. *Journal of virology*, 79(24), 15573–15577. <https://doi.org/10.1128/JVI.79.24.15573-15577.2005>
- (212) Michaud, H. A., de Mulder, M., SenGupta, D., Deeks, S. G., Martin, J. N., Pilcher, C. D., Hecht, F. M., Sacha, J. B., & Nixon, D. F. (2014). Trans-activation, post-transcriptional maturation, and induction of antibodies to HERV-K (HML-2) envelope transmembrane protein in HIV-1 infection. *Retrovirology*, 11, 10. <https://doi.org/10.1186/1742-4690-11-10>

- (213) Forrest, M. E., Pinkard, O., Martin, S., Sweet, T. J., Hanson, G., & Collier, J. (2020). Codon and amino acid content are associated with mRNA stability in mammalian cells. *PLoS one*, *15*(2), e0228730. <https://doi.org/10.1371/journal.pone.0228730>
- (214) Zuker M. (2003). Mfold web server for nucleic acid folding and hybridization prediction. *Nucleic acids research*, *31*(13), 3406–3415. <https://doi.org/10.1093/nar/gkg595>
- (215) Bao, C., Zhu, M., Nykonchuk, I., Wakabayashi, H., Mathews, D. H., & Ermolenko, D. N. (2022). Specific length and structure rather than high thermodynamic stability enable regulatory mRNA stem-loops to pause translation. *Nature communications*, *13*(1), 988. <https://doi.org/10.1038/s41467-022-28600-5>
- (216) Zhang, Y. J., Pan, H. Y., & Gao, S. J. (2001). Reverse transcription slippage over the mRNA secondary structure of the LIP1 gene. *BioTechniques*, *31*(6), . <https://doi.org/10.2144/01316st02>
- (217) Bao, C., Loerch, S., Ling, C., Korostelev, A. A., Grigorieff, N., & Ermolenko, D. N. (2020). mRNA stem-loops can pause the ribosome by hindering A-site tRNA binding. *eLife*, *9*, e55799. <https://doi.org/10.7554/eLife.55799>
- (218) Brierley I. (1995). Ribosomal frameshifting viral RNAs. *The Journal of general virology*, *76* (Pt 8), 1885–1892. <https://doi.org/10.1099/0022-1317-76-8-1885>
- (219) Advani, V. M., & Dinman, J. D. (2016). Reprogramming the genetic code: The emerging role of ribosomal frameshifting in regulating cellular gene expression. *BioEssays : news and reviews in molecular, cellular and developmental biology*, *38*(1), 21–26. <https://doi.org/10.1002/bies.201500131>
- (220) Dulude, D., Baril, M., & Brakier-Gingras, L. (2002). Characterization of the frameshift stimulatory signal controlling a programmed -1 ribosomal frameshift in the human immunodeficiency virus type 1. *Nucleic acids research*, *30*(23), 5094–5102. <https://doi.org/10.1093/nar/gkf657>
- (221) Staple, D. W., & Butcher, S. E. (2003). Solution structure of the HIV-1 frameshift inducing stem-loop RNA. *Nucleic acids research*, *31*(15), 4326–4331. <https://doi.org/10.1093/nar/gkg654>
- (222) Giedroc, D. P., & Cornish, P. V. (2009). Frameshifting RNA pseudoknots: structure and mechanism. *Virus research*, *139*(2), 193–208. <https://doi.org/10.1016/j.virusres.2008.06.008>
- (223) Kim, H. K., Liu, F., Fei, J., Bustamante, C., Gonzalez, R. L., Jr, & Tinoco, I., Jr (2014). A frameshifting stimulatory stem loop destabilizes the hybrid state and impedes ribosomal translocation. *Proceedings of the National Academy of Sciences of the United States of America*, *111*(15), 5538–5543. <https://doi.org/10.1073/pnas.1403457111>
- (224) Korniy, N., Samatova, E., Anokhina, M. M., Peske, F., & Rodnina, M. V. (2019). Mechanisms and biomedical implications of -1 programmed ribosome frameshifting on viral

- and bacterial mRNAs. *FEBS letters*, 593(13), 1468–1482. <https://doi.org/10.1002/1873-3468.13478>
- (225) Dittmar, K. A., Goodenbour, J. M., & Pan, T. (2006). Tissue-specific differences in human transfer RNA expression. *PLoS genetics*, 2(12), e221. <https://doi.org/10.1371/journal.pgen.0020221>
- (226) Rak, R., Dahan, O., & Pilpel, Y. (2018). Repertoires of tRNAs: The Couplers of Genomics and Proteomics. *Annual review of cell and developmental biology*, 34, 239–264. <https://doi.org/10.1146/annurev-cellbio-100617-062754>
- (227) Netzer, N., Goodenbour, J. M., David, A., Dittmar, K. A., Jones, R. B., Schneider, J. R., Boone, D., Eves, E. M., Rosner, M. R., Gibbs, J. S., Embry, A., Dolan, B., Das, S., Hickman, H. D., Berglund, P., Bennink, J. R., Yewdell, J. W., & Pan, T. (2009). Innate immune and chemically triggered oxidative stress modifies translational fidelity. *Nature*, 462(7272), 522–526. <https://doi.org/10.1038/nature08576>
- (228) Kirchner, S., & Ignatova, Z. (2015). Emerging roles of tRNA in adaptive translation, signalling dynamics and disease. *Nature reviews. Genetics*, 16(2), 98–112. <https://doi.org/10.1038/nrg3861>
- (229) van Weringh, A., Ragonnet-Cronin, M., Pranckeviciene, E., Pavon-Eternod, M., Kleiman, L., & Xia, X. (2011). HIV-1 modulates the tRNA pool to improve translation efficiency. *Molecular biology and evolution*, 28(6), 1827–1834. <https://doi.org/10.1093/molbev/msr005>
- (230) Pavon-Eternod, M., David, A., Dittmar, K., Berglund, P., Pan, T., Bennink, J. R., & Yewdell, J. W. (2013). Vaccinia and influenza A viruses select rather than adjust tRNAs to optimize translation. *Nucleic acids research*, 41(3), 1914–1921. <https://doi.org/10.1093/nar/gks986>
- (231) Herbst, H., Sauter, M., & Mueller-Lantzsch, N. (1996). Expression of human endogenous retrovirus K elements in germ cell and trophoblastic tumors. *The American journal of pathology*, 149(5), 1727–1735. PMID: 8909261; PMCID: PMC1865275.
- (232) Santoni, F. A., Guerra, J., & Luban, J. (2012). HERV-H RNA is abundant in human embryonic stem cells and a precise marker for pluripotency. *Retrovirology*, 9, 111. <https://doi.org/10.1186/1742-4690-9-111>
- (233) Sun, T., Xu, Y., Xiang, Y., Ou, J., Soderblom, E. J., & Diao, Y. (2023). Crosstalk between RNA m⁶A and DNA methylation regulates transposable element chromatin activation and cell fate in human pluripotent stem cells. *Nature genetics*, 55(8), 1324–1335. <https://doi.org/10.1038/s41588-023-01452-5>
- (234) Hoehner, J. C., Gestblom, C., Hedborg, F., Sandstedt, B., Olsen, L., & Pahlman, S. (1996). A developmental model of neuroblastoma: differentiating stroma-poor tumors'

- progress along an extra-adrenal chromaffin lineage. *Laboratory investigation; a journal of technical methods and pathology*, 75(5), 659–675. PMID: 8941212.
- (235) Kamijo T. (2012). Role of stemness-related molecules in neuroblastoma. *Pediatric research*, 71(4 Pt 2), 511–515. <https://doi.org/10.1038/pr.2011.54>
- (236) Walton, J. D., Kattan, D. R., Thomas, S. K., Spengler, B. A., Guo, H. F., Biedler, J. L., Cheung, N. K., & Ross, R. A. (2004). Characteristics of stem cells from human neuroblastoma cell lines and in tumors. *Neoplasia (New York, N.Y.)*, 6(6), 838–845. <https://doi.org/10.1593/neo.04310>
- (237) Zimmerman, M. W., Liu, Y., He, S., Durbin, A. D., Abraham, B. J., Easton, J., Shao, Y., Xu, B., Zhu, S., Zhang, X., Li, Z., Weichert-Leahey, N., Young, R. A., Zhang, J., & Look, A. T. (2018). MYC Drives a Subset of High-Risk Pediatric Neuroblastomas and Is Activated through Mechanisms Including Enhancer Hijacking and Focal Enhancer Amplification. *Cancer discovery*, 8(3), 320–335. <https://doi.org/10.1158/2159-8290.CD-17-0993>
- (238) Matsuno, R., Gifford, A. J., Fang, J., Warren, M., Lukeis, R. E., Trahair, T., Sugimoto, T., Marachelian, A., Asgharzadeh, S., Maris, J. M., Ikegaki, N., & Shimada, H. (2018). Rare MYC-amplified Neuroblastoma With Large Cell Histology. *Pediatric and developmental pathology : the official journal of the Society for Pediatric Pathology and the Paediatric Pathology Society*, 21(5), 461–466. <https://doi.org/10.1177/1093526617749670>
- (239) Zafar, A., Wang, W., Liu, G., Wang, X., Xian, W., McKeon, F., Foster, J., Zhou, J., & Zhang, R. (2021). Molecular targeting therapies for neuroblastoma: Progress and challenges. *Medicinal research reviews*, 41(2), 961–1021. <https://doi.org/10.1002/med.21750>
- (240) Ziller, C., Dupin, E., Brazeau, P., Paulin, D., & Le Douarin, N. M. (1983). Early segregation of a neuronal precursor cell line in the neural crest as revealed by culture in a chemically defined medium. *Cell*, 32(2), 627–638. [https://doi.org/10.1016/0092-8674\(83\)90482-8](https://doi.org/10.1016/0092-8674(83)90482-8)
- (241) Löfstedt, T., Jögi, A., Sigvardsson, M., Gradin, K., Poellinger, L., Pählman, S., & Axelsson, H. (2004). Induction of ID2 expression by hypoxia-inducible factor-1: a role in dedifferentiation of hypoxic neuroblastoma cells. *The Journal of biological chemistry*, 279(38), 39223–39231. <https://doi.org/10.1074/jbc.M402904200>
- (242) Hörner, S. J., Couturier, N., Bruch, R., Koch, P., Hafner, M., & Rudolf, R. (2021). hiPSC-Derived Schwann Cells Influence Myogenic Differentiation in Neuromuscular Cocultures. *Cells*, 10(12), 3292. <https://doi.org/10.3390/cells10123292>
- (243) Maruyama, H., Kleeff, J., Wildi, S., Friess, H., Büchler, M. W., Israel, M. A., & Korc, M. (1999). Id-1 and Id-2 are overexpressed in pancreatic cancer and in dysplastic lesions in chronic pancreatitis. *The American journal of pathology*, 155(3), 815–822. [https://doi.org/10.1016/S0002-9440\(10\)65180-2](https://doi.org/10.1016/S0002-9440(10)65180-2)

- (244) Langlands, K., Down, G. A., & Kealey, T. (2000). Id proteins are dynamically expressed in normal epidermis and dysregulated in squamous cell carcinoma. *Cancer research*, *60*(21), 5929–5933. PMID: 11085505.
- (245) Lin, C. Q., Singh, J., Murata, K., Itahana, Y., Parrinello, S., Liang, S. H., Gillett, C. E., Campisi, J., & Desprez, P. Y. (2000). A role for Id-1 in the aggressive phenotype and steroid hormone response of human breast cancer cells. *Cancer research*, *60*(5), 1332–1340. PMID: 10728695.
- (246) Desprez, P. Y., Hara, E., Bissell, M. J., & Campisi, J. (1995). Suppression of mammary epithelial cell differentiation by the helix-loop-helix protein Id-1. *Molecular and cellular biology*, *15*(6), 3398–3404. <https://doi.org/10.1128/MCB.15.6.3398>
- (247) Desprez, P. Y., Lin, C. Q., Thomasset, N., Sympson, C. J., Bissell, M. J., & Campisi, J. (1998). A novel pathway for mammary epithelial cell invasion induced by the helix-loop-helix protein Id-1. *Molecular and cellular biology*, *18*(8), 4577–4588. <https://doi.org/10.1128/MCB.18.8.4577>
- (248) Lyden, D., Young, A. Z., Zagzag, D., Yan, W., Gerald, W., O'Reilly, R., Bader, B. L., Hynes, R. O., Zhuang, Y., Manova, K., & Benezra, R. (1999). Id1 and Id3 are required for neurogenesis, angiogenesis and vascularization of tumour xenografts. *Nature*, *401*(6754), 670–677. <https://doi.org/10.1038/44334>
- (249) Iavarone, A., Garg, P., Lasorella, A., Hsu, J., & Israel, M. A. (1994). The helix-loop-helix protein Id-2 enhances cell proliferation and binds to the retinoblastoma protein. *Genes & development*, *8*(11), 1270–1284. <https://doi.org/10.1101/gad.8.11.1270>
- (250) Lasorella, A., Nosedà, M., Beyna, M., Yokota, Y., & Iavarone, A. (2000). Id2 is a retinoblastoma protein target and mediates signalling by Myc oncoproteins. *Nature*, *407*(6804), 592–598. <https://doi.org/10.1038/35036504>
- (251) Lasorella, A., Boldrini, R., Dominici, C., Donfrancesco, A., Yokota, Y., Inserra, A., & Iavarone, A. (2002). Id2 is critical for cellular proliferation and is the oncogenic effector of N-myc in human neuroblastoma. *Cancer research*, *62*(1), 301–306. PMID: 11782392.
- (252) Zhao, Z., Bo, Z., Gong, W., & Guo, Y. (2020). Inhibitor of Differentiation 1 (Id1) in Cancer and Cancer Therapy. *International journal of medical sciences*, *17*(8), 995–1005. <https://doi.org/10.7150/ijms.42805>
- (253) Jögi, A., Øra, I., Nilsson, H., Lindeheim, A., Makino, Y., Poellinger, L., Axelson, H., & Pålman, S. (2002). Hypoxia alters gene expression in human neuroblastoma cells toward an immature and neural crest-like phenotype. *Proceedings of the National Academy of Sciences of the United States of America*, *99*(10), 7021–7026. <https://doi.org/10.1073/pnas.102660199>
- (254) Du, Y., & Yip, H. (2010). Effects of bone morphogenetic protein 2 on Id expression and neuroblastoma cell differentiation. *Differentiation; research in biological diversity*, *79*(2), 84–92. <https://doi.org/10.1016/j.diff.2009.10.003>

- (255) Prasad, M. S., Sauka-Spengler, T., & LaBonne, C. (2012). Induction of the neural crest state: control of stem cell attributes by gene regulatory, post-transcriptional and epigenetic interactions. *Developmental biology*, 366(1), 10–21. <https://doi.org/10.1016/j.ydbio.2012.03.014>
- (256) Light, W., Vernon, A. E., Lasorella, A., Iavarone, A., & LaBonne, C. (2005). Xenopus Id3 is required downstream of Myc for the formation of multipotent neural crest progenitor cells. *Development (Cambridge, England)*, 132(8), 1831–1841. <https://doi.org/10.1242/dev.01734>
- (257) Kim, J., Lo, L., Dormand, E., & Anderson, D. J. (2003). SOX10 maintains multipotency and inhibits neuronal differentiation of neural crest stem cells. *Neuron*, 38(1), 17–31. [https://doi.org/10.1016/s0896-6273\(03\)00163-6](https://doi.org/10.1016/s0896-6273(03)00163-6)
- (258) McKeown, S. J., Lee, V. M., Bronner-Fraser, M., Newgreen, D. F., & Farlie, P. G. (2005). Sox10 overexpression induces neural crest-like cells from all dorsoventral levels of the neural tube but inhibits differentiation. *Developmental dynamics : an official publication of the American Association of Anatomists*, 233(2), 430–444. <https://doi.org/10.1002/dvdy.20341>
- (259) Mundell, N. A., & Labosky, P. A. (2011). Neural crest stem cell multipotency requires Foxd3 to maintain neural potential and repress mesenchymal fates. *Development (Cambridge, England)*, 138(4), 641–652. <https://doi.org/10.1242/dev.054718>
- (260) McCaughan, G. W., Clark, M. J., & Barclay, A. N. (1987). Characterization of the human homolog of the rat MRC OX-2 membrane glycoprotein. *Immunogenetics*, 25(5), 329–335. <https://doi.org/10.1007/BF00404426>
- (261) Wright, G. J., Jones, M., Puklavec, M. J., Brown, M. H., & Barclay, A. N. (2001). The unusual distribution of the neuronal/lymphoid cell surface CD200 (OX2) glycoprotein is conserved in humans. *Immunology*, 102(2), 173–179. <https://doi.org/10.1046/j.1365-2567.2001.01163.x>
- (262) Liu, J. Q., Hu, A., Zhu, J., Yu, J., Talebian, F., & Bai, X. F. (2020). CD200-CD200R Pathway in the Regulation of Tumor Immune Microenvironment and Immunotherapy. *Advances in experimental medicine and biology*, 1223, 155–165. https://doi.org/10.1007/978-3-030-35582-1_8
- (263) Liao, K. L., Bai, X. F., & Friedman, A. (2013). The role of CD200-CD200R in tumor immune evasion. *Journal of theoretical biology*, 328, 65–76. <https://doi.org/10.1016/j.jtbi.2013.03.017>
- (264) Choe, D., & Choi, D. (2023). Cancel cancer: The immunotherapeutic potential of CD200/CD200R blockade. *Frontiers in oncology*, 13, 1088038. <https://doi.org/10.3389/fonc.2023.1088038>
- (265) Moreaux, J., Hose, D., Reme, T., Jourdan, E., Hundemer, M., Legouffe, E., Moine, P., Bourin, P., Moos, M., Corre, J., Möhler, T., De Vos, J., Rossi, J. F., Goldschmidt, H., & Klein,

- B. (2006). CD200 is a new prognostic factor in multiple myeloma. *Blood*, *108*(13), 4194–4197. <https://doi.org/10.1182/blood-2006-06-029355>
- (266) Love, J. E., Thompson, K., Kilgore, M. R., Westerhoff, M., Murphy, C. E., Papanicolaou-Sengos, A., McCormick, K. A., Shankaran, V., Vandeven, N., Miller, F., Blom, A., Nghiem, P. T., & Kussick, S. J. (2017). CD200 Expression in Neuroendocrine Neoplasms. *American journal of clinical pathology*, *148*(3), 236–242. <https://doi.org/10.1093/ajcp/axx071>
- (267) Petermann, K. B., Rozenberg, G. I., Zedek, D., Groben, P., McKinnon, K., Buehler, C., Kim, W. Y., Shields, J. M., Penland, S., Bear, J. E., Thomas, N. E., Serody, J. S., & Sharpless, N. E. (2007). CD200 is induced by ERK and is a potential therapeutic target in melanoma. *The Journal of clinical investigation*, *117*(12), 3922–3929. <https://doi.org/10.1172/JCI32163>
- (268) Alapat, D., Coviello-Malle, J., Owens, R., Qu, P., Barlogie, B., Shaughnessy, J. D., & Lorschach, R. B. (2012). Diagnostic usefulness and prognostic impact of CD200 expression in lymphoid malignancies and plasma cell myeloma. *American journal of clinical pathology*, *137*(1), 93–100. <https://doi.org/10.1309/AJCP59UORCYZEVQO>
- (269) Siva, A., Xin, H., Qin, F., Oltean, D., Bowdish, K. S., & Kretz-Rommel, A. (2008). Immune modulation by melanoma and ovarian tumor cells through expression of the immunosuppressive molecule CD200. *Cancer immunology, immunotherapy : CII*, *57*(7), 987–996. <https://doi.org/10.1007/s00262-007-0429-6>
- (270) Xin, C., Zhu, J., Gu, S., Yin, M., Ma, J., Pan, C., Tang, J., Zhang, P., Liu, Y., Bai, X. F., Mo, X., Xu, M., & Zhu, H. (2020). CD200 is overexpressed in neuroblastoma and regulates tumor immune microenvironment. *Cancer immunology, immunotherapy : CII*, *69*(11), 2333–2343. <https://doi.org/10.1007/s00262-020-02589-6>
- (271) Clark, D. A., Dhesy-Thind, S., Ellis, P., & Ramsay, J. (2014). The CD200-tolerance signaling molecule associated with pregnancy success is present in patients with early-stage breast cancer but does not favor nodal metastasis. *American journal of reproductive immunology (New York, N.Y. : 1989)*, *72*(5), 435–439. <https://doi.org/10.1111/aji.12297>
- (272) Erin, N., Podnos, A., Tanriover, G., Duymuş, Ö., Cote, E., Khatri, I., & Gorczynski, R. M. (2015). Bidirectional effect of CD200 on breast cancer development and metastasis, with ultimate outcome determined by tumor aggressiveness and a cancer-induced inflammatory response. *Oncogene*, *34*(29), 3860–3870. <https://doi.org/10.1038/onc.2014.317>
- (273) Bustamante Rivera, Y. Y., Brütting, C., Schmidt, C., Volkmer, I., & Staeger, M. S. (2018). Endogenous Retrovirus 3 - History, Physiology, and Pathology. *Frontiers in microbiology*, *8*, 2691. <https://doi.org/10.3389/fmicb.2017.02691>
- (274) Lee, S. H., Kang, Y. J., Jo, J. O., Ock, M. S., Baek, K. W., Eo, J., Lee, W. J., Choi, Y. H., Kim, W. J., Leem, S. H., Kim, H. S., & Cha, H. J. (2014). Elevation of human ERV3-1 env protein expression in colorectal cancer. *Journal of clinical pathology*, *67*(9), 840–844. <https://doi.org/10.1136/jclinpath-2013-202089>

- (275) Strissel, P. L., Ruebner, M., Thiel, F., Wachter, D., Ekici, A. B., Wolf, F., Thieme, F., Ruprecht, K., Beckmann, M. W., & Strick, R. (2012). Reactivation of codogenic endogenous retroviral (ERV) envelope genes in human endometrial carcinoma and prestages: Emergence of new molecular targets. *Oncotarget*, 3(10), 1204–1219. <https://doi.org/10.18632/oncotarget.679>
- (276) Taruscio, D., Florida, G., Zoraqi, G. K., Mantovani, A., & Falbo, V. (2002). Organization and integration sites in the human genome of endogenous retroviral sequences belonging to HERV-E family. *Mammalian genome : official journal of the International Mammalian Genome Society*, 13(4), 216–222. <https://doi.org/10.1007/s00335-001-2118-7>
- (277) Repaske, R., Steele, P. E., O'Neill, R. R., Rabson, A. B., & Martin, M. A. (1985). Nucleotide sequence of a full-length human endogenous retroviral segment. *Journal of virology*, 54(3), 764–772. <https://doi.org/10.1128/JVI.54.3.764-772.1985>
- (278) Turbeville, M. A., Rhodes, J. C., Hyams, D. M., Distler, C. M., & Steele, P. E. (1997). Characterization of a putative retroviral env-related human protein. *Pathobiology : journal of immunopathology, molecular and cellular biology*, 65(3), 123–128. <https://doi.org/10.1159/000164113>
- (279) Wang-Johanning, F., Frost, A. R., Jian, B., Azerou, R., Lu, D. W., Chen, D. T., & Johanning, G. L. (2003). Detecting the expression of human endogenous retrovirus E envelope transcripts in human prostate adenocarcinoma. *Cancer*, 98(1), 187–197. <https://doi.org/10.1002/cncr.11451>
- (280) Yi, J. M., & Kim, H. S. (2007). Molecular phylogenetic analysis of the human endogenous retrovirus E (HERV-E) family in human tissues and human cancers. *Genes & genetic systems*, 82(1), 89–98. <https://doi.org/10.1266/ggs.82.89>
- (281) Stricker, E., Peckham-Gregory, E. C., & Scheurer, M. E. (2023). CancerHERVdb: Human Endogenous Retrovirus (HERV) Expression Database for Human Cancer Accelerates Studies of the Retrovirome and Predictions for HERV-Based Therapies. *Journal of virology*, 97(6), e0005923. <https://doi.org/10.1128/jvi.00059-23>
- (282) Weyerer, V., Strissel, P. L., Stöhr, C., Eckstein, M., Wach, S., Taubert, H., Brandl, L., Geppert, C. I., Wullich, B., Cynis, H., Beckmann, M. W., Seliger, B., Hartmann, A., & Strick, R. (2021). Endogenous Retroviral-K Envelope Is a Novel Tumor Antigen and Prognostic Indicator of Renal Cell Carcinoma. *Frontiers in oncology*, 11, 657187. <https://doi.org/10.3389/fonc.2021.657187>
- (283) Buslei, R., Strissel, P. L., Henke, C., Schey, R., Lang, N., Ruebner, M., Stolt, C. C., Fabry, B., Buchfelder, M., & Strick, R. (2015). Activation and regulation of endogenous retroviral genes in the human pituitary gland and related endocrine tumours. *Neuropathology and applied neurobiology*, 41(2), 180–200. <https://doi.org/10.1111/nan.12136>

- (284) Gray, L. R., Jackson, R. E., Jackson, P. E. H., Bekiranov, S., Rekosh, D., & Hammar skjöld, M. L. (2019). HIV-1 Rev interacts with HERV-K RcREs present in the human genome and promotes export of unspliced HERV-K proviral RNA. *Retrovirology*, 16(1), 40. <https://doi.org/10.1186/s12977-019-0505-y>
- (285) Christensen T. (2006). The role of EBV in MS pathogenesis. *International MS journal*, 13(2), 52–57. PMID: 16635422.
- (286) Lassmann H. (2019). Pathogenic Mechanisms Associated With Different Clinical Courses of Multiple Sclerosis. *Frontiers in immunology*, 9, 3116. <https://doi.org/10.3389/fimmu.2018.03116>
- (287) Greenfield, A. L., & Hauser, S. L. (2018). B-cell Therapy for Multiple Sclerosis: Entering an era. *Annals of neurology*, 83(1), 13–26. <https://doi.org/10.1002/ana.25119>
- (288) Sellebjerg, F., Blinkenberg, M., & Sorensen, P. S. (2020). Anti-CD20 Monoclonal Antibodies for Relapsing and Progressive Multiple Sclerosis. *CNS drugs*, 34(3), 269–280. <https://doi.org/10.1007/s40263-020-00704-w>
- (289) Frisch, E. S., Pretzsch, R., & Weber, M. S. (2021). A Milestone in Multiple Sclerosis Therapy: Monoclonal Antibodies Against CD20-Yet Progress Continues. *Neurotherapeutics : the journal of the American Society for Experimental NeuroTherapeutics*, 18(3), 1602–1622. <https://doi.org/10.1007/s13311-021-01048-z>
- (290) 't Hart, B. A., Jagessar, S. A., Haanstra, K., Verschoor, E., Laman, J. D., & Kap, Y. S. (2013). The Primate EAE Model Points at EBV-Infected B Cells as a Preferential Therapy Target in Multiple Sclerosis. *Frontiers in immunology*, 4, 145. <https://doi.org/10.3389/fimmu.2013.00145>
- (291) Oh, J. H., Kim, Y. J., Moon, S., Nam, H. Y., Jeon, J. P., Lee, J. H., Lee, J. Y., & Cho, Y. S. (2013). Genotype instability during long-term subculture of lymphoblastoid cell lines. *Journal of human genetics*, 58(1), 16–20. <https://doi.org/10.1038/jhg.2012.123>
- (292) Toritsuka, M., Makinodan, M., Yamauchi, T., Yamashita, Y., Ikawa, D., Komori, T., Kimoto, S., Hamano-Iwasa, K., Matsuzaki, H., & Kishimoto, T. (2018). Altered gene expression in lymphoblastoid cell lines after subculture. *In vitro cellular & developmental biology. Animal*, 54(7), 523–527. <https://doi.org/10.1007/s11626-018-0267-1>
- (293) Hsiao, F. C., Lin, M., Tai, A., Chen, G., & Huber, B. T. (2006). Cutting edge: Epstein-Barr virus transactivates the HERV-K18 superantigen by docking to the human complement receptor 2 (CD21) on primary B cells. *Journal of immunology (Baltimore, Md. : 1950)*, 177(4), 2056–2060. <https://doi.org/10.4049/jimmunol.177.4.2056>
- (294) Vrazo, A. C., Chauchard, M., Raab-Traub, N., & Longnecker, R. (2012). Epstein-Barr virus LMP2A reduces hyperactivation induced by LMP1 to restore normal B cell phenotype in transgenic mice. *PLoS pathogens*, 8(4), e1002662. <https://doi.org/10.1371/journal.ppat.1002662>

- (295) Panagopoulos, D., Victoratos, P., Alexiou, M., Kollias, G., & Mosialos, G. (2004). Comparative analysis of signal transduction by CD40 and the Epstein-Barr virus oncoprotein LMP1 in vivo. *Journal of virology*, 78(23), 13253–13261. <https://doi.org/10.1128/JVI.78.23.13253-13261.2004>
- (296) Rasmussen, H. B., Geny, C., Deforges, L., Perron, H., Tourtelotte, W., Heltberg, A., & Clausen, J. (1995). Expression of endogenous retroviruses in blood mononuclear cells and brain tissue from multiple sclerosis patients. *Multiple sclerosis (Houndmills, Basingstoke, England)*, 1(2), 82–87. <https://doi.org/10.1177/135245859500100205>
- (297) Rasmussen, H. B., Heltberg, A., Lisby, G., & Clausen, J. (1996). Three allelic forms of the human endogenous retrovirus, ERV3, and their frequencies in multiple sclerosis patients and healthy individuals. *Autoimmunity*, 23(2), 111–117. <https://doi.org/10.3109/08916939608995334>
- (298) Pisano, M. P., Grandi, N., Cadeddu, M., Blomberg, J., & Tramontano, E. (2019). Comprehensive Characterization of the Human Endogenous Retrovirus HERV-K(HML-6) Group: Overview of Structure, Phylogeny, and Contribution to the Human Genome. *Journal of virology*, 93(16), e00110-19. <https://doi.org/10.1128/JVI.00110-19>
- (299) Schiavetti, F., Thonnard, J., Colau, D., Boon, T., & Coulie, P. G. (2002). A human endogenous retroviral sequence encoding an antigen recognized on melanoma by cytolytic T lymphocytes. *Cancer research*, 62(19), 5510–5516. PMID: 12359761.
- (300) Seifarth, W., Frank, O., Zeilfelder, U., Spiess, B., Greenwood, A. D., Hehlmann, R., & Leib-Mösch, C. (2005). Comprehensive analysis of human endogenous retrovirus transcriptional activity in human tissues with a retrovirus-specific microarray. *Journal of virology*, 79(1), 341–352. <https://doi.org/10.1128/JVI.79.1.341-352.2005>
- (301) Zhang, H., Wang, Y., & Lu, J. (2019). Identification of lung-adenocarcinoma-related long non-coding RNAs by random walking on a competing endogenous RNA network. *Annals of translational medicine*, 7(14), 339. <https://doi.org/10.21037/atm.2019.06.69>
- (302) Lin, J., Zhang, X., Xue, C., Zhang, H., Shashaty, M. G., Gosai, S. J., Meyer, N., Grazioli, A., Hinkle, C., Caughey, J., Li, W., Susztak, K., Gregory, B. D., Li, M., & Reilly, M. P. (2015). The long noncoding RNA landscape in hypoxic and inflammatory renal epithelial injury. *American journal of physiology. Renal physiology*, 309(11), F901–F913. <https://doi.org/10.1152/ajprenal.00290.2015>
- (303) Shah, A. H., Govindarajan, V., Doucet-O'Hare, T. T., Rivas, S., Ampie, L., DeMarino, C., Banasavadi-Siddegowda, Y. K., Zhang, Y., Johnson, K. R., Almsned, F., Gilbert, M. R., Heiss, J. D., & Nath, A. (2022). Differential expression of an endogenous retroviral element [HERV-K(HML-6)] is associated with reduced survival in glioblastoma patients. *Scientific reports*, 12(1), 6902. <https://doi.org/10.1038/s41598-022-10914-5>

- (304) Mugneret, F., Chaffanet, M., Maynadié, M., Guasch, G., Favre, B., Casasnovas, O., Birnbaum, D., & Pébusque, M. J. (2000). The 8p12 myeloproliferative disorder. t(8;19)(p12;q13.3): a novel translocation involving the FGFR1 gene. *British journal of haematology*, *111*(2), 647–649. <https://doi.org/10.1046/j.1365-2141.2000.02355.x>
- (305) Guasch, G., Popovici, C., Mugneret, F., Chaffanet, M., Pontarotti, P., Birnbaum, D., & Pébusque, M. J. (2003). Endogenous retroviral sequence is fused to FGFR1 kinase in the 8p12 stem-cell myeloproliferative disorder with t(8;19)(p12;q13.3). *Blood*, *101*(1), 286–288. <https://doi.org/10.1182/blood-2002-02-0577>
- (306) Liu, Z., Mi, M., Li, X., Zheng, X., Wu, G., & Zhang, L. (2019). lncRNA OSTN-AS1 May Represent a Novel Immune-Related Prognostic Marker for Triple-Negative Breast Cancer Based on Integrated Analysis of a ceRNA Network. *Frontiers in genetics*, *10*, 850. <https://doi.org/10.3389/fgene.2019.00850>
- (307) Liao, X., Wang, X., Huang, K., Han, C., Deng, J., Yu, T., Yang, C., Huang, R., Liu, X., Yu, L., Zhu, G., Su, H., Qin, W., Zeng, X., Han, B., Han, Q., Liu, Z., Zhou, X., Gong, Y., Liu, Z., Huang, J., Winkler, C. A., O'Brien, S. J., Ye, X., Peng, T. (2019). Integrated analysis of competing endogenous RNA network revealing potential prognostic biomarkers of hepatocellular carcinoma. *Journal of Cancer*, *10*(14), 3267–3283. <https://doi.org/10.7150/jca.29986>
- (308) Subramanian, R. P., Wildschutte, J. H., Russo, C., & Coffin, J. M. (2011). Identification, characterization, and comparative genomic distribution of the HERV-K (HML-2) group of human endogenous retroviruses. *Retrovirology*, *8*, 90. <https://doi.org/10.1186/1742-4690-8-90>
- (309) Hughes, J. F., & Coffin, J. M. (2001). Evidence for genomic rearrangements mediated by human endogenous retroviruses during primate evolution. *Nature genetics*, *29*(4), 487–489. <https://doi.org/10.1038/ng775>
- (310) Cakmak Guner, B., Karlik, E., Marakli, S., & Gozukirmizi, N. (2018). Detection of HERV-K6 and HERV-K11 transpositions in the human genome. *Biomedical reports*, *9*(1), 53–59. <https://doi.org/10.3892/br.2018.1096>
- (311) Grabski, D. F., Ratan, A., Gray, L. R., Bekiranov, S., Rekosh, D., Hammarskjold, M. L., & Rasmussen, S. K. (2021). Upregulation of human endogenous retrovirus-K (HML-2) mRNAs in hepatoblastoma: Identification of potential new immunotherapeutic targets and biomarkers. *Journal of pediatric surgery*, *56*(2), 286–292. <https://doi.org/10.1016/j.jpedsurg.2020.05.022>
- (312) Grabski, D. F., Ratan, A., Gray, L. R., Bekiranov, S., Rekosh, D., Hammarskjold, M. L., & Rasmussen, S. K. (2020). Human endogenous retrovirus-K mRNA expression and genomic alignment data in hepatoblastoma. *Data in brief*, *31*, 105895. <https://doi.org/10.1016/j.dib.2020.105895>

- (313) Gonzalez-Hernandez, M. J., Cavalcoli, J. D., Sartor, M. A., Contreras-Galindo, R., Meng, F., Dai, M., Dube, D., Saha, A. K., Gitlin, S. D., Omenn, G. S., Kaplan, M. H., & Markovitz, D. M. (2014). Regulation of the human endogenous retrovirus K (HML-2) transcriptome by the HIV-1 Tat protein. *Journal of virology*, 88(16), 8924–8935. <https://doi.org/10.1128/JVI.00556-14>
- (314) Gonzalez-Hernandez, M. J., Swanson, M. D., Contreras-Galindo, R., Cookinham, S., King, S. R., Noel, R. J., Jr, Kaplan, M. H., & Markovitz, D. M. (2012). Expression of human endogenous retrovirus type K (HML-2) is activated by the Tat protein of HIV-1. *Journal of virology*, 86(15), 7790–7805. <https://doi.org/10.1128/JVI.07215-11>
- (315) Hughes, J. F., & Coffin, J. M. (2004). Human endogenous retrovirus K solo-LTR formation and insertional polymorphisms: implications for human and viral evolution. *Proceedings of the National Academy of Sciences of the United States of America*, 101(6), 1668–1672. <https://doi.org/10.1073/pnas.0307885100>
- (316) Grandi, N., & Tramontano, E. (2018). Human Endogenous Retroviruses Are Ancient Acquired Elements Still Shaping Innate Immune Responses. *Frontiers in immunology*, 9, 2039. <https://doi.org/10.3389/fimmu.2018.02039>
- (317) Ramasamy, R., Mohammed, F., & Meier, U. C. (2020). HLA DR2b-binding peptides from human endogenous retrovirus envelope, Epstein-Barr virus and brain proteins in the context of molecular mimicry in multiple sclerosis. *Immunology letters*, 217, 15–24. <https://doi.org/10.1016/j.imlet.2019.10.017>
- (318) Schmidt, H., Williamson, D., & Ashley-Koch, A. (2007). HLA-DR15 haplotype and multiple sclerosis: a HuGE review. *American journal of epidemiology*, 165(10), 1097–1109. <https://doi.org/10.1093/aje/kwk118>
- (319) De Silvestri, A., Capittini, C., Mallucci, G., Bergamaschi, R., Rebuffi, C., Pasi, A., Martinetti, M., & Tinelli, C. (2019). The Involvement of HLA Class II Alleles in Multiple Sclerosis: A Systematic Review with Meta-analysis. *Disease markers*, 2019, 1409069. <https://doi.org/10.1155/2019/1409069>
- (320) Garcia-Montojo, M., Rodriguez-Martin, E., Ramos-Mozo, P., Ortega-Madueño, I., Dominguez-Mozo, M. I., Arias-Leal, A., García-Martínez, M. Á., Casanova, I., Galan, V., Arroyo, R., Álvarez-Lafuente, R., & Villar, L. M. (2020). Syncytin-1/HERV-W envelope is an early activation marker of leukocytes and is upregulated in multiple sclerosis patients. *European journal of immunology*, 50(5), 685–694. <https://doi.org/10.1002/eji.201948423>
- (321) Alvarez-Lafuente, R., García-Montojo, M., De Las Heras, V., Domínguez-Mozo, M. I., Bartolome, M., Benito-Martin, M. S., & Arroyo, R. (2008). Herpesviruses and human endogenous retroviral sequences in the cerebrospinal fluid of multiple sclerosis patients. *Multiple sclerosis (Houndmills, Basingstoke, England)*, 14(5), 595–601. <https://doi.org/10.1177/1352458507086425>

- (322) Flockerzi, A., Maydt, J., Frank, O., Ruggieri, A., Maldener, E., Seifarth, W., Medstrand, P., Lengauer, T., Meyerhans, A., Leib-Mösch, C., Meese, E., & Mayer, J. (2007). Expression pattern analysis of transcribed HERV sequences is complicated by ex vivo recombination. *Retrovirology*, 4, 39. <https://doi.org/10.1186/1742-4690-4-39>
- (323) Laufer, G., Mayer, J., Mueller, B. F., Mueller-Lantsch, N., & Ruprecht, K. (2009). Analysis of transcribed human endogenous retrovirus W env loci clarifies the origin of multiple sclerosis-associated retrovirus env sequences. *Retrovirology*, 6, 37. <https://doi.org/10.1186/1742-4690-6-37>
- (324) Ruprecht, K., & Mayer, J. (2019). On the origin of a pathogenic HERV-W envelope protein present in multiple sclerosis lesions. *Proceedings of the National Academy of Sciences of the United States of America*, 116(40), 19791–19792. <https://doi.org/10.1073/pnas.1911703116>
- (325) Kremer, D., Perron, H., & Küry, P. (2019). Reply to Ruprecht and Mayer: Unearthing genomic fossils in the pathogenesis of multiple sclerosis. *Proceedings of the National Academy of Sciences of the United States of America*, 116(40), 19793–19794. <https://doi.org/10.1073/pnas.1912315116>
- (326) Dolei, A., Serra, C., Mameli, G., Pugliatti, M., Sechi, G., Cirotto, M. C., Rosati, G., & Sotgiu, S. (2002). Multiple sclerosis-associated retrovirus (MSRV) in Sardinian MS patients. *Neurology*, 58(3), 471–473. <https://doi.org/10.1212/wnl.58.3.471>
- (327) Cossu, D., Tomizawa, Y., Sechi, L. A., & Hattori, N. (2023). Epstein-Barr Virus and Human Endogenous Retrovirus in Japanese Patients with Autoimmune Demyelinating Disorders. *International journal of molecular sciences*, 24(24), 17151. <https://doi.org/10.3390/ijms242417151>
- (328) Mafi, S., Savadi Oskoe, D., Bannazadeh Baghi, H., Azadi, A., & Ahangar Oskouee, M. (2023). Association of Epstein-Barr Virus (EBV) and Human Endogenous Retroviruses (HERV) with Multiple Sclerosis in Northwest of Iran. *International journal of inflammation*, 2023, 8175628. <https://doi.org/10.1155/2023/8175628>
- (329) Dolei, A., Uleri, E., Iba, G., Caocci, M., Piu, C., & Serra, C. (2015). The aliens inside human DNA: HERV-W/MSRV/syncytin-1 endogenous retroviruses and neurodegeneration. *Journal of infection in developing countries*, 9(6), 577–587. <https://doi.org/10.3855/jidc.6916>
- (330) Pérez-Pérez, S., Domínguez-Mozo, M. I., García-Martínez, M. Á., García-Frontini, M. C., Villarrubia, N., Costa-Frossard, L., Villar, L. M., Arroyo, R., & Álvarez-Lafuente, R. (2021). Anti-Human Herpesvirus 6 A/B Antibodies Titers Correlate With Multiple Sclerosis-Associated Retrovirus Envelope Expression. *Frontiers in immunology*, 12, 798003. <https://doi.org/10.3389/fimmu.2021.798003>
- (331) Serafini, B., Rosicarelli, B., Franciotta, D., Magliozzi, R., Reynolds, R., Cinque, P., Andreoni, L., Trivedi, P., Salvetti, M., Faggioni, A., & Aloisi, F. (2007). Dysregulated

- Epstein-Barr virus infection in the multiple sclerosis brain. *The Journal of experimental medicine*, 204(12), 2899–2912. <https://doi.org/10.1084/jem.20071030>
- (332) Tzartos, J. S., Khan, G., Vossenkamper, A., Cruz-Sadaba, M., Lonardi, S., Sefia, E., Meager, A., Elia, A., Middeldorp, J. M., Clemens, M., Farrell, P. J., Giovannoni, G., & Meier, U. C. (2012). Association of innate immune activation with latent Epstein-Barr virus in active MS lesions. *Neurology*, 78(1), 15–23. <https://doi.org/10.1212/WNL.0b013e31823ed057>
- (333) Hassani, A., Corboy, J. R., Al-Salam, S., & Khan, G. (2018). Epstein-Barr virus is present in the brain of most cases of multiple sclerosis and may engage more than just B cells. *PloS one*, 13(2), e0192109. <https://doi.org/10.1371/journal.pone.0192109>
- (334) Lassmann, H., Niedobitek, G., Aloisi, F., Middeldorp, J. M., & NeuroproMiSe EBV Working Group (2011). Epstein-Barr virus in the multiple sclerosis brain: a controversial issue--report on a focused workshop held in the Centre for Brain Research of the Medical University of Vienna, Austria. *Brain : a journal of neurology*, 134(Pt 9), 2772–2786. <https://doi.org/10.1093/brain/awr197>
- (335) de-Thé, G., Day, N. E., Geser, A., Lavoué, M. F., Ho, J. H., Simons, M. J., Sohler, R., Tukei, P., Vonka, V., & Zavadova, H. (1975). Sero-epidemiology of the Epstein-Barr virus: preliminary analysis of an international study - a review. *IARC scientific publications*, (11 Pt 2), 3–16. PMID: 191375.
- (336) Venkitaraman, A. R., Lenoir, G. M., & John, T. J. (1985). The seroepidemiology of infection due to Epstein-Barr virus in southern India. *Journal of medical virology*, 15(1), 11–16. <https://doi.org/10.1002/jmv.1890150103>
- (337) Levin, L. I., Munger, K. L., O'Reilly, E. J., Falk, K. I., & Ascherio, A. (2010). Primary infection with the Epstein-Barr virus and risk of multiple sclerosis. *Annals of neurology*, 67(6), 824–830. <https://doi.org/10.1002/ana.21978>
- (338) Angelini, D. F., Serafini, B., Piras, E., Severa, M., Coccia, E. M., Rosicarelli, B., Ruggieri, S., Gasperini, C., Buttari, F., Centonze, D., Mechelli, R., Salvetti, M., Borsellino, G., Aloisi, F., & Battistini, L. (2013). Increased CD8+ T cell response to Epstein-Barr virus lytic antigens in the active phase of multiple sclerosis. *PLoS pathogens*, 9(4), e1003220. <https://doi.org/10.1371/journal.ppat.1003220>
- (339) Jilek, S., Schlupe, M., Meylan, P., Vingerhoets, F., Guignard, L., Monney, A., Kleeberg, J., Le Goff, G., Pantaleo, G., & Du Pasquier, R. A. (2008). Strong EBV-specific CD8+ T-cell response in patients with early multiple sclerosis. *Brain : a journal of neurology*, 131(Pt 7), 1712–1721. <https://doi.org/10.1093/brain/awn108>
- (340) Salzer, J., Nyström, M., Hallmans, G., Stenlund, H., Wadell, G., & Sundström, P. (2013). Epstein-Barr virus antibodies and vitamin D in prospective multiple sclerosis biobank samples. *Multiple sclerosis (Houndmills, Basingstoke, England)*, 19(12), 1587–1591. <https://doi.org/10.1177/1352458513483888>

- (341) Ascherio, A., Munger, K. L., Lennette, E. T., Spiegelman, D., Hernán, M. A., Olek, M. J., Hankinson, S. E., & Hunter, D. J. (2001). Epstein-Barr virus antibodies and risk of multiple sclerosis: a prospective study. *JAMA*, 286(24), 3083–3088. <https://doi.org/10.1001/jama.286.24.3083>
- (342) Levin, L. I., Munger, K. L., Rubertone, M. V., Peck, C. A., Lennette, E. T., Spiegelman, D., & Ascherio, A. (2005). Temporal relationship between elevation of Epstein-Barr virus antibody titers and initial onset of neurological symptoms in multiple sclerosis. *JAMA*, 293(20), 2496–2500. <https://doi.org/10.1001/jama.293.20.2496>
- (343) Lünemann, J. D., Tintoré, M., Messmer, B., Strowig, T., Rovira, A., Perkal, H., Caballero, E., Münz, C., Montalban, X., & Comabella, M. (2010). Elevated Epstein-Barr virus-encoded nuclear antigen-1 immune responses predict conversion to multiple sclerosis. *Annals of neurology*, 67(2), 159–169. <https://doi.org/10.1002/ana.21886>
- (344) Tatfi, M., Perthame, E., Hillion, K. H., Dillies, M. A., Menager, H., Hermine, O., & Suarez, F. (2021). Gene expression analysis in EBV-infected ataxia-telangiectasia cell lines by RNA-sequencing reveals protein synthesis defect and immune abnormalities. *Orphanet journal of rare diseases*, 16(1), 288. <https://doi.org/10.1186/s13023-021-01904-3>
- (345) Mentzer, A. J., Brenner, N., Allen, N., Littlejohns, T. J., Chong, A. Y., Cortes, A., Almond, R., Hill, M., Sheard, S., McVean, G., UKB Infection Advisory Board, Collins, R., Hill, A. V. S., & Waterboer, T. (2022). Identification of host-pathogen-disease relationships using a scalable multiplex serology platform in UK Biobank. *Nature communications*, 13(1), 1818. <https://doi.org/10.1038/s41467-022-29307-3>
- (346) Cortese, M., Munger, K. L., Martínez-Lapiscina, E. H., Barro, C., Edan, G., Freedman, M. S., Hartung, H. P., Montalbán, X., Foley, F. W., Penner, I. K., Hemmer, B., Fox, E. J., Schippling, S., Wicklein, E. M., Kappos, L., Kuhle, J., Ascherio, A., & BENEFIT Study Group (2020). Vitamin D, smoking, EBV, and long-term cognitive performance in MS: 11-year follow-up of BENEFIT. *Neurology*, 94(18), e1950–e1960. <https://doi.org/10.1212/WNL.00000000000009371>
- (347) Pierrot-Deseilligny, C., & Souberbielle, J. C. (2010). Is hypovitaminosis D one of the environmental risk factors for multiple sclerosis?. *Brain : a journal of neurology*, 133(Pt 7), 1869–1888. <https://doi.org/10.1093/brain/awq147>
- (348) Décard, B. F., von Ahnen, N., Grunwald, T., Streit, F., Stroet, A., Niggemeier, P., Schottstedt, V., Riggert, J., Gold, R., & Chan, A. (2012). Low vitamin D and elevated immunoreactivity against Epstein-Barr virus before first clinical manifestation of multiple sclerosis. *Journal of neurology, neurosurgery, and psychiatry*, 83(12), 1170–1173. <https://doi.org/10.1136/jnnp-2012-303068>
- (349) Niino M. (2012). Risk factors for multiple sclerosis: decreased vitamin D level and remote Epstein-Barr virus infection in the pre-clinical phase of multiple sclerosis. *Journal of*

- neurology, neurosurgery, and psychiatry*, 83(12), 1135. <https://doi.org/10.1136/jnnp-2012-303245>
- (350) Moosazadeh, M., Nabinezhad-Male, F., Afshari, M., Nasehi, M. M., Shabani, M., Kheradmand, M., & Aghaei, I. (2021). Vitamin D status and disability among patients with multiple sclerosis: a systematic review and meta-analysis. *AIMS neuroscience*, 8(2), 239–253. <https://doi.org/10.3934/Neuroscience.2021013>
- (351) Brütting, C., Stangl, G. I., & Staege, M. S. (2021). Vitamin D, Epstein-Barr virus, and endogenous retroviruses in multiple sclerosis - facts and hypotheses. *Journal of integrative neuroscience*, 20(1), 233–238. <https://doi.org/10.31083/j.jin.2021.01.392>
- (352) Cencioni, M. T., Magliozzi, R., Nicholas, R., Ali, R., Malik, O., Reynolds, R., Borsellino, G., Battistini, L., & Muraro, P. A. (2017). Programmed death 1 is highly expressed on CD8⁺ CD57⁺ T cells in patients with stable multiple sclerosis and inhibits their cytotoxic response to Epstein-Barr virus. *Immunology*, 152(4), 660–676. <https://doi.org/10.1111/imm.12808>
- (353) Vietzen, H., Berger, S. M., Kühner, L. M., Furlano, P. L., Bsteh, G., Berger, T., Rommer, P., & Puchhammer-Stöckl, E. (2023). Ineffective control of Epstein-Barr-virus-induced autoimmunity increases the risk for multiple sclerosis. *Cell*, 186(26), 5705–5718.e13. <https://doi.org/10.1016/j.cell.2023.11.015>
- (354) Pender, M. P., Csurhes, P. A., Lenarczyk, A., Pfluger, C. M., & Burrows, S. R. (2009). Decreased T cell reactivity to Epstein-Barr virus infected lymphoblastoid cell lines in multiple sclerosis. *Journal of neurology, neurosurgery, and psychiatry*, 80(5), 498–505. <https://doi.org/10.1136/jnnp.2008.161018>
- (355) Kusunoki, Y., Huang, H., Fukuda, Y., Ozaki, K., Saito, M., Hirai, Y., & Akiyama, M. (1993). A positive correlation between the precursor frequency of cytotoxic lymphocytes to autologous Epstein-Barr virus-transformed B cells and antibody titer level against Epstein-Barr virus-associated nuclear antigen in healthy seropositive individuals. *Microbiology and immunology*, 37(6), 461–469. <https://doi.org/10.1111/j.1348-0421.1993.tb03237.x>
- (356) Sohlberg, E., Saghafian-Hedengren, S., Rasul, E., Marchini, G., Nilsson, C., Klein, E., Nagy, N., & Sverremark-Ekström, E. (2013). Cytomegalovirus-seropositive children show inhibition of in vitro EBV infection that is associated with CD8⁺CD57⁺ T cell enrichment and IFN- γ . *Journal of immunology (Baltimore, Md. : 1950)*, 191(11), 5669–5676. <https://doi.org/10.4049/jimmunol.1301343>
- (357) Guerrero, G., Ruggieri, S., Picozza, M., Piras, E., Gargano, F., Placido, R., Gasperini, C., Salvetti, M., Buscarinu, M. C., Battistini, L., Borsellino, G., & Angelini, D. F. (2020). EBV-specific CD8 T lymphocytes and B cells during glatiramer acetate therapy in patients with MS. *Neurology(R) neuroimmunology & neuroinflammation*, 7(6), e876. <https://doi.org/10.1212/NXI.0000000000000876>

- (358) Johnson, K. P., Brooks, B. R., Cohen, J. A., Ford, C. C., Goldstein, J., Lisak, R. P., Myers, L. W., Panitch, H. S., Rose, J. W., & Schiffer, R. B. (1995). Copolymer 1 reduces relapse rate and improves disability in relapsing-remitting multiple sclerosis: results of a phase III multicenter, double-blind placebo-controlled trial. The Copolymer 1 Multiple Sclerosis Study Group. *Neurology*, *45*(7), 1268–1276. <https://doi.org/10.1212/wnl.45.7.1268>
- (359) Comi, G., Martinelli, V., Rodegher, M., Moiola, L., Leocani, L., Bajenaru, O., Carra, A., Elovaara, I., Fazekas, F., Hartung, H. P., Hillert, J., King, J., Komoly, S., Lubetzki, C., Montalban, X., Myhr, K. M., Preziosa, P., Ravnborg, M., Rieckmann, P., Rocca, M. A., Wynn, D., Young, C., & Filippi, M. (2013). Effects of early treatment with glatiramer acetate in patients with clinically isolated syndrome. *Multiple sclerosis (Houndmills, Basingstoke, England)*, *19*(8), 1074–1083. <https://doi.org/10.1177/1352458512469695>
- (360) Miller, D. H., Chard, D. T., & Ciccarelli, O. (2012). Clinically isolated syndromes. *The Lancet. Neurology*, *11*(2), 157–169. [https://doi.org/10.1016/S1474-4422\(11\)70274-5](https://doi.org/10.1016/S1474-4422(11)70274-5)
- (361) Confavreux, C., O'Connor, P., Comi, G., Freedman, M. S., Miller, A. E., Olsson, T. P., Wolinsky, J. S., Bagulho, T., Delhay, J. L., Dukovic, D., Truffinet, P., Kappos, L., & TOWER Trial Group (2014). Oral teriflunomide for patients with relapsing multiple sclerosis (TOWER): a randomised, double-blind, placebo-controlled, phase 3 trial. *The Lancet. Neurology*, *13*(3), 247–256. [https://doi.org/10.1016/S1474-4422\(13\)70308-9](https://doi.org/10.1016/S1474-4422(13)70308-9)
- (362) Bar-Or A. (2014). Teriflunomide (Aubagio®) for the treatment of multiple sclerosis. *Experimental neurology*, *262 Pt A*, 57–65. <https://doi.org/10.1016/j.expneurol.2014.06.005>
- (363) Miller, A. E., Wolinsky, J. S., Kappos, L., Comi, G., Freedman, M. S., Olsson, T. P., Bauer, D., Benamor, M., Truffinet, P., O'Connor, P. W., & TOPIC Study Group (2014). Oral teriflunomide for patients with a first clinical episode suggestive of multiple sclerosis (TOPIC): a randomised, double-blind, placebo-controlled, phase 3 trial. *The Lancet. Neurology*, *13*(10), 977–986. [https://doi.org/10.1016/S1474-4422\(14\)70191-7](https://doi.org/10.1016/S1474-4422(14)70191-7)
- (364) Henao-Martínez, A. F., Weinberg, A., Waldman, W. J., & Levi, M. E. (2012). Successful treatment of acyclovir-resistant herpes simplex virus type 2 proctitis with leflunomide in an HIV-infected man. *Journal of clinical virology : the official publication of the Pan American Society for Clinical Virology*, *54*(3), 276–278. <https://doi.org/10.1016/j.jcv.2012.02.026>
- (365) Knight, D. A., Hejmanowski, A. Q., Dierksheide, J. E., Williams, J. W., Chong, A. S., & Waldman, W. J. (2001). Inhibition of herpes simplex virus type 1 by the experimental immunosuppressive agent leflunomide. *Transplantation*, *71*(1), 170–174. <https://doi.org/10.1097/00007890-200101150-00031>
- (366) Mei-Jiao, G., Shi-Fang, L., Yan-Yan, C., Jun-Jun, S., Yue-Feng, S., Ting-Ting, R., Yong-Guang, Z., & Hui-Yun, C. (2019). Antiviral effects of selected IMPDH and DHODH inhibitors against foot and mouth disease virus. *Biomedicine & pharmacotherapy* =

<https://doi.org/10.1016/j.biopha.2019.109305>

- (367) Bilger, A., Plowshay, J., Ma, S., Nawandar, D., Barlow, E. A., Romero-Masters, J. C., Bristol, J. A., Li, Z., Tsai, M. H., Delecluse, H. J., & Kenney, S. C. (2017). Leflunomide/teriflunomide inhibit Epstein-Barr virus (EBV)- induced lymphoproliferative disease and lytic viral replication. *Oncotarget*, 8(27), 44266–44280. <https://doi.org/10.18632/oncotarget.17863>
- (368) Gold, J., Holden, D., Parratt, J., Yiannikas, C., Ahmad, R., Sedhom, M., & Giovannoni, G. (2022). Effect of teriflunomide on Epstein-Barr virus shedding in relapsing-remitting multiple sclerosis patients: Outcomes from a real-world pilot cohort study. *Multiple sclerosis and related disorders*, 68, 104377. <https://doi.org/10.1016/j.msard.2022.104377>
- (369) Domínguez-Mozo, M. I., González-Suárez, I., Villar, L. M., Costa-Frossard, L., Villarrubia, N., Aladro, Y., Pilo, B., Montalbán, X., Comabella, M., Casanova-Peño, I., Martínez-Ginés, M. L., García-Domínguez, J. M., García-Martínez, M. Á., Arroyo, R., & Álvarez-Lafuente, R. (2023). Teriflunomide and Epstein-Barr virus in a Spanish multiple sclerosis cohort: *in vivo* antiviral activity and clinical response. *Frontiers in immunology*, 14, 1248182. <https://doi.org/10.3389/fimmu.2023.1248182>
- (370) Zivadínov, R., Ramanathan, M., Hagemeyer, J., Bergsland, N., Ramasamy, D. P., Durfee, J., Kolb, C., & Weinstock-Guttman, B. (2019). Teriflunomide's effect on humoral response to Epstein-Barr virus and development of cortical gray matter pathology in multiple sclerosis. *Multiple sclerosis and related disorders*, 36, 101388. <https://doi.org/10.1016/j.msard.2019.101388>
- (371) Paul, F., & Berthele, A. (2022). Arzneimittelversorgung bei Multipler Sklerose. In: Schröder, H., Thürmann, P., Telschow, C., Schröder, M., & Busse, R. (eds) *Arzneimittel-Kompass 2022*. Springer, Berlin, Heidelberg. https://doi.org/10.1007/978-3-662-66041-6_9
- (372) Polman, C. H., O'Connor, P. W., Havrdova, E., Hutchinson, M., Kappos, L., Miller, D. H., Phillips, J. T., Lublin, F. D., Giovannoni, G., Wajgt, A., Toal, M., Lynn, F., Panzara, M. A., Sandrock, A. W., & AFFIRM Investigators (2006). A randomized, placebo-controlled trial of natalizumab for relapsing multiple sclerosis. *The New England journal of medicine*, 354(9), 899–910. <https://doi.org/10.1056/NEJMoa044397>
- (373) Miller, D. H., Soon, D., Fernando, K. T., MacManus, D. G., Barker, G. J., Yousry, T. A., Fisher, E., O'Connor, P. W., Phillips, J. T., Polman, C. H., Kappos, L., Hutchinson, M., Havrdova, E., Lublin, F. D., Giovannoni, G., Wajgt, A., Rudick, R., Lynn, F., Panzara, M. A., Sandrock, A. W., & AFFIRM Investigators (2007). MRI outcomes in a placebo-controlled trial of natalizumab in relapsing MS. *Neurology*, 68(17), 1390–1401. <https://doi.org/10.1212/01.wnl.0000260064.77700.fd>

- (374) Fernández Ó. (2017). Is there a change of paradigm towards more effective treatment early in the course of apparent high-risk MS?. *Multiple sclerosis and related disorders*, 17, 75–83. <https://doi.org/10.1016/j.msard.2017.07.003>
- (375) Freeman, L., Longbrake, E. E., Coyle, P. K., Hendin, B., & Vollmer, T. (2022). High-Efficacy Therapies for Treatment-Naïve Individuals with Relapsing-Remitting Multiple Sclerosis. *CNS drugs*, 36(12), 1285–1299. <https://doi.org/10.1007/s40263-022-00965-7>
- (376) Melamed, E., & Lee, M. W. (2020). Multiple Sclerosis and Cancer: The Ying-Yang Effect of Disease Modifying Therapies. *Frontiers in immunology*, 10, 2954. <https://doi.org/10.3389/fimmu.2019.02954>
- (377) Havrdova, E., Galetta, S., Hutchinson, M., Stefoski, D., Bates, D., Polman, C. H., O'Connor, P. W., Giovannoni, G., Phillips, J. T., Lublin, F. D., Pace, A., Kim, R., & Hyde, R. (2009). Effect of natalizumab on clinical and radiological disease activity in multiple sclerosis: a retrospective analysis of the Natalizumab Safety and Efficacy in Relapsing-Remitting Multiple Sclerosis (AFFIRM) study. *The Lancet. Neurology*, 8(3), 254–260. [https://doi.org/10.1016/S1474-4422\(09\)70021-3](https://doi.org/10.1016/S1474-4422(09)70021-3)
- (378) Spelman, T., Kalincik, T., Jokubaitis, V., Zhang, A., Pellegrini, F., Wiendl, H., Belachew, S., Hyde, R., Verheul, F., Lugaresi, A., Havrdová, E., Horáková, D., Grammond, P., Duquette, P., Prat, A., Iuliano, G., Terzi, M., Izquierdo, G., Hupperts, R. M., Boz, C., Pucci, E., Giuliani, G., Sola, P., Spitaleri, D. L., Lechner-Scott, J., Bergamaschi, R., Grand'Maison, F., Granella, F., Kappos, L., Trojano, M., Butzkueven, H. (2016). Comparative efficacy of first-line natalizumab vs IFN- β or glatiramer acetate in relapsing MS. *Neurology. Clinical practice*, 6(2), 102–115. <https://doi.org/10.1212/CPJ.0000000000000227>
- (379) Spelman, T., Frisell, T., Piehl, F., & Hillert, J. (2018). Comparative effectiveness of rituximab relative to IFN- β or glatiramer acetate in relapsing-remitting MS from the Swedish MS registry. *Multiple sclerosis (Houndmills, Basingstoke, England)*, 24(8), 1087–1095. <https://doi.org/10.1177/1352458517713668>
- (380) Harding, K., Williams, O., Willis, M., Hrastelj, J., Rimmer, A., Joseph, F., Tomassini, V., Wardle, M., Pickersgill, T., Robertson, N., & Tallantyre, E. (2019). Clinical Outcomes of Escalation vs Early Intensive Disease-Modifying Therapy in Patients With Multiple Sclerosis. *JAMA neurology*, 76(5), 536–541. <https://doi.org/10.1001/jamaneurol.2018.4905>
- (381) Raffel, J., Dobson, R., Gafson, A., Mattoscio, M., Muraro, P., & Giovannoni, G. (2014). Multiple sclerosis therapy and Epstein-Barr virus antibody titres. *Multiple sclerosis and related disorders*, 3(3), 372–374. <https://doi.org/10.1016/j.msard.2013.12.004>
- (382) Castellazzi, M., Delbue, S., Elia, F., Gastaldi, M., Franciotta, D., Rizzo, R., Bellini, T., Bergamaschi, R., Granieri, E., & Fainardi, E. (2015). Epstein-Barr Virus Specific Antibody Response in Multiple Sclerosis Patients during 21 Months of Natalizumab Treatment. *Disease markers*, 2015, 901312. <https://doi.org/10.1155/2015/901312>

- (383) Persson Berg, L., Eriksson, M., Longhi, S., Kockum, I., Warnke, C., Thomsson, E., Bäckström, M., Olsson, T., Fogdell-Hahn, A., & Bergström, T. (2022). Serum IgG levels to Epstein-Barr and measles viruses in patients with multiple sclerosis during natalizumab and interferon beta treatment. *BMJ neurology open*, 4(2), e000271. <https://doi.org/10.1136/bmjno-2022-000271>
- (384) Serafini, B., Scorsi, E., Rosicarelli, B., Rigau, V., Thouvenot, E., & Aloisi, F. (2017). Massive intracerebral Epstein-Barr virus reactivation in lethal multiple sclerosis relapse after natalizumab withdrawal. *Journal of neuroimmunology*, 307, 14–17. <https://doi.org/10.1016/j.jneuroim.2017.03.013>
- (385) Dominguez-Mozo, M. I., Perez-Perez, S., Villar, L. M., Oliver-Martos, B., Villarrubia, N., Matesanz, F., Costa-Frossard, L., Pinto-Medel, M. J., García-Sánchez, M. I., Ortega-Madueño, I., Lopez-Lozano, L., Garcia-Martinez, A., Izquierdo, G., Fernández, Ó., Álvarez-Cermeño, J. C., Arroyo, R., & Alvarez-Lafuente, R. (2020). Predictive factors and early biomarkers of response in multiple sclerosis patients treated with natalizumab. *Scientific reports*, 10(1), 14244. <https://doi.org/10.1038/s41598-020-71283-5>
- (386) Hagemann, S., Misiak, D., Bell, J. L., Fuchs, T., Lederer, M. I., Bley, N., Hämmerle, M., Ghazy, E., Sippl, W., Schulte, J. H., & Hüttelmaier, S. (2023). IGF2BP1 induces neuroblastoma via a druggable feedforward loop with MYCN promoting 17q oncogene expression. *Molecular cancer*, 22(1), 88. <https://doi.org/10.1186/s12943-023-01792-0>
- (387) Torkildsen, Ø., Myhr, K. M., Brugger-Synnes, P., & Bjørmevik, K. (2024). Antiviral therapy with tenofovir in MS. *Multiple sclerosis and related disorders*, 83, 105436. Advance online publication. <https://doi.org/10.1016/j.msard.2024.105436>

6. Anhang

6.1. Eidesstattliche Erklärung / Declaration of Oath

Ich erkläre gemäß § 5 der Promotionsordnung der Naturwissenschaftlichen Fakultäten I, II & III der Martin-Luther-Universität Halle-Wittenberg an Eides statt, dass ich die Arbeit selbstständig und ohne fremde Hilfe verfasst, keine anderen als die von mir angegebenen Quellen und Hilfsmittel benutzt und die den benutzten Werken wörtlich oder inhaltlich entnommenen Stellen als solche kenntlich gemacht habe.

Weiterhin erkläre ich, dass ich mich mit der vorliegenden Dissertationsarbeit erstmals um die Erlangung eines Doktorgrades bewerbe.

I declare according to § 5 of “Promotionsordnung der Naturwissenschaftlichen Fakultäten I, II & III der Martin-Luther-Universität Halle-Wittenberg” under penalty of perjury that this thesis is my own work entirely and has been written without any help from other people. I used only the sources mentioned and included all the citations correctly both in word or content. Furthermore, I declare that this thesis has not been submitted to another faculty. This is my first application for a PhD title.

15.03.2024

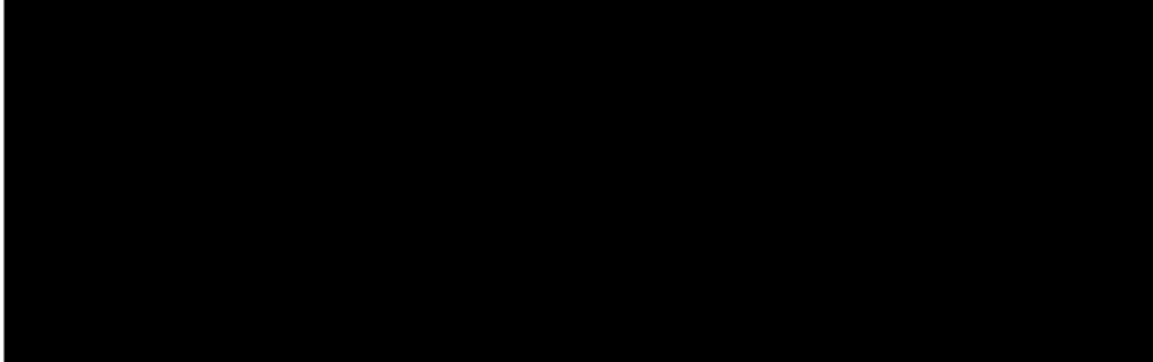
Datum / Date

Unterschrift der Antragstellerin / Signature of the applicant

6.2. Lebenslauf

Lisa Marie Wieland

Persönliche Daten



Beruflicher Werdegang

- 10/2012 – 09/2015: Studium der Biochemie an der MLU Halle-Wittenberg
Abschluss - *Bachelor of Science*
Abschlussarbeit am Institut für Pharma- und Toxikologie,
MLU Halle-Wittenberg
- 10/2015 – 11/2017: Weiterführendes Studium der Biochemie an der MLU Halle-Wittenberg
Abschluss - *Master of Science*
Abschlussarbeit am Fraunhofer-Institut für Zelltherapie und
Immunologie (IZI), Außenstelle Halle (Saale)
- 11/2017 – 04/2018: Hilfswissenschaftlerin am Fraunhofer-Institut für Zelltherapie und
Immunologie (IZI), Außenstelle Halle (Saale)
- 06/2018-09/2021: Wissenschaftliche Mitarbeiterin am Universitätsklinikum der
Medizinischen Fakultät der MLU Halle-Wittenberg
Universitätsklinik und Poliklinik für Neurologie
- 11/2020: Sachkunde-Erwerb für tierexperimentelle Tätigkeiten an Maus und Ratte
- Seit 10/2021: Wissenschaftliche Mitarbeiterin am Universitätsklinikum der
Medizinischen Fakultät der MLU Halle-Wittenberg
Universitätsklinik und Poliklinik für Innere Medizin IV

6.3. Publikationen

Gröger, V., **Wieland, L.**, Naumann, M., Meinecke, A. C., Meinhardt, B., Rossner, S., Ihling, C., Emmer, A., Staege, M. S., & Cynis, H. (2020). Formation of HERV-K and HERV-Fc1 Envelope Family Members is Suppressed on Transcriptional and Translational Level. *International journal of molecular sciences*, 21(21), 7855. <https://doi.org/10.3390/ijms21217855>

Wieland, L., Engel, K., Volkmer, I., Krüger, A., Posern, G., Kornhuber, M. E., Staege, M. S., & Emmer, A. (2021). Overexpression of Endogenous Retroviruses and Malignancy Markers in Neuroblastoma Cell Lines by Medium-Induced Microenvironmental Changes. *Frontiers in oncology*, 11, 637522. <https://doi.org/10.3389/fonc.2021.637522>

Engel, K., **Wieland, L.**, Krüger, A., Volkmer, I., Cynis, H., Emmer, A., & Staege, M. S. (2021). Identification of Differentially Expressed Human Endogenous Retrovirus Families in Human Leukemia and Lymphoma Cell Lines and Stem Cells. *Frontiers in oncology*, 11, 637981. <https://doi.org/10.3389/fonc.2021.637981>

Wieland, L., Schwarz, T., Engel, K., Volkmer, I., Krüger, A., Tarabuko, A., Junghans, J., Kornhuber, M.E., Hoffmann, F., Staege, M.S., & Emmer, A. (2022). Epstein-Barr Virus-Induced Genes and Endogenous Retroviruses in Immortalized B Cells from Patients with Multiple Sclerosis. *Cells*, 11, 3619. <https://doi.org/10.3390/cells11223619>

6.4. Konferenzbeiträge (*Abstracts*) und Publikationen ohne *Peer-Review-Verfahren*

- 01/2019: **Wieland L**, Emmer A, Staege MS. B-Zell-Superantigene und oligoklonale Banden – ein in-vitro-Modell. In: *Research Day MS 2019 Multiple Sklerose – Ein Update aus klinischer und präklinischer Forschung* (Simon U, Hartung HP, Hrsg.), S. 78-79. Nürnberg, Novartis Pharma GmbH (2019).
- 02/2019: Emmer A, **Wieland L**, Kornhuber M, Zierz S, Klusmann JH, Gröger V, Cynis H, Staege MS. Grundlagenforschung: Endogene Retroviren. *Leben* 19:II,22-23 (2019).
- 05/2019: Joshi PR, Müller S, **Wieland L**, Schneider I, Kraya T, Stoltenberg G, Zschüntzsch J, Kornhuber M, Staege MS, Zierz S, Emmer A. Erhöhte Expression des humanen endogenen Retrovirus (HERV) K im Muskelgewebe von Patienten mit Polymyositis und Einschlusskörper-Myositis. 24. *Kongress des Medizinisch-Wissenschaftlichen Beirates der Deutschen Gesellschaft für Muskelkranke (DGM) e.V.* 09.-11.05.2019, Göttingen. *Nervenheilkunde* 38:285 (2019).
- 01/2020: **Wieland L**, Emmer A, Staege MS. Transaktivierung endogener Retroviren durch das Epstein-Barr-Virus - Pathophysiologisch relevanter Schlüsselmechanismus der Multiplen Sklerose. *Research Day MS 2020*. 23.-24.01.2020, Berlin (2020).
- 05/2020: **Wieland L**, Emmer A, Kornhuber NE, Staege MS. Transactivation of endogenous retroviruses by the Epstein-Barr virus - pathophysiologically relevant key mechanism of multiple sclerosis? 6th Congress of the European-Academy of Neurology (EAN). 23.-26.05.2020. Online congress. *Eur J Neurol* 27:479-480 (2020).
- 11/2020: **Wieland L**, Engel K, Krüger A, Schwarz T, Hoffmann F, Emmer A, Kornhuber ME, Staege MS. Identifizierung differenzieller Genexpressionsmuster in Epstein-Barr Virus-immortalisierten B-Zelllinien von Multiple Sklerose-Patienten und gesunden Kontrollen. 93. *Kongress der Deutschen Gesellschaft für Neurologie (DGN)*. 04.07.11.2020, online (2020).
- 09/2021: **Wieland L**, Engel K, Volkmer I, Krüger A, Posern G, Kornhuber M, Staege MS, Emmer A. Overexpression of endogenous retroviruses and immune checkpoint molecule CD200 under microenvironmental changes in neuroblastoma cell lines. 6th European Congress of Immunology. 01.-04.09.2021, Online-Kongress. *Eur J Immunol* 51(S1):320 (2021).

Ilse V, **Wieland L**, Naumann M, Meinecke AC, Meinhardt B, Rossner S, Ihling A, Emmer A, Staege MS, Cynis H. Suppressed expression and incomplete maturation of HERV-K and HERV-Fc1 envelope proteins in mammalian cells. 6th European Congress of Immunology. 01.-04.09.2021, Online-Kongress. *Eur J Immunol* 51(S1):230 (2021).

02/2022: **Wieland L**, Emmer A, Engel K, Hoffmann F, Staege MS. Einfluss des S1PR1/5-Modulators Siponimod auf die Genexpression in EBV-immortalisierten B-Zellen von MS-Patienten und Kontrollen. *Research Day MS – Virtual 2022*. 28.01.2022, online (2022).

Krüger A, Engel K, **Wieland L**, Hoffmann F, Emmer A, Staege MS. Analyse neuartiger Np9-Transkripte im Kontext der Multiplen Sklerose. *Research Day MS – Virtual 2022*. 28.01.2022, online (2022).

01/2023: **Wieland L**, Schwarz T, Engel K, Volkmer I, Krüger A, Tarabuko A, Junghans J, Kornhuber ME, Hoffmann F, Emmer A, Staege MS. Identification of differentially expressed genes in multiple sclerosis using an EBV-immortalized B cell approach. *Research Day MS 2023*. 26.-27.01.2023, Berlin (2023).

6.5. Danksagung

An dieser Stelle möchte ich mich zu tiefst bei allen Personen bedanken, die mich während meiner Promotionszeit unterstützt und begleitet haben.

Prof. Dr. Gary Sawers gilt mein besonderer Dank für die fachliche Betreuung der Promotionsarbeit an der Martin-Luther-Universität Halle-Wittenberg. Die Hinweise zum Aufbau und Struktur der kumulativen Arbeit waren äußerst hilfreich und für die freundliche, offene Art mir und meinem Promotionsthema gegenüber möchte ich mich herzlich bedanken.

Apl. Prof. Dr. Martin Staeger möchte ich für die fachliche Betreuung im Forschungslabor der Kinder- und Jugendmedizin I des UKH und die Begutachtung der Promotionsarbeit danken. Die Welt hinter den Kulissen der Transkriptomanalysen hat sich zu Beginn für mich wie eine Fremdsprache angehört, die ich im Laufe der Zeit immer besser zu beherrschen gelernt habe. Dabei war es sehr hilfreich, auch manchmal kurzfristig bei dir vorbeikommen zu können, um ein Problem direkt zu besprechen.

Prof. Steffen Roßner danke ich für die Begleitung der Promotionsarbeit. Der offene und auch kritische Diskurs innerhalb der HERV-Projektbesprechungen haben diese Arbeit bereichert.

Dr. Alexander Emmer möchte ich für den medizinisch-fachlichen Input und die Begleitung während meiner Promotionszeit in der AG Neuroimmunologie des UKH danken. Der Austausch zu klinischen Fragestellungen hat mir geholfen meine Perspektive um einen Blickwinkel zu erweitern.

Dr. Heiner Höltkötter danke ich herzlich für die finanzielle Unterstützung des HERV-Projektes. Dein besonderes Interesse an unserer Arbeit war mir stets ein Antrieb. Ich werde die interessanten Gespräche bei vorzüglichem Speis und Trank in guter Erinnerung behalten.

Allen Kolleg:innen der Forschungslabore der Neurologie und der Kinder- und Jugendmedizin I, die mich in den vergangenen Jahren auf verschiedenen Ebenen unterstützt haben, möchte ich herzlich danken. Hierbei seien insbesondere die nachfolgenden Kolleginnen und Kollegen namentlich erwähnt:

PD Dr. Leila Scholle – Dir gilt mein herzlicher Dank für die vielen kleinen und großen Hindernisse, die du mit mir aus dem Weg geräumt hast. Vielen Dank, dass deine Tür für mich immer offen war und mich deine Kaffee-Reserven mehr als einmal gerettet haben.

Beate Hinrichsen – Als Leidensgenossin (sowohl in der Klinik, als auch auf der Strecke) danke ich dir für dein absolutes Verständnis der „Hochs“ und „Tiefs“ während meiner Promotionszeit. Danke für deine immer fachlich kompetenten Tipps und Tricks im Laboralltag und definitiv auch außerhalb hinsichtlich Allem, was sehens- und lesenswert ist.

Katrin Schulz, Kathleen Zietz und Angela Rosemeier – Euch macht in Sachen Labororganisation und Histologie so schnell keiner was vor. Vielen Dank, dass ihr euer Wissen und eure Fertigkeiten mit mir geteilt habt.

Dr. Kristina Engel – Du bist mir auf dem Weg die „Transkriptom-Sprache“ zu erlernen eine hervorragende Mentorin gewesen, die auch bei noch so großen Datenbergen den Überblick behält. Vielen lieben Dank auch für dein kompetentes Feedback bei den Publikationen. Ich freue mich auf weiterhin gute Zusammenarbeit im neuen Laborteam.

Ines Volkmer – Dein Einsatz und das nahezu fotografische Gedächtnis deiner gut 20-jährigen Laborbuch-Notizen hat so manchem Studenten das Leben erleichtert. Ich bedanke mich für deine labortechnische Expertise, dein lösungsorientiertes Denken und deine herzlich ehrliche Art.

Zudem gilt ein besonderer Dank auch den Kolleginnen und Kollegen der Hallenser Außenstelle Molekulare Wirkstoffbiochemie und Therapieentwicklung des Fraunhofer Instituts für Zelltherapie und Immunologie (IZI-MWT), die mein Interesse an neurodegenerativen und entzündlichen Erkrankungen, sowie den HERVs vor gut sieben Jahren geweckt haben. Namentlich seien hier Jun.-Prof. Holger Cynis, Victoria Ilse und Dr. Anke Piechotta genannt. Ich habe den fachlichen Austausch, sowie die gute Zusammenarbeit im HERV-Projekt mit euch immer sehr geschätzt.

Der größte Dank von Allen gilt meiner Familie und Freunden. Liebe Mama, lieber Papa, lieber Lukas, liebe Carla, liebe Sandra, lieber Thorsten, liebe Petra - Ihr seid mein Anker, mein Motor, mein Ein und Alles. Mein abschließender Dank gebührt meinem Mann - Deine Unterstützung, Liebe und Kraft, die du mir spendest, sind der Grund, dass jedes noch so scheinbar unerreichbare Ziel greifbar wird. Ich kann es kaum erwarten mit der Geburt unserer Tochter die nächste Herausforderung mit dir annehmen zu dürfen.